New Late-Stage Strategies Towards Difluoromethylarenes

A thesis submitted to the Board of the Faculty of Physical Sciences, in partial fulfilment of the requirements for the degree of Doctor of Philosophy at the University of Oxford

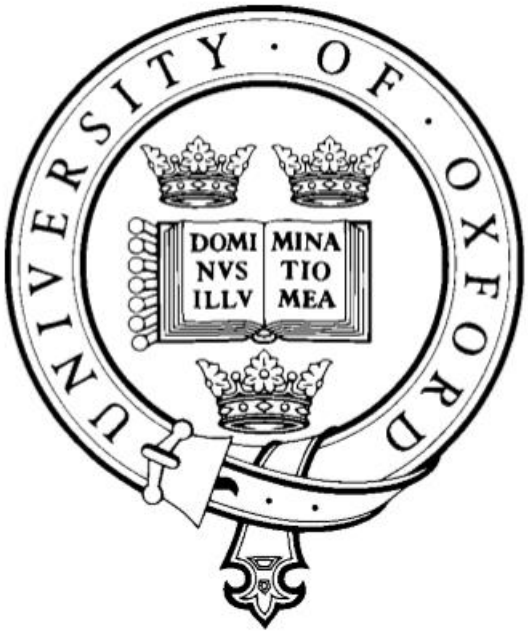

Jeroen B. I. Sap
Merton College
University of Oxford

Declaration

I hereby declare that the work presented in this thesis was conducted under the supervision of Prof. Véronique Gouverneur FRS FRSC and carried out at the Chemistry Research Laboratory and Siemens Molecular Imaging Lab, University of Oxford, unless otherwise specified. All the work is my own, except where otherwise stated, and has not been submitted for any other degree at this or any other university.

Jeroen Sap

22nd of July 2020

Dedication

This thesis is dedicated in its entirety to Björn Gugu, a friend, a scholar and a brilliant scientist who left us far too early.

Jeroen Sap Merton College DPhil Chemistry Trinity Term 2020

Abstract: New Late-Stage Strategies Towards Difluoromethylarenes

This thesis consists of the development of novel methodology to access difluoromethylated compounds both in the context of photoredox catalysis and fluorine-18 radiochemistry for Positron Emission Tomography (PET). First a general introduction to late-stage difluoromethylation will be showcased in **Chapter I**. In **Chapter II**, a metal-free visible light catalysed synthesis of difluoromethylarenes *via* a controlled hydrodefluorination of electron-poor trifluoromethylarenes is described. The reaction works both in batch and in flow and proves to be useful in the context of late-stage functionalisation. In **Chapter III**, a general introduction to PET is provided. General radiochemistry concepts are also introduced. In **Chapter IV**, a facile and robust radiochemical methodology for PET describing the synthesis of ^{18}F-difluoromethylarenes from aryl boronic acids, ethyl bromofluoroacetate and cyclotron produced [^{18}F]fluoride is presented. The two key steps involve a copper catalysed cross-coupling reaction using bench-stable aryl boronic acids to yield 2-fluoro-2-arylacetic acids in a two-step one-pot reaction followed by a manganese mediated ^{18}F-fluorodecarboxylation to afford ^{18}F-difluoromethylarenes in a streamlined fashion. **Chapter V** discusses the synthesis of the first ^{18}F-difluorocarbene reagent and its application to react as a difluoromethylating reagent with phenols, thiophenols, *N*-heterocycles, and boronic acids. **Chapter VI** provides experimental data for compounds described within this thesis.

Acknowledgements

First and foremost, I would like to thank Véronique for giving me the opportunity to work in her fantastic research group. It has been a great experience where I had the opportunity to do great science and work alongside very intelligent scientists. Throughout all four years she has been a supportive supervisor who taught me the ropes from day one. Her passion and excitement for science is truly inspiring and rubs off onto everyone who has the privilege to work for her. Her mentorship and guidance have made me the scientist I am today and for this I could not be more grateful. I will always take with me the countless chats we had about my future career, thank you very much for giving me so much of your precious time, Véronique.

I would also like to thank the EPSRC and Pfizer for my generous funding. In particular, I would like to thank Christopher amEnde, for the continuous support he has given me since day one of my DPhil. I want to thank you for all the scientific input you have given me along the way and all the resources from Pfizer you have made available to me throughout these four years. I would also like to thank Paramita Mukherjee and Thomas Knaußer both from Pfizer for their input on the various projects I have been involved in throughout my DPhil. Matthew Tredwell, thank you for allowing Claudio and I to come to Cardiff for labelling. We have learnt so much from you, a truly inspirational and knowledgeable radiochemist!

Over my four years the group has changed a lot. First, I would like to thank the initial F12 crew who very much made me feel at home. Plum, Hyde, Gregor, Enrico, Sean, Paolo thank you for the initial guidance you gave me in the lab as well as more general advice on radiolabelling or lab techniques.

Nick, I'll never forget all the chats we had during our late nights of work during my first year, thank you for having those late burritos with me and Anna at Mission Burrito.

Tom, my buddy since day one, thank you for looking after me, thank you for asking whether I was doing ok when I seemed stressed. I thoroughly enjoy our conversations even though you are on the other side of the ocean. Véronique has compared me to you in the past and I can only say how honoured I felt when she said that, big shoes to fill! Thank you also for proofreading this thesis.

Greg, we didn't overlap much, but thank you for all those chats and drinks at the pub when things were not going so well!

Moving on to the current VG lab crew. Anna, thank you for being one of the kindest human beings I have met during my DPhil. Francesco, thanks for always being there with an unbiased opinion when I needed it most, and for all the chats about football and other shenanigans, FORZA SAMPDORIA! Osman, thank you for spending all those late nights in the lab with me and tolerating my goofiness in the late-hours. Thank you also for sharing with me your love and talent for piano. Jimmy, cheers for all the good times chatting about chemistry, and being one of 'the boys,' your knowledge of named reactions is impressive! Rob, cheers for all the good times in the hot lab, our chats about life and last but not least for bestowing the title of 'Daddy Cool' upon me. Sandrine, thank you for all the great collaborative work over the years, your drive and dedication to science are inspiring! I thoroughly enjoy working with you and Claudio! Tim, Tobi, Adeline, Konstantinos, Zijun, cheers for all the drinks and laughs over the last few years, you are all talented chemists who will go on to do fantastic things! Giulia, thank you for being such a great friend, you are a driven, passionate and talented chemist! Thanks for all those weekends working together in F12! Claudio, my CF_2H buddy since day one! Thank you for all the great collaborative efforts throughout our

three year overlap. More importantly, as a friend you were always there for a chat over coffee about science or random things. Thank you for all the good times in SOMIL and Cardiff, labelling with you for the carbene project was and continuously to be a joy! Marie, thanks for being a good friend in the often-stressful environment that is the CRL. Your friendship is much appreciated and thank you for proofreading this thesis.

The post docs: there have been quite a few since I started! Gabri: Thank you for being the go-to guy for advice on my career, and continuously challenging me to think 'big.' Thank you also for sharing your love of food with me. Alex (Dürr), 100% you are the funniest one of the bunch 'I tell you.' Thank you for the late-evening chats and ensuring there is always something to laugh about in the office. Alex (Grozavu), you are a very bright chemist and I admire your dedication to understand every single detail about your reactions! Matt, thank you for all the chats about chemistry, academia and Spain! Florian, thank you for running the hot lab, and being available for a chat whether chemistry or personal. Having Chinese New Year at your place, is something I'll never forget! David, thank you for all the formals we had together, I truly enjoyed every single one of them! Natan, thanks for all the banter in the (hot)lab and being my go-to lunch buddy! I very much enjoyed the board game nights we had! Kee, thanks for being my mentor, I respect your efficiency! I enjoyed playing board games and having our weekly Merton lunch together! Patrick, thank you for being a listening ear when I needed someone mature to have a personal conversation with. Thank you for all the good times in the hot lab! I'm proud to have a friend like you in my life!

My parents, the ones that have not just been there for me since day one of my DPhil but for my entire life. If it wasn't for you, I wouldn't even have studied in the UK and perhaps I would have

become a magician instead of a scientist (jokes). Thanks for bearing with me and my obsession for science, letting me pursue my dreams and allowing me to spread my wings away from home in order to pursue my goals! Thank you also to my siblings, Pieter and Annelies and my brother and sister in law, Yentl and Sofie, being able to wind down when I'm back in Belgium has helped me through this DPhil! Thank you also to my parents in law Alice and Sammy and my sister in law Sherry for welcoming me to Hong Kong and accepting my ridiculous working hours.

Björn: This thesis is written in your honour. I always dreamed about starting and finishing our PhDs together, sadly, this is no longer possible. I hope you have found peace and look down with pride. I will never be as talented or smart as you, but I will continuously strive to raise the bar, as you always did.

Finally, last but definitely not least…Renee, first my girlfriend but now with pride I can say, my wife. Thank you for keeping up with my often-ridiculous passion or should I say 'obsession' with chemistry. Thank you for all the long evenings you sat in the office, so I could do my experiments! Thank you for bearing with me all the times I would chat about chemistry with my colleagues, I apologise (maybe getting a 'chemistry jar' would help)! My achievements are equally yours, I would not be the chemist, partner and now husband if it wasn't for all the things you took care of so I could do my chemistry, words will never be enough to describe how grateful I am to you for this, I love you!

Abbreviations

1,2-DCB	1,2-Dichlorobenzene
3-DPAFIPN	2,4,6-Tris(diphenylamino)-5-fluoroisophthalonitrile
4-DPA-IPN	2,4,5,6-tetrakis(diphenylamino)isophthalonitrile
4-HTP	4-hydroxythiophenol
ADME	Absorption, distribution, metabolism, and excretion
AY	Activity yield
B_2Pin_2	Bis(pinacolato)diboron
BDE	Bond dissociation energy
BEMP	2-tert-Butylimino-2-diethylamino-1,3-dimethylperhydro-1,3,2-diazaphosphorine
BTMG	2-tert-Butyl-1,1,3,3-tetramethylguanidine
BTTP	tert-Butylimino-tri(pyrrolidino)phosphorane
$CDCl_3$	Deuterated chloroform
CFCs	Chlorofluoro carbons
CRTh2	Prostaglandin D2 receptor 2
CT	Computed tomography
CV	Cyclic voltammetry
CYP-450	Cytochrome P450
CySH	Cyclohexanethiol
DABCO	1,4-Diazabicyclo(2,2,2)octane
DAST	(Diethylamino)sulfur trifluoride
DBN	1,5-Diazabicyclo[4.3.0]non-5-ene
DBU	1,8-Diazabicyclo(5.4.0)undec-7-ene
DCE	Dichloroethane
DCM	Dichloromethane
Deoxy-Fluor	Bis(2-methoxyethyl)aminosulfur trifluoride
DFC	Difluorocarbene
DFMS	Zinc difluoromethanesulfinate
DIPA	*N,N*-Diisopropylethylamine
DMA	*N,N*-Dimethylacetamide
DME	Dimethoxyethane
DMF	Dimethylformamide
DMI	1,3-Dimethyl-2-imidazolidinone
DMPU	*N*, *N*'-Dimethylpropyleneurea
DMSO	Dimethyl sulfoxide
DPEPhos	Bis[(2-diphenylphosphino)phenyl] ether
DPPF	1,1'-Bis(diphenylphosphino)ferrocene
Dtbpy	4,4′-Di-tert-butyl-2,2′-dipyridyl
DTBPY	2,6-Di-tert-butylpyridine
E.O.B	End of bombardment

FDG	Fluorodeoxyglucose
GC-MS	Gas-chromatography coupled mass spectrometry
HAD	Hydrogen atom donor
HBD	Hydrogen bond donor
HBPin	4,4,5,5-Tetramethyl-1,3,2-dioxaborolane
HDF	Hydrodefluorination
HFIP	1,1,1,3,3,3-Hexafluoro-2-propanol
HMPA	Hexamethylphosphoramide
HOMO	Highest occupied molecular orbital
HPLC	High-performance liquid chromatography
HRMS	High resolution mass spectrometry
HTS	High throughput screening
IR	Infrared
ISC	Inter-system crossing
K_{222}	Kryptofix® 222
LC-MS	Liquid chromatography coupled mass spectrometry
LSF	Late-stage functionalisation
LUMO	Lowest unoccupied molecular orbital
MA	Molar activity
MeCN	Acetonitrile
MeNER	(S)-2-((S)-(2-methoxyphenoxy)(phenyl)methyl)morpholine
mpgCN	Mesoporous graphitic carbon nitride
MRI	Magnetic resonance imaging
MTBD	7-Methyl-1,5,7-triazabicyclo(4.4.0)dec-5-ene
NET	Norepinephrine transporter
NMP	*N*-Methyl-2-pyrrolidone
NMR	Nuclear magnetic resonance
PC	Photocatalyst
PDFA	Difluoromethylene phosphobetaine
PET	Positron Emission Tomography
PIDA	(Diacetoxyiodo)benzene
PMP	1,2,2,6,6-Pentamethylpiperidine
PTH	10-phenyl-10H-phenothiazine
Py	Pyridine
QMA	Quaternary methyl ammonium
RCY	Radiochemical yield
r.t.	Room temperature
SAR	Structure activity relationship
SCE	Standard calomel electrode
SET	Single Electron Transfer
TBAF	Tetra-n-butylammonium fluoride
TEAF	Tetraethylammonium fluoride
$TEAHCO_3$	tetraethylammonium bicarbonate
TEMPO	(2,2,6,6-Tetramethylpiperidin-1-yl)oxyl or (2,2,6,6-tetramethylpiperidin-1-yl)oxidanyl

TFT	α,α,α-Trifluorotoluene
THF	Tetrahydrofuran
TMEDA	Tetramethylethylenediamine
TMG	1,1,3,3-Tetramethylguanidine
TMP	2,2,6,6-Tetramethylpiperidine
UV	Ultra-violet
Xantphos	4,5-Bis(diphenylphosphino)-9,9-dimethylxanthene
XPhos	[2-Dicyclohexylphosphino-2',4',6'-triisopropylbiphenyl]

Table of Contents

Chapter 1: Late-stage Methods to Install the Difluoromethyl Group

1.1 Late-Stage Functionalisation to Access Fluorinated Motifs

Late-stage functionalisation (LSF) is a powerful strategy to generate novel fluorinated analogues of a lead structure, without employing *de novo* synthesis.[1] Traditional methods to construct small fluorinated molecules often start from fluorinated building blocks which serve as reaction partners to generate structural complexity.[2] Such strategies can be time consuming, expensive and thus inefficient for highly complex scaffolds. As such, LSF provides an alternative to build on existing complexity. The field of LSF is progressing rapidly. In general, four main strategies are employed. The first, is to exploit a reactive handle which can be pre-installed to facilitate cross-coupling reactions.[3] These reactions are often highly selective. The second, is to activate inert bonds such as the C-H bond to introduce functional groups. However, many of these reactions typically require a directing group in order to promote reactivity and to ensure site selectivity.[4] A third strategy has recently surfaced which takes advantage of seemingly inert chemical bonds, such as the C-F bond, which are significantly less prominent in complex targets than C-H bonds, allowing for site-selectivity.[5] Finally, a fourth strategy which exploits reactive handles which are native to the molecule and not pre-installed has become popular amongst medicinal chemists to allow quick derivatisation of existing lead compounds. Such a strategy typically harnesses the reactive nature of nucleophilic functionalities such as alcohols, amines or carboxylic acids already present on the target of interest (**Scheme 1.1**).[6]

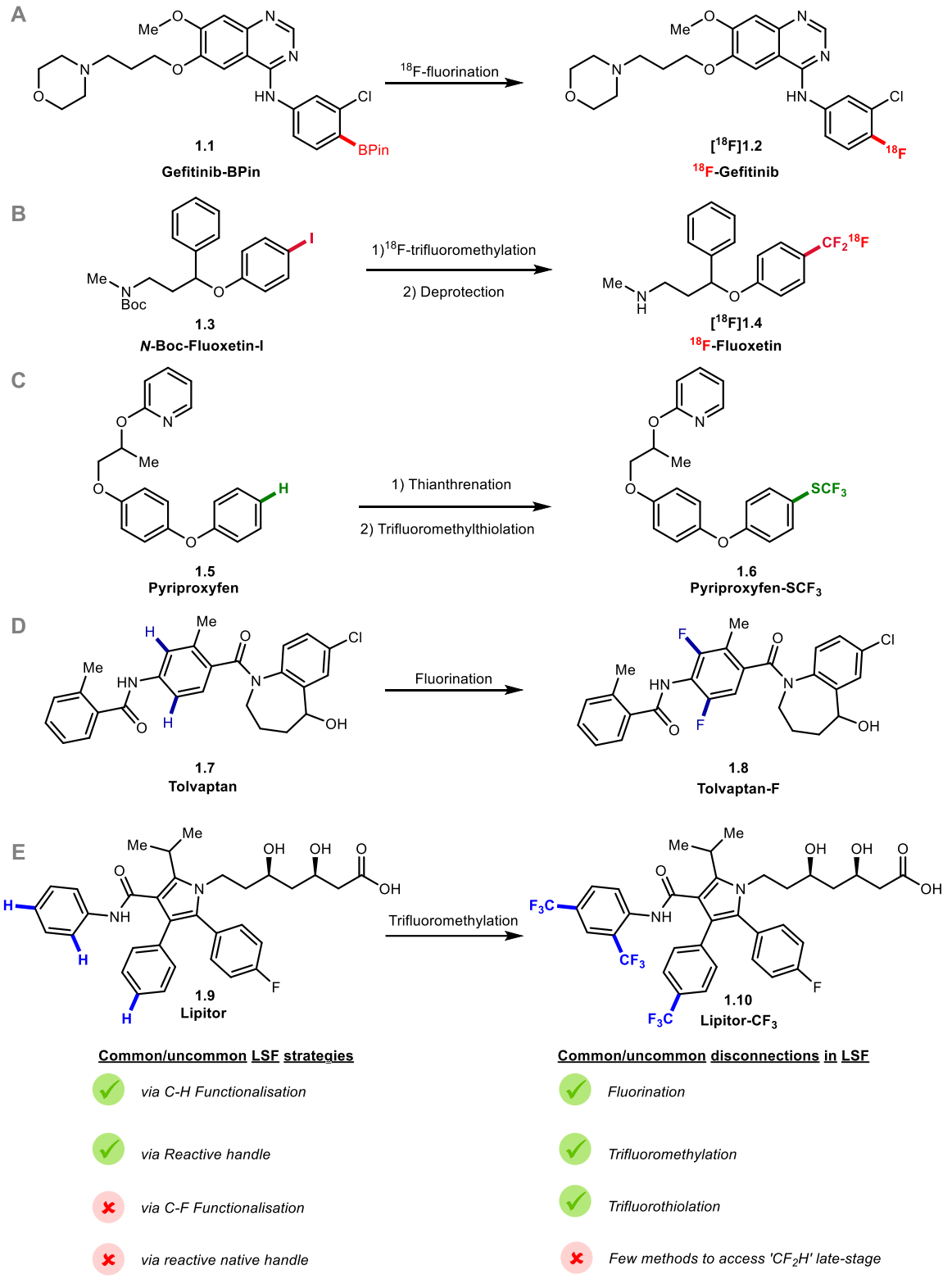

Scheme 1.1 Strategies to introduce fluorinated motifs in the context of LSF. Late-stage ^{18}F-fluorination (A) and ^{18}F-trifluoromethylation (B) facilitated by a reactive handle. Late stage thianthrenation/trifluoromethylthiolation (C), fluorination (D) and trifluoromethylation of innate C-H bonds (E).

LSF is often employed with a given application in mind. One powerful application is the ability to rapidly access metabolites for the assessment in ADME studies, in which LSF oxidations play a critical role.[7] Another key application of LSF can be found in the context of radiolabelling. In such processes the late-stage introduction of the radioactive label is often desirable to decrease the overall synthesis time and complexity of the radiosynthesis.[8] The application of LSF to F-18 radiochemistry will be discussed in **Chapters IV and V.** A further application of LSF is the modulation of lipophilicity of drug candidates. Being able to modulate lipophilicity, for example by tailoring fluorine content, is a powerful tool in drug discovery. This will be the topic of discussion in **Chapter II**. This thesis will showcase the development of new LSF strategies to access $ArCF_2H$ and its F-18 labelled analogue $ArCHF^{18}F$ as well as other $-CHF^{18}F$ motifs **(Scheme 1.2)**.

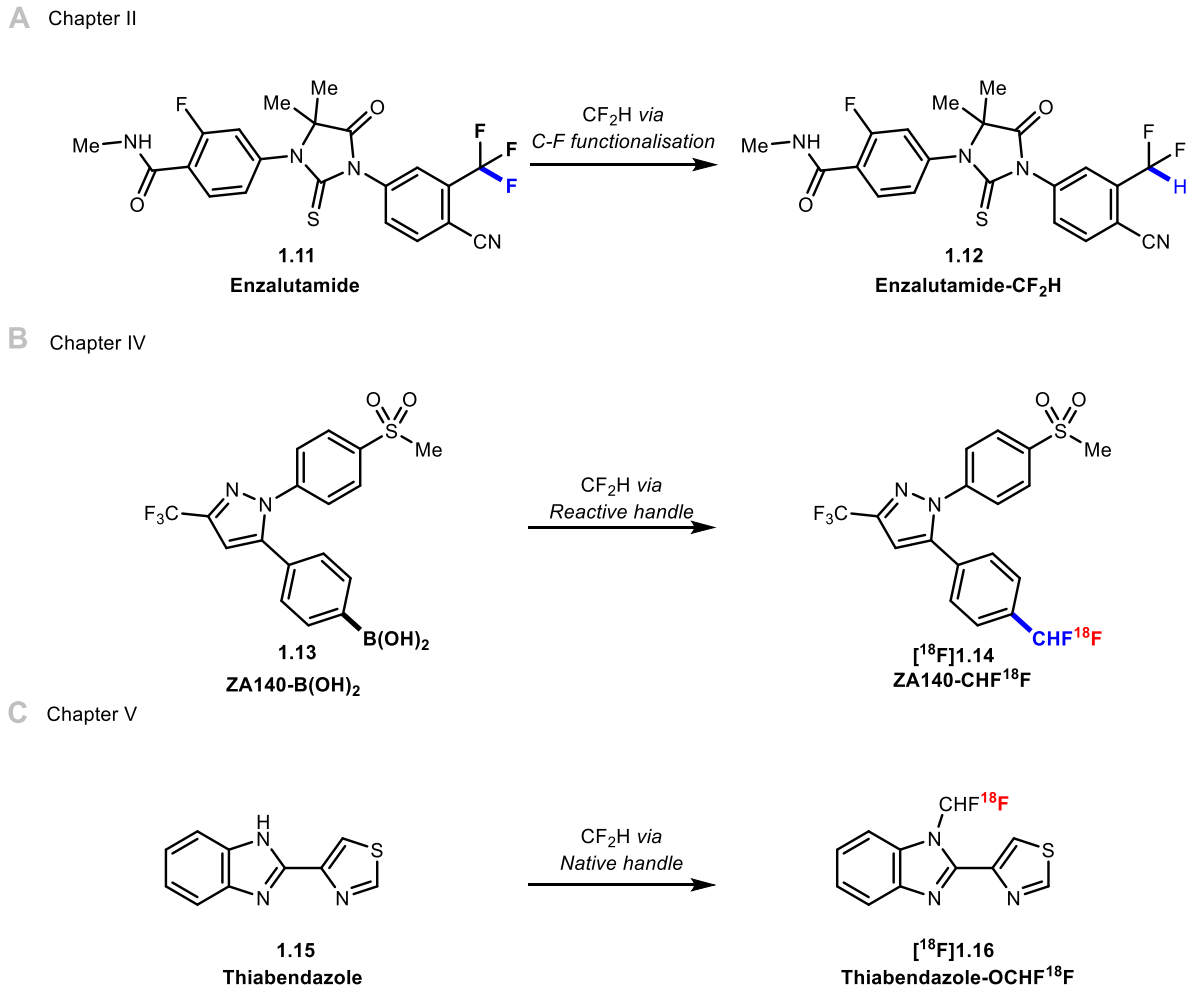

Scheme 1.2 Overview of late-stage methods to access CF_2H motifs addressed in this thesis. A) Late-stage site-selective hydrodefluorination of trifluoromethylarenes. B) Late-stage radiosynthesis of [^{18}F]ArCF_2H *via* ^{18}F-fluorodecarboxylation. C) Late-stage ^{18}F-difluoromethylation of a native handle.

1.2 Properties of The Difluoromethyl Group

The CF_2H group has similarities to other fluorinated functional groups such as the CFH_2 and CF_3 groups, but some significant differences which make it unique. These distinct features have made the CF_2H group popular in the pharmaceutical and agrochemical industries to tune the properties of drugs, herbicides, fungicides, and agrochemicals.[9]

1.2.1 Difluoromethyl Compared to Other Fluorinated Functional Groups

With respect to its physiochemical properties, the CF_2H group possesses a polarised C-H bond, which can act as a hydrogen bond donor (HBD). This unusual property is illustrated by comparing 2-nitro-1-difluoromethylbenzene and 2-nitrophenol, which both readily dimerise (**Figure 1.1**).[10]

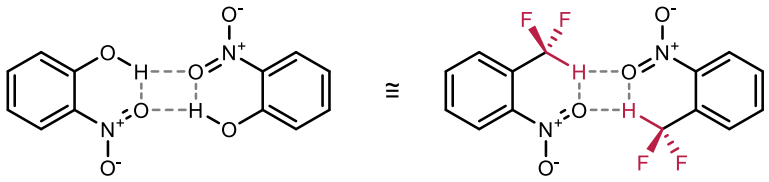

1.17 ≅ **1.18**

Figure 1.1 Hydrogen bonding properties of the -CF_2H group.

The ability of the CF_2H group to participate in hydrogen bonding can be rationalised by referring to its hydrogen bond acidity [*A*] (higher [*A*] corresponds to higher acidity). This parameter can be calculated directly from the ^1H NMR shifts of a molecule in different solvents, and quantifies a molecule's ability to participate in hydrogen bonding interactions. As depicted in **Figure 1.2**, molecules with a CF_2H group are more likely to exhibit HBD properties than their corresponding non-fluorinated counterparts.[11,12]

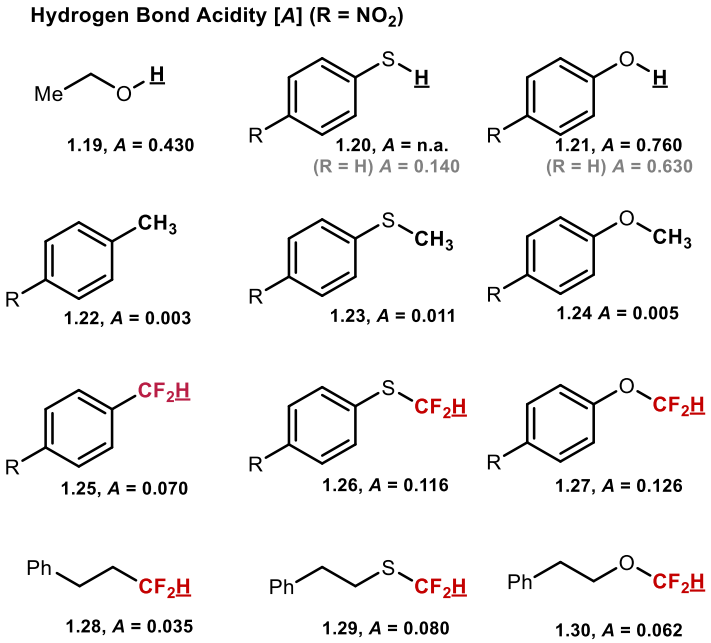

Figure 1.2 Reported [*A*] values of the functional groups with known HBD properties. Hydrogen bond acidity ([*A*]) calculated through the NMR chemical shift difference of a proton in DMSO vs $CDCl_3$ solvent.

In addition to its hydrogen bonding properties, the effects of the CF_2H group on the overall lipophilicity of compounds has also been studied. As shown in **Figure 1.3**, toluene derivatives have a higher logP than their difluoromethyl analogues. However, when comparing the relative lipophilicities of aliphatic difluoromethylated compounds to aliphatic methyl (thio)ethers, the former exhibits drastically increased logP values. A similar trend is observed when comparing phenol to (difluoromethyl)benzene.[13]

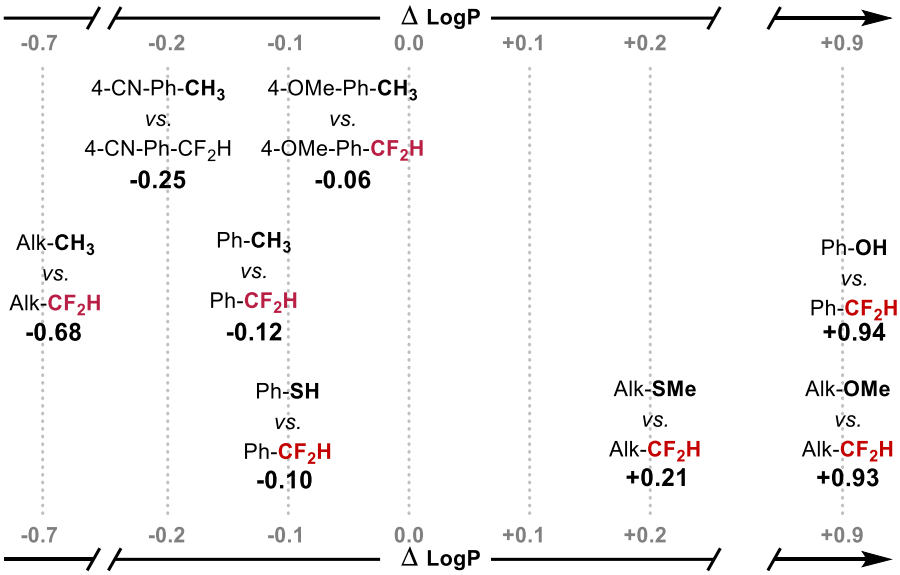

Figure 1.3 Relative lipophilicity of the CF_2H group.

With regards to ADME (absorption, distribution, metabolism and elimination) properties, Pfizer conducted a case study in which they studied the differences between anisoles and their fluorinated derivatives (OMe, OCF_2H, OCF_3) on a variety of lead drug candidates. Their findings suggest that on average, $ArOCF_2H$ compounds exhibit a >0.5 reduction in logP and higher membrane permeability compared to their OCF_3 counterparts. They also found that on average, $ArOCF_2H$ drug structures showed an increased metabolic stability compared to $ArOCH_2F$. With respect to conformational preference, $ArOCF_2H$ compounds were shown to display less conformational bias compared to their $ArOCF_3$, due to a less pronounced anomeric effect(**Figure 1.4**).[13]

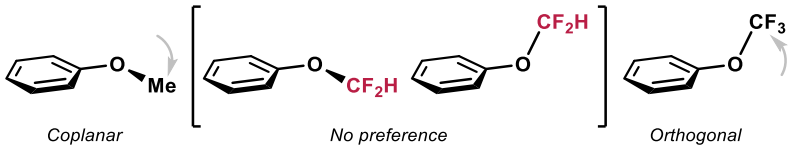

Figure 1.4 Conformational preference of fluoromethyl ethers.

In light of these studies, the demand for new, mild, selective and late-stage methods to introduce the CF_2H group into complex organic molecules through C-C or X-C bond formation has increased. Technologies which allow the late-stage introduction of the CF_2H group into complex bioactive molecules are advantageous for medicinal chemistry, agrochemistry as well as F-18 radiochemistry for positron emission tomography (PET) applications.[14]

1.2.2 Conventional Methods to Access the CF_2H Motif

In 1920 when Swarts reported the synthesis of several halofluorocarbons, including chlorodifluoromethane ($ClCF_2H$), commonly referred to as *Freon-22*.[15,16] These polyfluorinated compounds were initially primarily used as refrigerants, fire repellents, and industrial cooling agents.[17] Further applications of this reagent and other chlorofluorocarbons (CFCs) came when the interest in incorporating the CF_2H group into organic molecules surged. However, the realisation that these CFCs contribute to ozone depletion, soon led to their phasing out. In 1987, the Montreal protocol manifested the agreement of the strict regulation on the use of CFCs. This agreement encouraged the chemistry community to rethink the development of polyfluoroalkylation reagents, including but not limited to those used in difluoromethylation reactions. In recent decades, the mostly widely used strategy to construct the CF_2H moiety was *via* deoxyfluorination; in this transformation, an aldehyde is converted into a CF_2H group. (**Scheme 1.3**).[18] A plethora of reagents have since been developed to facilitate the reaction whereby an aldehyde is converted into a difluoromethyl group. Reagents used to accomplish this transformation are commonly derived from gaseous sulfur

tetrafluoride (SF_4, **1.31**) including *N,N'*-diethyl amino sulfur trifluoride (DAST, **1.32**) and bis-(2-methoxyethyl) amino sulfur trifluoride (Deoxo-Fluor®, **1.33**).[19] This chemistry has led to a variety of CF_2H containing compounds, however limitations of these reagents with regards to scope, scalability, toxicity, and explosivity, have paved the way to the development of new deoxyfluorination reagents.[20] In the last decade, several advancements have been made to overcome some of these limitations. The development of bench stable, crystalline solid alternative reagents such as XtalFluor-M® (**1.35**) which exhibit similar reactivity has been welcomed by the community.[21]

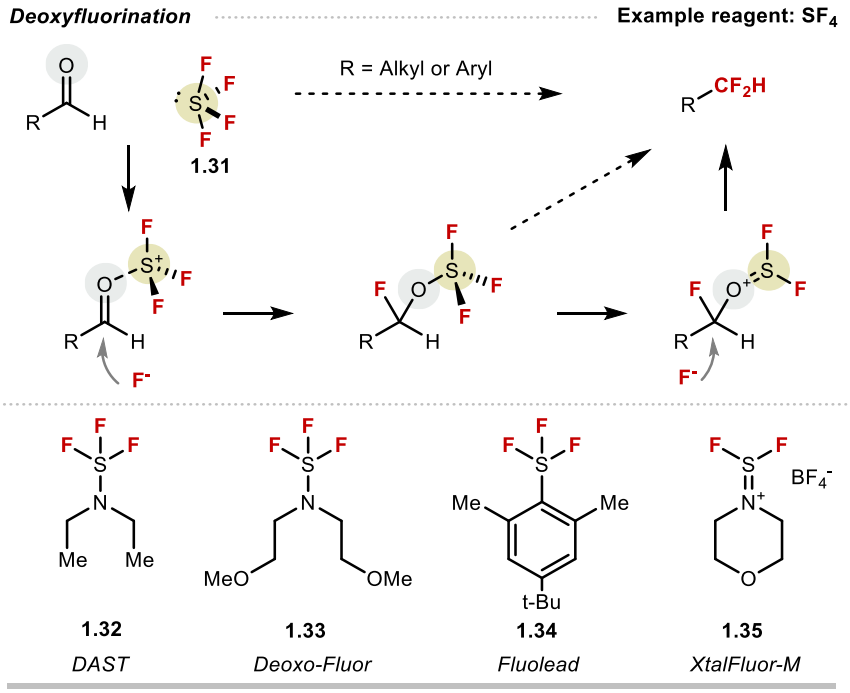

Scheme 1.3 Deoxyfluorination of aldehyde functional group.

In the context of LSF, the necessity to install an aldehyde functionality, limits the utility of these reagents.[22] CF_2H groups are often incorporated into more complex structures such as those shown in **Figure 1.5** *via* pre-functionalised building blocks. As such, new technologies which exploit easy to install reactive handles

which allow cross-coupling from aryl halide or aryl boron motifs are attractive. Equally attractive are methods which allow the late-stage modulation in fluorine content *via* site-specific fluorination or defluorination, the latter of which will be discussed in **Chapter II**.

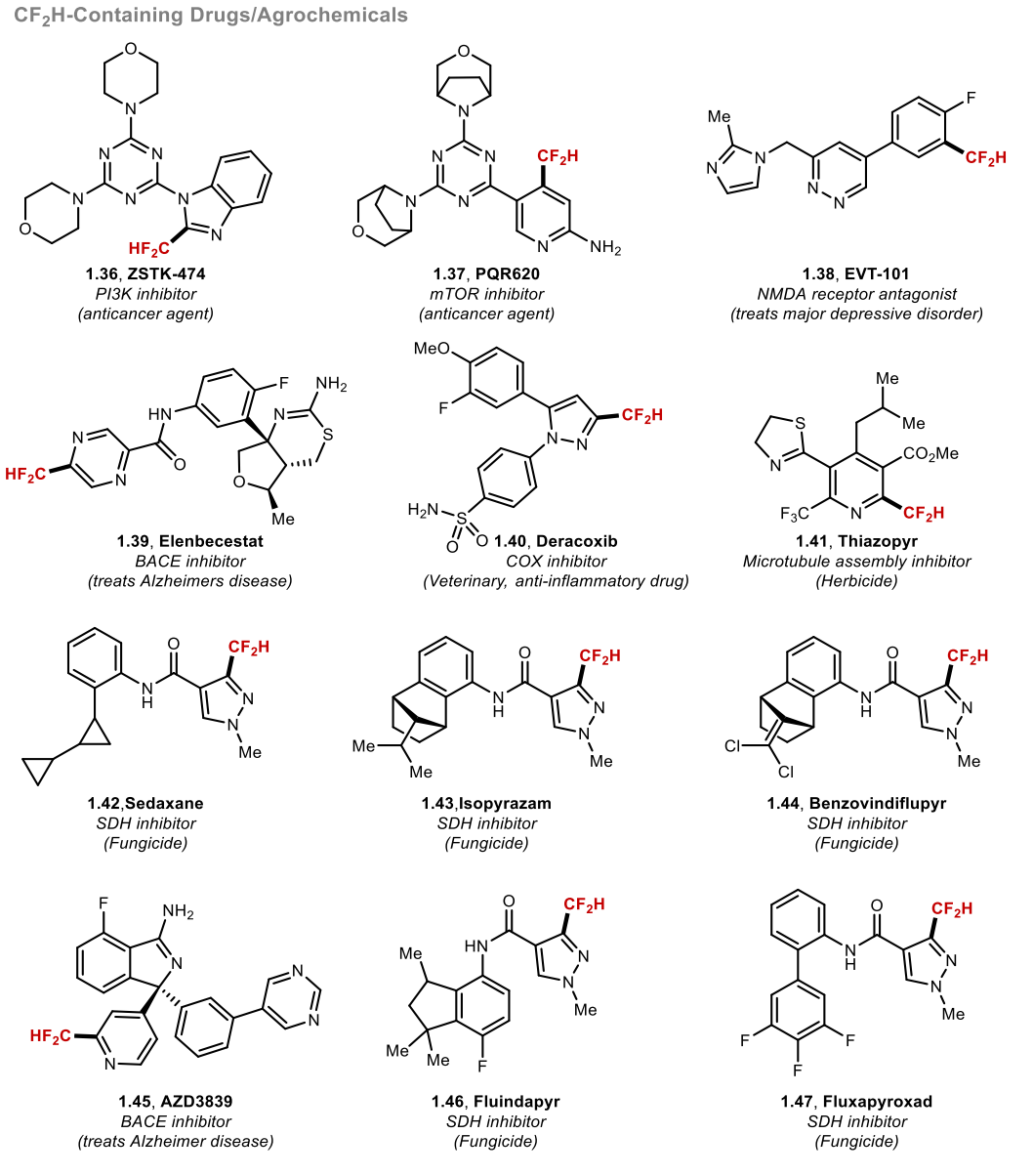

Figure 1.5 Examples of bioactive molecules which contain a (hetero)arene C(sp^2)-CF_2H bond.

1.3 State-of-The Art in C(sp^2)CF_2H Bond Formation

1.3.1 C(sp2)-CF_2H: Arenes and Heteroarenes

The introduction of a CF_2H group onto a (hetero)arene can be accomplished through a stepwise method involving the transfer of a CF_2X group (where X = stabilising group) facilitated by a metal. In these cases, the stabilising groups help increase the stability of the metal-carbon bond, thereby facilitating cross-coupling. A variety of reagents can be employed for such a strategy including $BrCF_2CO_2Et$, $FSO_2CF_2CO_2H$, $TMSCF_2SO_2Ph$, $BrCF_2SO_2Ph$, $BrCF_2P(O)(OEt)_2$, ICF_2SO_2Ph and $R_3SiCF_2CO_2Et$. After the coupling step, the stabilising group is then subsequently cleaved under reductive conditions, liberating the CF_2H motif (**Scheme 1.4**).[23]

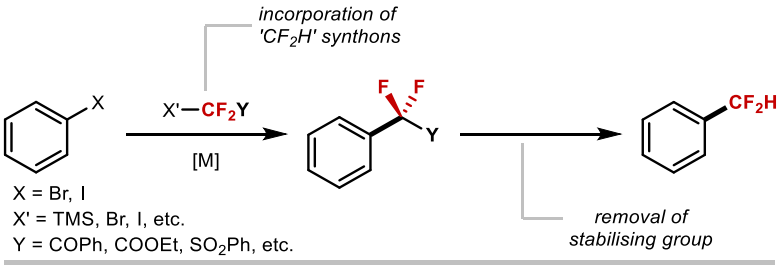

Scheme 1.4 Metal-mediated stepwise difluoromethylation reactions.

Alternatively, the introduction of a CF_2H group can be achieved in a direct fashion, either facilitated by a metal *via* cross-coupling or by applying radical chemistry. In the context of LSF, direct methods are typically more attractive than stepwise approaches which often require harsh conditions to remove the activating group.

From a mechanistic point of view, cross-coupling difluoromethylation reactions more often rely on the formation of a high-valent transition metal [MCF_2H] complex, which can undergo reductive elimination to facilitate carbon-carbon bond formation between an aromatic carbon and a CF_2H group. Over the last decade, chemists have developed a

series of strategies to access such [MCF_2H] complexes (**Scheme 1.5A**). Nucleophilic reagents such as $TMSCF_2H$ and [(SiPr)$AgCF_2H$] were found to readily undergo transmetallation to yield the [MCF_2H] complex (**Scheme 1.5B**). The carbon-bromine bond in bromodifluoromethane was shown to readily undergo radical addition to transition metals, such as nickel, to afford a [MCF_2H] complex with an increased oxidation state (**Scheme 1.5C**). Electrophilic difluoromethylation reagents such as difluoroiodomethane have been shown to undergo oxidative addition (**Scheme 1.5D**). More recently, the addition of difluorocarbene to metal centres has gained considerable interest. In this pathway, difluorocarbene first coordinates to the metal generating a [$M{=}CF_2$] complex and is subsequently protonated to give the desired [MCF_2H] complex (**Scheme 1.5E**).

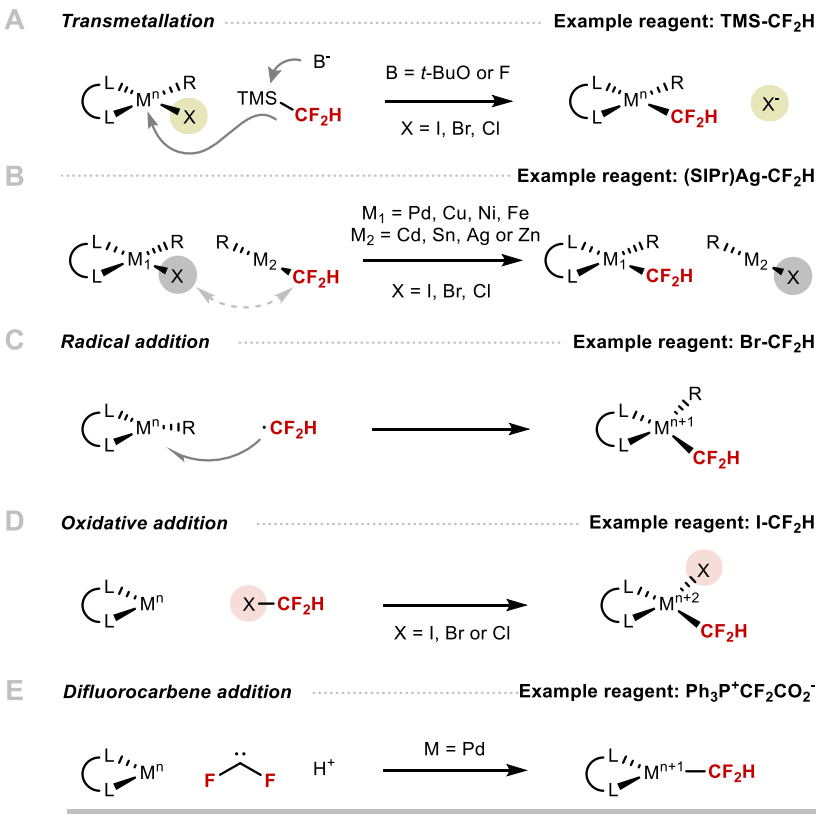

Scheme 1.5 Different strategies to access metal-CF_2H complexes.

1.3.1.2 C(Sp^2)-CF_2H Bond Formation: Copper-Mediated Difluoromethylation of Arenes and Heteroarenes

Prior to methods which allowed the direct transfer of a CF_2H group on to an aromatic scaffold facilitated by copper, seminal work from Amii and co-workers represents one of the most widely used transformation to access difluoromethylated aromatics (**Scheme 1.6**). [24]

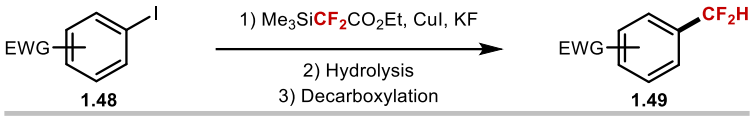

Scheme 1.6 Three-step copper mediated synthesis of difluoromethylated arenes.

In 2012, Hartwig and co-workers reported the first copper-mediated difluoromethylation of aryl iodides, using CuI, CsF and commercially available $TMSCF_2H$ as the source of CF_2H. Difluoromethylcopper complexes are known to be less stable than their trifluoromethylcopper analogues. Hartwig however, discovered that by using a large excess of $TMSCF_2H$ (5.0 equiv.), the equilibrium could be shifted from unstable $[CuCF_2H]$ to the more stable disubstituted cuprate intermediate $[Cu(CF_2H)_2]^-$. This allowed for the difluoromethylation of electron-neutral, electron-rich and sterically hindered aryl iodides to be achieved (**Scheme 1.7A**).[25] In tandem to this work, Prakash and co-workers illustrated that using $TMSCF_2H$-derived Bu_3SnCF_2H could be utilised as a CF_2H source to functionalise a variety of (hetero)aryl iodides. Complementary to Hartwig's method, electron deficient substrates including carbonyl containing substrate, 2-iodobenzaldehyde were readily difluoromethylated (**Scheme 1.7B**).[26] In 2014, Gooßen and co-workers reported that difluoromethylation of (hetero)arenediazonium salts using $TMSCF_2H$ and CuSCN as the copper source was feasible (**Scheme 1.7C**). These

pioneering efforts paved the way to catalytic methods and the use of different metals to allow the construction of C(sp^2)-CF_2H bonds.[27]

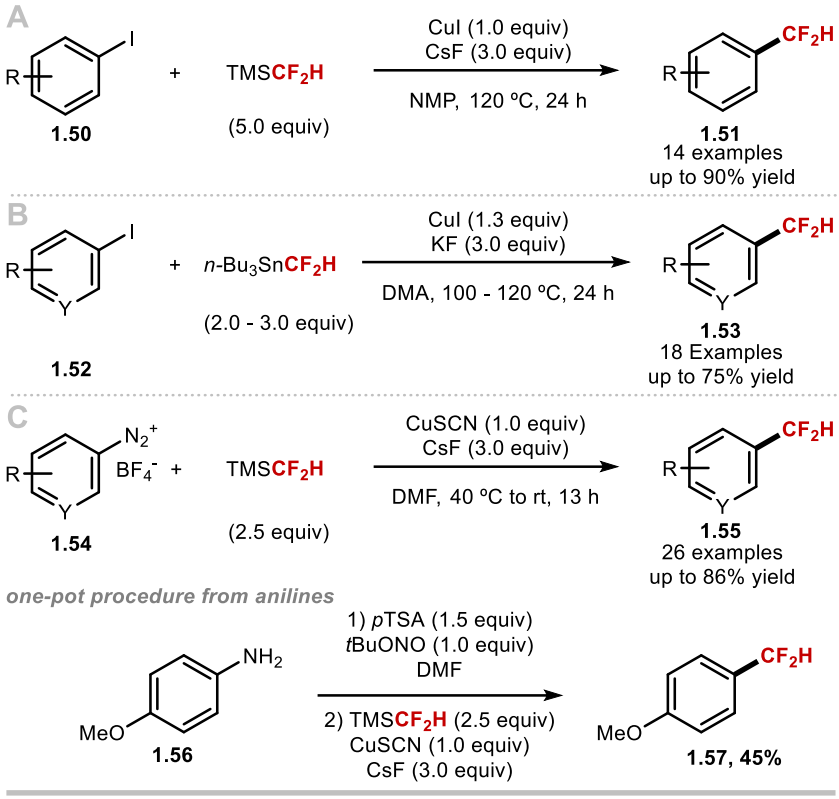

Scheme 1.7 Copper-mediated cross coupling methods for the synthesis aryl-CF_2H from aryl (pseudo)halides.

Within the realm of metal-mediated difluoromethylation processes, new mechanistic insights are essential to unlock reactivity of alternative precursors. The lack of electrophilic difluoromethylating reagents was a significant hurdle to the development of an electrophilic difluoromethylation process. Qing and co-workers however suggested that the cross-coupling of heteroarenes with [$CuCF_2H$] might be feasible under oxidative conditions. Indeed, when Qing and co-workers generated [$CuCF_2H$] *in situ*, a variety of deprotonated heterocycles readily coordinated to the Cu^I centre. Upon oxidation of this complex mediated by 9-10-phenanthrenequinone, reductive elimination could take place to afford

the difluoromethylated products. C-H bonds of oxazoles, thiazoles, imidazoles, 1,3,4-oxadiazoles, benzo[*d*]oxazoles, benzo[*d*]thiazoles, benzo[*b*]thiophenes, pyridines, thiophenes, and thiazolo[5,4-*c*]pyridines were readily difluoromethylated in good to excellent yields (**Scheme 1.8**).[28]

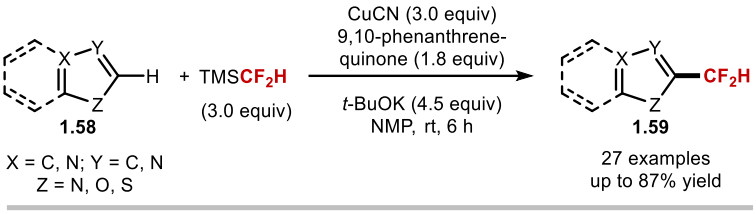

Scheme 1.8 Copper mediated oxidative C-H difluoromethylation.

1.3.1.3 C(sp^2)–CF_2H Bond Formation: Copper Catalysed Difluoromethylation of Aryl (pseudo)halide Precursors

The above-mentioned methods are copper-mediated difluoromethylation processes which use stoichiometric copper. Mikami and co-workers developed the copper catalysed difluoromethylation of aryl iodides, employing $(DMPU)_2Zn(CF_2H)_2$ as the CF_2H source (**Scheme 1.9A**). They found that CuI in the absence of a ligand readily underwent transmetallation to generate the stable $[Cu(CF_2H)_2]^-$ cuprate. Under their optimised conditions, a variety of electron-deficient aryl iodides, readily reacted to furnish the desired products in moderate to good yields.[29] More recently, in 2017, Sanford and co-workers disclosed the synthesis of the first isolable $[CuCF_2H]$ complex. Using 10 mol% of a *N*-heterocyclic carbene copper(I) pre-catalyst, and $TMSCF_2H$ as the CF_2H source, a variety of simple aryl iodides were difluoromethylated (**Scheme 1.9B**).[30]

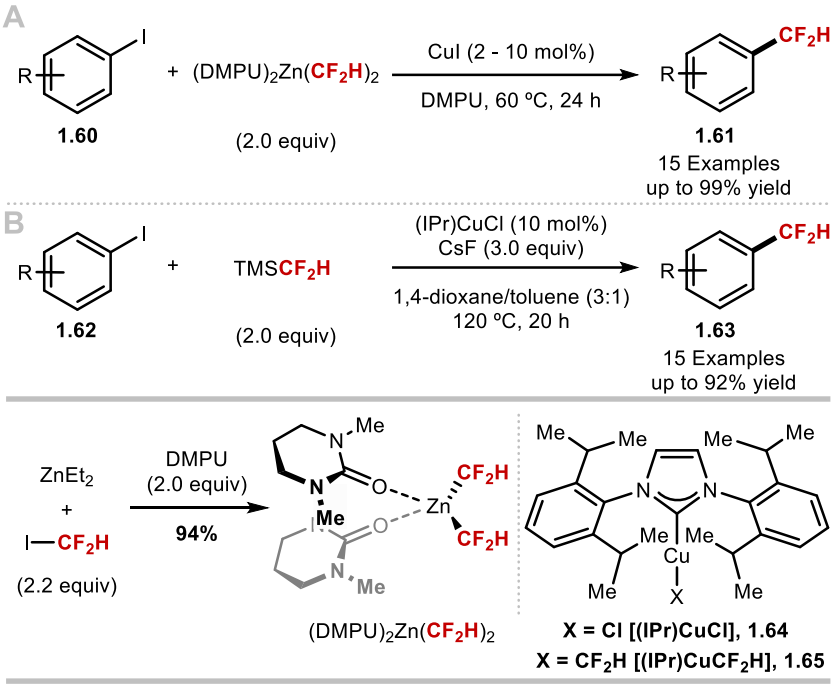

Scheme 1.9 Copper catalysed cross coupling methods for the synthesis aryl-CF_2H from (pseudo)halides.

1.3.1.4 C(sp^2)–CF_2H Bond Formation: Palladium Catalysed Difluoromethylation of Aryl (pseudo)halide Precursors

In 2014, Shen and co-workers disclosed the first palladium catalysed difluoromethylation of aryl bromides and iodides. This was accomplished with a dual catalytic system comprised of palladium and silver, and $TMSCF_2H$ as the CF_2H source. Extensive mechanistic work demonstrated that two successive transmetallation processes involving Si to Ag to Pd were faster than direct Si to Pd transmetallation, proving that the *in situ* formation of a [$AgCF_2H$] stabilised by an NHC ligand acted as a transmetallation shuttle.[31] Under their optimised conditions, numerous difluoromethylated bioactive molecules were prepared (**Scheme 1.10A**). Shen and co-workers later expanded the scope of this methodology to aryl chlorides and aryl triflates, although in this case a pre-formed [$AgCF_2H$] was necessary (**Scheme 1.10B**).[32] In 2017, the same group found that by substituting the palladium source to [$Pd(dba)_2$] (5.0 mol%)

and the ligand to DPEPhos (10 mol%) a wide variety heterocyclic halides could be difluoromethylated (**Scheme 1.10C**); this methodology is highly complementary to radical methods described in **Section 1.3.1.7** where the CF_2H radical reacts at the innately most reactive C-H bonds.[33] Mikami and co-workers disclosed a palladium-catalysed Negishi coupling where aryl halides were readily difluoromethylated, employing an organo zinc reagent ([$(TMEDA)_2Zn(CF_2H)$]. The authors illustrated that transmetallation of the organozinc reagent to the palladium centre readily occurred without the need of an external activator. Electron-deficient and electron-rich (hetero)aryl halides were suitable substrates for this transformation (**Scheme 1.10D**).[34]

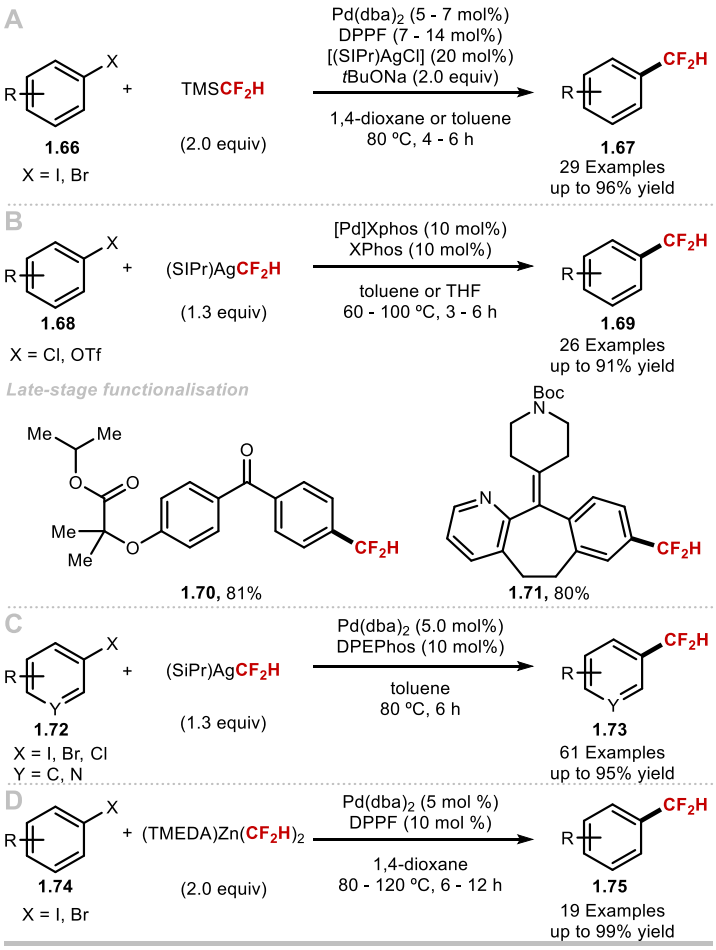

Scheme 1.10 Palladium catalysed cross coupling methods for the synthesis aryl-CF_2H from (pseudo)halides.

1.3.1.5 C(sp^2)-CF_2H Bond Formation: Palladium Catalysed Difluoromethylation of Aryl Boronic Acid Precursors

Aryl boron reagents are commonly used synthetic precursors in organic chemistry due to their versatility as intermediates in the synthesis of bioactive molecules. Their ease of preparation, as well as their commercial availability make them attractive precursors for difluoromethylation.[35] Zhang and co-workers developed a protocol which employs a commercially available palladium catalyst and ethyl bromodifluoroacetate as the CF_2H source (**Scheme 1.11A**).[36] Preliminary mechanistic experiments in this report suggest a difluorocarbene intermediate is formed during this reaction. These mechanistic insights led the Xiao group to probe the existence of a palladium difluorocarbene catalytic intermediate and prove it could successfully act as a difluorocarbene transfer reagent, to difluoromethylate aryl boronic acids (**Scheme 1.11B**).[37] In 2019, Zhang and Houk developed a controllable palladium catalysed difluorocarbene transfer reaction which employs aryl boronic acids and $BrCF_2P(O)(OEt)_2$ as difluorocarbene source. They illustrated that their difluorocarbene transfer enables access to four distinct types of products: difluoromethylated and tetrafluoroethylated arenes and their corresponding fluoroalkylated ketones through alterations of the reaction conditions (**Scheme 1.11C**).[38]

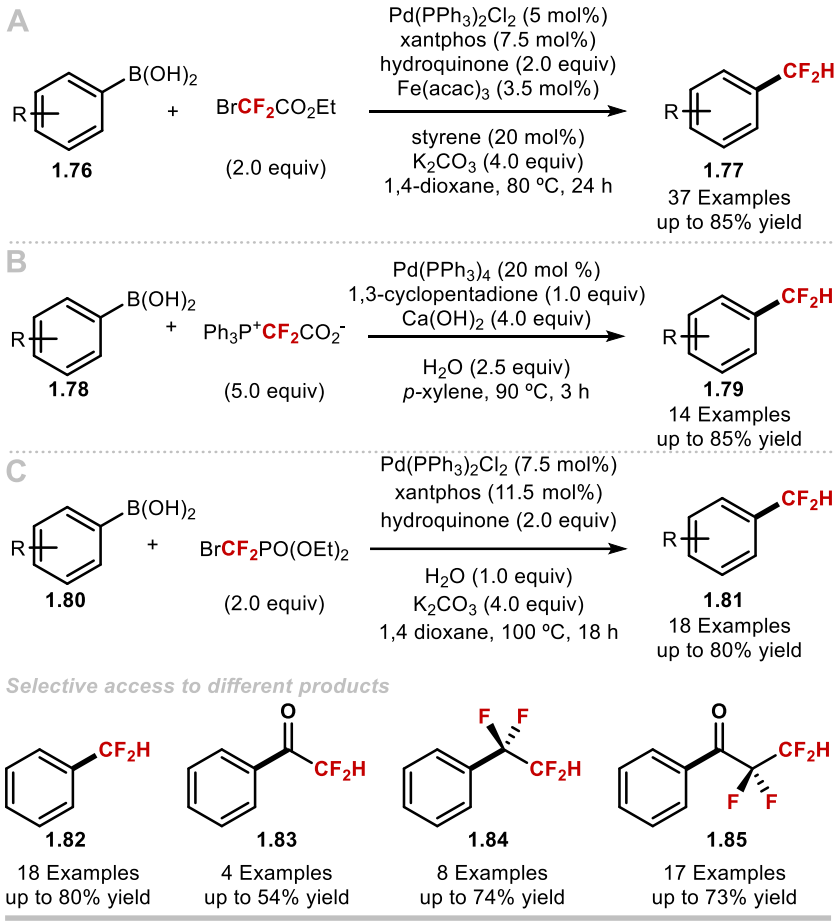

Scheme 1.11 Palladium catalysed cross coupling methods for the synthesis aryl-CF_2H from aryl boron acids.

1.3.1.6 C(sp^2)–CF_2H Bond Formation: Iron Catalysed Difluoromethylation

The desire for a cross-coupling method using a more sustainable and cost-effective catalyst derived from earth-crust abundant iron, encouraged Hu and co-workers to develop a mild and broadly applicable cross-coupling methodology for the difluoromethylation of aryl zinc reagents using commercially available 2-[((difluoromethyl)sulfonyl)]pyridine as the difluoromethylating reagent. Their reaction proceeds under mild conditions and gives access to electron-rich and electron-deficient difluoromethylarenes (**Scheme 1.12**).[39]

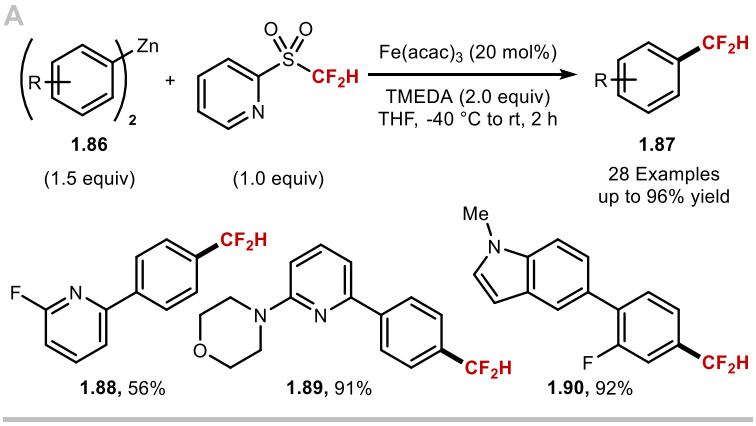

Scheme 1.12 Iron catalysed cross coupling methods for the synthesis aryl-CF_2H from aryl zinc reagents.

1.3.1.7 C(sp^2)-CF_2H Bond Formation Mediated by a Radical Initiator

The field of radical difluoromethylation has expanded rapidly over the last few years. Several reagents to generate the CF_2H radical have been developed. These reagents are activated through a variety of processes such as single electron oxidation (i.e. for $Zn(SO_2CF_2H)_2$, **Scheme 1.13A**), single electron reduction (i.e. for $ClSO_2CF_2H$, **Scheme 1.13B**), homolytic cleavage of weak bonds under UV light (i.e. for $[Ph_3PCF_2H][Br]$, **Scheme 1.13C**), or radical abstraction of a halide (i.e. for $BrCF_2H$, **Scheme 1.13D**). The stability of fluoroalkylated radicals changes as a function of the degree of fluorine substitution (CF_3>CF_2H>CH_2F, **Scheme 1.13E**).[40] Furthermore, the geometry of these fluoroalkyl radicals becomes progressively more distorted toward a tetrahedral geometry with higher degrees of fluorine substitution. Combined with less prominent electron withdrawing effects (two fluorine versus three), the CF_2H radical is considered to be nucleophilic in contrast to the electrophilic nature of the CF_3 radical.[41] This feature leads to prominent differences in reactivity and selectivity between CF_2H and CF_3 radicals in Minisci-type chemistry.

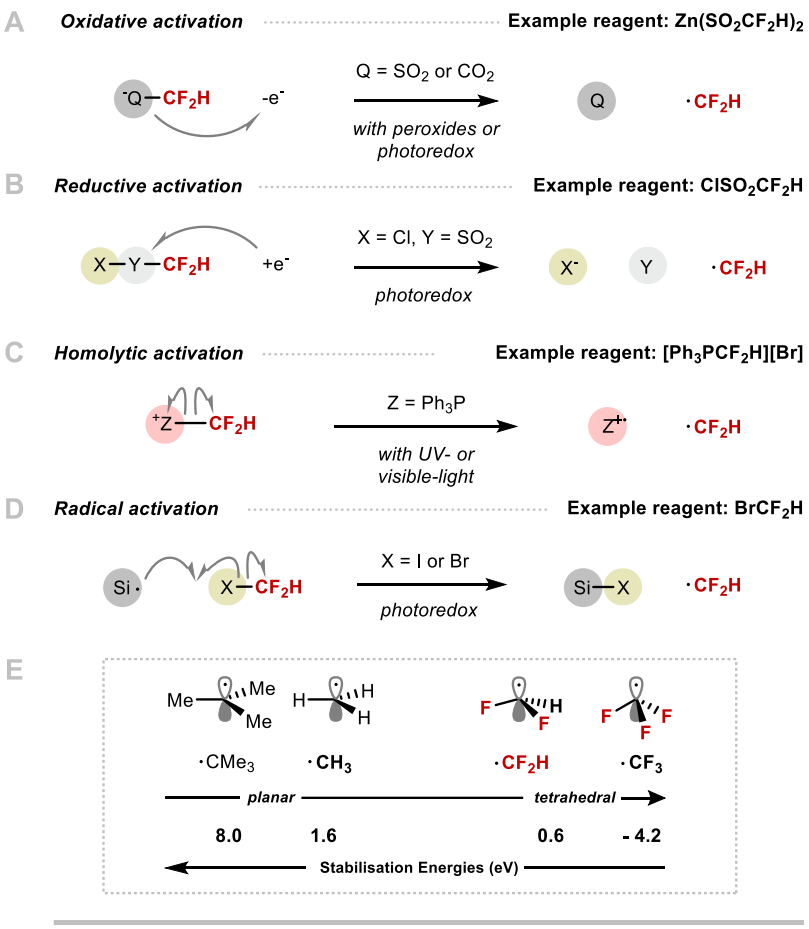

Scheme 1.13 Relative stability and structure of the CF_2H radical.

Baran and co-workers pioneered the development of $[Zn(SO_2CF_2H)_2]$ (DFMS), the first reagent which allowed for direct C–H difluoromethylation of heteroarenes. It was found that DFMS could generate CF_2H radicals readily under peroxide activation (**Scheme 1.14A**). A wide array of heterocycles was readily difluoromethylated under acidic biphasic conditions at room temperature.[41] Nielsen and co-workers developed an alternative procedure for the direct C–H difluoromethylation of heteroaromatic compounds, through the generation of CF_2H radicals from cheap and commercially available difluoroacetic acid under persulfate activation (**Scheme 1.14B**).[42] More recently, MacMillan and co-workers employed metallaphotoredox catalysis, merging photoredox catalysis and nickel catalysis to facilitate the difluoromethylation of a broad

range of heteroaromatic halides. They illustrated that by employing silyl radical activation to generate CF_2H radicals directly from CF_2BrH under visible light activation. A series of heteroaryl halides (18 examples, up to 84% yield) were readily difluoromethylated (**Scheme 1.14C**). This method allowed the successful difluoromethylation of 1-(3-bromo-1*H*-pyrazol-1-yl)ethan-1-one, which is significant considering the presence of 3-(difluoromethyl)-1-methyl-1H-pyrazole in targets of interest to the agrochemical industry (see **Figure 1.5**).[43] Other methods which employ alternative modes of activation such as UV light or single electron transfer (SET) to generate CF_2H radicals, are summarised in **Scheme 1.14D** and **Scheme 1.14E** respectively.[44,45]

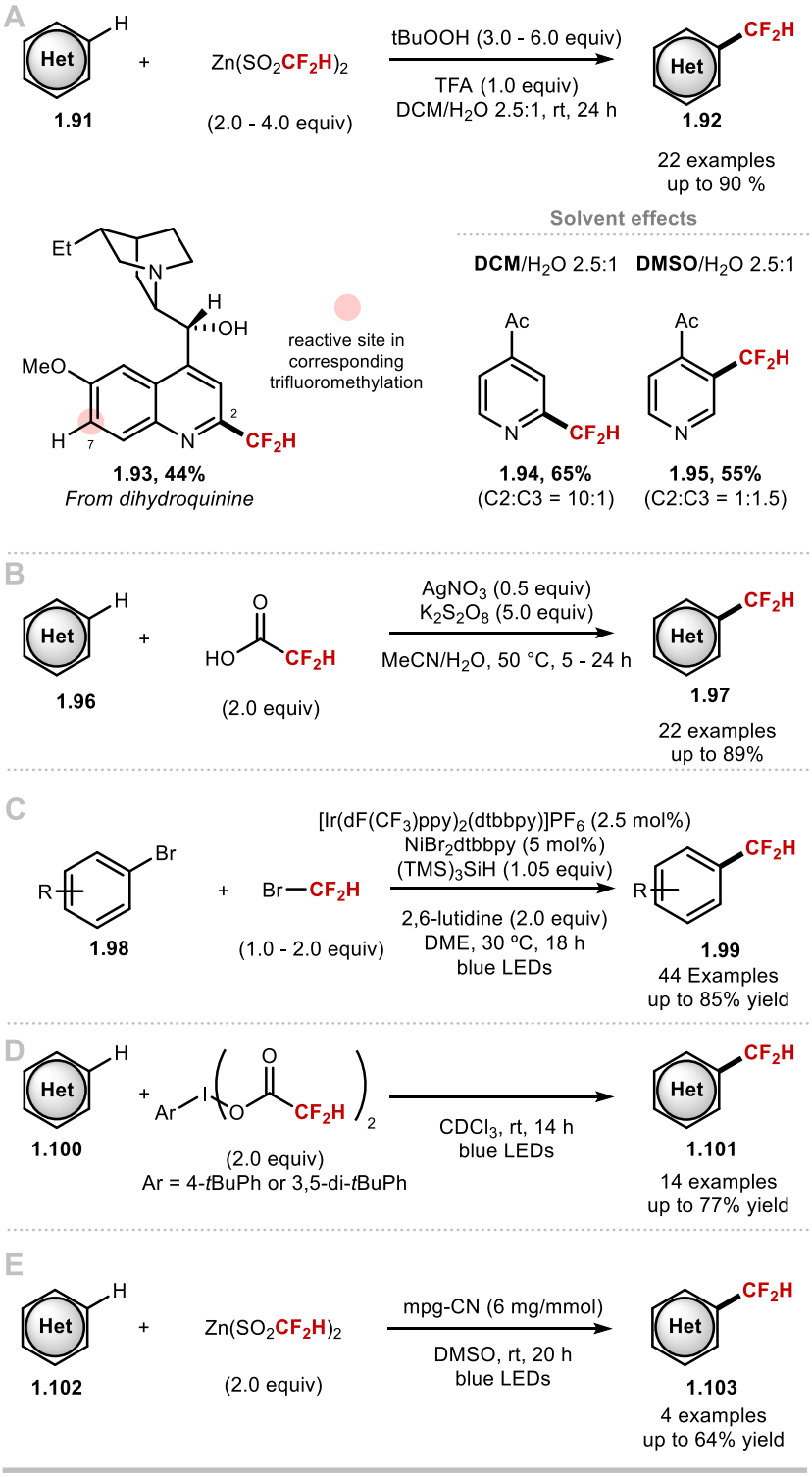

Scheme 1.14 Synthesis of heteroaryl-CF_2H *via* radical initiation, mpgCN = mesoporous graphitic carbon nitride.

1.4 State-of-The Art in X-CF_2H Bond Formation (Where X = O, N and S)

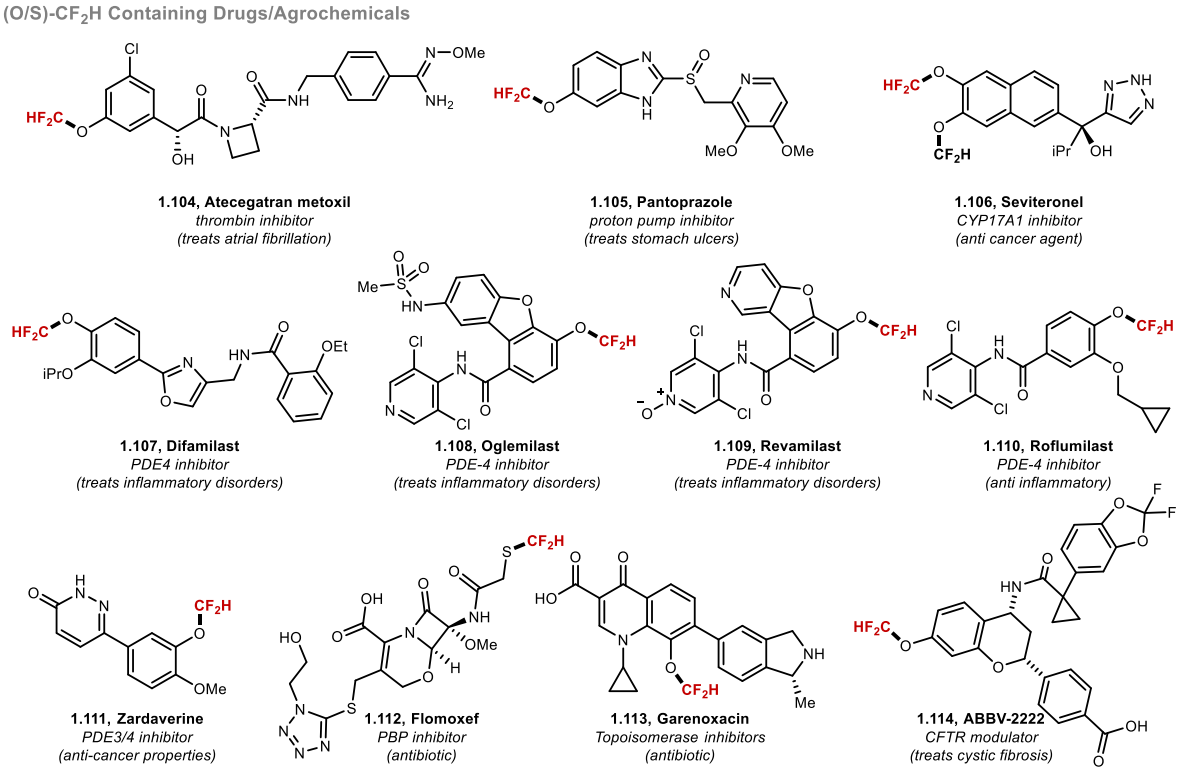

Figure 1.6 Examples of drugs, herbicides, fungicides, and agrochemicals which contain a (hetero)arene $C(sp^2)$-OCF_2H bond or $C(sp^3)$-SCF_2H bond.

The majority of reported methodologies which construct a X–CF_2H bond, where X is either oxygen, nitrogen or sulfur employ a difluorocarbene reagent which is activated in one of three modes: alkaline, nucleophilic, or thermal activation. Other methods to access this motif involve radical conditions, such as decarboxylative fluorination, which are well described in published review articles.[46] The conditions and type of reagent govern how difluorocarbene is generated. For the difluoromethylation of heteroatoms (-SH, -OH and -NH) the formation of difluorocarbene is usually initiated by a base (**Scheme 1.15A**), which is also used to activate the pro-nucleophile. When difluorocarbene is generated *via* nucleophilic activation, aliphatic alcohols can be selectively

difluoromethylated in preference to phenols (**Scheme 1.15B**). In the case of difluorocarbene reaction with alkenes or alkynes, the fast release of difluorocarbene and its rapid reaction with base can inhibit [2 + 1] cycloadditions leading to the difluorocyclopropanated products, respectively. Thermal activation is preferred to enable these cycloadditions. (**Scheme 1.15C**).[47]

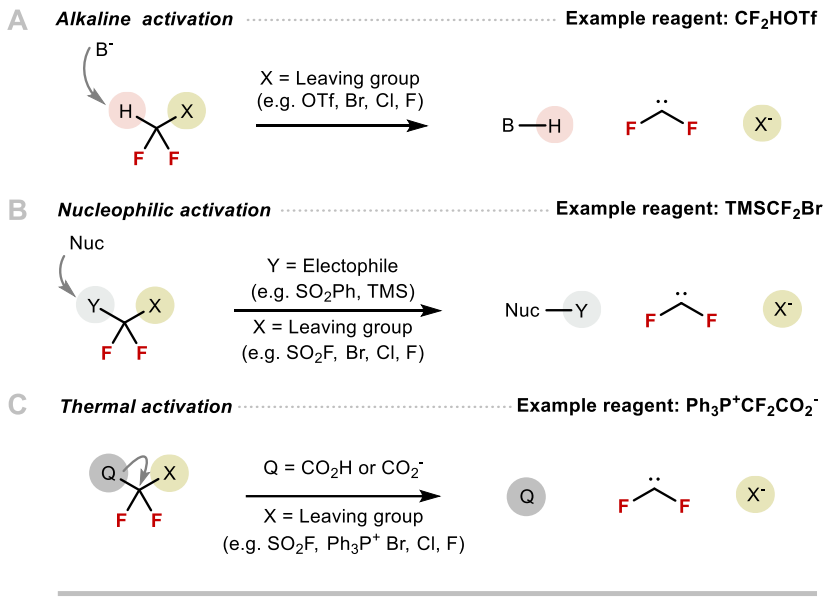

Scheme 1.15 Different modes of activation to generate difluorocarbene.

This section will mainly focus on methods which employ a difluorocarbene reagent and show broad scope (i.e. react with different classes of nucleophiles).

1.4.1 Difluoromethylation of Phenols/Thiophenols Under Difluorocarbene Conditions

In 2007, Hu and co-workers disclosed the synthesis of a non-ozone depleting difluorocarbene reagent in the form of chlorodifluoromethylphenylsulfone. They illustrated the application of this reagent for the difluoromethylation of a series of *N*-heterocycles as well as phenols with a variety of ring electronics under aqueous basic conditions (**Scheme 1.16A**).[48] In 2011, the same authors reported that aryl substituents

for the DFC reagent with positive Hammett σ_{para} values such as *p*-chlorophenyl chlorodifluoromethyl sulfone and *p*-nitrophenyl chlorodifluoromethyl sulfone were more easily activated under aqueous basic conditions (**Scheme 1.16C**).[49]

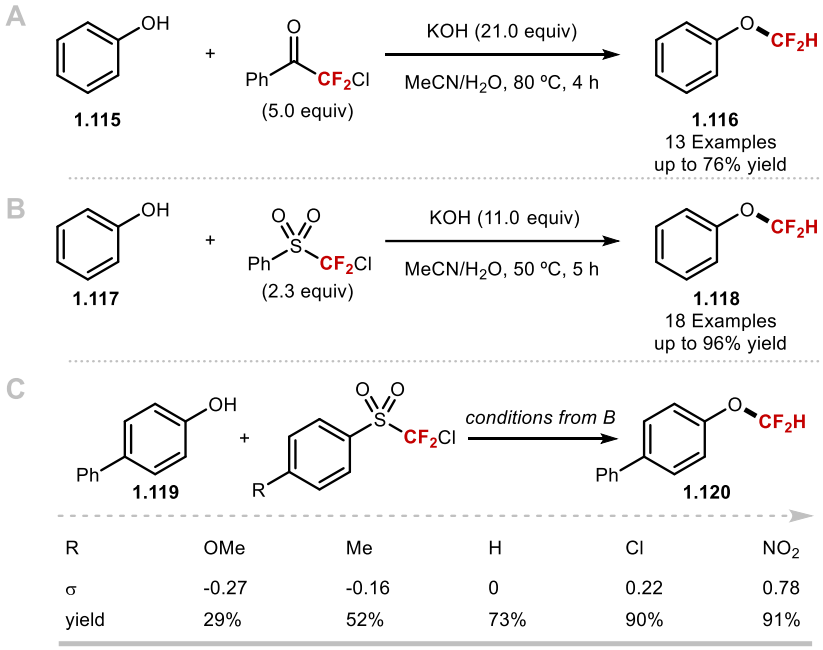

Scheme 1.16 ((Chlorodifluoromethyl)sulfonyl)arenes as difluorocarbene reagents for phenols.

In 2009, Zafrani and Segall described for the first time the difluorocarbene reactivity of $BrCF_2P(O)(OEt)_2$ on both phenols (9 examples, up to 96% yield) and thiophenols (6 examples, up to 98% yield) (**Scheme 1.17A**).[50] Influenced by this seminal report, Wu and Zou proposed that a general method to access $ArOCF_2D$ would be a valuable addition to methods available for medicinal chemists. Substitution of hydrogen for deuterium may affect the pharmacokinetics, pharmacodynamics and overall metabolic stability of a drug molecule. The authors found that their methodology was broad in scope, tolerating electron-rich, electron-deficient and heterocyclic substrates (22 examples, up to 93% yield), as well as showing excellent deuterium incorporation (>98% D

incorporation) (**Scheme 1.17B**).[51] The high %D incorporation observed with readily available deuterated solvents is an attractive feature of difluorocarbene chemistry, because it circumvents the need for pre-deuterated starting materials, which may not be trivial to synthesise.

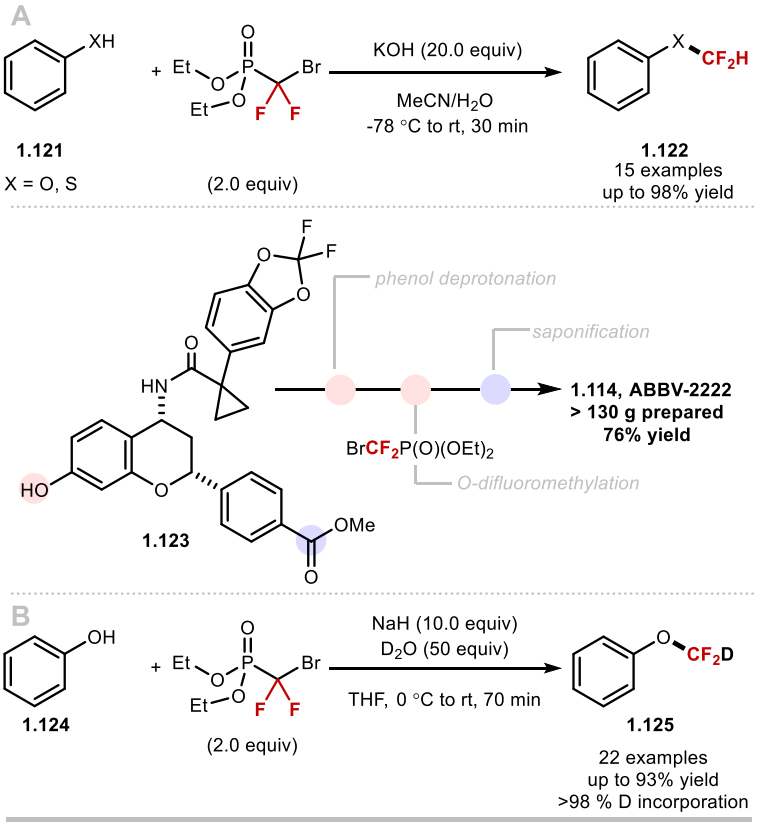

Scheme 1.17 Diethyl (bromodifluoromethyl)phosphonate as a difluorocarbene reagent to access $ArOCF_2H$ or $ArOCF_2D$.

In 2013, the Hartwig group disclosed the synthesis and application of difluoromethyl triflate. This now commercially available, non-ozone depleting difluorocarbene reagent is able to difluoromethylate phenols and thiophenols in short reaction times at ambient conditions. The fast reaction times allow this reagent to be used in one-pot sequences such as those which generate phenols *in situ* from readily available aryl boronic acids (**Scheme 1.18**).[52]

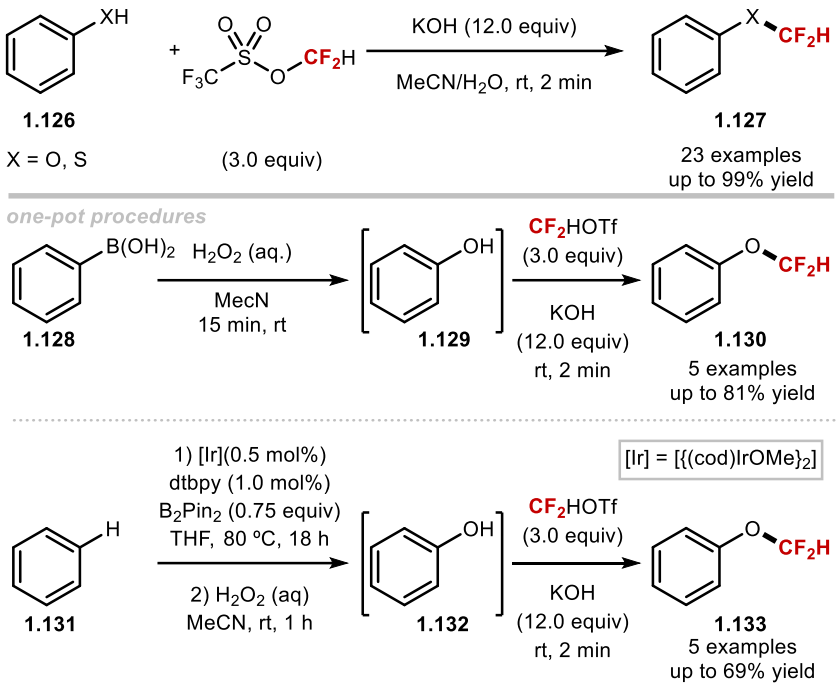

Scheme 1.18 Difluoromethyl triflate as a difluorocarbene reagent to access $ArOCF_2H$.

In 2017, Fu and co-workers generated difluorocarbene for the first time *via* photoredox catalysis. They found that the cesium salt of bromodifluoroacetic acid ($BrCF_2CO_2Cs$) was able to quench the excited state of the photocatalyst (PC*), the resulting oxidised Ir(IV) catalyst was then returned to its native oxidation state through SET from the carboxylate anion, releasing difluorocarbene in the process. The difluorocarbene reacted with a selection of phenolates and thiophenolates to yield difluoromethylated products in excellent yields (**Scheme 1.19**).[53]

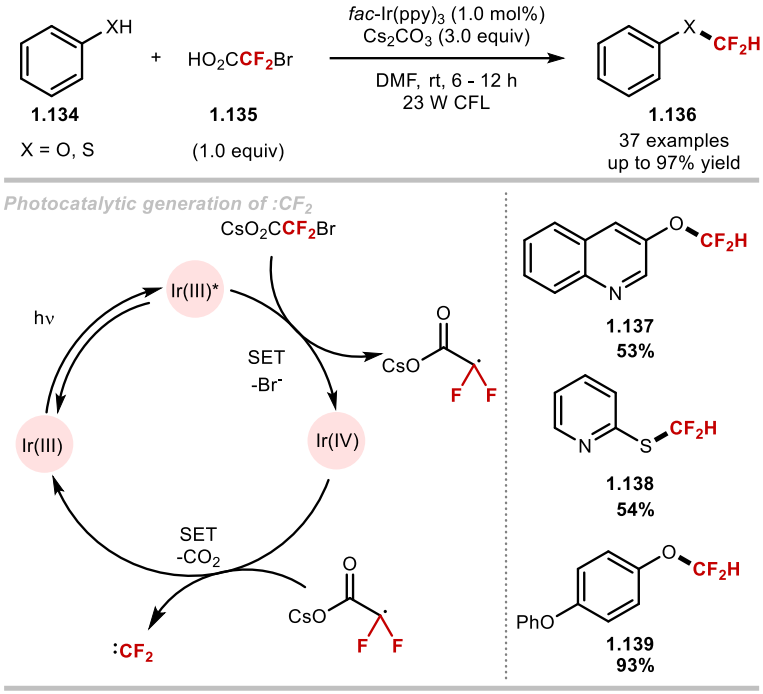

Scheme 1.19 Difluorocarbene generation under photoredox catalysis for the difluoromethylation of (thio)phenols.

1.4.2 Difluoromethylation of Aliphatic Alcohols/Thiols Under Difluorocarbene Conditions

Due to differences in pKa the difluoromethylation of aliphatic alcohols/thiols often does not lie within the same realm as those used for the difluoromethylation of (thio)phenols. Hine and Tababe and later Mizukado illustrated that the difluoromethylation of aliphatic alcohols was possible under basic activation of $ClCF_2H$.[54,55] Similarly, Burton and Hu also illustrated that basic activation of $BrCF_2P(O)OEt_2$ and $TMSCF_2Br$ allowed aliphatic alcohols to be difluoromethylated albeit in low conversions.[56] In addition to these reports, a variety of early reports in the literature by Mitsch, Robertson, Miethchen and Mizukado have shown the successful difluoromethylation of aliphatic alcohols

under neutral conditions. Despite these advances, these methods lack generality in scope and generally exhibit poor reactivity (**Scheme 1.20**).[57]

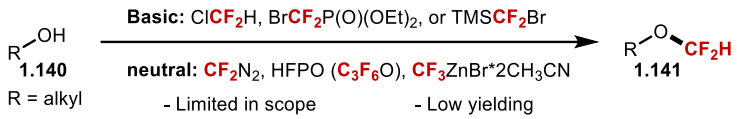

Scheme 1.20 Difluoromethylation of aliphatic alcohols under basic and neutral difluorocarbene conditions.

In 2016, Shen and co-workers disclosed that the difluoromethylation of aliphatic alcohols could be accomplished by difluoromethyl-(4-nitrophenyl)-*bis*-(carbomethoxy)-methylide sulfoniumylide. With this reagent in conjunction with $LiBF_4$ as the activator, a series of alkyl difluoromethyl ethers could be accessed in good yields (**Scheme 1.21A**).[58] In the same year, Mykhailiuk and co-workers reported the use of $FSO_2CF_2CO_2H$ as a difluorocarbene surrogate for the synthesis of difluoromethyl ethers from polyfunctional alcohols (**Scheme 1.21B**). This methodology astutely employs copper catalysis to mediate the transfer of the reactive difluorocarbene. This methodology is only applicable to primary and secondary alcohols with much lower yields obtained for tertiary alcohols.[59] In 2017, the Hu group disclosed a mild and general *O*-difluoromethylation method, using $TMSCF_2Br$ as a difluorocarbene source (**Scheme 1.21C**). Their method uniquely allows tertiary alkyl difluoromethylethers to be synthesized in very good yields albeit excess amount of $TMSCF_2Br$ reagent was required to obtain high yields. The authors found that the higher nucleophilic character of aliphatic alcohols compared to phenols, aliphatic alcohols can be difluoromethylated under mild acidic conditions, while phenols require basic conditions and

difluoromethylation generally proceeds *via* phenolates. In their report, Hu and co-workers illustrate that chemoselective difluoromethylation can be achieved through variation of the reaction conditions (**Scheme 21C**).[60]

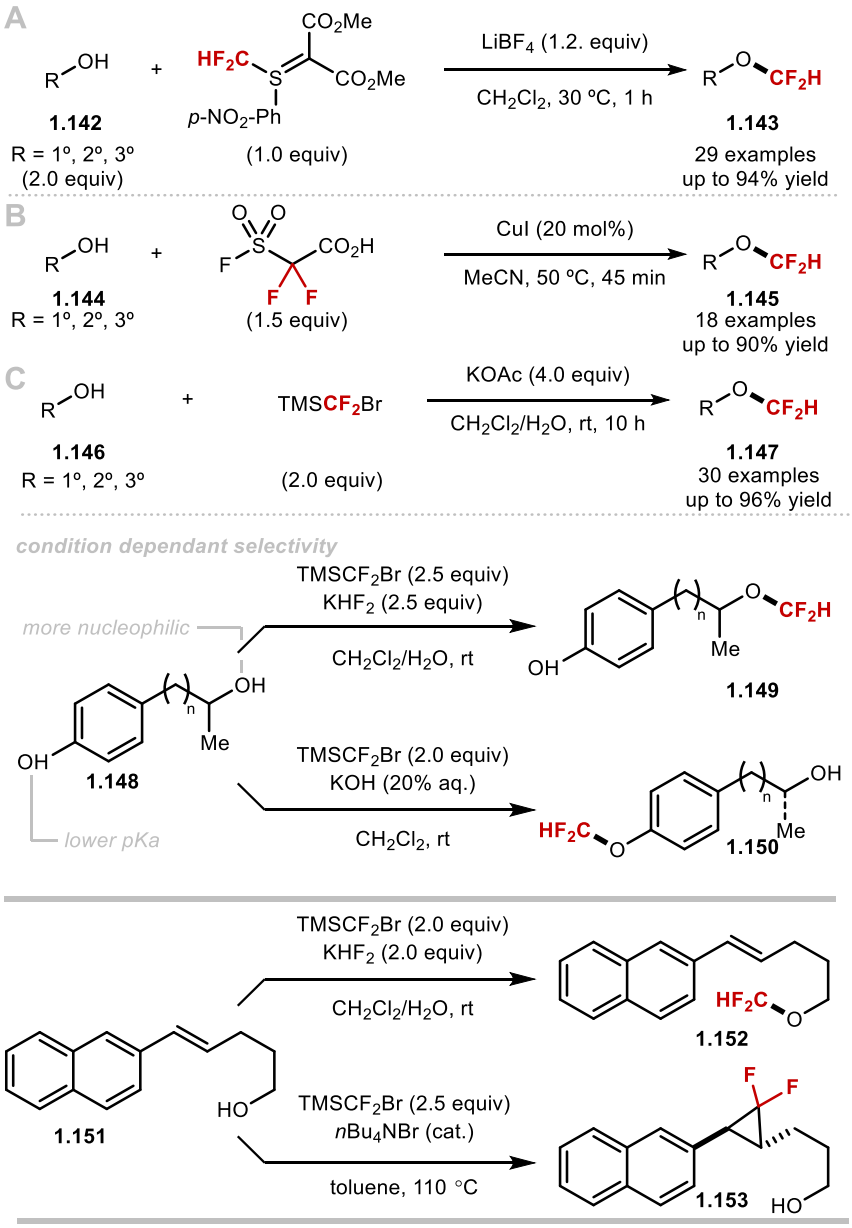

Scheme 1.21 Difluoromethylation of aliphatic alcohols.

Zhang and co-workers expanded upon the seminal work of Shen in 2019, when they published the facile difluoromethylation of aliphatic alcohols using S-(difluoro-methyl)sulfonium salt. The authors found that their optimum reaction

conditions were: 5.0 equivalents of NaOAc as the base and 20 mol% of Bu_4NBF_4 as an initiator, in a solvent mixture of CH_2Br_2 and H_2O at room temperature. They found that similarly to the seminal reports of Hu and Shen, a wide array of functional groups including ester, nitro, methoxy, and boronic ester were tolerated under their optimal reaction conditions. Notably, aliphatic OH site reacts preferentially in the presence of functional groups such as phenol OH, carbamate, alkyne, alkene, or N-heterocycle (**Scheme 1.22A**). When omitting the initiator (Bu_4NBF_4), changing the counterion of their reagent from PF_6 to BF_4, altering the base from NaOAc to KOH (2.4 equiv.) and the solvent to MeCN, aliphatic thiols were successfully subjected to difluoromethylation (4 examples, up to 57% yield) (**Scheme 1.22B**).[61]

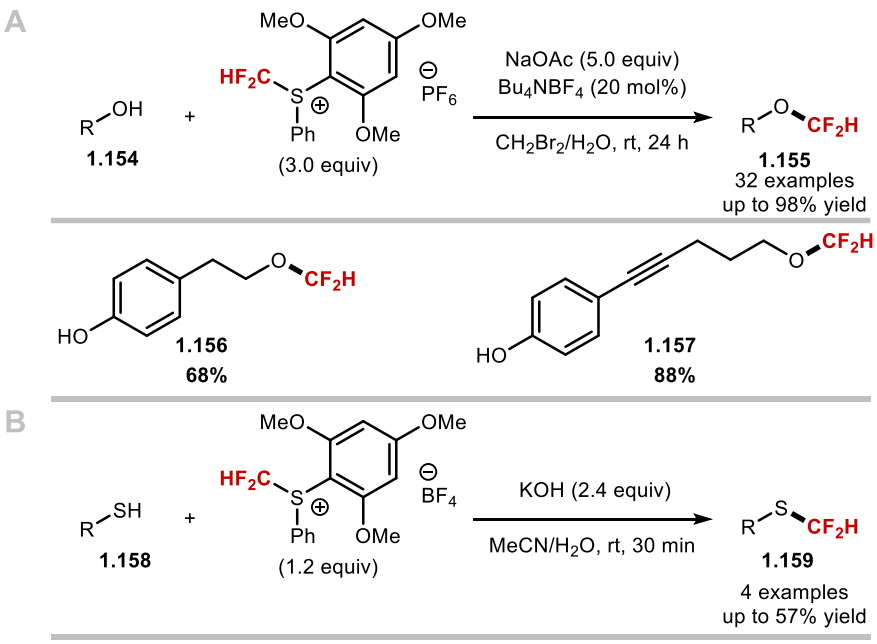

Scheme 1.22 Difluoromethylation of aliphatic alcohols and thiols.

1.4.3 *N*-Difluoromethylation

N-heteroaromatic scaffolds such as imidazoles are prevalent structural motifs in biological systems.[62] Analogous to methods which allow insertion of the CF_2H group in O-H and S-H bonds, methods which allow for the selective insertion of a CF_2H group into a N-H bond have a plethora of applications in medicinal chemistry and agrochemistry. Specifically, *N*-difluoromethylated pyrazoles have been investigated in structure activity relationship (SAR) studies as calpain inhibitors (**Figure 1.7**).[63] Recently, Andrés et al achieved increased receptor residence times for CRTh2 antagonists. The authors discovered that *N*-difluoromethylated 2-pyridones have a significantly higher dissociation half-life than their methylated or naked pyridines counterpart.[64]

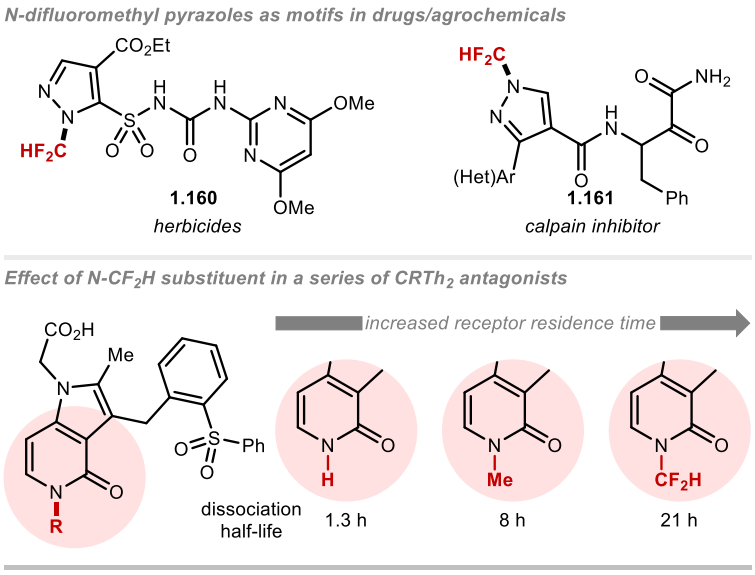

Figure 1.7 Application of N-CF_2H compounds.

Unlike molecules bearing the OCF_2H or SCF_2H motifs which are generally either directly bound to an aliphatic (sp^3) carbon or an aromatic (sp^2) carbon, the

electronic environment of the NCF_2H motif is highly dependent on the nature of the *N*-heterocycle (**Scheme 1.23**).[65]

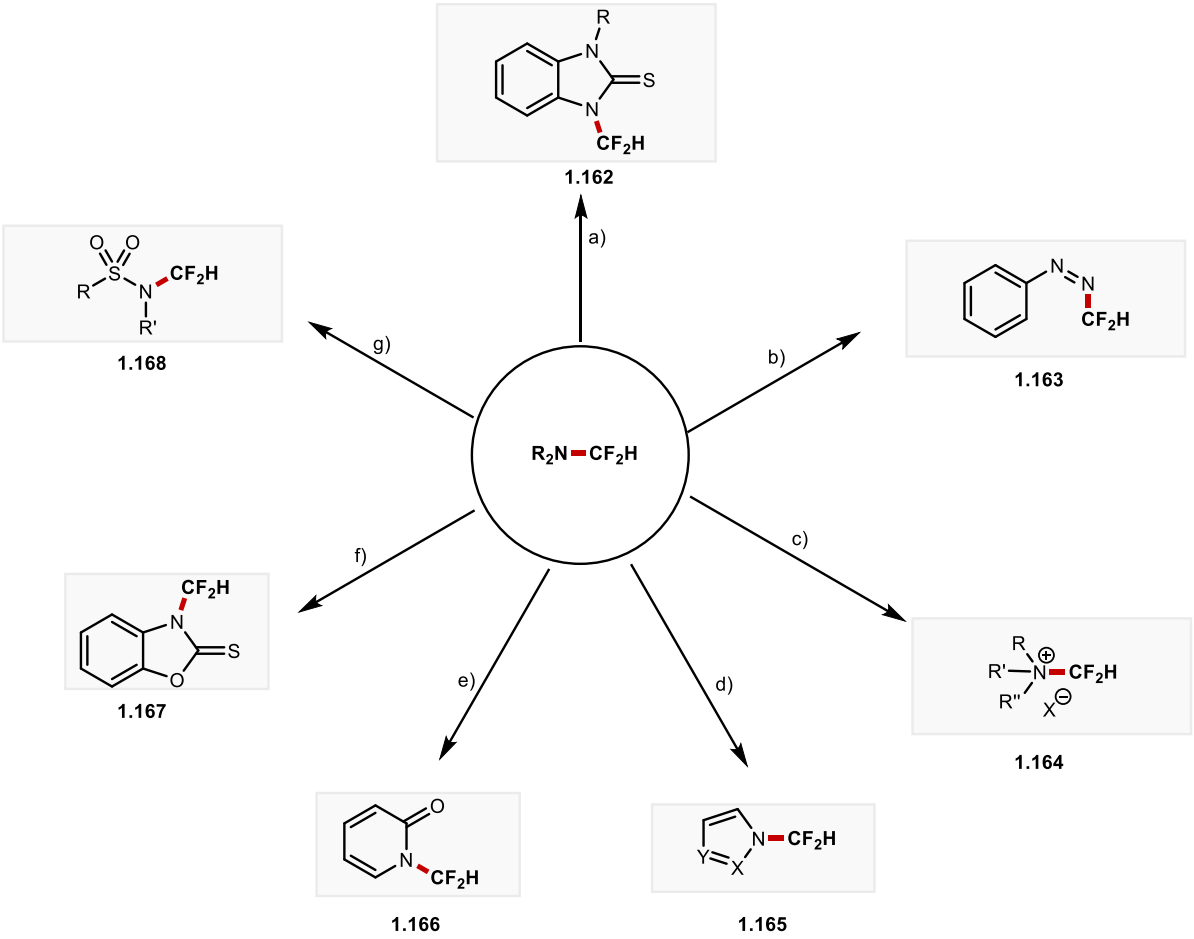

Scheme 1.23 NCF_2H chemical space.

While late-stage difluoromethylation is a growing field of interest within organic chemistry, methods which can incorporate the CF_2H group in complex drug manifolds are lacking. In **Chapters II, IV** and **V** we will show the development of new late-stage strategies to incorporate the CF_2H group.

1.5 References

1 (a) J. Wencel-Delord and F. Glorius, *Nat. Chem.,* 2013, **5**, 369; (b) M. Abid Masood, E. Farrant, I. Morao, M. Bazin, M. Perez, M. E. Bunnage, S.-A. Fancy and T. Peakman, *Bioorg. Med. Chem. Lett.,* 2012, **22**, 723.

2 A. W. Dombrowski, N. J. Gesmundo, A. L. Aguirre, K. A. Sarris, J. M. Young, A. R. Bogdan, M. C. Martin, S. Gedeon and Y. Wang, *ACS Med. Chem. Lett.,* 2020, **11**, 597.

3 N. J. Taylor, E. Emer, S. Preshlock, M. Schedler, M. Tredwell, S. Verhoog, J. Mercier, C. Genicot and V. Gouverneur, *J. Am. Chem. Soc.,* 2017, **139**, 8267.

4 H. Dai, A. F. Stepan, M. S. Plummer, Y. Zhang and J. Yu, *J. Am. Chem. Soc.,* 2011, **133**, 7222.

5 J. B. I. Sap, N. J. Straathof, T. Knauber, C. F. Meyer, M. Médebielle, L. Buglioni, C. Genicot, A. A. Trabanco, T. Noël and C. W. am Ende, and V. Gouverneur, *J. Am. Chem. Soc.,* 2020, **142**, 9181.

6 (a) J. Wu, R. M. Bär, L. Guo, A. Noble and V. K. Aggarwal, *Angew. Chem. Int. Ed.,* 2019, **58**, 18830; (b) E. B. Corcoran, M. T. Pirnot, S. Lin, S. D. Dreher, D. A. DiRocco, I. W. Davies, S. L. Buchwald and D. W. MacMillan, *Science,* 2016, **353**, 279; (c) Y. Liang, X. Zhang and D. W. MacMillan, *Nature,* 2018, **559**, 83.

7 M. S. Chen and M. C. White, *Science,* 2007, **318**, 783.

8 J. B. I. Sap, T. C. Wilson, C. W. Kee, N. J. Straathof, C. W. am Ende, P. Mukherjee, L. Zhang, C. Genicot and V. Gouverneur, *Chem. Sci.* 2019*,* **10**, 3237.

9 (a) Drug Bank. Available online: https://http://www.drugbank.ca (accessed on 2 May 2020); (b) D. Rageot, T. Bohnacker, A. Melone, J. B. Langlois, C. Borsari, P

.Hillmann, A. M. Sele, F. Beaufils, M. Zvelebil, P. Hebeisen, W. Löscher, J. Burke, D. Fabbro and M. P. Wymann*, J. Med. Chem.,* 2018, **61**, 10084.

10 C. D. Sessler, M. Rahm, S. Becker, J. M. Goldberg, F. Wang and S. J. Lippard, *J. Am. Chem. Soc.,* 2017, **139**, 9325.

11 M. H. Abraham, R. J. Abraham, J. Byrne and L. Griffiths, *J. Org. Chem.,* 2006, **71**, 3389–3394.

12 Y. Zafrani, G. Sod-Moriah, D. Yeffet, A. Berliner, D. Amir, D. Marciano, S. Elias, S. Katalan, N. Ashkenazi, M. Madmon, E. Gershonov and S. Saphier, *J. Med. Chem.*, 2019, **62**, 5628–5637.

13 L. Xing, D. C. Blakemore, A. Narayanan, R. Unwalla, F. Lovering, R. A. Denny, H. Zhou and M. E. Bunnage, *ChemMedChem,* 2015, **10**, 715.

14 P. Villard, *C. R. Acad. Sci.*, 1890, **111**, 303.

15 F. Swarts, *Bull. Acad. my. Belg.,* 1920, **78**, 389

16 A. McCulloch, P. M. Midgley and A. A. Lindley, *Atmos*., 2006, **40**, 936–942.

17 (a) W. J. Middleton, *J. Org. Chem.,* 1975, **40**, 574; (b) G. S. Lal, G. P. Pez, R. J. Pesaresi, F. M. Prozonic and H. Cheng, *J. Org.Chem.,* 1999, **64**, 7048; (c) T. Umemoto, R. P. Singh, Y. Xu, N. Saito, *J. Am. Chem. Soc.* 2010, **132**, 18199.

18 R. Szpera, N. Kovalenko, K. Natarajan, N. Paillard and B. Linclau, *Beilstein J. Org. Chem.,*2017, **13**, 2883.

19 F. Beaulieu, L-P. Beauregard, G. Courschesne, M. Couturier*,* F. LaFlamme and A. L'Heureux, *Org. Lett.,* 2009, **11**, 5050.

20 G. W. Rewcastle, S. A. Gamage, J. U. Flanagan, R. Frederick, W. A. Denny, B. C. Baguley, P. Kestell, R. Singh, J. D. Kendall, E. S. Marshall, C. L. Lill, W-J. Lee, S.

Kolekar, C. M. Buchanan, S. M. F. Jamieson and P. R. Shepherd, *J. Med. Chem.,* 2011, **54**, 7105.

21 F. Beaulieu, L. Beauregard, G. Courchesne, M. Couturier, F. LaFlamme and A. L'Heureux, *Org. Lett.,* 2009, **11**, 5050.

22 H. Huang, C. Yu, X. Li, Y. Zhang, Y. Zhang, X. Chen, P. S. Mariano, H. Xie and W. Wang, *Angew. Chem. Int. Ed,* 2017, **56**, 8201.

23 J. Rong, C. Ni and J. Hu, *Asian J. Org. Chem.,* 2017, **6**, 139.

24 K. Fujikawa, Y. Fujioka, A.Kobayashi and H. Amii, *Org. Lett.*, 2011, **13**, 5560.

25 P. S. Fier, J. F. Hartwig, *J. Am. Chem. Soc.,* 2012, **134**, 5524.

26 G. K. S. Prakash, S. K. Ganesh, J. P. Jones, A. Kulkarni, K. Masood, J. K. Swabeck, G. A. Olah, *Angew. Chem. Int. Ed.,* 2012, **51**, 12090.

27 C. Matheis, K. Jouvin, L. J. Gooßen, *Org. Lett.,* 2014, **16**, 5984.

28 S-Q. Zhu, Y-L. Liu, H. Li, X-H. Xu and F-L. Qing, *J. Am. Chem. Soc.,* 2018, **140**, 11613.

29 H. Serizawa, K. Ishii, K. Aikawa and K. Mikami, *Org. Lett.,* 2016, **18**, 3686.

30 J. R. Bour, S. K. Kariofillis and M. S. Sanford*, Organometallics*, 2017, 36, 1220.

31 Y. Gu and Q. Shen, *Nat. Commun.,* 2014, **5**, 5405.

32 C. Lu, H, Lu, J. Wu, H. C. Shen, T. Hu, Y. Gu and Q. Shen, *J. Org. Chem.*, 2018, **83**, 1077.

33 C. Lu, Y. Gu, J. Wu, Y. Gu, Q. Shen, *Chem. Sci.*, 2017, **8**, 4848.

34 K. Aikawa, Y. Nakamura, Y. Yokota, W. Toya and K. Mikami, *Chem. Eur. J.,* 2015, **21**, 96.

35 (a) T. C. Wilson, T. Cailly and V. Gouverneur, *Chem. Soc. Rev.*, 2018, **47**, 6990; (b) J. W. B. Fyfe, A. J. B. Watson, *Chem.*, 2017, **3**, 31; (c) T. C. Wilson, G. McSweeney,

S. Preshlock, S. Verhoog, M. Tredwell, T. Cailly and V. Gouverneur, *Chem. Commun.,* 2016, **52**, 13277.

36 Z. Feng, Q-Q. Min and X. Zhang, *Org. Lett.,* 2016, **18**, 44.

37 X-Y. Deng, J-H. Lin, J-C. Xiao, *Org. Lett.*, 2016, **18**, 4384.

38 X-P. Fu, X-S. Xue, X-Y. Zhang, Y-L. Xiao, S. Zhang, Y-L. Guo, X. Leng, K. N. Houk, and X. Zhang, *Nat. Chem.*, 2019, **11**, 948.

39 W. Miao, Y. Zhao, C. Ni, B. Gao, W. Zhang and J. Hu, *J. Am. Chem. Soc.*, 2018, **140**, 880.

40 X. Jiang, G. Ji and J. R. Xie, *J. Fluorine Chem.,* 1996, **79**, 133.

41 Y. Fujiwara, J. A. Dixon, R. A. Rodriguez, R. D. Baxter, D. D. Dixon, M. R. Collins, D. G. Blackmond and P. S. Baran., *J. Am. Chem. Soc.*, 2012, **134**, 1494.

42 T. T. Tung, S. B. Christensen and J. Nielsen, *Chem. Eur. J.,* 2017, **23**, 18125.

43 V. Bacauanu, S. Cardinal, M. Yamauchi, M. Kondo, D. F. Fernández, R. Remy and D. W. C. MacMillan, *Angew. Chem. Int. Ed.,* 2018, **57**, 12543.

44 R. Sakamoto, H. Kashiwagi and K. Maruoka, *Org. Lett.*, 2017, **19**, 5126.

45 I. Ghosh, J. Khamrai, A. Savateev, N. Shlapakov, M. Antonietti and B. König, *Science*, 2019, **365**, 360.

46 (a) S. Mizuta, I. S. Stenhagen, M. O'Duill, J. Wolstenhulme, A. K. Kirjavainen, S. J. Forsback, M. Tredwell, G. Sandford, P. R. Moore and M. Huiban, *Org. Lett.,* 2013, **15**, 2648; (b) N. Yoneda and T. Fukuhara, *Chem. Lett.,* 2001, **30**, 222; (c) J. W. Lee, W. Zheng, C. A. Morales-Rivera, P. Liu and M. Ngai, *Chem. Sci.,* 2019, **10**, 3217.

47 C. Ni and J. Hu, *Synthesis,* 2014, **46**, 842.

48 J. Zheng, Y. Li, L. Zhang, J. Hu, G. J. Meuzelaar and H. Federsel, *Chem. Commun.,* 2007, 5149.

49 F. Wang, L. Zhang, J. Zheng and J. Hu, *J. Fluorine Chem.,* 2011, **132**, 521.

50 Y. Zafrani, G. Sod-Moriah and Y. Segall, *Tetrahedron,* 2009, **65**, 5278.

51 Y. Geng, M. Zhu, A. Liang, C. Niu, J. Li, D. Zou, Y. Wu and Y. Wu, *Org. Biomol. Chem.,* 2018, **16**, 1807.

52 P. S. Fier and J. F. Hartwig, *Angew. Chem. Int. Ed.,* 2013, **52**, 2092.

53 J. Yang, M. Jiang, Y. Jin, H. Yang and H. Fu, *Org. Lett.,* 2017, **19**, 2758.

54 J. Hine and K. Tanabe, *J. Am. Chem. Soc.,* 1957, **79**, 2654.

55 J. Mizukado, Y. Matsukawa, H. Quan, M. Tamura and A. Sekiya, *J. Fluorine Chem.,* 2006, **127**, 400.

56 R. M. Flynn and D. J. Burton, *J. Fluorine Chem.,* 2011, **132**, 815.

57 J. Mizukado, Y. Matsukawa, H. Quan, M. Tamura and A. Sekiya, *J. Fluorine Chem.,* 2005, **126**, 365.

58 J. Zhu, Y. Liu and Q. Shen, *Angew. Chem. Int. Ed.,* 2016, **55**, 9050.

59 K. Levchenko, O. P. Datsenko, O. Serhiichuk, A. Tolmachev, V. O. Iaroshenko and P. K. Mykhailiuk, *J. Org. Chem.,* 2016, **81**, 5803.

60 Q. Xie, C. Ni, R. Zhang, L. Li, J. Rong and J. Hu, *Angew. Chem. Int. Ed.,* 2017, **56**, 3206.

61 G. Liu, X. Li, W. Qin, X. Peng, H. N. Wong, L. Zhang and X. Zhang, *Chem. Commun.,* 2019, **55**, 7446.

62 M. Gaba and C. Mohan, *Med. Chem. Res.,* 2016, **25**, 173.

63 (a) S. Lim, P. Ibrahim and M. Fuentes, WO2020006294A1; (b) B. O. Buckman, P. Ibrahim and P. T. R. Rajagopalan, WO2019190999A1; c) B. O. Buckman, S. Yuan, K. Emayan, M. Adler and P. Ibrahim, WO2019190885A1; d) B. O. Buckman, S. Yuan, M. Adler, K. Emayan, J. Ma, J. B. Nicholas, WO2018064119A1; (e) K. Morimoto, K. Makino, S. Yamamoto and G. Sakata, *J. Heterocyclic Chem.*, 1990, **27**, 807.

64 M. Andrés, M. A. Buil, M. Calbet, O. Casado, J. Castro, P. R. Eastwood, P. Eichhorn, M. Ferrer, P. Forns, I. Moreno, S. Petit and R. S. Roberts, *Bioorg. Med. Chem. Lett.*, 2014, **24**, 5111.

65 Y. Zafrani, D. Amir, L. Yehezkel, M. Madmon, S. Saphier, N. Karton-Lifshin and E. Gershonov, *J. Org. Chem.,* 2016, **81**, 9180.

Chapter 2: Organophotoredox Hydrodefluorination of Trifluoromethylarenes with Application to Drug Discovery

The work discussed in this chapter was published in *The Journal of the American Chemical Society.*

Sap, J. B. I.; Straathof, N. J.; Knauber, T.; Meyer, C. F.; Médebielle, M.; Buglioni, L.; Genicot, C.; Trabanco, A. A.; Noël, T.; am Ende, C. W. Gouverneur, V. *J. Am. Chem. Soc.* **2020**, *142,* 9181-9187

Author contributions: Reaction optimisation was performed by Jeroen Sap with the help of Dr. Natan Straathof. Scope and continuous flow experiments were performed by Jeroen Sap. Mechanistic experiments were performed by Jeroen Sap. Luminescence quenching experiments were performed by Jeroen Sap with assistance from Claudio Meyer. Robustness screening experiments were performed by Dr. Thomas Knauber and Jeroen Sap. Cyclic voltammetry measurements of **2.70**, **2.71** and **2.72** were performed by Dr. Laura Buglioni.

2.1 Trifluoromethyl Groups in Organic Synthesis

Over the past decade, the trifluoromethyl (CF_3) group has become an increasingly prominent moiety amongst blockbuster drugs, examples of which include: Celecoxib (**2.1**), Enzalutamide (**2.2**), refrigerants such as 2,2-dichloro-1,1,1-trifluoroethane (**2.3**) and agrochemicals such as Fluopyram (**2.4**) (**Figure 2.1**).[1]

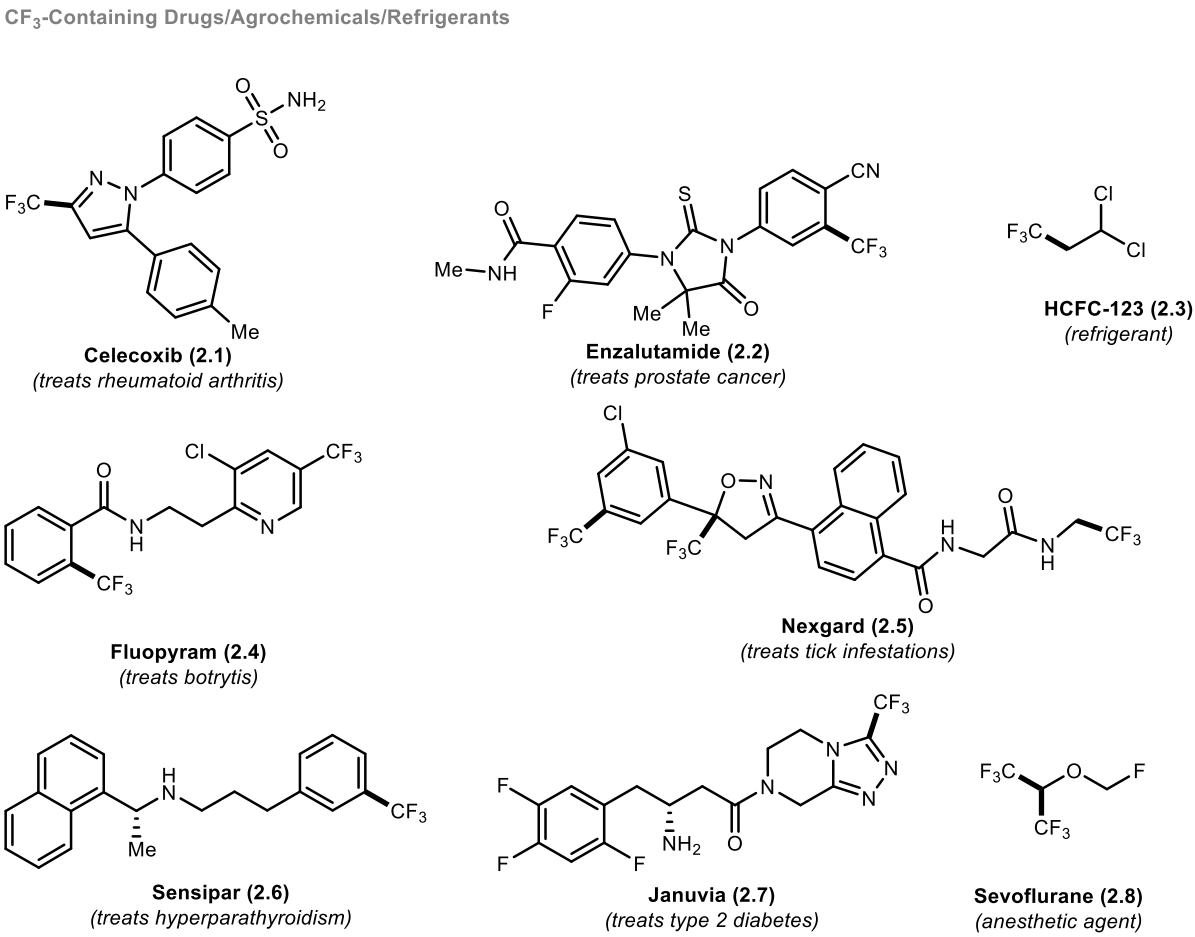

Figure 2.1 Examples of drugs, agrochemicals and refrigerants, which contain a CF_3 group.

The CF_3 group is often used as a bioisostere of other functionalities such as chloride and methyl groups due to its favourable metabolic stability.[2] Since the seminal reports by Kobayashi and Kumadaki, and McLoughlin and Thrower in 1969, the CF_3 group within

the context of (hetero)aromatics has received significant attention.[3,4] The field has grown at a rapid pace resulting in a large toolbox of reported methods available to incorporate this motif onto complex molecular structures. Practical and versatile strategies have been developed for the trifluoromethylation of (hetero)aryl halides (**2.9**),[5] (hetero)aryl boronic acid derivatives (**2.10**)[6] and (hetero)aryl diazonium tetrafluoroborate salts (**2.11**).[7] More recently directed C−H activation and photoinduced radical methods have been devised to access trifluoromethylarenes.[8] These strategies are summarised in **Scheme 2.1**.

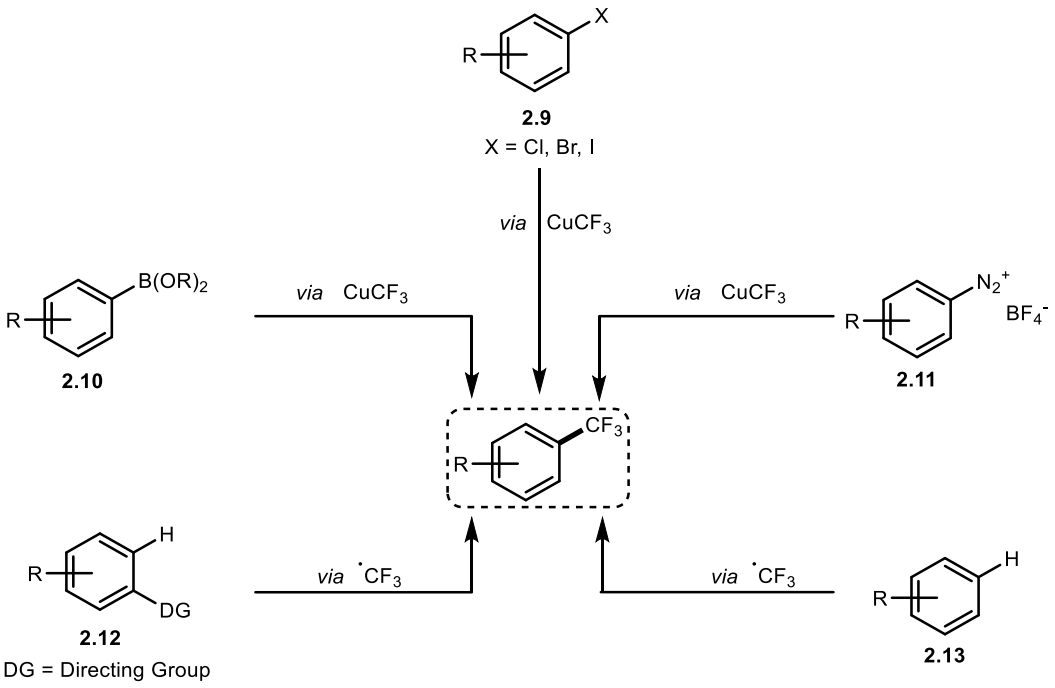

Scheme 2.1 Common strategies to access trifluoromethylarenes.

2.2 Introduction to The Hydrodefluorination Strategy

In contrast to the number of methods available to access CF_3-substituted arenes, methods which allow for the incorporation of a CF_2H functionality, especially those methods with applications to LSF, remain underdeveloped with respect to drug

molecules (see **Chapter I**). This is partly due to the decreased thermodynamic stability of MCF_2H complexes compared to their MCF_3 counterparts.[9] Indeed, reliable, scalable and robust difluoromethylation protocols, specifically for LSF remain elusive.

Alternative strategies which build up complexity through increase or decrease of fluorine content *via* C−H fluorination or hydrodefluorination (HDF) provide attractive alternatives to access difluoromethylarenes, due to the prevalence of methyl groups and abundance of methods to install trifluoromethyl groups.[10] The latter of these two strategies will be the focus of this chapter, specifically the synthesis of CF_2H functionalities directly from CF_3 groups through HDF. Such an approach relies on existing trifluoromethylation technologies to first furnish the desired CF_3-containing scaffold prior to accessing the CF_2H group with an 'end-game' HDF strategy. From a medicinal chemistry point of view, such a strategy could facilitate access to multiple drug analogues with varying fluorine content. One of the major advantages of this approach is that it alleviates the need to redesign the existing synthetic route used to access the parent CF_3 compound.

2.3 The Potential and Challenges of Defluorination Reactions

Within the field of late-stage functionalisation, the ability to target inert bonds that are found infrequently within complex targets is highly desirable. Despite the obvious appeal of an HDF strategy, significant challenges must be overcome. The high bond dissociation energy (BDE) of the carbon-fluorine bond (115 kcal/mol) poses one significant challenge.[11] Moreover, several studies have shown that the activation of consecutive C−F bonds of trifluoromethylarenes is thermodynamically more facile (see

Scheme 2.13). This provides a challenge to selectively cleave a single C−F bond and trap the resulting intermediate, in favour of exhaustive defluorination.[12] The stability and therefore unreactive nature of the C−F bond provides an explanation for the long environmental lifetime of compounds functionalised with CF_3 groups.[13] Due to the toxicity of many organofluorine compounds, their efficient degradation under mild and efficient conditions is an important area of research. A common strategy to degrade fluoroaromatic pollutants to nonfluorinated organics is to strip their entire fluorine content through electrochemical reduction.[14] Derivatisation and repurposing of such compounds *via* selective mono HDF would provide an alternative use for end-of-lifecycle CF_3-containing compounds and is therefore an attractive endeavour. Furthermore, if such a strategy is successful in an LSF context, it would allow immediate expansion of drug libraries.

2.4 Reductive Defluorination

2.4.1 Lewis Acid Catalysed Uncontrolled Hydrodefluorination of Trifluoromethylarenes

Uncontrolled defluorination of polyfluorinated molecules mediated by alkali metals is a highly exothermic process, generally leading to the complete consumption of the starting material. For example, it is well-documented that defluorination of organic molecules is facile but controlling such processes has proven to be more difficult. This lack of control is illustrated in **Scheme 2.2**. A niobium Lewis acid in conjunction with a strong reducing agent ($LiAlH_4$) can induce reductive defluorination of trifluoromethylarenes. Due to the highly reactive nature of this system, partial

defluorination of 2-(trifluoromethyl)-1,1'-biphenyl (**2.14**) was not observed, and 9H-fluorene (**2.15**), a product which does not contain fluorine, was detected instead.[15]

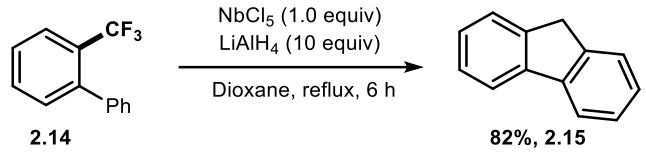

2.14 **82%, 2.15**

Scheme 2.2 Non-selective hydrodefluorination of trifluoromethylarenes.

Exhaustive defluorination is commonly observed in HDF reactions which employ a hydride source ($LiAlH_4$, Et_3SiH or $LiEt_3BH$) to reduce C−F bonds in trifluoromethylarenes (**2.16, 2.18**, **2.20**). As such, these methods lack the necessary selectivity control to prevent exhaustive defluorination (**2.17, 2.19, 2.21**). Furthermore, the need for strong hydride sources to reduce the C−F bond make these methods unsuitable for LSF (**Scheme 2.3**)[16-18]

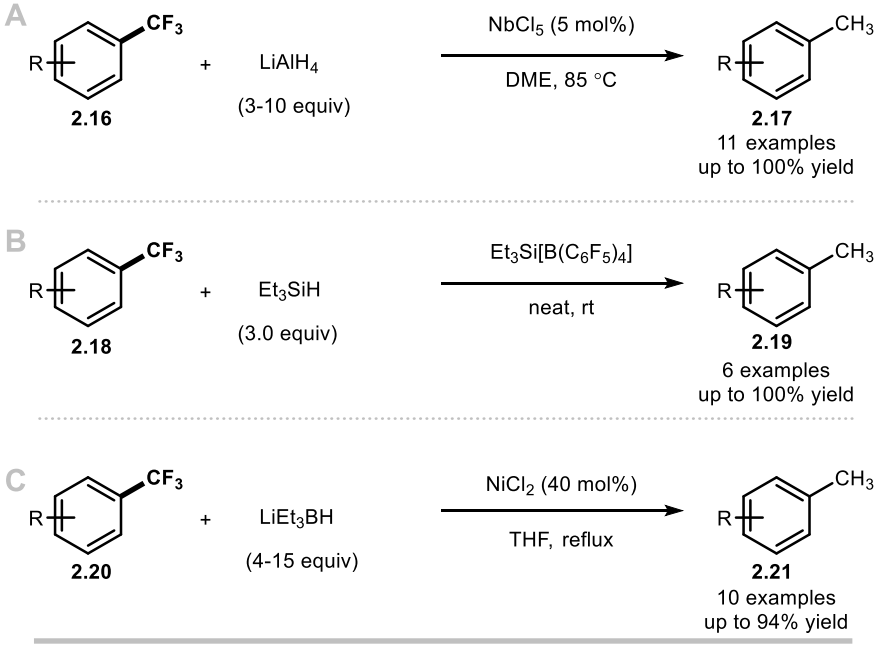

Scheme 2.3 Non-selective hydrodefluorination of trifluoromethylarenes.

Despite the absence in HDF methods to access difluoromethylarenes selectively from trifluoromethylarenes, several reports have illustrated that controlled mono defluoroalkylation of trifluoromethylarenes is feasible.[19,20]

2.4.2 Controlled Defluorination of Trifluoromethylarenes

While controlled HDF poses a great challenge, the partial electrochemical defluoroalkylation of trifluoromethylarenes in the presence of a sacrificial anode and a strong electrophile is more facile. Indeed, the difluoromethyl anion resulting from reduction of the trifluoromethylarene readily reacts with electrophiles such as CO_2, (**Scheme 2.4A**) acetone (**Scheme 2.4B**) or DMF (**Scheme 2.4C**) affording the acid, dimethyl carbinol, or aldehyde adducts respectively upon acidic work-up.[20] Unlike the HDF reactions described in **Section 2.4.1**, the electrochemical reduction reactions described in **Scheme 2.4** are controlled and chemoselective for the CF_3 group. This chemoselectivity likely stems from the fact that the products themselves are not prone to defluorination. In contrast to HDF reactions, where the loss of C−F bonds results in the formation of a C-H bond and consequently decreased stability towards reduction (order of stability: CF_3>CF_2H>CH_2F).

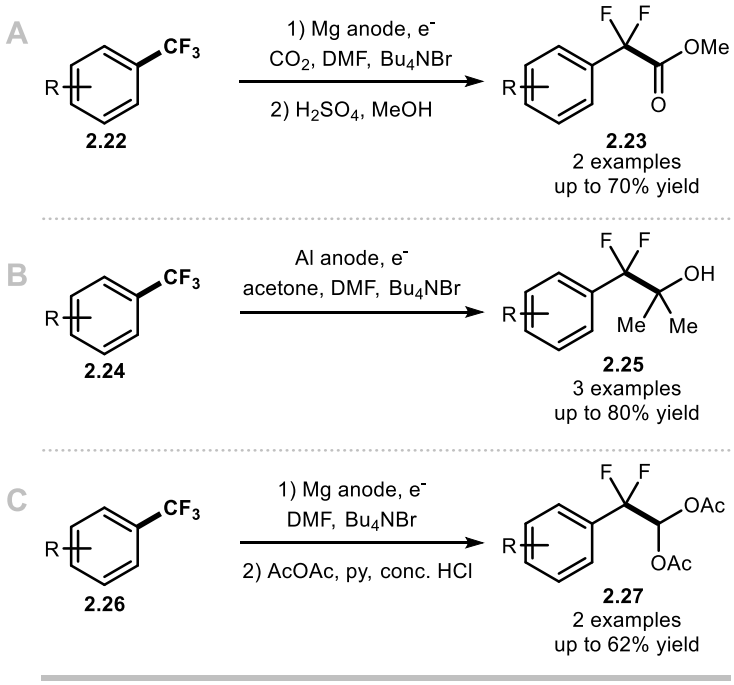

Scheme 2.4 Selective single hydrodefluoroalkylation of trifluoromethylarenes.

The successful cleavage of a single C−F bond found within CF_3 groups under oxidative conditions was first described by Lectka and co-workers in 1997. They accomplished this through carefully engineered biphenyl diazonium salts (**2.28** and **2.29**) which they proposed could generate a difluorocarbenium intermediate which could trigger a fluoride ion shift through a Friedel-Crafts-type reaction, generating **2.30**. The authors suggested that one of the driving forces for this transformation is the six-membered transition state necessary for the process. The authors also report the formation of by-product **2.31** which stems from hydrolysis of the difluorocarbenium intermediate. (**Scheme 2.5**).[21]

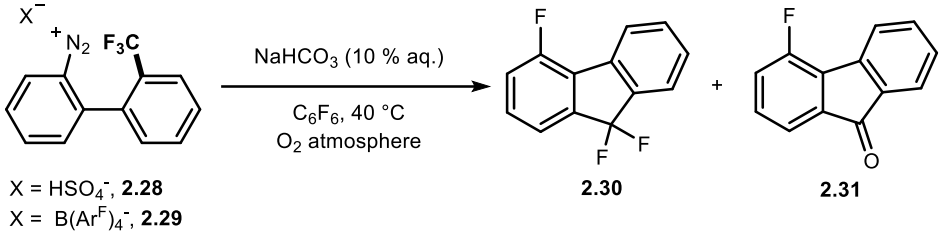

Scheme 2.5 C−F bond activation by aryl carbocations through intramolecular fluoride shift.

Nineteen years later, Hosoya and co-workers disclosed the first general protocol for the selective single C−F bond cleavage of trifluoromethylarenes (**2.32**) by employing an *ortho*-silyl group. Their proposed mechanism suggests *in situ* generation of a silylium cation which, due to its proximity and fluorophilicity, readily abstracts fluoride. The resulting difluorocarbenium cation then reacts with a range of nucleophiles such as allyl silanes to access a variety of difluoromethylene compounds (**2.33**) (**Scheme 2.6**).[22]

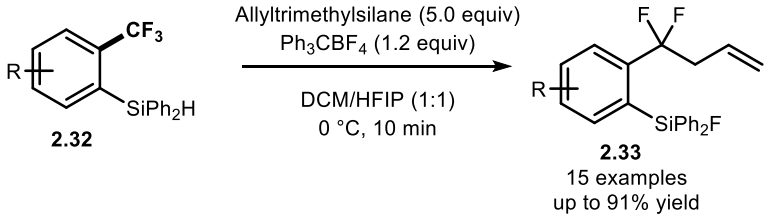

Scheme 2.6 Selective C−F bond activation of trifluoromethylarenes with an *ortho*-silyl directing group.

2.5 Photoredox-Catalysed Defluorination

Despite these advances, alternative defluorination methods which are milder and broader in scope, and do not require a directing group are necessary for defluoroalkylation and HDF reactions to become synthetically useful, especially in the case of LSF. Employing photoredox catalysis provides an alternative mechanistic pathway to generate C-centered difluorobenzylic radicals. Due to the LUMO-lowering effects of electron withdrawing CF_3 groups as well as their proximity to the aromatic ring, this privileged substrate class can be activated under photoredox catalysis.

Activation of these substrates occurs through single electron reduction into the LUMO of the trifluoromethylarene, generating a radical anion in the process. This radical anion readily undergoes fluoride extrusion resulting in the generation of a C-centered difluorobenzylic radical, a reactive intermediate which can be harnessed for further functionalisation.[23]

2.5.1 Introduction to photoredox catalysis

Photoredox catalysis is generally defined as the process where electromagnetic energy is converted into chemical energy through a catalyst which absorbs visible light. This occurs either in the form of an organic dye sensitiser or a metal complex. Recently, photoredox catalysis has undergone rapid expansion within organic synthesis due to its ability to access reaction pathways which are otherwise inaccessible through thermal energy-driven processes. From a mechanistic point of view, a photoredox reaction typically commences with the visible-light excitation of a photocatalyst (PC), which facilitates the transfer of an excited electron from a PC metal-centered orbital (t_2g) to a ligand-centred π^* orbital, revealing an electron hole in the t_2g orbital. At this stage, the photoexcited state catalyst can act as a reductant or an oxidant. In the first case, the high energy electron in the π^* orbital undergoes intersystem crossing (ISC) generating a long-lived triplet excited species (1900 ns for $[Ir(ppy)_3]$), which can then undergo spin-allowed single electron transfer (SET) with an organic substrate. This pathway is generally preferred over direct spin-forbidden decay from the singlet excited state. In the latter case, where the photoexcited catalyst acts as an oxidant, an electron can be accepted in the metal-based t_2g orbital. Visible-light photoredox reactions are especially convenient, since most organic compounds do not absorb visible light (i.e. 455 nm),

allowing selective activation of the PC whilst circumventing undesired decay pathways of the substrate.[24]

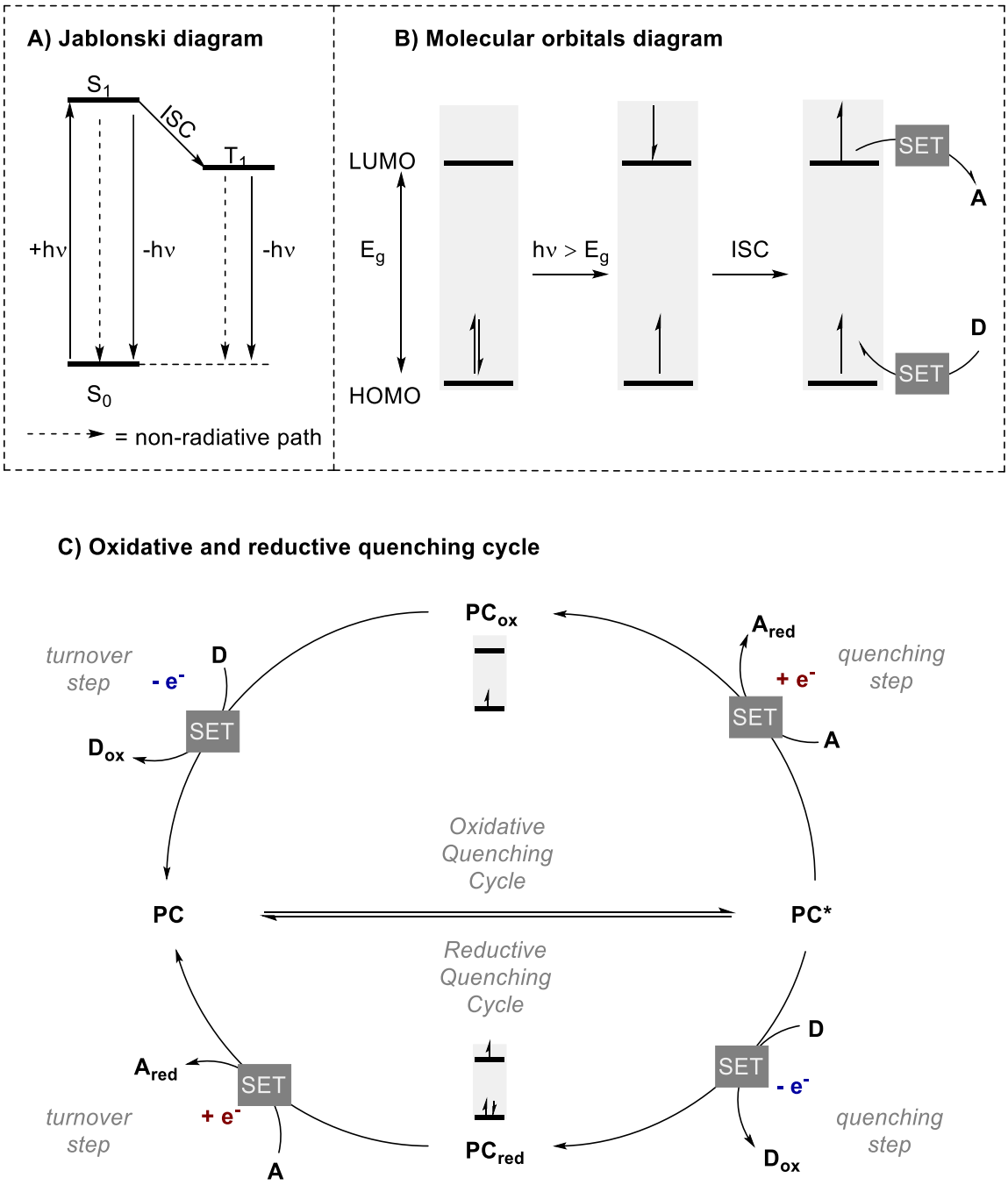

Figure 2.2 Main concepts of photoredox catalysis. A) Jablonski photophysics diagram. B) Molecular orbitals diagram. C) Oxidative and reductive quenching cycles.

2.5.2 Photoredox-Catalysed Selective C-F bond Functionalization in Aromatic Fluorides

Numerous strategies exist to activate perfluoroarenes such as nucleophilic aromatic substitution and defluorinative functionalisation *via* benzynes. However, the first photocatalytic C-F bond activation technology was not reported until 2014 (**Figure 2.3**).[25]

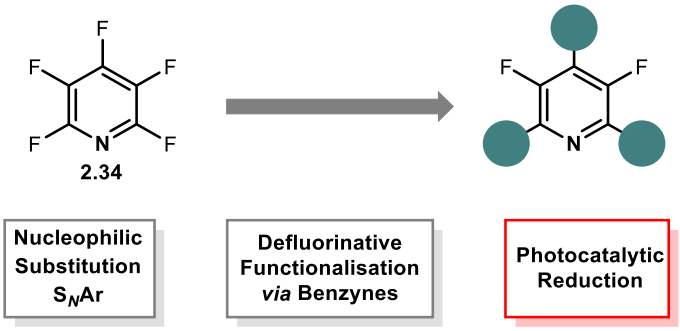

Figure 2.3 Common strategies for the defluorination of perfluoroarenes.

This pioneering work by Weaver and co-workers illustrated that the photocatalytic HDF of perfluorinated pyridines (**2.34**) was feasible using catalytic amounts of commercially available iridium catalyst ($[Ir(ppy)_3]$), an organic quencher ($EtNiPr_2$) and blue light. The same authors also illustrated that defluoro-alkylation, arylation and alkenylation reactions were feasible under similar photochemical conditions. In each instance, $[Ir(ppy)_3]$ was employed as the PC. Upon excitation of this PC with blue light, $[Ir(ppy)_3]^*$ is formed. The excited state PC then undergoes reductive quenching to yield the reduced ground state PC, $[Ir(ppy)_3]^-$ which has a sufficiently high ground state reduction potential to induce C−F bond cleavage of perfluoropyridine. The resulting aryl radical intermediate (**2.36**) then terminates in a bimolecular fashion to yield the products (**2.37 – 2.40**) outlined in **Scheme 2.7**.[25]

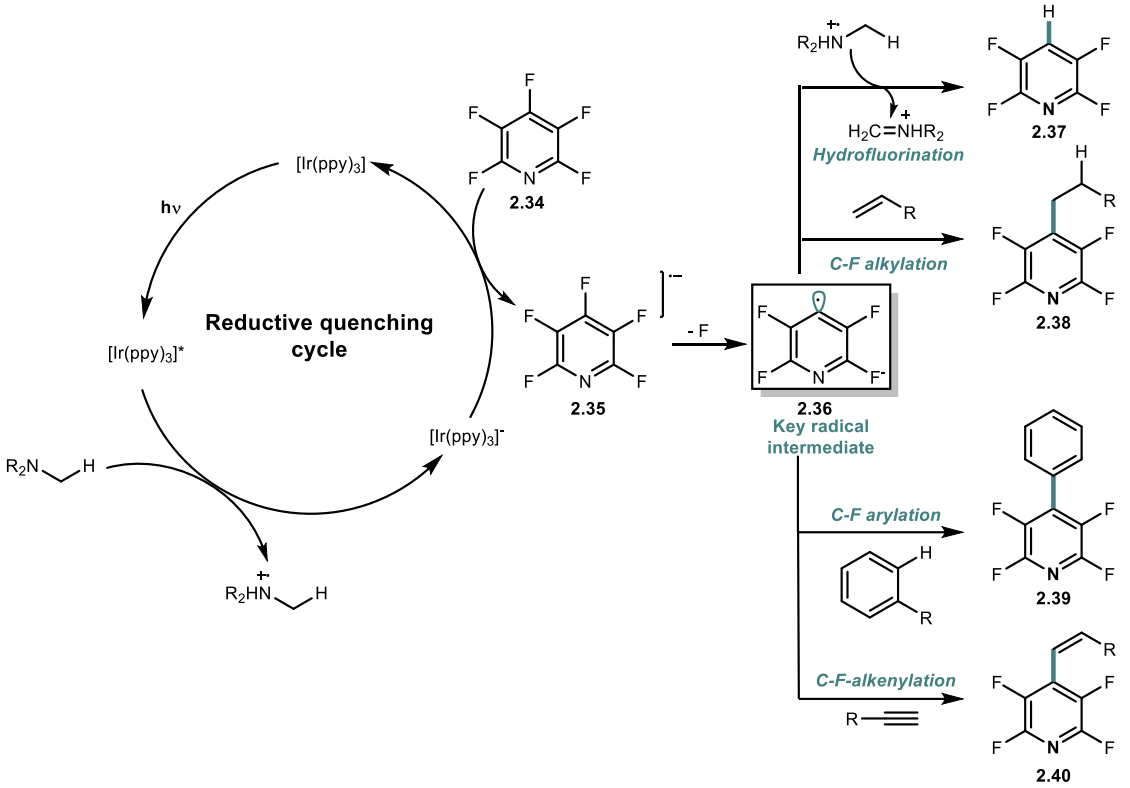

Scheme 2.7 Photoredox-catalysed defluorination of perfluoroarenes.

2.5.3 Selective C-F bond Functionalisation of Trifluoromethylarenes Under Photoredox Catalysis

Inspired by the seminal works of Weaver and co-workers, both Jui and König disclosed technologies which allow photocatalytic defluoroalkylation of trifluoromethylarenes (**2.41**).[25-27] In König's report, the authors propose a mechanism whereby the excited state PC*, $[Ir(ppy)_3]^*$, is generated through blue light irradiation. $[Ir(ppy)_3]^*$ is then reductively quenched by 2,2,6,6-tetramethylpiperidine (TMP) resulting in a stable radical cation (**2.45**). The resulting Ir(II) species then reduces trifluoromethylarene **2.41** through a ground-state single electron transfer process. The resulting radical anion intermediate (**2.48**) then undergoes mesolytic cleavage facilitated by an *in situ* generated borenium cation **2.47** which abstracts F^- from **2.48**. This process affords the intermediary C-centered difluorobenzylic radical **2.49**. This radical may then react

directly with one equivalent of methacrylamide to yield radical **2.50,** which upon oxidation and subsequent rearomatisation yields the aryl difluoroalkylated product (**2.43**) (**Scheme 2.8**). [26]

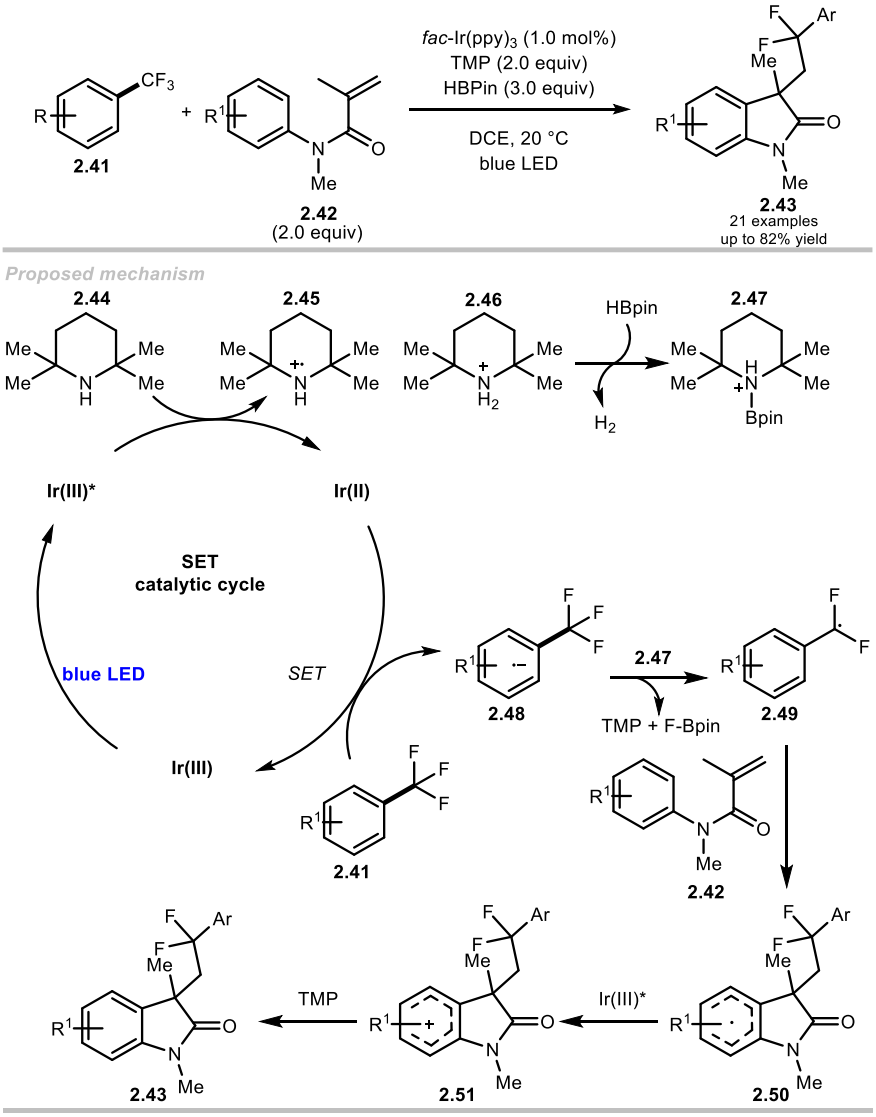

Scheme 2.8 Photoredox-catalysed selective hydrodefluoroalkylation of trifluorometylarenes.

In Jui's report, an organophotoredox catalyst, *N*-phenylphenothiazine (PTH, $E_{1/2}$* = −2.10 V vs SCE) is employed. In contrast to König's report, an oxidative quenching cycle operates whereby SET takes place directly from PC*. In this case, the trifluoromethylarene **2.52** acts as the oxidant. The authors found that the C-centered

difluorobenzylic radical **2.57,** which forms upon extrusion of fluoride, readily engages in radical addition reactions with a wide selection of unactivated alkenes (**2.53**). After the radical addition step, a new radical intermediate (**2.58**) is formed, and readily quenched with cyclohexanethiol (CySH), which acts as a catalytic hydrogen atom donor (HAD) reagent. The authors propose that both catalysts, (HAD and PC) are regenerated by sodium formate (**2.54**), which is used stoichiometrically (**Scheme 2.9**).[27]

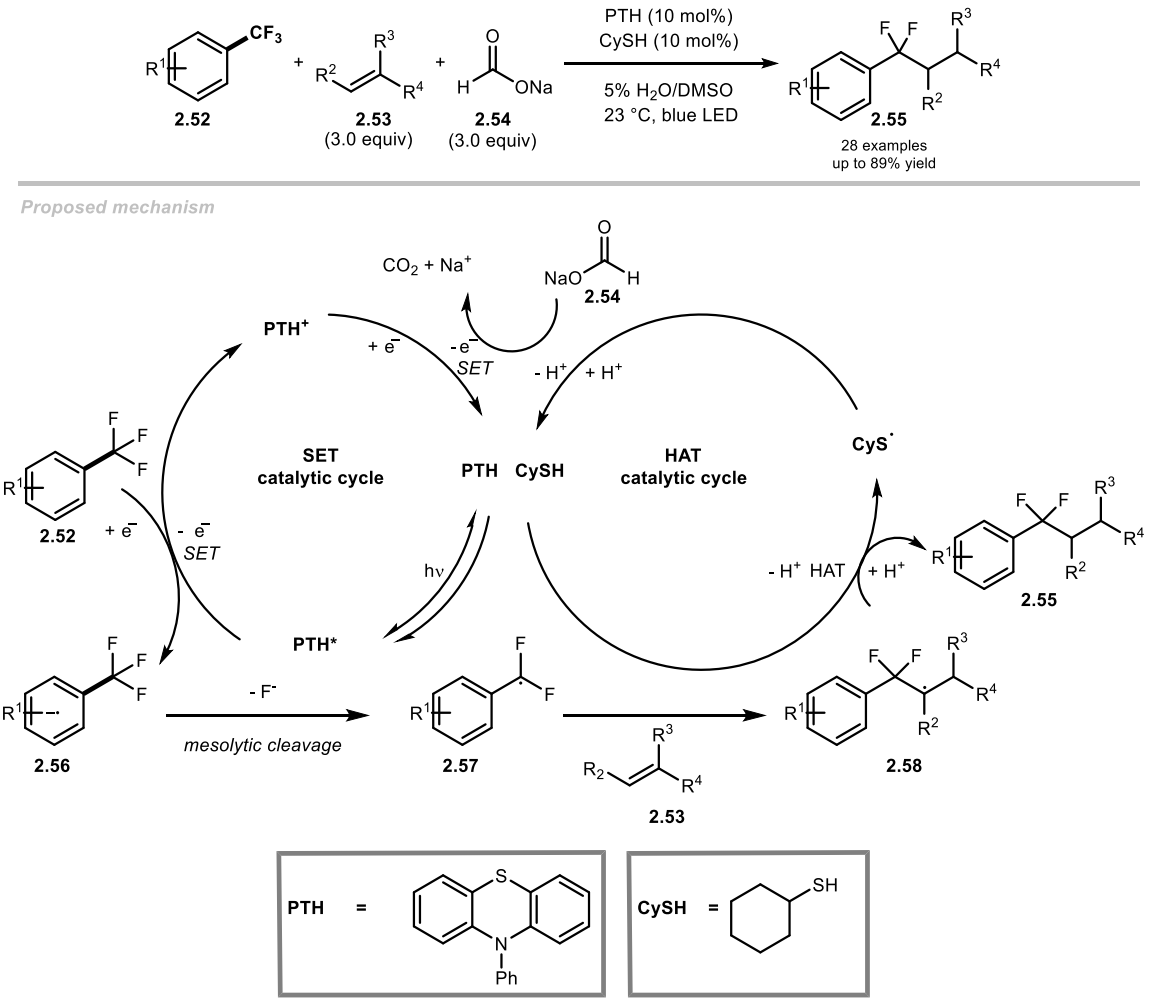

Scheme 2.9 Photoredox-catalysed mono-selective hydrodefluoroalkylation of trifluorometylarenes.

Despite the advances in photocatalysed defluoroalkylation of trifluoromethylarenes, methods which allow these precursors to undergo HDF have not been reported. In Jui's

report, **2.57** preferentially undergoes a radical addition reaction with **2.53** generating the radical intermediate **2.58** which can be trapped with a polarity matched HAD.[27] Direct termination of **2.57** was not observed, most likely due to a polarity mismatch between this radical and the HAD reagent. In König's report, the absence of HAD alleviates the possibility of an HDF pathway.[26]

2.6 State of The Art: Selective Mono-Hydrodefluorination of Trifluoromethylarenes

Concurrent to those photocatalytic HDF technologies, alternative mono selective HDF protocols have been reported. In 2016, Lalic developed a two-step one-pot HDF method utilising catalytic amounts of palladium and copper in the presence of triphenylsilane (**2.60**) and potassium *tert*-butoxide. Upon *in situ* generation of a nucleophilic addition adduct to DMF (**2.61**), the intermediate could react with *tert*-butanol to afford the desired mono-HDF product (**2.62**) in good selectivity (up to >50:1) in favour of the difluoromethylated product (**Scheme 2.10**). With the exception of one example, Lalic's method was limited to substituted biphenyl trifluoromethylarenes and not amenable to LSF.[28]

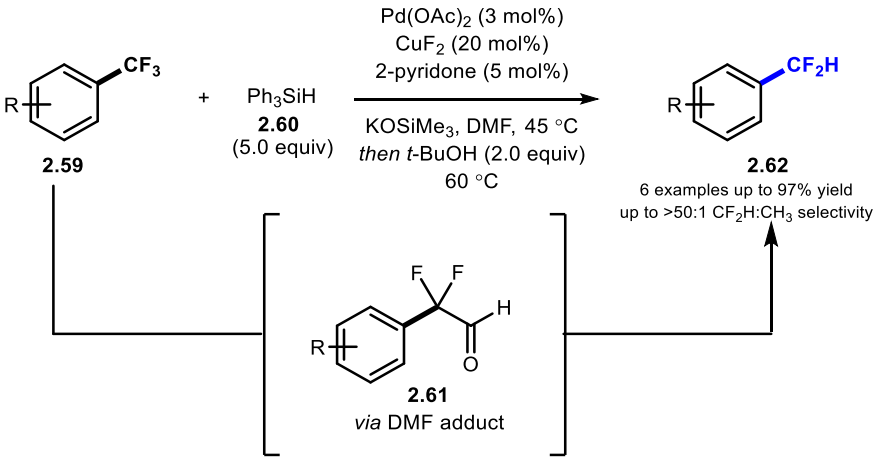

Scheme 2.10 Two-step-one pot metal catalysed hydrodefluorination of trifluoromethylarenes.

In 2017, Prakash and co-workers disclosed the mono selective HDF of substituted 1,3-bis(trifluoromethyl)arenes (**2.63**). In this report, the authors employed super stoichiometric amounts of elemental magnesium to successfully induce mono HDF to a selection of substituted 1,3-bis(trifluoromethyl)arenes. While attractive, the authors illustrated that the applicability of their technology did not span beyond 1,3-bis(trifluoromethyl)arene substrates. Furthermore, the authors found that electron-deficient substrates bearing deactivating functionalities such as nitrile or nitro groups readily underwent exhaustive defluorination. The poor selectivity of this technology towards electron deficient systems can be explained by the fact that the products themselves are likely susceptible to further reduction (**Scheme 2.11**).[29]

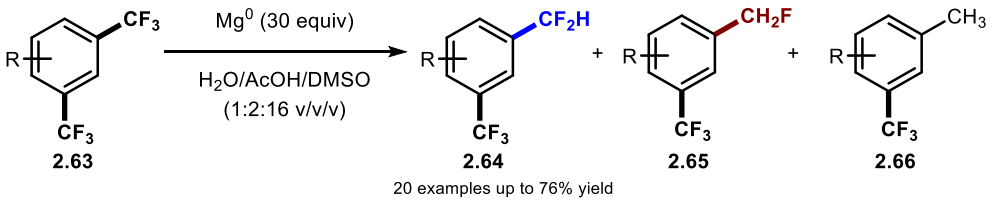

Scheme 2.11 Metal-mediated hydrodefluorination of 1,3-bis(trifluoromethyl)arenes.

2.7 Selection of Strategy and Approach

Applying the concept of molecular editing to a highly functionalised molecular framework is an aspirational goal for all chemists. To this end, we developed an HDF protocol which could be useful in the context of drug discovery. Late-stage alterations, in this case variation of fluorine content, could help medicinal chemists introduce subtle changes to the lipophilicity of lead compounds in an *ad hoc* fashion. Such a strategy would avoid the need for an existing synthetic route to be redesigned, an often laborious and costly process. Despite significant advances, the HDF of trifluoromethylarenes with

a broad scope and with a direct application to drug discovery has not been accomplished, prior to the work outlined in this chapter.

Due to their increased thermal and metabolic stability and their resistance to CYP-450 enzymes, electron deficient di- and trifluoromethylarenes are more prevalent amongst pharmaceuticals than their electron-rich counterparts (85% of all $ArCF_2H$ drugs and 65% of all $ArCF_3$ drugs are electron poor). The likely reason for the lower stability of difluoromethyarenes adorned with electron-donating groups is that these substrates are prone to decomposition through spontaneous defluorination. Electron-donating functionalities such as amine and methoxy functionalities possess lone pairs which facilitate heterolytic cleavage of the C_{alkyl}–F bond. 5-(Difluoromethyl)-1*H*-indole (**2.67**), for example, suffers spontaneous defluorination in aqueous buffer solutions at neutral pH. Decomposition through defluorination of this compound is fast. In addition to its chemical instability, metabolism can also liberate fluoride from CF_2H-substituted arenes through benzylic oxidation by CYP450 enzymes (**Scheme 2.12**).[30] As such, these concerns have been considered in drug-design. We therefore chose to focus primarily on developing a selective HDF methodology focusing on electron deficient trifluoromethylarenes as these are the most prominent in the context of medicinal chemistry.

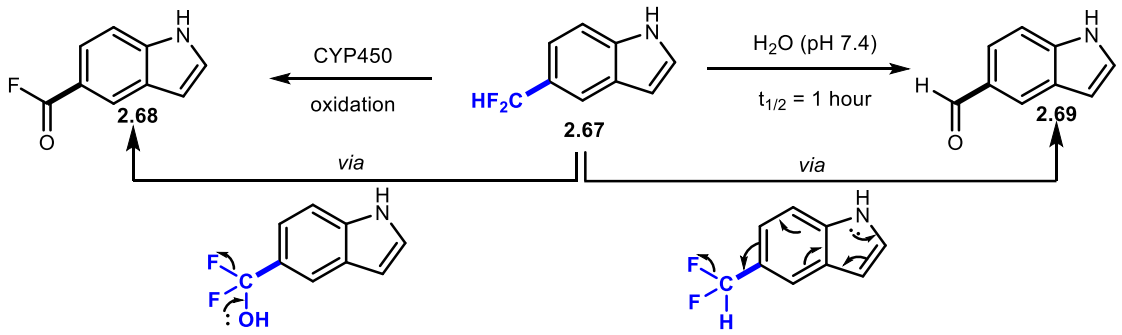

Scheme 2.12 Decomposition of 5-(difluoromethyl)-1*H*-indole through spontaneous defluorination.

Mechanistic studies by Savéant and Thiébault provided useful information on the electrochemical reductive cleavage of C−F bonds for 4-cyanofluorotoluenes **2.70**–**2.72** and trifluoromethylbenzene (**2.73**). The process involves fluoride expulsion from an anion radical, followed by reduction of the radical intermediate, and subsequent protonation. The standard reduction potential measured versus the standard calomel electrode (SCE) for the formation of the radical anion, increases from -1.79 V (**2.70**) to -2.02 V (**2.72**), although these are closely spaced, while the instability of the radical anion towards fluoride mesolytic cleavage increases as shown by the increase in cleavage rate constants (K_{cleave}) from **2.70** to **2.72**. These kinetic studies indicating facile exhaustive defluorination highlight the challenge at hand for these highly-activated substrates (**Scheme 2.13**).[31]

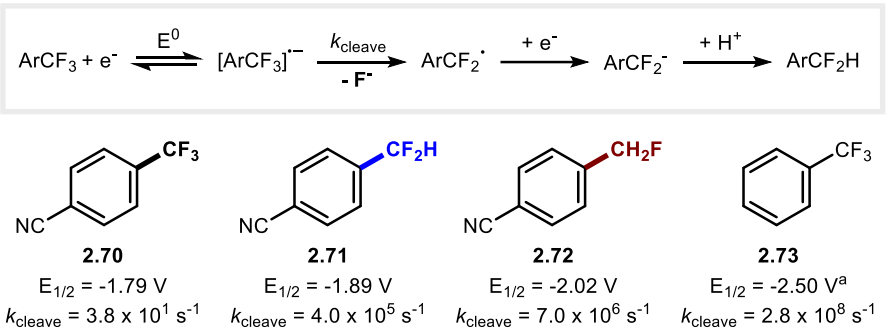

Scheme 2.13 Electrochemical reductive cleavage of **2.70 – 2.73**: standard reduction potentials (V vs standard calomel electrode (SCE) in DMF) and cleavage rate constants. [a]$E_{1/2}$ (V vs SCE in DMF), value taken from **Ref. 31**.

Cyclic voltammetry measurements:

Procedure: All the cyclic voltammetry experiments were performed in a batch setup. The analysis was performed with a PalmSens EmStat3+ instrument equipped with a

glassy carbon working electrode (3 mm), a platinum wire counter electrode, and a SCE reference electrode. All measurements were carried out at a concentration of 0.1 M in anhydrous DMF with an electrolyte (Me_4NBF_4, 0.05 M), with a scan rate of 100 mV. CV measurements of **2.70**, **2.71** and **2.72** indicate that the reduction potential becomes progressively more negative from **2.70** to **2.72**, but are closely spaced.

4-(Trifluoromethyl)benzonitrile (2.70, -1.79 V)

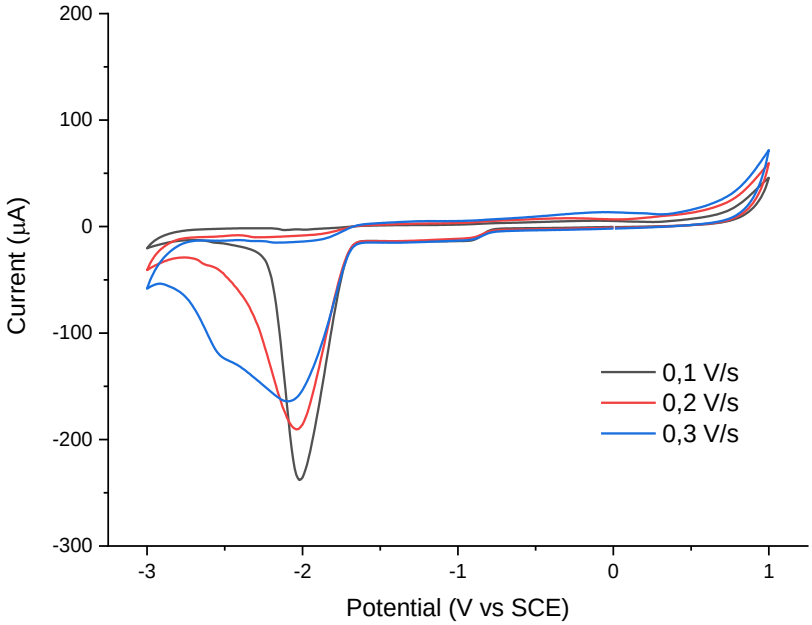

Figure 2.4 Cyclic Voltammetry of **2.70** (-1.79 V) in DMF Right: from 1.0 V to -3.0 V.

4-(Difluoromethyl)benzonitrile (2.71, -1.89 V)

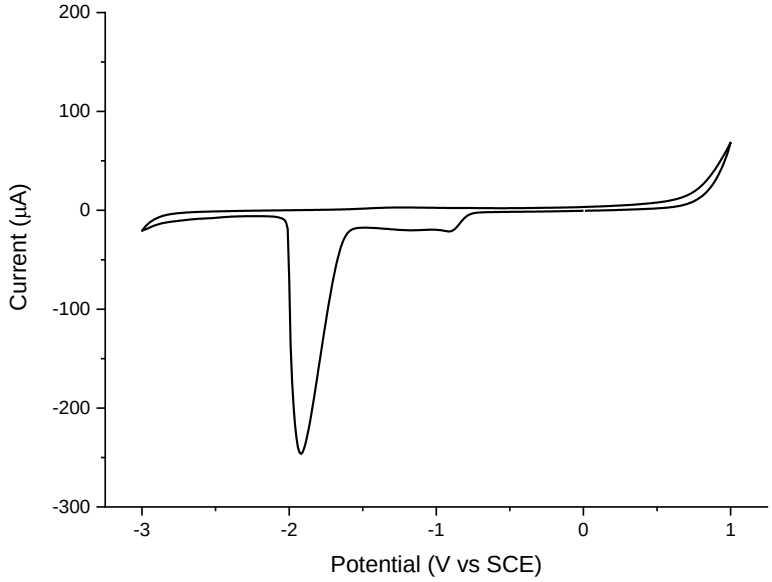

Figure 2.5 Cyclic Voltammetry of **2.71** (-1.89 V) in DMF Right: from 1.0 V to -3.0 V.

4-(Fluoromethyl)benzonitrile (2.72, -2.02 V)

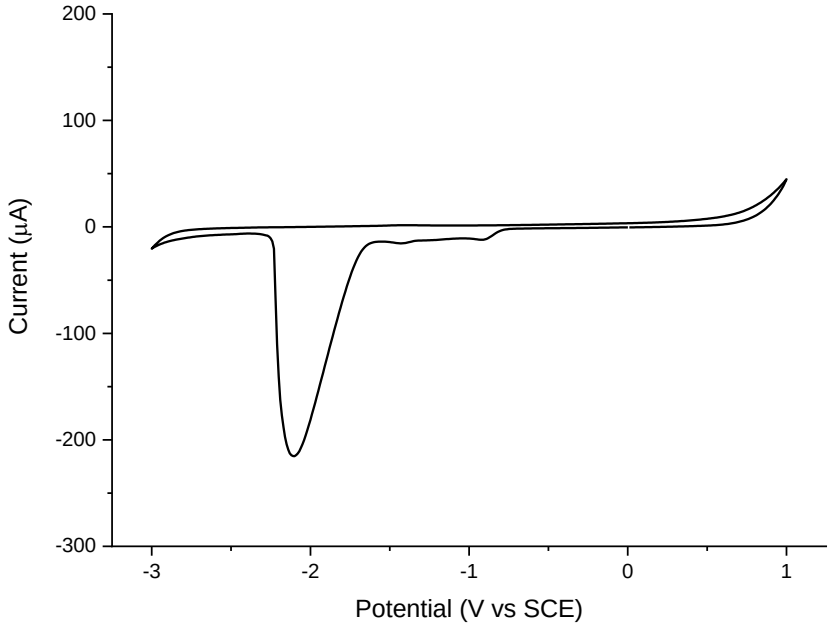

Figure 2.6 Cyclic Voltammetry of **2.72** (-2.02 V) in DMF Right: from 1.0 V to -3.0 V.

2.8 Initial Optimisation of The Reaction Conditions

With the aspirational goal of developing a method which could substitute a single fluorine atom in a highly functionalised trifluoromethylarene for a hydrogen atom, our HDF technology would need to be mild and chemoselective in order to be amenable to LSF. We elected **2.70** as a model substrate for reaction development and optimisation studies. To highlight any limitations of current mono-selective HDF protocols, **2.70** was exposed to the reaction conditions of Lalic and co-workers **(Scheme 2.14A)** and Prakash **(Scheme 2.14B)** and co-workers.[28,29] Neither methods resulted in conversion towards **2.71** or **2.72,** and led primarily to the recovery of starting material.

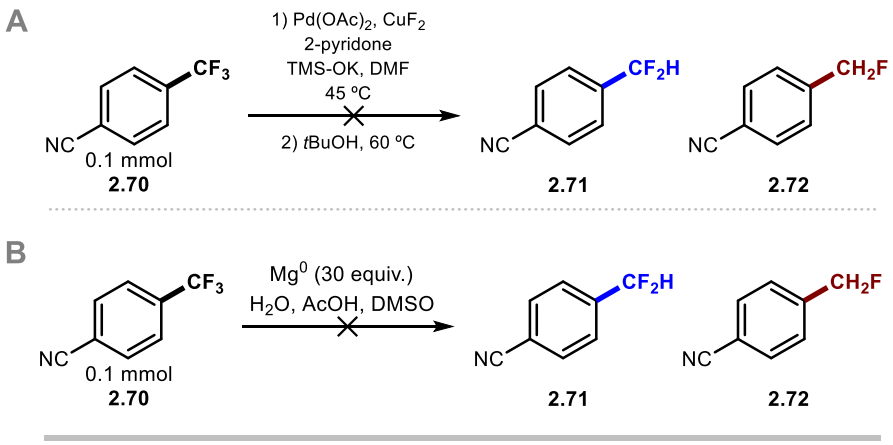

Scheme 2.14 (A) Attempted hydrodefluorination of **2.70** under the conditions of **ref. 28.** (B) Attempted hydrodefluorination of **2.70** under the conditions of **ref. 29**.

With neither the conditions of Lalic and Prakash being suitable, the works of both König and Jui served as a starting point. Exposing our model substrate to the reaction conditions of König's protocol in absence of alkene, no product formation was observed (**Scheme 2.15A**). Similarly, the conditions of Jui and co-workers in absence of alkene led to no product conversion (**Scheme 2.15B**).[26] In all cases, the starting material was mostly recovered.

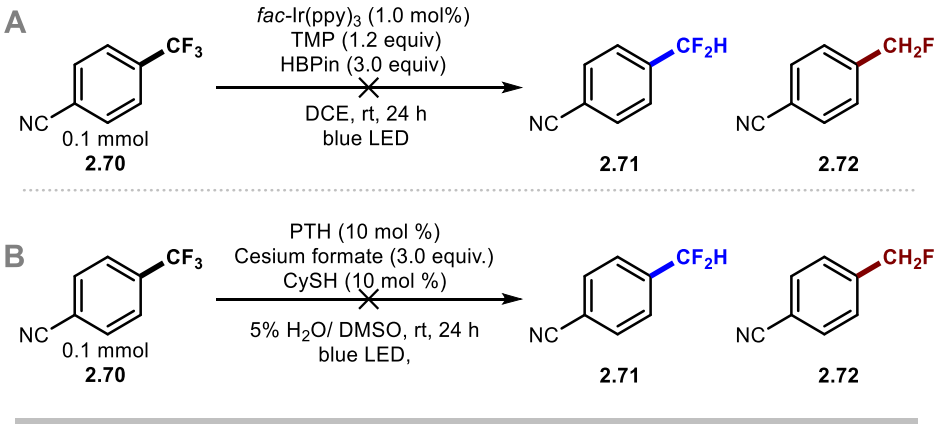

Scheme 2.15 Attempted hydrodefluorination of **2.70** under the conditions of **ref. 26** and **ref. 27** in the absence of alkene.

These findings illustrated the need for a new photoredox protocol which would allow access to **2.71** in high yield and selectivity. From both König and Jui's studies we learned that a PC with a sufficiently high reduction potential can reduce electron deficient trifluoromethylarenes. We knew that a SET process facilitated by such a PC would result in a radical anion which undergoes spontaneous mesolytic cleavage, generating a C-centered difluorobenzylic radical in the process. The electrophilic nature of this difluorinated benzylic radical derived from electron-deficient **2.70** encouraged us to conduct an optimisation study examining HAD reagents other than cesium formate and CySH employed in Jui's defluoroalkylation protocol. A selection of HAD reagents were screened as additives, using conditions analogous to those employed by König and co-workers (**Scheme 2.15A**).

Reaction procedure: To an oven-dried 8 mL screw top reaction tube, equipped with a stirrer bar, a photoredox catalyst (0.0025 mmol, 2.5 mol%) was added. To this reaction tube was added: **2.70** (0.1 mmol, 1 equiv.), varying amounts of hydrogen atom transfer donor, and TMP (0.12 mmol, 1.2 equiv). The reaction tube was capped and further diluted with 1,2-dichloroethane to afford a 0.1 M reaction mixture. The mixture was

sparged with nitrogen for 2 minutes and then placed 5 cm away from a UFO Blue (460 - 470 nm) LED Grow Light 'Morbo' – 50 Watt photobox, stirred and irradiated for an appropriate time at room temperature. After the reaction time, internal standard was added (0.1 mmol of 4-fluoroanisole from a 1 M stock solution in $CDCl_3$) to the crude reaction mixture, further diluted with $CDCl_3$ and analysed by quantitative ^{19}FNMR and GC-MS.

Initial optimisation reaction results indicated, as expected, that the nature of the HAD reagent was critical to observe HDF (**Table 2.1**). $(TMS)_3SiH$ and cesium formate (**2.74**) employed by Jui led to no or only trace amounts of **2.71** (**Table 2.1**, entries 1 and 2). However, when 4-hydroxythiophenol (4-HTP) was used as HAD reagent, selective mono HDF of **2.70** could be achieved yielding **2.71** and **2.72** in a combined yield of 20% (9:1) (**Table 2.1**, entry 2). When substituting 4-HTP for 1,4-cylohexadiene (**2.75**) (**Table 2.1**, entry 4) or the Hantzsch ester (**2.76**) (**Table 2.1**, entry 5), trace to no product was observed. Further experiments indicated that only thiophenol derivatives containing substituents with a negative hammett parameter (σ_p) resulted in moderate product formation (**Table 2.1**, entries 3, 9 and 10). An increased yield of 38% (5:1) was obtained when the loading of TMP and 4-HTP was increased to 3.0 equivalents (**Table 2.1**, entry 11). Interestingly, unlike the conditions of Lalic and Prakash, the fully reduced product was not observed by GC-MS analysis of the crude reaction mixture under the conditions of entry 11. Increasing the reaction time to 60 hours did not result in an increased combined yield of **2.71** and **2.72** (**Table 2.1**, entry 12). This, in addition to a lack of luminescence of the reaction mixture under blue light, could indicate that catalyst deactivation took place.

Table 2.1 Optimisation studies investigating the effect of the hydrogen atom donor.

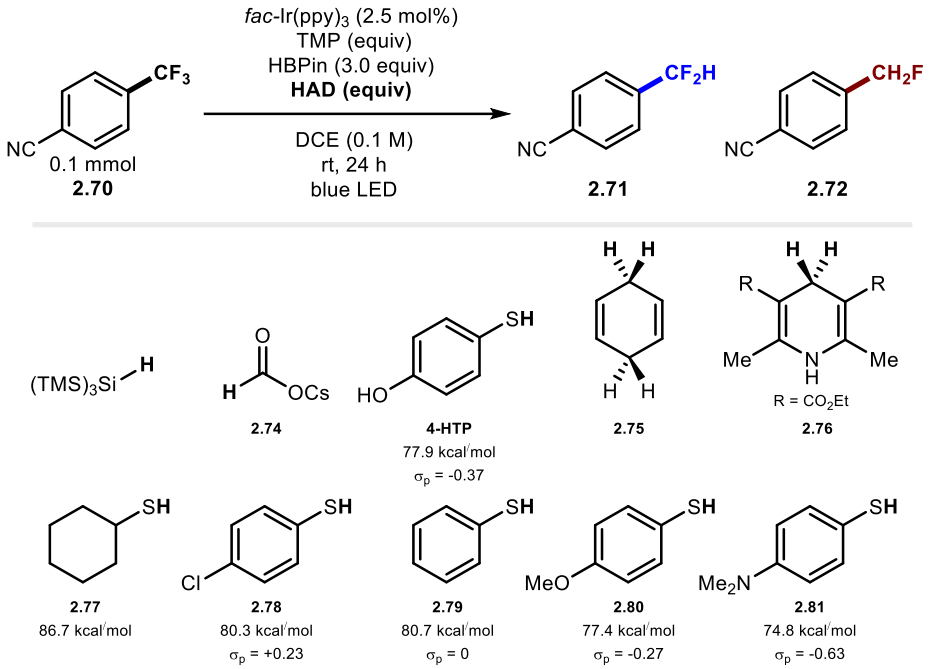

Entry[a]	HAD	2.71	2.72	2.71:2.72
1	2.73	0%	0%	-
2	2.74	Trace	-	-
3	**4-HTP**	**18%**	**2%**	**9:1**
4	2.75	Trace	-	-
5	2.76	0%	0%	-
6	2.77	3%	1	3:1
7	2.78	Trace	-	-
8	2.79	5%	1%	5:1
9	2.80	8%	1%	8:1
10	2.81	9%	1%	9:1
11	**4-HTP**	**32%**	**6%**	**5:1**
12	**4-HTP**	**30%**	**6%**	**5:1**

[a]Reaction performed with HAD reagent (0.12 mmol, 1.2 equiv) and base (0.1 mmol, 1.0 equiv). [b]Reaction performed with HAD reagent (0.3 mmol, 3.0 equiv) and base (0.3 mmol, 3.0 equiv). Reactions analysed with ^{19}FNMR and GC-MS with 4-fluoroanisole as internal standard. *Abbreviations:* 4-HTP = 4-hydroxythiophenol, TMP = 2,2,6,6-tetramethylpipyridine. [b]reaction time = 60 hours.

A variety of bases and additives were screened. TMP was the best base with no improvement observed when alternative organic nitrogen-containing bases were used (**Table 2.2**).

Table 2.2 Optimisation studies investigating the effect of the base.

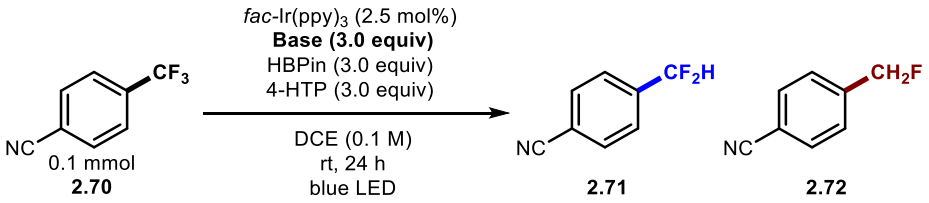

Entry	Base	2.71	2.72	2.71:2.72
13	Et_3N	12%	7%	2:1
14	DIPEA	12%	4%	3:1
15	TMEDA	19%	15%	1:1
16	DBU	14%	11%	1:1
17	TMP	21%	4%	5:1
18	Et_3N	23%	9%	3:1
19	DIPEA	14%	2%	7:1
20	TMEDA	17%	12%	1:1
21	DBU	14%	12%	1:1
11	**TMP**	**32%**	**6%**	**5:1**

Reaction performed with HAD reagent (0.3 mmol, 3.0 equiv) and base (0.3 mmol, 3.0 equiv). Reactions analysed with ^{19}F-NMR and GC-MS with 4-fluoroanisole as internal standard. *Abbreviations:* 4-HTP = 4-hydroxythiophenol, TMP = 2,2,6,6-tetramethylpipyridine.

A variety of solvents and co-solvents were screened (**Table 2.3**). DCE was found to be optimal, although other solvents were tolerated as co-solvents. Chlorinated solvents such as DCE, DCM, 1,2-DCB and chlorobenzene were the only solvents which resulted in conversion towards **2.71**. The tolerance of co-solvents was beneficial for substrates that were otherwise not sufficiently soluble. One common by-product observed in our screening reactions with DCE comes from an S_N2 reaction between the anion of 4-HTP and DCE affording 4-[(chloromethyl)thio]phenol (**Scheme 2.16**). This, however, was only a minor side-product which was later almost supressed entirely by lowering the concentration of the reaction mixture.

Table 2.3 Optimisation studies investigating the effect of solvent.

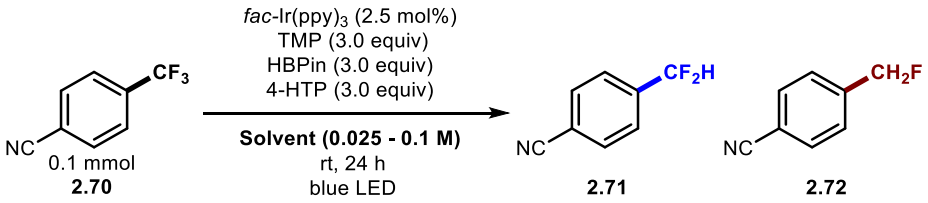

Entry	Solvent	2.71	2.72	2.71:2.72
22	DCE/EtOH	10%	1%	-
23	DCM	13%	5%	-
24	DCE/H_2O	22%	6%	4:1
25	DMF	1%	0%	-
26	1,2-DFB	9%	2%	5:1
27	TFT	4%	0%	-

28	PhCl	12%	2%	6:1
29	1,2-DCB (0.1 M)	12%	2%	6:1
30	1,2-DCB (0.025 M)	15%	3%	5:1
31	DCE/HFIP	25%	6%	4:1
11	**DCE**	**32%**	**6%**	**5:1**

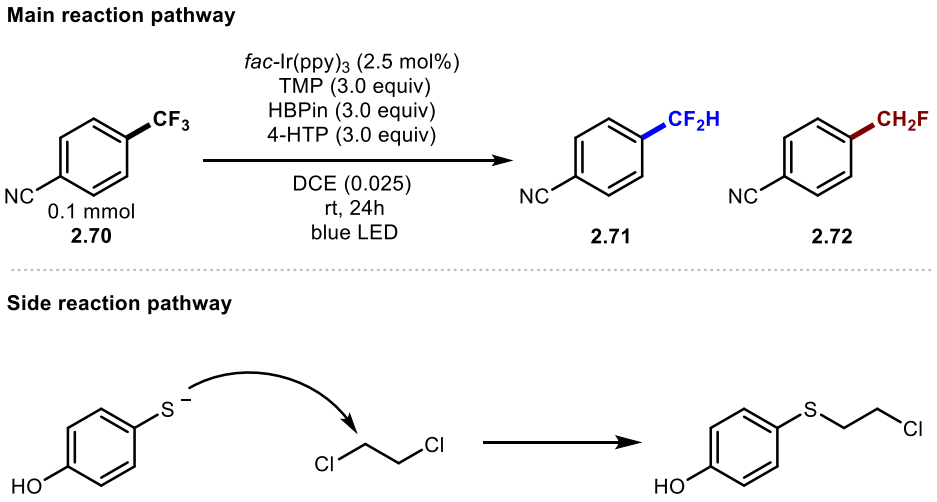

Scheme 2.16 Side reaction pathway between the anion of 4-HTP and DCE.

2.9 Further Optimisation via Design of Experiment

With the optimised conditions in hand, we next performed a design of experiment (DOE) high throughput-screening (HTS) to further improve conversion and selectivity towards **2.71**.

2.9.1 General Considerations

HDF reactions were performed in HTS format using a Lumidox 96-well plate (**Figure 2.7**). The scale of each reaction was 2.5 µmol. All screening reactions were run using 30 mA/470 nm light. The stirring rate was set to 1150 rpm.

Procedure: A stock solution of reaction mixture was prepared in a nitrogen filled glovebox and an aliquot (25 µL) was added in each vial. The vials were transferred into an argon-filled glovebox and DCE was added. Aliquots (25 µL) of the resulting stock solutions were added to the corresponding vials. All conversions are calculated with respect to *n*-tetradecane as internal standard and not corrected with response factors. Samples of crude mixtures were analysed by GC-FID/MS. HTS experiments were primarily used to evaluate trends, not to provide absolute yields.

Figure 2.7 Pictures of the Lumidox 96-well plate set up used in for HTS experiments.

2.9.2 Base Screening

The base screening confirmed that TMP is a good base for the transformation, although a series of other inorganic and organic bases performed well under analogous reaction conditions. A control experiment without base resulted in no conversion towards the desired product, indicating that the addition of base was essential for HDF (**Figure 2.8**).

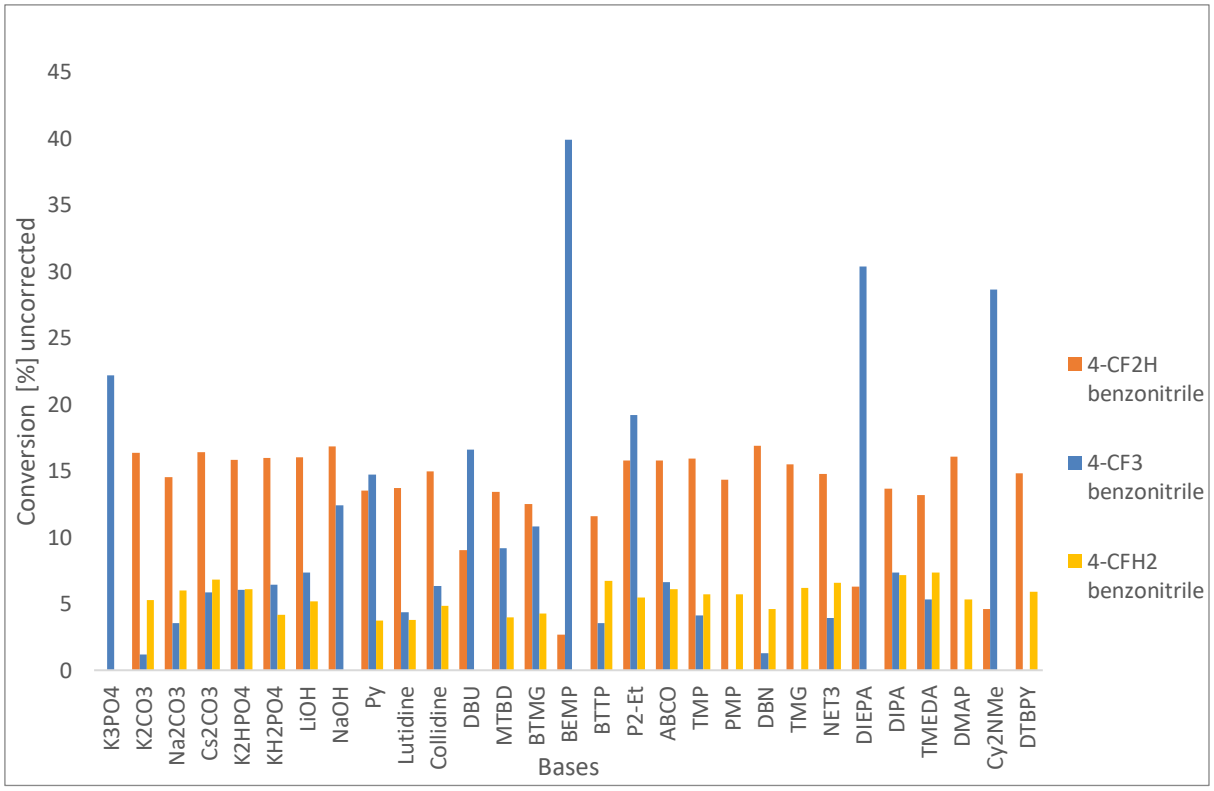

Figure 2.8 High throughput screening investigations examining the effect of base on reactivity and selectivity.

2.9.3 Photocatalyst Screening

Next, the effect of the PC was investigated. As expected, only PCs with a sufficiently high reduction potential were able to catalyse HDF (**Figure 2.9**). Organophotocatalyst 2,4,5,6-tetrakis(diphenylamino)isophthalonitrile (4-DPA-IPN) was identified as a suitable metal-free replacement for $[Ir(ppy)_3]$. Interestingly, Miyake phenoxazine, another commonly used organophotocatalyst, gave significantly less conversion to desired product (low conversion of starting material), despite having a higher reduction potential. This observation can possibly be explained by an increased rate of catalyst deactivation compared to 4-DPA-IPN or $[Ir(ppy)_3]$.

2.9.3 Photocatalyst Screening

With the discovery of 4-DPA-IPN as a suitable metal-free replacement for [Ir(ppy)$_3$], we re-evaluated the reaction conditions of our HDF protocol with 4-DPA-IPN as catalyst. Low catalyst loadings of 0.25 mol% were found to be optimal. Increasing the loading to 2.5 mol% did not lead to an increased combined conversion of **2.71** and **2.72**. Control experiments indicated that the photocatalyst, HAD, base, and blue light are all essential components for this transformation to proceed. In the absence of PMP, a slight decrease in yield was observed (**Table 2.4,** entry 3); in the absence of TMP, the conversion decreased to 31% (**Table 2.4,** entry 4). In the absence of base, **2.71** was not detected (**Table 2.4,** entry 5). Removal of the light source, 4-HTP or photocatalyst all prevented HDF (**Table 2.4,** entries 6-8).

Table 2.4 Optimisation and control reactions with 4-DPA-IPN as photocatalyst.

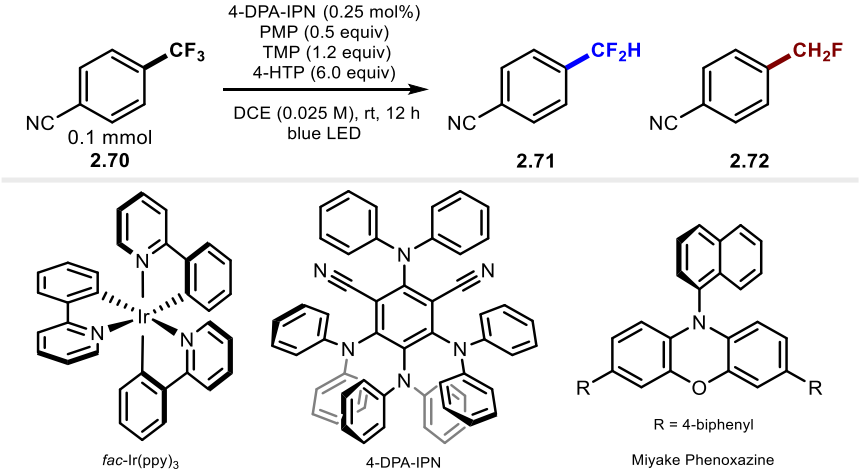

Entry	Alterations to conditions	Yield[a] (ratio 2.71:2.72)
1	4-DPA-IPN (2.5 mol%)	62% (5:1)
2	**No alteration**	**65% (5:1)**
3	no PMP	51% (5:1)
4	no TMP	31% (>20:1)
5	no TMP and no PMP	0%
6	no light	0%

7	no 4-HTP	0%
8	no photocatalyst	0%

2.10 Synthesis of 4-DPA-IPN

Having elected 4-DPA-IPN as the optimal PC for HDF, it is noteworthy to point out that the synthesis of 4-DPA-IPN proved unsuccessful under the conditions originally reported in the literature. Zhang and co-workers prepared 4-DPA-IPN in a single step from tetrafluoroisophthalonitrile and diphenylamine through an S_NAr reaction.[32] In our hands, however, this protocol led only to traces of 4-DPA-IPN (<1%). Instead, we obtained 2,4,6-tris(diphenylamino)-5-fluoroisophthalonitrile (**3-DPAFIPN**) in high selectivity and yield (**Scheme 2.17A**). Full-characterisation by ^{13}C NMR and ^{1}H NMR, and a distinctive ^{19}F NMR signal at -121.30 ppm confirmed the identity of **3-DPAFIPN**. In order to successfully access 4-DPA-IPN, we reoptimised the original conditions and successfully obtained 4-DPA-IPN by employing the conditions outlined in **Scheme 2.17B**.

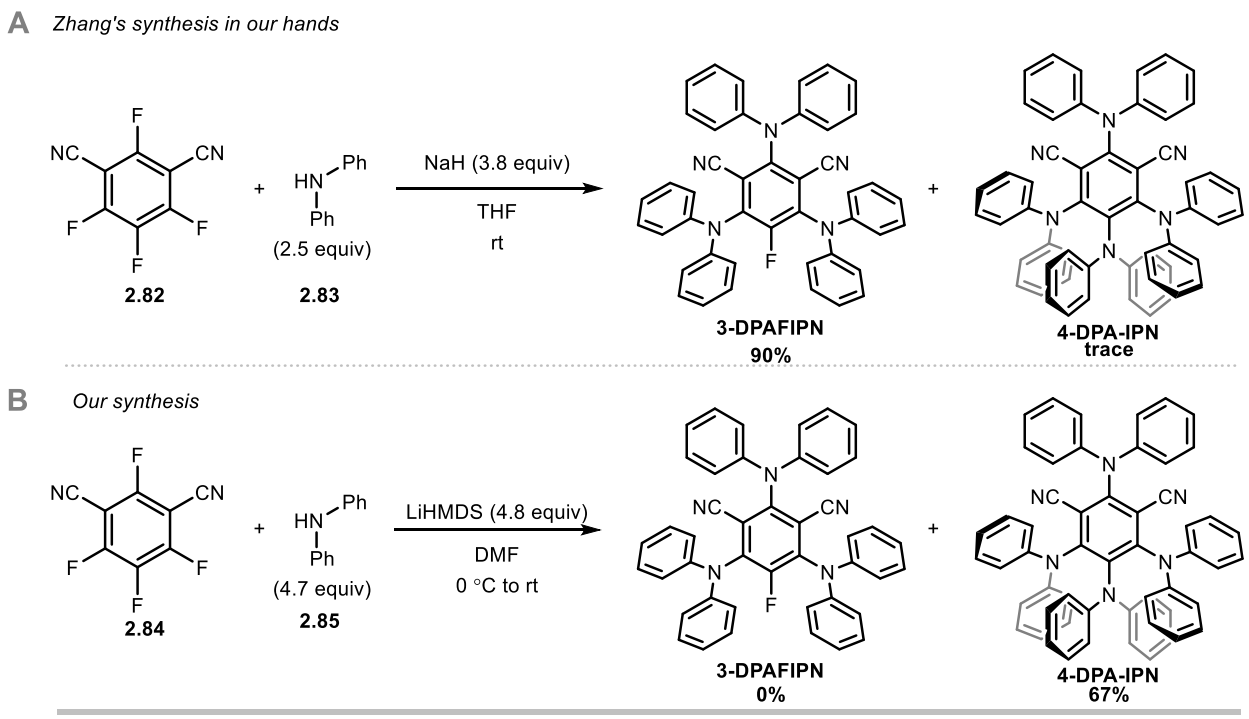

Scheme 2.17 A) Synthesis of 4-DPA-IPN following the protocol in **ref. 32** in our hands. B) Modified synthesis of 4-DPA-IPN.

Prior to the publication of the work outlined in this chapter, the Waser group employed a similar strategy to the one depicted in **Scheme 2.17B** to access 4-DPA-IPN.[33] In addition to reassigning the structure of 4-DPA-IPN by NMR and HRMS, Waser and co-workers also disclosed the crystal structure of 4-DPA-IPN. Our spectral data were consistent with Waser and co-workers. ^{19}F NMR analysis confirmed the absence of fluorine in the compound that was formed and isolated.[33]

2.11 Scope

2.11.1 Scope of Small Molecule Trifluoromethylarenes

With the optimal reaction conditions in hand (**Table 2.4, entry 2**), we explored the generality of our HDF reaction towards electron-deficient trifluoromethylarenes on a 0.1 mmol scale. 2-(Trifluoromethyl)benzonitrile gave **2.86** in 63% yield and >20:1 selectivity in favour of the mono hydrodefluorinated CF_2H product (**2.86**). This observation was confirmed by the characteristic ^{19}F NMR shift at -113.21 ppm with corresponding $^{2}J_{H\text{-}F}$

coupling constant of 55.9 Hz. The relative selectivity between CF_2H and CH_2F products was determined through integration of the ^{19}F NMR signals corresponding to the CF_2H product (doublet, -113.21 ppm $^2J_{H-F}$ coupling constant of 55.9 Hz) and the signal attributed to the CH_2F product (triplet, -215.1 ppm, $^2J_{H-F}$ = 46.8 Hz). Additional functionalities on the aromatic ring including fluorine, acetamido, and methoxy with a ten-fold increased PC loading for the latter were tolerated and the corresponding products isolated in good yields (**2.87**, **2.91** and **2.89**, 42-88%) and in high selectivity for CF_2H (>10:1). Methyl and ethyl-4-(trifluoromethyl)benzoate which contain a carboxylic ester in place of a cyano group, were readily transformed into CF_2H analogues **2.88** and **2.92** in moderate yields (30% and 40%) and moderate selectivity (3:1). Interestingly, increasing the catalyst loading ten-fold to 2.5 mol% gave preferentially the CH_2F analogue resulting from double reductive defluorination of **2.92** (**CF_2H vs CH_2F** = 1:2). 4-(Trifluoromethyl)benzenesulfonamide, which contains an unprotected sulfonamide functionality, was within reach and readily underwent mono-hydrodefluorinated to afford **2.90** with excellent selectivity (>20:1) (**Scheme 2.18**). Electron-poor trifluoromethylarenes which were incompatible under the optimised reaction conditions include 1,3-bis(trifluoromethyl)benzene, diethyl (4-(trifluoromethyl)phenyl)-phosphonate and 5-(trifluoromethyl)picolinonitrile, all of which gave no or only traces of the HDF products **2.93** – **2.95**. Instead of **2.93** and **2.94**, CF_3 starting materials were recovered. For the reaction towards **2.95**, several singlet signals were observed ~ -63 ppm (^{19}F NMR), characteristic for (het)ArCF_3 signals. This observation indicates possible starting material decomposition.

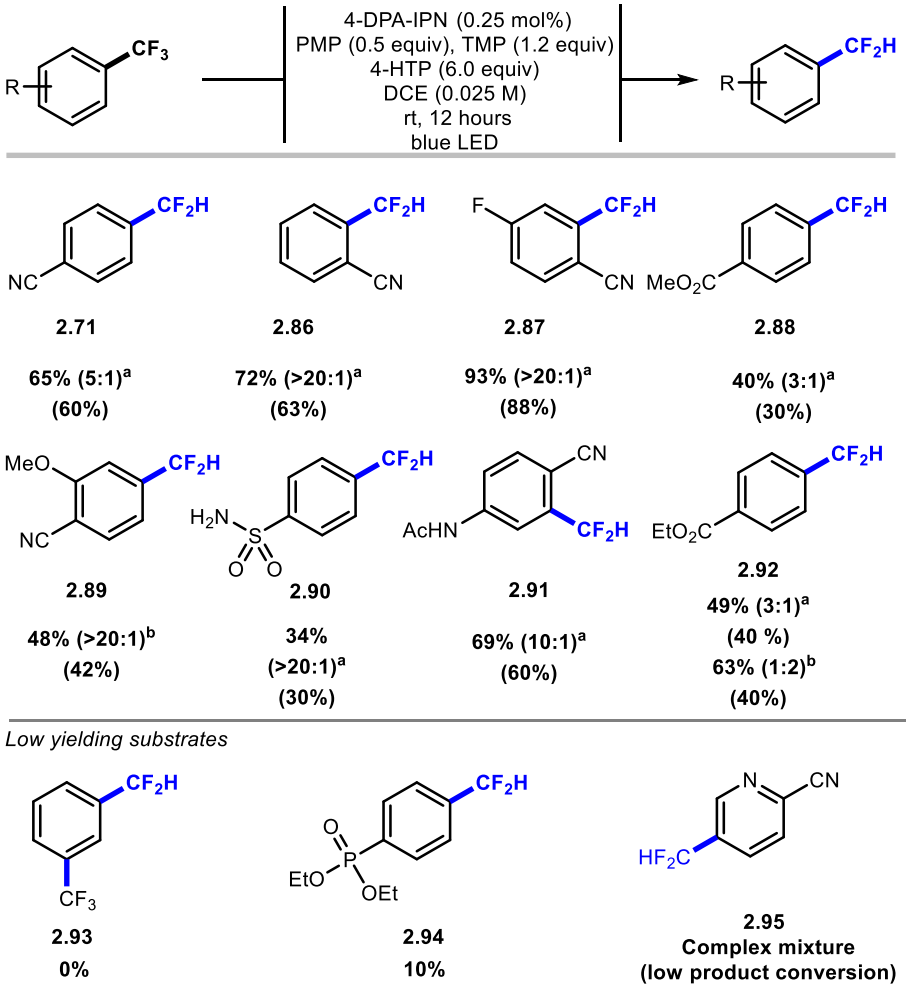

Scheme 2.18 Scope of HDF (with simple trifluoromethylarene building blocks). [a]Yields and CF_2H/CH_2F ratio determined by quantitative ^{19}F NMR spectroscopy using 4-fluoroanisole as internal standard. Yields of isolated products (RCF_2H only) are given in parentheses. [b]2.5 mol % of 4-DPA-IPN.

2.11.2 Scope of CF_3-Containing Biologically Active Molecules

Complex molecules with biological relevance were examined next. We decided to use our results on the HDF of small molecules as a guide to successfully perform this reaction on a selection of CF_3-containing drug molecules. If successful, this would provide access to the CF_2H analogues of these drugs, many of which being either previously inaccessible, or requiring multi-step synthetic routes for their preparation.

Bicalutamide, a drug used to treat prostate cancer, underwent reductive defluorination affording **2.96** isolated in 43% yield and 10:1 CF_2H/CH_2F selectivity.[34] The doubly trifluoromethylated cannabinoid receptor agonist BAY 59-3074 reacted exclusively at the arene site with complete chemoselectivity. The chemoselectivity can be explained by the preferential SET reduction of the aromatic ring, where the π-system acts as an electron sink for single electron reduction. An analogue of Enobosarm featuring three trifluoromethylaryl groups served the purpose to investigate a more complex case of "arene versus arene" chemoselectivity.[35] HDF occurred with excellent CF_2H/CH_2F selectivity (> 20:1) at a single site, leaving the 3,5-bis(trifluoromethyl)arene motif untouched (**2.98**, 53%). This result corroborates a control experiment that demonstrated 3,5-*bis*-trifluoromethylbenzene to be unreactive under our reaction conditions. Having found that 4-(trifluoromethyl)benzenesulfonamide was a viable substrate for our HDF protocol, we were interested to see whether trifluoromethylarene drug molecules substituted with sulfonamides, such as bendroflumethiazide, a drug used for mild heart failure and hypertension *via* vasodilation, is a viable substrate for our HDF technology.[36] Subjecting Bendroflumethiazide to a slightly modified protocol (solvent mixture DCE/DMSO to aid solubility) gave CF_2H-bendroflumethiazide (**2.99**) in 56% yield although with decreased selectivity (CF_2H:CH_2F ratio = 4:1). This result is significant because sulfonamides and/or amines can chelate metals such as copper, rendering late stage cross-coupling strategies towards aryl–CF_2H bond construction more challenging.[37] Enzalutamide, a hormonal therapy drug used to treat prostate cancer also underwent HDF. This reaction yielded **2.100** in 40% yield and in excellent selectivity (>20:1). The usefulness of this HDF protocol was further illustrated with the

synthesis of **2.101**, a molecule with strong androgen receptor binding affinity *in vivo*. This biologically relevant compound was previously prepared in eight steps. With our protocol, **2.101** was obtained in two steps; the CF_3 precursor was prepared in one step from commercially available materials, and HDF gave **2.101** isolated in 60% yield (**Scheme 2.19**).[38] Alternative HDF protocols were not successful to access **2.101**.

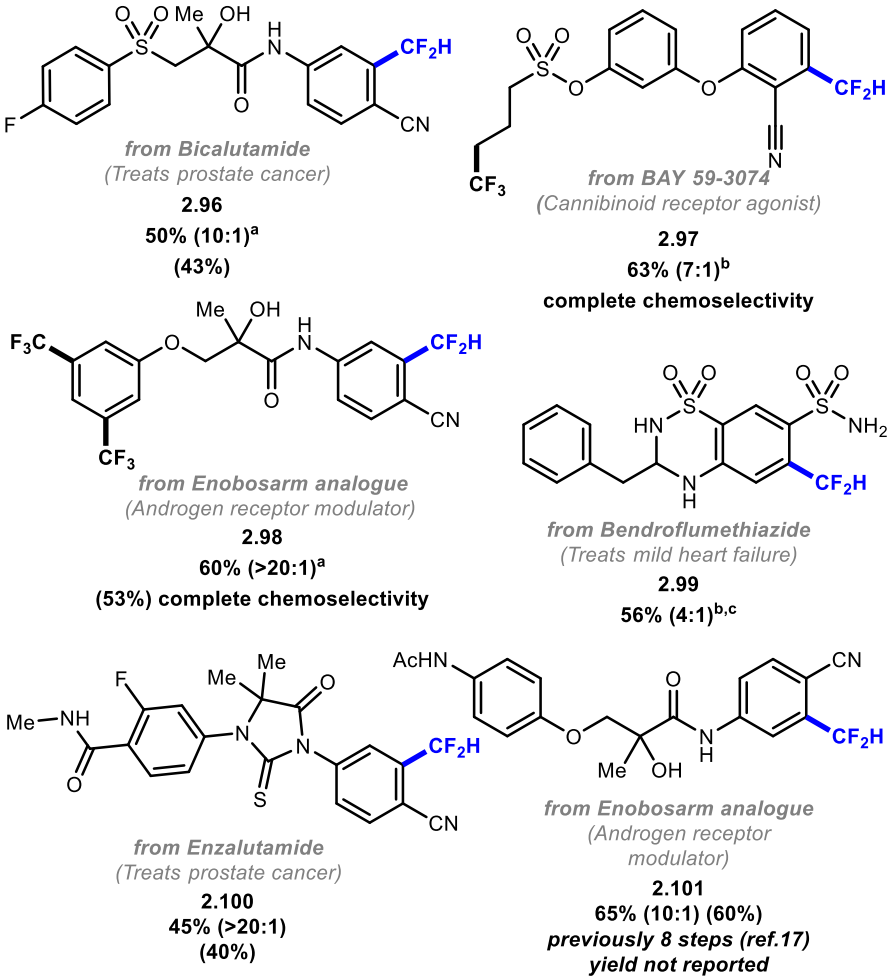

Scheme 2.19 Scope of HDF (biologically active trifluoromethylarenes). [a]Yields and CF_2H/CH_2F ratio determined by quantitative ^{19}F NMR spectroscopy using 4-fluoroanisole as internal standard. Yields of isolated products (RCF_2H only) are given in parentheses. [b]2.5 mol% 4-DPA-IPN. [c]Solvent is DCE/DMSO (19:1 v/v, c = 0.025 M).

2.11.3 Purification

Due to similarities in polarity, several of the CF_2H products had to be purified by reverse-phase preparative HPLC using a Synergi C-18 HYDRO-RP prep column. In all cases, the peaks corresponding to the parent compound and the products of mono- and bis-HDF were readily separated in an eluent mixture of acetonitrile and water.

2.11.4 Determination of Chemoselectivity

In the case of BAY 59-3074 which possess two CF_3 groups (one aliphatic and one aromatic) and an analogue of enobosarm which features three trifluoromethyl groups, we studied the implications towards chemoselectivity for the reactions towards **2.97** and **2.98**. To assign chemoselectivity, we used quantitative ^{19}F NMR analysis. The distinct multiplicity and chemical shift of the alkyl CF_3 group versus the aromatic CF_3 peak allowed us to determine through relative integration, the overall chemoselectivity of the reaction. From the crude mixture of the reaction towards **2.97**, it was evident that only a single CF_2H species had formed (**^{19}F-NMR:** (376 MHz, Chloroform-*d*) δ -112.48 (d, *J* = 54.6 Hz, 2F)). This provided us with the information that either the aliphatic or aromatic CF_3 moiety was reduced selectively. To determine which of the two moieties was reduced, we analysed the peaks corresponding to the CF_3 entities. The CF_3 peak corresponding to the starting material (**^{19}F-NMR** (376 MHz, Chloroform-*d*) δ -66.17 (s, 3F)) had an identical integration pattern as one of the two overlapping multiplets corresponding to the alkyl CF_3 groups. This allowed us to infer that it was the aromatic CF_3 group which was selectively reduced (**Figure 2.10**).

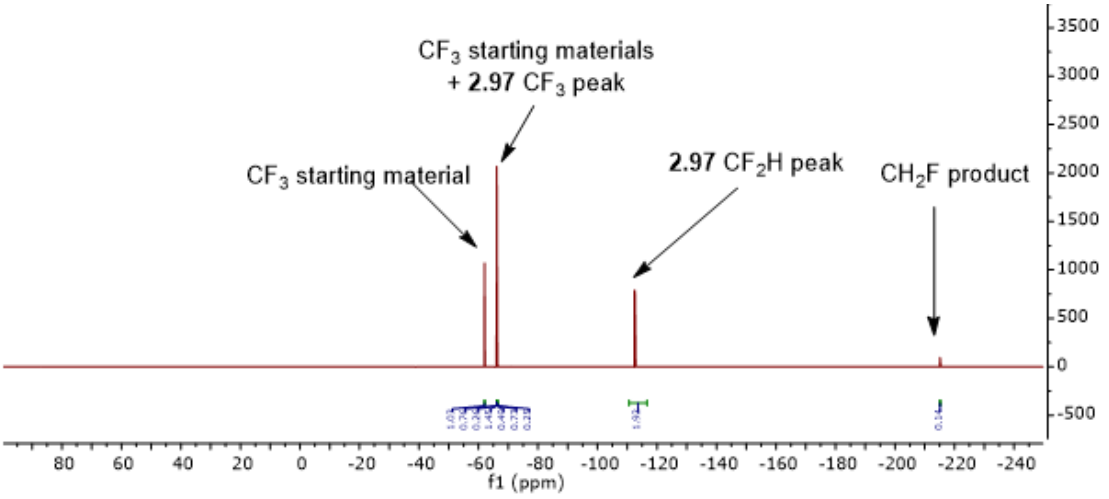

Figure 2.10 ^{19}F NMR analysis of **c**rude reaction mixture towards **2.97**.

Next we investigated the chemoselectivity of the reaction towards **2.98**. A previous experiment which illustrated that 3,5-*bis*-trifluoromethylbenzene was unreactive under the optimised reaction conditions, provided an indicator that chemoselective HDF could be feasible at the CF_3 site *ortho* to the cyano functionality. With this information at hand, we analysed the crude reaction mixture towards **2.98**. Analogously to the reaction of BAY 59-3074, a single CF_2H product was observed (**^{19}F NMR** (376 MHz, Chloroform-*d*) δ -112.47 (d, *J* = 54.6 Hz)), indicating complete chemoselectivity. To determine which CF_3 group had been selectively reduced, we integrated the distinct peaks in the CF_3 region of the ^{19}F NMR spectrum. Through relative integrations, we assigned the peak at δ -62.25 (s) as the peak corresponding to unreacted CF_3 starting material. The peak at δ -63.08 (s) was determined as the combined 3,5-*bis*-CF_3 fragments of the CF_3 starting material and **2.98**. Upon isolation of the product, we confirmed that the reaction towards **2.98** was chemoselective and that only the CF_3 group positioned ortho to the cyano group was reduced (**Figure 2.11**).

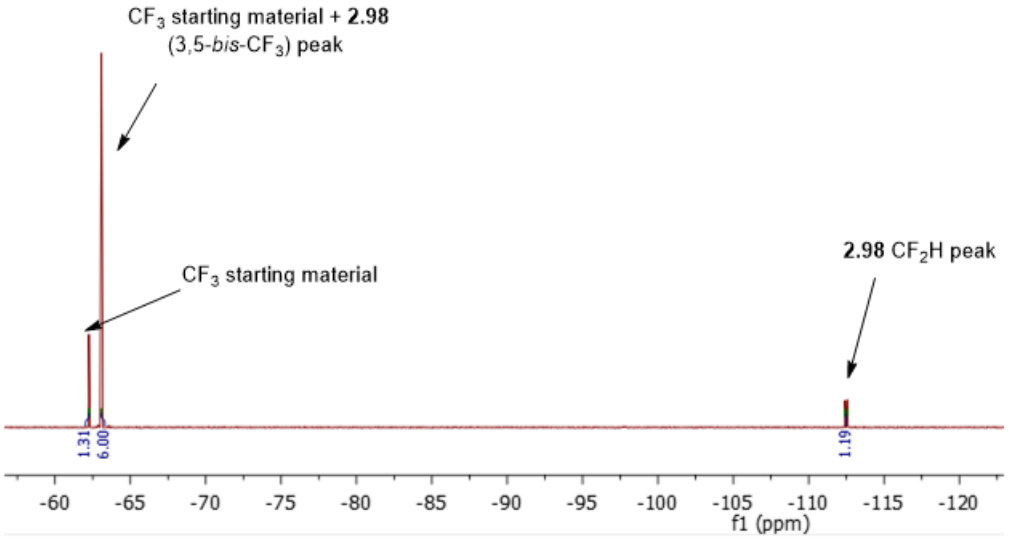

Figure 2.11 Crude mixture of reaction towards **2.98**.

2.12 Robustness Screening

The synthesis of complex drug molecules is a timely endeavour. Given that the attrition of small molecules in drug development is high, route design helps minimize the risk of late-stage failure in multi-step syntheses. Typically, basic or acidic functional groups and heterocycles which coordinate to metals cause chemical reactions to fail unexpectedly. Glorius and co-workers have explored robustness screening as a tool to evaluate the likely success of a chemical reaction before it is performed.[39,40] Such an approach can be especially useful for predicting the reactivity of complex scaffolds which may be time-consuming or expensive to prepare. In a typical robustness screening reaction, the model reaction, in this case the HDF reaction of **2.70** under optimised conditions, is performed in the presence of one equivalent of heterocycle. The functional group robustness factor can then be quantified (**Equation 1**).

Equation 1: $(100)x\frac{Yield\ with\ additive}{Yield\ in\ absence\ of\ additive}$

While the determination of the functional group robustness is not a substitute for assessing the scope of a reaction, spiking of additives (in this case functionalized heterocycles) to the reaction mixture does emulate the presence of that heterocycle within a target molecule (**Figure 2.12**).

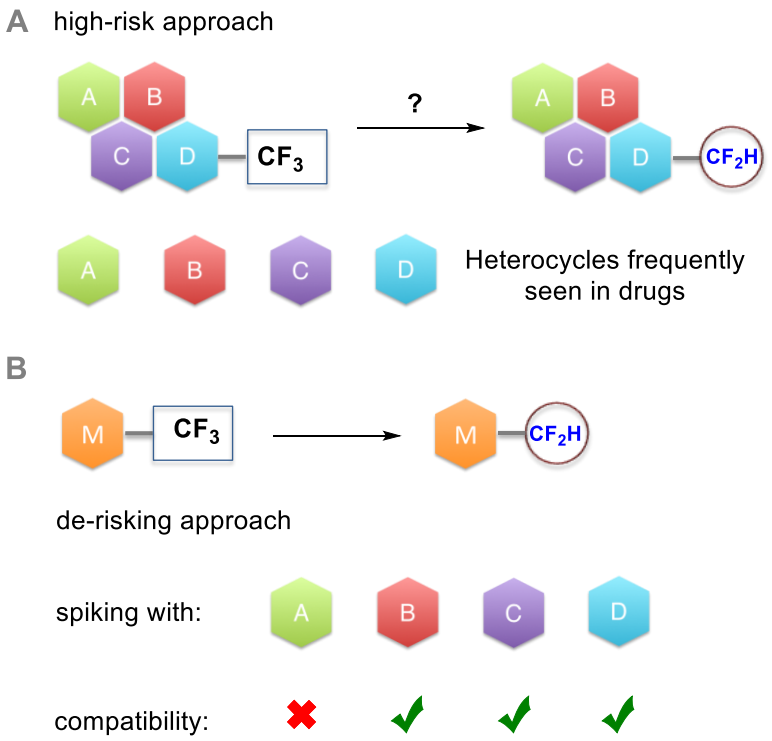

Figure 2.12 (A) Late-stage hydrodefluorination of complex targets featuring multiple heterocycles (A, B, C, D) is a high-risk approach. (B) A rapid screen on the compatibility of the reaction of a readily available model substrate (M) in the presence of each heterocycle provides information on feasibility for a final step hydrodefluorination.

Given the relevance of our HDF methodology to drug discovery, we conducted a robustness screening experiment. In order to obtain our data in high throughput, we performed our robustness screening experiments in an HTS fashion with in-line GC-MS analysis of the crude reaction mixtures. This would allow us to evaluate the overall

tolerance of our HDF reaction towards a variety of pharmacophores and reactive functional groups commonly found in pharmaceutical lead structures. First, we investigated the effect of common functional groups by spiking *para*-substituted toluenes **A** to our model reaction. *Para*-substituted toluenes bearing bromo, primary amine, carboxylic acid, alcohol, tertiary amine and aldehyde functionalities were all tolerated, with little to no effect on the reaction yield. Next, we exposed our model reaction to a range of 6-membered *N*-heterocycles such as 2-pyridines **B**, 5-pyrimidines **C**, 3-pyridazines **D**. While 2-pyridines and 5-pyrimidines were broadly tolerated, 3-pyridazines and 2-pyrazines often prevented hydrodefluorination of our model substrate. Five membered heterocycles including isoxazoles **G** and pyrazoles **H** with varying substitution patterns were also well tolerated. In addition, fused heterocycles including pyrazolpyridines **F**, benzooxazoles **I**, benzothiazoles **J**, indazoles **K** and benzimidazoles **L** did not hamper HDF of **2.70**. The broad tolerance to these substituted heterocycles is significant, given the frequency of these motifs in modern pharmaceutical drugs and agrochemicals. Many of the heterocycles investigated in this study contain basic nitrogen atoms which could deactivate transition-metal catalysts by strongly coordinating to the metal through ligand displacement. Furthermore, the tolerance of our protocol towards halides and boronic acids further illustrates the complementarity of our approach to cross-coupling strategies. The tolerance towards aldehydes is also remarkable given that these groups can be converted to CF_2H groups applying deoxyfluorination (**Scheme 2.20**). In conclusion, the experimental findings of our robustness screening indicate that our method serves as a valuable addition to the existing toolbox of synthetic methods currently used to access difluoromethylarenes.

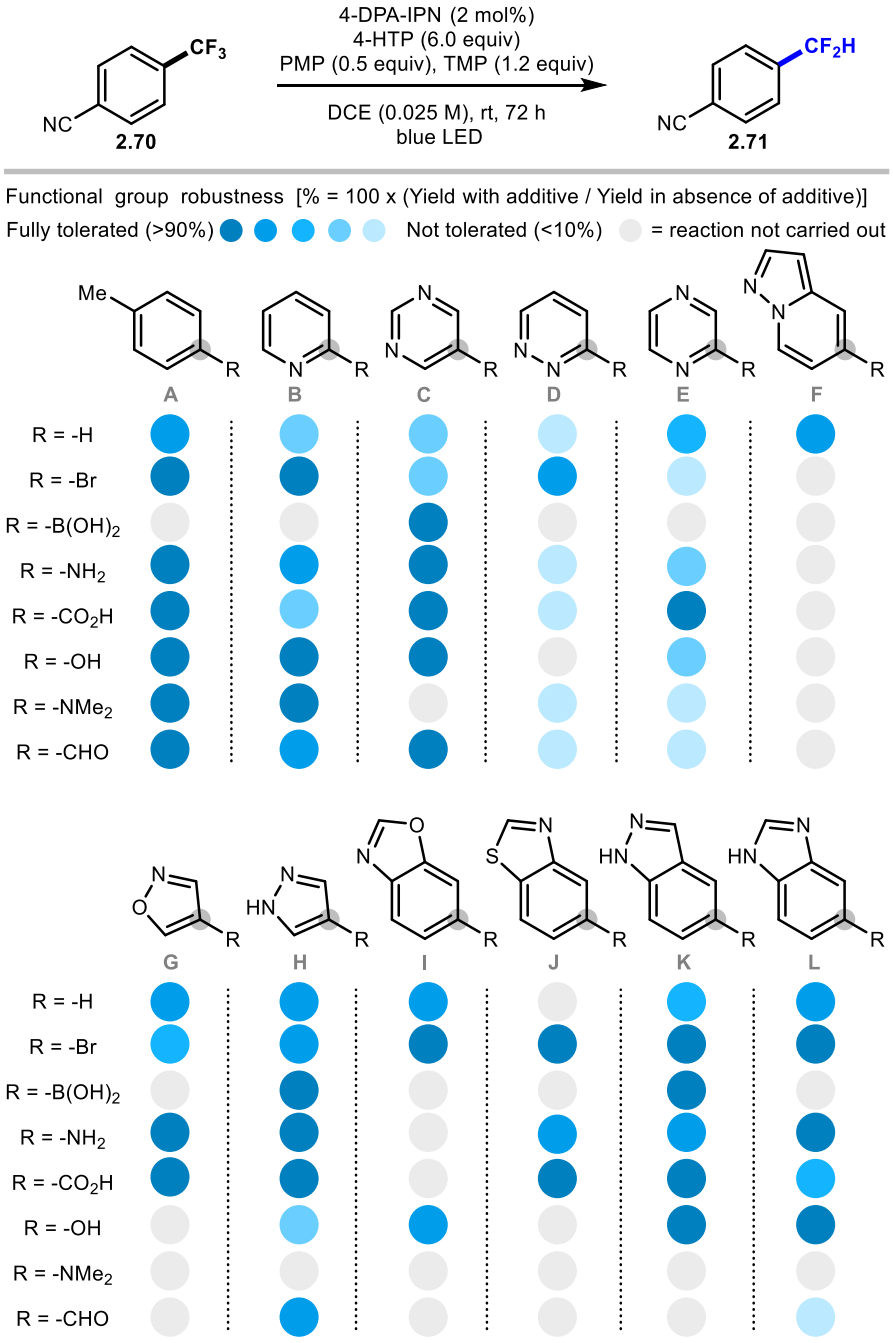

Scheme 2.20 Additive-based screening. [a]All reactions were performed on 2.5 µmol scale in a 96-well plate suited for photoredox chemistry. Crude mixtures were analyzed by GC-FID/MS.

Apart from the robustness factor, another parameter commonly assessed in robustness screening experiments is whether the additive is consumed throughout the reaction. In many cases, providing that the additive was not low in molecular weight, the additive

was detected by GC-MS after the reaction. Quantities of remaining additive were measured qualitatively and not quantified; the results are summarised in **Scheme 2.21**.

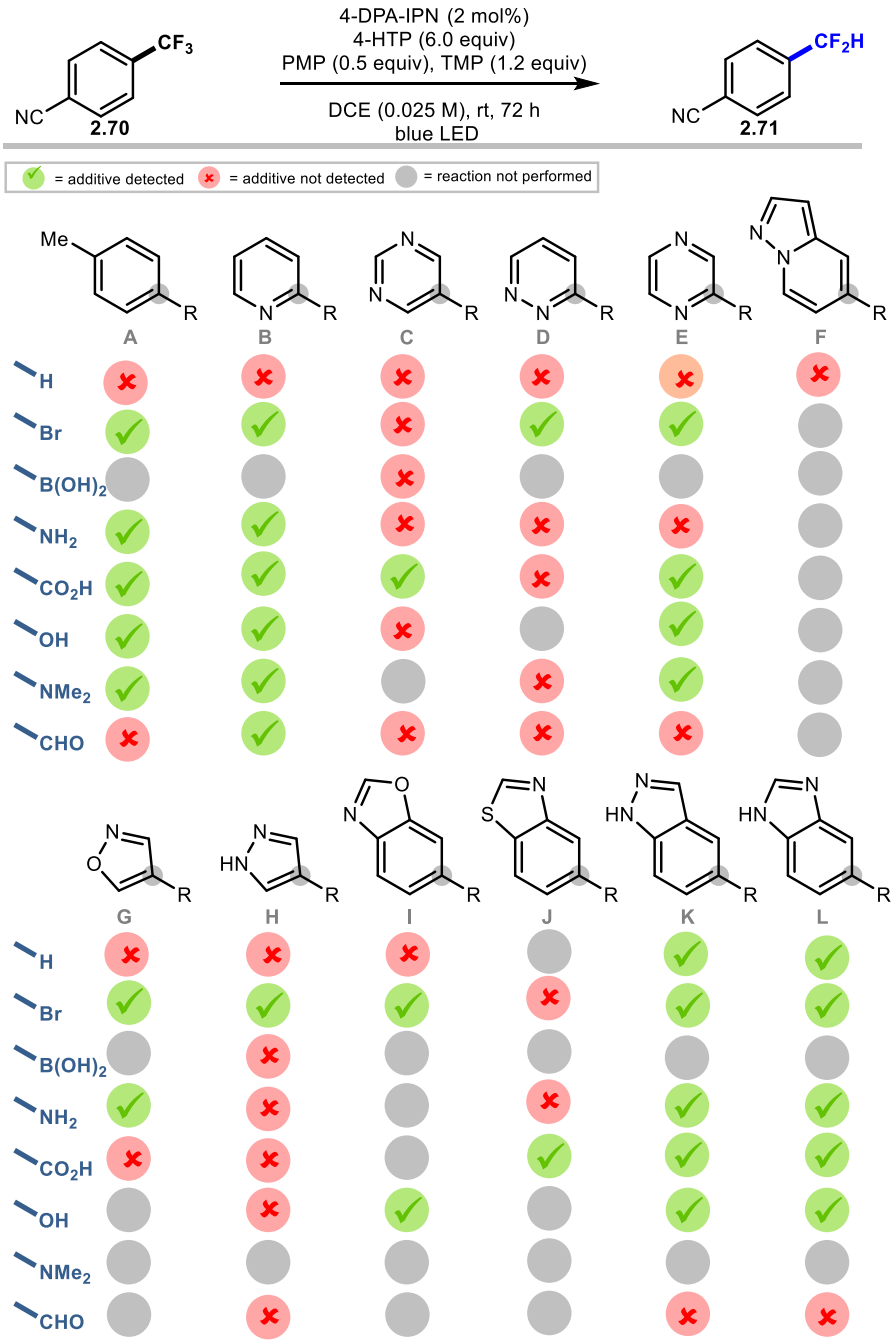

Scheme 2.21 Additive-based screening. [a]All reactions were performed on 2.5 µmol scale in a 96-well plate suited for photoredox chemistry. Crude mixtures were analyzed by GC-FID/MS to determine remaining additive.

2.13 Scaling of the HDF Reaction

One of the limitations of photocatalysis and photochemistry is that such processes may be difficult to scale up due to limited absorption of light (Beer-Lambert law).[41] Furthermore, the low concentration required in our reaction (0.025 M) meant that large batch reactors with minimal depth penetration of visible light were likely to be unsuitable to scale-up our HDF protocol.[42] As such, we considered developing a continuous flow method in order to efficiently scale-up the synthesis of **2.70**. Initial reactions were performed in a microflow system made of a perfluoroalkoxyalkane capillary (internal diameter = 0.5 mm, internal volume = 2.0 mL) on a scale similar to the reactions performed in batch (0.2 mmol); **2.70** could be obtained in 69% yield with a selectivity (CF_2H/CH_2F) of 5:1 with residence time (t_R) of 15 minutes and a flow rate of 0.133 µL/min. Additionally, **2.100** (0.2 mmol) was isolated in 25% yield with 10:1 selectivity after a 7.5 min t_R at a flow rate of 0.266 µL/min. With a flow-protocol in hand, we scaled up the synthesis of **2.70**. Starting with 2.5 g of **2.70** (14.6 mmol), 1.4 g of **2.71** (5:1) was produced in 15 minutes t_R and with a flow rate of 0.133 µL/min (**Scheme 2.22**).

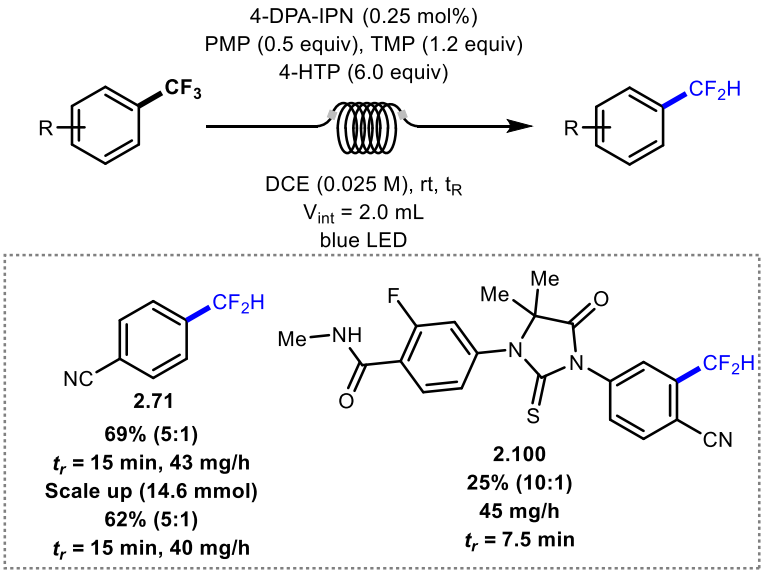

Scheme 2.22 Photoredox HDF under continuous-flow conditions. [a]Yields of isolated products.

2.14 Mechanistic Investigations

2.14.1 Initial Experiments

In order to gain mechanistic insights, control experiments were performed. A radical scavenger experiment performed with TEMPO (**2.102**) led to the formation of the TEMPO-adduct **2.103** which was observed by LC-MS (**Scheme 2.23A**). Moreover, when the reaction of **2.70** was carried out in the presence of five equivalents of styrene (**2.104)**, **2.105** was obtained in 56% yield (**Scheme 2.23B**). Taken together, these results are consistent with the formation of a C-centered difluorobenzylic radical species formed by mesolytic C–F bond cleavage of a primary radical anion. Deuterium enriched 4-cyano difluoromethylbenzene (**2.107**) could be obtained (40% yield, H/D ratio of 3:2) when d_2-4-HTP (**2.106**) was used instead of 4-HTP. The incorporation of deuterium into the final product suggests that 4-HTP is a plausible HAD in this reaction (**Scheme 2.23C**).

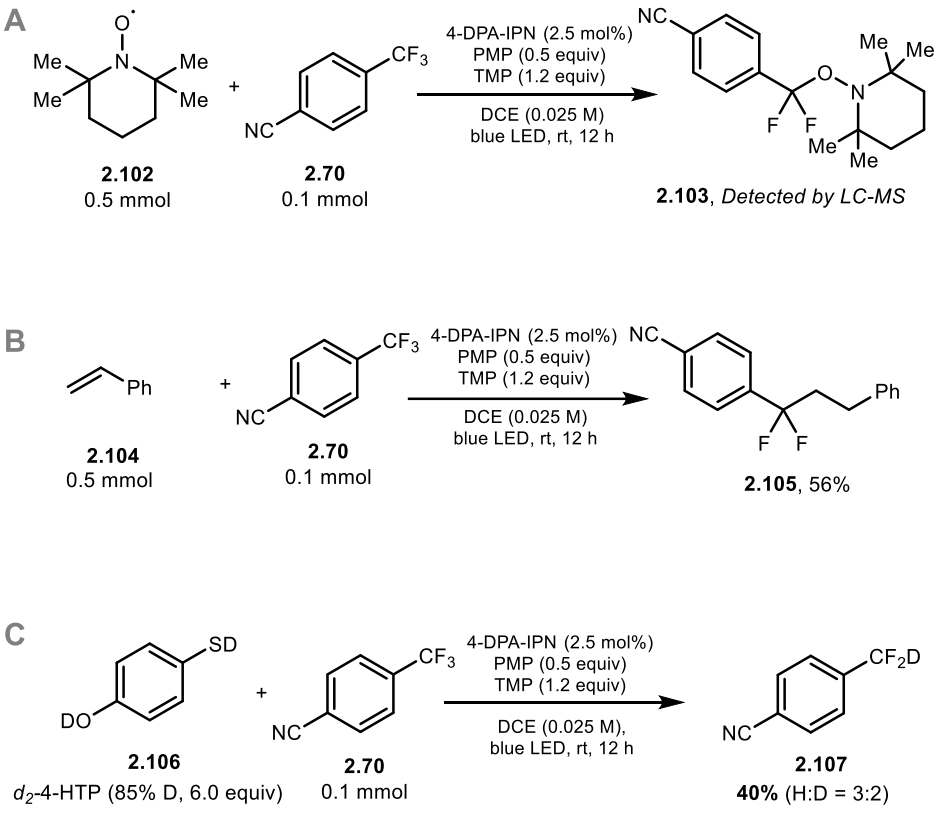

Scheme 2.23 Mechanistic investigations. Yields determined by quantitative ^{19}F NMR using 4-fluoroanisole as internal standard.

2.14.2 Stern-Volmer luminescence quenching experiments

Stern-Volmer luminescence quenching experiments provided additional information on which component in the reaction was quenching the excited state of the PC (**Figure 2.13**). We found that the combination of 4-HTP and TMP (1:1) quenches $*PC^n$. The ability of 4-HTP to quench $*PC^n$ suggests that it has a dual role, acting both as HAD and organic quencher. We also investigated whether other reaction components such as TMP, PMP or trifluoromethylarene **2.70** were able to quench $*PC^n$. Interestingly, cesium formate and $(TMS)_3SiH$, both common HAD reagents were unsuccessful in quenching $*PC^n$. The inability of trifluoromethylarene **2.70** to quench $^*PC^n$ advocates against an oxidative quenching cycle, whereby the radical anion would result from SET involving $^*PC^n/PC^{n+1}$ (-1.28 V).[32]

Stern-Volmer Luminescence Quenching Studies

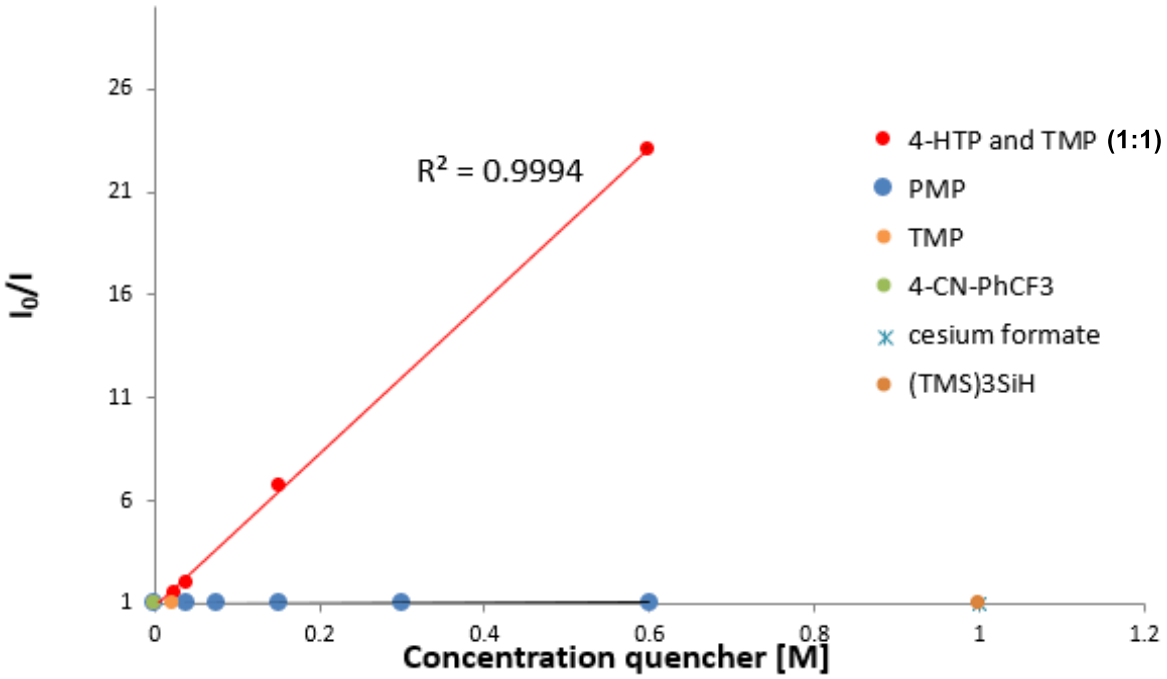

Figure 2.13 Stern−Volmer luminescence quenching studies.

2.14.3 Proposed catalytic cycle

These preliminary findings led us to propose the catalytic cycle shown in **Scheme 2.24** as a plausible mechanistic pathway. Irradiation with blue light affords the excited state catalyst PC*. Under basic conditions, deprotonation of 4-HTP leads to a thiolate (**2.108**) capable of reductive quenching of PC*, a process yielding the corresponding thiyl radical **2.109**, and the reduced PC^{n-1}.[43] In this scenario, the substrate acts as the oxidant to return the PC to its native oxidation state (PC^n/PC^{n-1} = -1.52 V) with concomitant release of the radical anion species that undergoes mesolytic cleavage of fluoride.[32] This latter process leads to the C-centered difluorobenzylic radical **2.112,** which is trapped by the hydrogen bond donor 4-HTP affording the difluoromethylarene **2.71**.

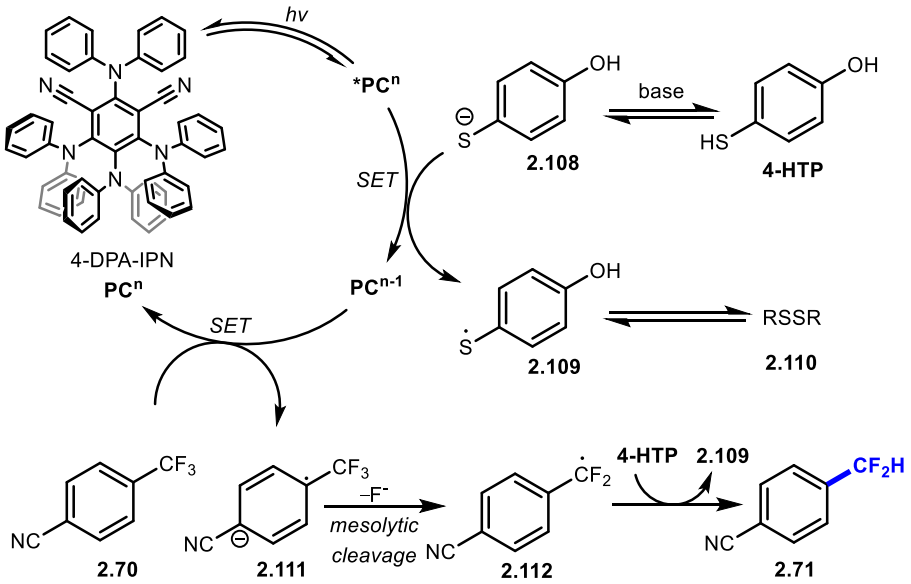

Scheme 2.24 Proposed HDF reaction mechanism.

2.15 Comparison of Our Technology to a Recently Disclosed Photoredox HDF Reaction

During the preparation of the manuscript in which we disclose the work outlined in this chapter, Jui and co-workers published a report on the selective C−F functionalisation of unactivated trifluoromethylarenes. The authors illustrate that in addition to photocatalysed defluoroalkylation, a selection of electron-rich trifluoromethylarenes readily underwent mono-selective HDF under modified reaction conditions (**Scheme 2.25**). Mechanistically Jui's protocol is distinct.[44] While our proposed catalytic cycle relies on a reductive quenching cycle and a ground state reduction process to induce mesolytic cleavage and fluoride expulsion, Jui's HDF reaction proceeds through an oxidative quenching cycle whereby the trifluoromethylarene directly quenches the excited state PC. Another element in which the respective methodologies differ is that while Jui's protocol was only applied to simple electron rich trifluoromethylarene building blocks, our protocol has direct applicability to complex drug structures. One

advantage of Jui's protocol over our method is that CF_3 substituted pyridines, a substrate class unsuccessful under our optimised reaction conditions are within reach.[44]

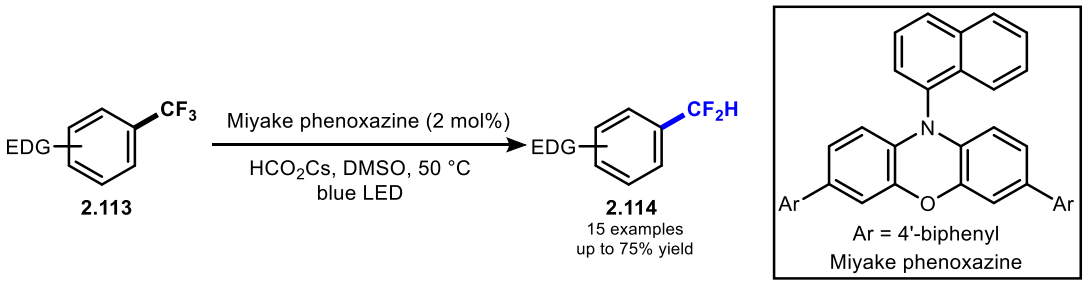

Scheme 2.25 HDF of electron-rich heteroarenes and pyridines.[44]

2.16 Conclusion

We have developed a new technology which allows controlled (mono-selective reductive defluorination of electron-poor trifluoromethylarenes. The reaction operates under basic conditions, employing 2,4,5,6-tetrakis(diphenylamino)isophthalonitrile (4-DPA-IPN) as the organo-photocatalyst, and 4-hydroxythiophenol acting both as the excited state catalyst quencher and the HAD. This operationally simple protocol tolerates a wide range of functional groups and heteroarenes commonly observed in pharmaceutically relevant lead structures. To the best of our knowledge, our technology is the first method which allows structures as complex as the bioactive molecules described in this chapter to undergo selective HDF, providing access to difluoromethyl drug analogues. Moreover, our reactions exhibit high CF_2H: CH_2F selectivity and chemoselectivity (no defluorination observed of other C−F bonds present in the parent structure). Mechanistic studies allude to a catalytic cycle whereby the PC is reduced by the HAD and returned to its native oxidation state by the trifluoromethylarene that acts as an oxidant. In conclusion, it is evident that molecular editing is a powerful strategy which can significantly reduce the time spent on re-configuring synthetic routes to

access analogues of lead structures. It is likely that other reaction methodologies which employ molecular editing, beyond HDF, will surface in the foreseeable future.

2.17 Future Work

Future aims of this project are to: 1) investigate the biological properties of **2.96** – **2.101**, through direct comparison of their properties to their CF_3 parent compounds; 2) expand our methodology further to electron-rich aromatics and analogously apply this to LSF; 3) successfully apply our HDF protocol to CF_3-containing *N*-heterocycles of interest to the pharmaceutical and agrochemical industries, including but not limited to six-membered heterocycles such as pyridines, pyrimidines, triazines, fused heterocycles such as (iso)quinolines, quinazolines and indoles, five-membered heteroaromatics such as pyrroles and imidazoles. A first step in this direction has been made through our robustness screening efforts which have shown our technology's tolerance to heterocycles not substituted with a CF_3 group. Initial efforts applying our HDF technology to an electron deficient CF_3-substituted pyridine were not fruitful (**Scheme 2.18**). Obtaining the conditions required to unlock these substrate classes will require re-optimisation of the HDF reaction. It is expected that electron-poor heteroarenes substrate classes will exhibit lower selectivity towards the desired mono-defluorinated product, due to their reduced reduction potentials. However, given that the most prominent side-products in our HDF protocol stem from exhaustive defluorination, the resulting products of which are themselves considered drug analogues, such technologies can still be useful to medicinal chemists. Our study shows that deuterium enriched **2.107** was accessible through deuteration of 4-HTP, but a more general

protocol that allows increased percentage deuterium incorporation would be welcomed by medicinal chemists.

2.18 References

1. (a) Drug Bank. Available online: https://http://www.drugbank.ca (accessed on 2 May 2020); (b) W. Zhu, J. Wang, S. Wang, Z. Gu, J. L. Aceña, K. Izawa, H. Liu and V. A. Soloshonok, *J. Fluorine Chem.,* 2014, **167**, 37.

2. C. Tseng, G. Baillie, G. Donvito, M. A. Mustafa, S. E. Juola, C. Zanato, C. Massarenti, S. Dall'Angelo, W. T. Harrison, A. H. Lichtman, R. A. Ross, M. Zanda and I. R. Greig, *J. Med. Chem.,* 2019, **62**, 5049.

3. Y. Kobayashi and I. Kumadaki, *Tetrahedron Lett.,* 1969, **10**, 4095.

4. V. C. R. McLoughlin, J. Thrower, *Tetrahedron*, 1969, **25**, 5921.

5. a) D. M. Wiemers, D. J. Burton, *J. Am. Chem. Soc.,* 1986, **108**, 832; b) H. Urata, T. Fuchikami, *Tetrahedron Lett.,* 1991, *32*, 91; c) G. G. Dubinina, H. Furutachi, D. A. Vicic, *J. Am. Chem. Soc.,* 2008, **130**, 9600; d) M. Oishi, H. Kondo, H. Amii, Chem. Commun., 2009, **45**, 1909; e) E. J. Cho, T. D. Senecal, T. Kinzel, Y. Zhang, D. A. Watson, S. L. Buchwald, *Science*, 2010, **328**, 1679; f) N. D. Ball, J. W. Kampf, M. S. Sanford, *J. Am. Chem., Soc.* 2010, **132**, 2878; g) A. Zanardi, M. A. Novikov, E. Martin, J. Benet-Buchholz, V. V. Grushin, *J. Am. Chem. Soc.,* 2011, **133**, 20901; h) C.-P. Zhang, Z.-L. Wang, Q.-Y. Chen, C.-T. Zhang, Y.-C. Gu, J.-C. Xiao, *Angew. Chem., Int. Ed.,* 2011, **50**, 1896; i) O. A. Tomashenko, E. C. Escudero-Adán, M. Martínez Belmonte, V. V. Grushin, *Angew. Chem., Int. Ed.,* 2011, **50**, 7655; j) H. Morimoto, T. Tsubogo, N. D. Litvinas, J. F. Hartwig, *Angew. Chem., Int. Ed.*,

2011, **50**, 3793; T. Knauber, F. Arikan, G.-V. Röschenthaler, L. J. Gooßen, *Chem. Eur. J.* 2011, **17**, 2689; k)V. I. Bakhmutov, F. Bozoglian, K. Gómez, G. González, V. V. Grushin, S. A. Macgregor, E. Martin, F. M. Miloserdov, M. A. Novikov, J. A. Panetier, L. V. Romashov, *Organometallics*, 2012, **31**, 1315; l) M. Chen S. L. Buchwald, *Angew. Chem., Int. Ed.,* 2013, **52**, 11628; m) A. Lishchynskyi, M. A. Novikov, E. Martin, E. C. Escudero-Adán, P. Novák, V. V. Grushin, *J. Org. Chem.,* 2013, **78**, 11126.

6. a) T. Liu, Q. Shen, *Org. Lett.* 2011, **13**, 2342; b) T. D. Senecal, A. Parsons, S. L. Buchwald, *J. Org. Chem.* 2011, **76**, 1174; c) J. Xu, D.-F. Luo, B. Xiao, Z.-J. Liu, T.-J. Gong, Y. Fu L. Liu, *Chem. Commun.,* 2011, **47**, 4300; d) C-P. Zhang, J. Cai, C.-B. Zhou, X.-P. Wang, X. Zheng, Y.-C. Gu Ji.-C. Xiao, *Chem. Commun.,* 2011, **47**, 9516; e) Y. Ye, M. S. Sanford, *J. Am. Chem. Soc.* 2012, **134**, 9034; f) X. Jiang, L. Chu, F.-L. Qing, *J. Org. Chem.* 2012, **77**, 1251; g) N. D. Litvinas, P. S. Fier, J. F. Hartwig, *Angew. Chem. Int. Ed.* 2012, **51**, 536; h) P. Novák, A. Lishchynskyi, V. V. Grushin, *Angew. Chem. Int. Ed.* 2012, **51**, 7767; i) B. A. Khan, A. E. Buba, L. J. Gooßen, *Chem. Eur. J.* 2012, **18**, 1577; j) Y. Ye, S. A. Künzi, M. S. Sanford, *Org. Lett.,* 2012, **14**, 4979; k) Y. Li, L. Wu, H. Neumann, M. Beller, *Chem. Commun.,* 2013, **49**, 2628; l) M. Presset, D. Oehlrich, F. Rombouts, G. A. Molander, *J. Org. Chem.* 2013, **78**, 12837.

7. a) J.-J. Dai, C. Fang, B. Xiao, J. Yi, J. Xu, Z.-J. Liu, X. Lu, L. Liu, Y. Fu, *J. Am. Chem. Soc.,* 2013, **135**, 8436; b) G. Danoun, B. Bayarmagnai, M. F. Grünberg, L. J. Gooßen, *Angew. Chem. Int. Ed.,* 2013, **52**, 7972; c) X. Wang, Y. Xu, F. Mo, G. Ji, D. Qiu, J. Feng, Y. Ye, S. Zhang, Y. Zhang, J. Wang, *J. Am. Chem. Soc.* 2013, **135**, 10330; d) B. Bayarmagnai, C.

Matheis, E. Risto, L. J. Goossen, *Adv. Synth. Catal.* 2014, **356**, 2343; e) A. Lishchynskyi, G. Berthon, V. V. Grushin, *Chem. Commun.* 2014, **50**, 10237.

8. N. Ichiishi, J. P. Caldwell, M. Lin, W. Zhong, X. Zhu, E. Streckfuss, H. Kim, C. A. Parish and S. W. Krska, *Chem. Sci.,* 2018, **9**, 4168.

9. J. Rong, C. Ni , J. Hu, *Asian J. Org. Chem.,* 2017, **6**, 139.

10. (a) E. J. Barreiro, A. E. Kümmerle and C. A. Fraga, *Chem. Rev.,* 2011, **111**, 5215; (b) R. Betageri, Y. Zhang, R. M. Zindell, D. Kuzmich, T. M. Kirrane, J. Bentzien, M. Cardozo, A. J. Capolino, T. N. Fadra, R. M. Nelson, *Bioorg. Med. Chem. Lett.,* 2005, **15**, 4761.

11. C. Luo, J. S. Bandar, *J. Am. Chem. Soc.,* 2019, **141**, 14120.

12. J. Hamel, J. Paquin, *Chem. Commun.,* 2018, **54**, 10224.

13. A. H. Neilson, A. Allard, in *Organofluorines*, Springer, 2002, p. 137.

14. M. J. Bentel, Y. Yu, L. Xu, Z. Li, B. M. Wong, Y. Men, J. Liu, *Environ. Sci. Technol.,* 2019, **53**, 3718.

15. K. Fuchibe, T. Akiyama, *J. Am. Chem. Soc.,* 2006, **128**, 1434.

16. T. Akiyama, K. Atobe, M. Shibata,K. Mori, *J. Fluorine Chem.,* 2013, **152**, 81.

17. V. J. Scott, R. Çelenligil-Çetinand O. V. Ozerov, *J. Am. Chem. Soc.,* 2005, **127**, 2852

18. W. Zhao, J. Wu, S. Cao, *Adv. Synth Catal.,* 2012, **354**, 574.

19. F. Forster, T. T. Metsänen, E. Irran, P. Hrobárik and M. Oestreich, *J. Am. Chem. Soc.,* 2017, **139**, 16334.

20. C. Saboureau, M. Troupel, S. Sibille and J. Périchon*, J. Chem. Soc., Chem. Commun.,* 1989, 1138.

21. D. Ferraris, C. Cox, R. Anand, T. Lectka, *J. Am. Chem. Soc.,* 1997, **119**, 4319.

22. S. Yoshida, K. Shimomori, Y. Kim, T. Hosoya, *Angew. Chem. Int. Ed.* 2016, **55**, 10406.

23. L. Kispert, H. Liu, C. Pittman, *J. Am. Chem. Soc.,* 1973, **95**, 1657.

24. M. H. Shaw, J. Twilton and D. W. C. MacMillan, *J. Org. Chem.,* 2016, **81**, 6898.

25. (a) S. M. Senaweera, A. Singh, J. D. Weaver, *J. Am. Chem. Soc.,* 2014, **136**, 3002; (b) S. Priya, J. D. Weaver III, *J. Am. Chem. Soc.,* 2018, **140**, 16020; (c) S. Senaweera, J. D. Weaver, *J. Am. Chem. Soc.,* 2016, **138**, 2520; (d) A. Singh, C. J. Fennell, J. D. Weaver, *Chem. Sci.,* 2016, **7**, 6796.

26. K. Chen, N. Berg, R. Gschwind, B. J. König, B. *J. Am. Chem. Soc.,* 2017, **139**, 18444.

27. H. Wang, N. T. Jui, *J. Am. Chem. Soc.,* 2018, **140**, 163.

28. H. Dang, A. M. Whittaker, G. Lalic, *Chem. Sci.,* 2016, **7**, 505.

29. S. B. Munoz, C. Ni, Z. Zhang, F. Wang, N. Shao, T. Mathew, G. A. Olah, G. S. Prakash, *Eur. J. Org. Chem.,* 2017, **2017**, 2322.

30. Y. Pan, *ACS Med. Chem. Lett.* 2019, **10**, 1016.

31. C. P. Andrieux, C. Combellas, F. Kanoufi, J. Saveant, A. Thiebault, *J. Am. Chem. Soc.,* 1997, **119**, 9527.

32. J. Luo, J. Zhang, *ACS Catalysis,* 2016, **6**, 873

33. M. Garreau, F. Le Vaillant, J. Waser, *Angew. Chem. Int. Ed.,* 2019, **58**, 8182.

34. M. L. Mohler, C. E. Bohl, A. Jones, C. C. Coss, R. Narayanan, Y. He, D. J. Hwang, J. T. Dalton and D. D. Miller, *J. Med. Chem.,* 2009, **52**, 3597.

35. V. A. Nair, S. M. Mustafa, M. L. Mohler, J. Yang, L. I. Kirkovsky, J. T. Dalton, D. D. Miller, *Tetrahedron Lett.,* 2005, **46**, 4821.

36. T. V. Macfarlane, F. Pigazzani, R. W. Flynn, T. M. MacDonald, *Br. J. Clin. Pharmacol.,* 2019, **85**, 285.

37. X. Li, Q. Gu, X. Dong, X. Meng, X. Liu, *Angew. Chem. Int. Ed.,* 2018, **57**, 7668.

38. J. D. Rozzell, R. McCague, Selective androgen receptor modulators. US 7205437 B2, April 17, 2007.

39. (a) K. D. Collins and F. Glorius, *Nat. Chem.,* 2013, **5**, 597; (b) K. D. Collins, A. Rühling and F. Glorius, *Nat. Protoc.,* 2014, **9**, 1348; (c) K. D. Collins, A. Rühling, F. Lied, F. Glorius, *Chem. Eur. J.,* 2014, **20**, 3800; (d) T. Gensch, M. Teders, F. Glorius, *J. Org. Chem.,* 2017, **82**, 9154.

40. N. J. Taylor, E. Emer, S. Preshlock, M. Schedler, M. Tredwell, S. Verhoog, J. Mercier, C. Genicot, V. Gouverneur, *J. Am. Chem. Soc.,* 2017, **139**, 8267.

41. B. Plutschack, C. A. Correia, P. H. Seeberger, K. Gilmore, *Top. Organomet. Chem.* 2015, **57**,

42. C. Sambiagio, T. Noël, *Trends in Chemistry,* 2020, **2**, 92.

43. N. A. Romero and D. A. Nicewicz, *J. Am. Chem. Soc.,* 2014, **136**, 17024.

44. D. B. Vogt, C. P. Seath, H. Wang, N. T. Jui, *J. Am. Chem. Soc.,* 2019, **141**, 13203.

Chapter 3: Introduction to F-18 radiochemistry

3.1 Introduction to Positron Emission Tomography

Positron Emission Tomography (PET) is a non-invasive imaging modality that can detect pre-symptomatic biochemical changes in body tissues where no evidence of abnormality from computed tomography (CT) or magnetic resonance imaging (MRI) are detectable.[1] This technology helps researchers to understand disease states as well as assisting clinicians in patient stratification. The sensitivity of PET makes this technique highly suitable to address questions fundamental to drug development for oncology, cardiology, neurosciences and inflammatory diseases. For example, PET enables biodistribution and receptor occupancies studies. The combination of PET with a structural imaging technique such as MRI or X-ray computed tomography (X-ray CT) is seen as symbiotic due the sensitivity of PET and the high spatial resolution of MRI which are unrivalled by either individual technique.[2,3]

3.2 The Key Principles of Positron Emission Tomography

PET is an imaging technique which relies on contributions of various scientific fields such as medicine, physics, engineering, biology and chemistry. In order to perform a PET scan, an appropriate radiotracer labelled with a positron emitting isotope such as carbon-11, fluorine-18 or Iodine-131 is administered to a patient. When positron-emitting isotopes decay, a positron is released. The positron travels a short distance until it encounters an electron. At this point, an annihilation event occurs emitting two gamma photons at 180 degrees with a given energy. A PET instrument does not directly detect positrons but instead detects the gamma rays through a ring of detectors which surrounds the patient. The incident gamma rays are initially converted into light and then into electrical pulses

which with the aid of a photomultiplier followed by informatic analysis allow the construction of a 3D image. The energy of emission dictates the resolution of a PET image (**Figure 3.1**). Of all PET radioi**s**otopes, fluorine-18 has the lowest emission energy (633 KeV) which results in the highest resolution images.[4]

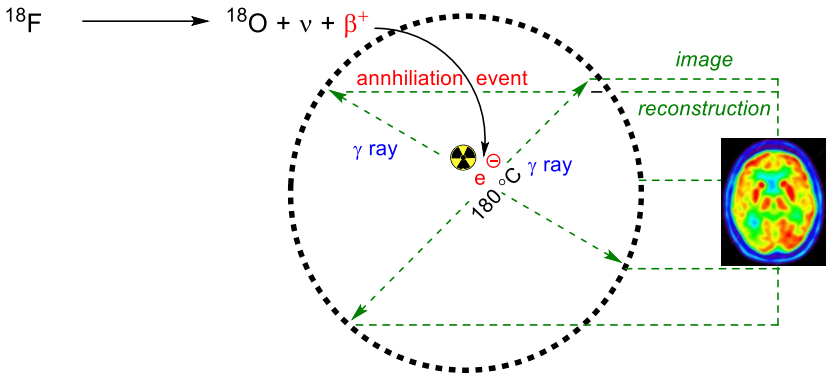

Figure 3.1 A workflow for PET imaging using fluorine-18.

Due to its sensitivity, PET scans typically require sub-nanomolar quantities of a tracer to be administered in order to generate enough annihilation events to provide an image of sufficiently high resolution.[5,6] This ability to administer low quantities of a given tracer, allows biological systems to remain unperturbed upon administration of the tracer. This property allows potentially toxic drugs or ones with high potency to be studied without triggering a biological response. Some of the most prominent applications include its utilisation in oncology for the detection of tumours, and in neuroscience for the monitoring of disorders such as Parkinson's and Alzheimer's disease, providing information such as receptor occupation and real time chemical information. In addition to its clinical applications, PET can be used to quantify the pharmacodynamic and pharmacokinetic properties of drug candidates complementing information gained from *in vitro* analysis. Therefore, PET has become a valuable tool in drug discovery where it is used as a screening technology in drug development programs. PET data can be used to

eliminate drug candidates prior to animal testing or clinical trials, ensuring an ethical and more cost-effective drug discovery process.[7,8]

3.3 Fluorine-18 Compared to Other Positron Emitting Isotopes

PET isotopes include but are not limited to carbon-11, nitrogen-13, oxygen-15, fluorine-18, copper-64, gallium-68 and zirconium-89. Each isotope is unique, differing in half-life, degree of positron emission, and positron emission energy (**Table 3.1**). Several factors need to be taken into account when choosing the appropriate isotope for a PET scan. The half-life is one crucial factor which needs to be considered. Given that the radiosynthesis should not exceed three half-lives from end of bombardment, the necessity to incorporate the PET isotope into a molecule of interest in a late-stage fashion is crucial, especially for short-lived isotopes such ^{13}N (half-life = 10 minutes) and ^{15}O (half-life = 2 minutes). Another crucial factor is the energy of the positron. Fluorine-18 has a relatively low maximum positron energy, meaning that its annihilation with an electron is in closer proximity to its site of decay when compared to radioisotopes of higher positron energy. In practice, this means that the spatial resolution of a PET scan for this isotope is better than other commonly used radioisotopes (2.4 mm in water). Provided fluorine-18 can be readily introduced in the tracer of interest, its favourable half-life (109.7 min) and lower maximum positron energy make it a privileged radioisotope. However, for larger biomolecules such as proteins and monoclonal antibodies which exhibit slower pharmacokinetics, fluorine-18's half-life may not be sufficient and another PET isotope such as zirconium-89 could be more suitable.[4]

Table 3.1 Physical properties of PET isotopes. ß$^+$ = positron.

Isotope	Typical production	Half-life	Proportion of ß$^+$ decay (%)	Maximum ß$^+$ energy (keV)	Decayed product
^{11}C	^{14}N(p,α)^{11}C	20.3 min	99.8	960	^{11}B
^{13}N	^{16}O(p,α)^{13}N	10.0 min	100	1190	^{13}C
^{15}O	^{15}N(d,n)^{15}O	2.04 min	99.9	1720	^{15}N
^{18}F	^{18}O(p,n)^{18}F ^{20}Ne(d,α)^{18}F	109.8 min	97	633	^{18}O
^{68}Ga	^{68}Ge generator	68.1 min	89	1920	^{68}Zn
^{64}Cu	^{64}Ni(p,n)^{64}Cu	762 min	19	653	^{64}Ni
^{89}Zr	^{89}Y(p,n)^{89}Zr	3.3 days	100	890	^{89}Y

3.4 Key Terms and Concepts

Several considerations need to be made to distinguish chemistry performed with fluorine-18 and fluorine-19. Many of the differences can be attributed to the half-life of fluorine-18. The instability of fluorine-18 means that ^{18}F-radiochemistry procedures which include the synthesis and purification should be performed rapidly and efficiently (ideally within 3 half-lives after end of bombardment). Fluorine-18 is treated as a gamma emitter, and as such, when large amounts of activity are used, hot cells made of lead walls of appropriate thickness must be used to perform radiosyntheses. Manual manipulations are difficult, or in cases when higher amounts of activity are used, impossible to perform. Routine productions of known radiopharmaceuticals used in the clinic are performed on automated synthesiser platforms. In order to develop new methodologies for F-18 radiochemistry, reactions can be performed with much smaller amounts of radioactivity allowing for more facile optimisation and for the reactions to be performed in lead-based gloveboxes. Given that the aim is to translate these methodologies to a clinical setting, reactions must be easy to perform and reproducible. In order to illustrate the reproducibility of ^{18}F-radiochemistry, reactions are run in triplicate at the minimum which allows for the quantification of a radiochemical yield

with a given error. In fluorine-19 chemistry, reagents and fluorinating reagents are typically present in equimolar quantities. Fluorine-18 reactions are not within the same realm, where reagents/substrate/precursors are present in several orders of magnitude greater than the ^{18}F-fluorinating reagent. Radiochemical yields (RCY) are always calculated based on the assumption that the ^{18}F source is the limiting reagent. It is generally accepted that a radiochemical yield is a defined as the percentage of activity of an isolated radiolabelled compound compared to the starting activity of the fluorine-18 reagent.[9] This yield may in certain cases be corrected for decay, and will then be referred to as a decay corrected yield (d.c). When reactions are run on a small scale without further purification, crude RCY's are reported. Due to the high costs of F-18, radiochemists often report crude RCY's because they allow for a faster assessment of a given methodology's generality. A crude RCY can be quantified using radioTLC and radioHPLC techniques, where radioTLC quantifies the consumption of ^{18}F fluorinating reagent, and radioHPLC is used to assess the purity of radiolabelled compounds. In order to accurately quantify a crude RCY, it is essential that reaction mixtures analysed by radioTLC and radioHPLC are homogenous.[9]

3.5 Production of Fluorine-18

Fluorine-18 can be produced by a cyclotron either in the form of [^{18}F]fluoride which can be prepared in high molar activity (MA) and introduced into organic molecules *via* nucleophilic substitution reactions, or as [^{18}F]F_2 gas, which is prepared in lower MA and can be introduced into organic molecules *via* electrophilic substitution reactions.[4] The form of fluorine-18 ([^{18}F]F^- or [^{18}F]F_2) will affect the production process, and the corresponding target used in its production (**Table 3.2)**.

Table 3.2 Methods to produce ^{18}F-containing sources. [a]Post-target production method.

^{18}F Source	Target	Nuclear Reaction	MA (GBq µmol^{-1})
[^{18}F]F^-	[^{18}O]H_2O	$^{18}O(p,n)^{18}F$	5000
[^{18}F]F_2	$Ne + F_2$	$^{20}Ne(d,\alpha)^{18}F$	0.37 – 0.74
[^{18}F]F_2	$^{18}O_2 + F_2$	$^{18}O(p,n)^{18}F$	1
[^{18}F]F_2[a]	[^{18}O]H_2O	$^{18}O(p,n)^{18}F$	55

3.5.1 Production of [^{18}F]fluoride

[^{18}F]fluoride is produced through proton bombardment of ^{18}O-enriched water (**Table 3.2**).[10] This method affords fluorine-18 in the highest molar activity (MA), a property defined as the ratio between activity and mass of a radiolabelled compound (usually measured in GBq/µmol).[9] The MA of radiotracers is often required to be high to prevent receptor occupation with unlabelled compound. For low-density receptors, this is a necessity to avoid high background in the PET image. Furthermore, the higher the MA, the lower the amount of tracer needs to be administered. When the MA of a given radiosynthesis is lower, it can still be useful for applications such as biodistribution profiling, or for radiotracers which occupy receptors present in high concentration *in vivo*. At the end of bombardment, [^{18}F]fluoride is then delivered in a solution of ^{18}O-enriched water.[11] Due to the high solvation energy in water, [^{18}F]fluoride lacks nucleophilicity and can not be used directly as an effective nucleophilic ^{18}F fluorinating reagent.[12] [^{18}F]Fluoride is therefore first separated from ^{18}O-enriched water by passing the aqueous solution through a pre-activated quaternary methyl ammonium anion exchange cartridge (QMA). After the [^{18}F]fluoride is trapped onto the QMA, it can be eluted using a basic solution with an appropriate counter cation. Most often, the solution used to elute [^{18}F]fluoride consists of a acetonitrile-water solution containing potassium carbonate (K_2CO_3) in addition to a cryptand such as kryptofix 2.2.2 (K_{222}) (used

to sequester potassium), or cation derived from a tetraalkylammonium bicarbonate salt which does not require the use of K_{222} or other phase transfer catalyst. Once eluted, the solution is further diluted with anhydrous acetonitrile, and azeotropically dried. After this process, $[^{18}F]F^-$ can be used to perform nucleophilic fluorination reactions to either directly label a compound of interest or to prepare first a known fluorinate prosthetic or fluorination reagent. In the vast majority of F-18 radiochemical reactions, $[^{18}F]$fluoride is employed as the fluorinating reagent. Analogously to chemistry with fluorine-19, the desired ^{18}F-labelled target or motif cannot always be accessed by employing $[^{18}F]$fluoride as the fluorinating reagent.[4] For this reason, there is a continuous effort from radiochemistry research groups to develop routes towards new ^{18}F-labelled reagents to expand the radiochemical space (**Scheme 3.1**).[13] One example is the development and application of **$[^{18}F]$3.1**, which will be discussed in further detail in **Chapter V**.

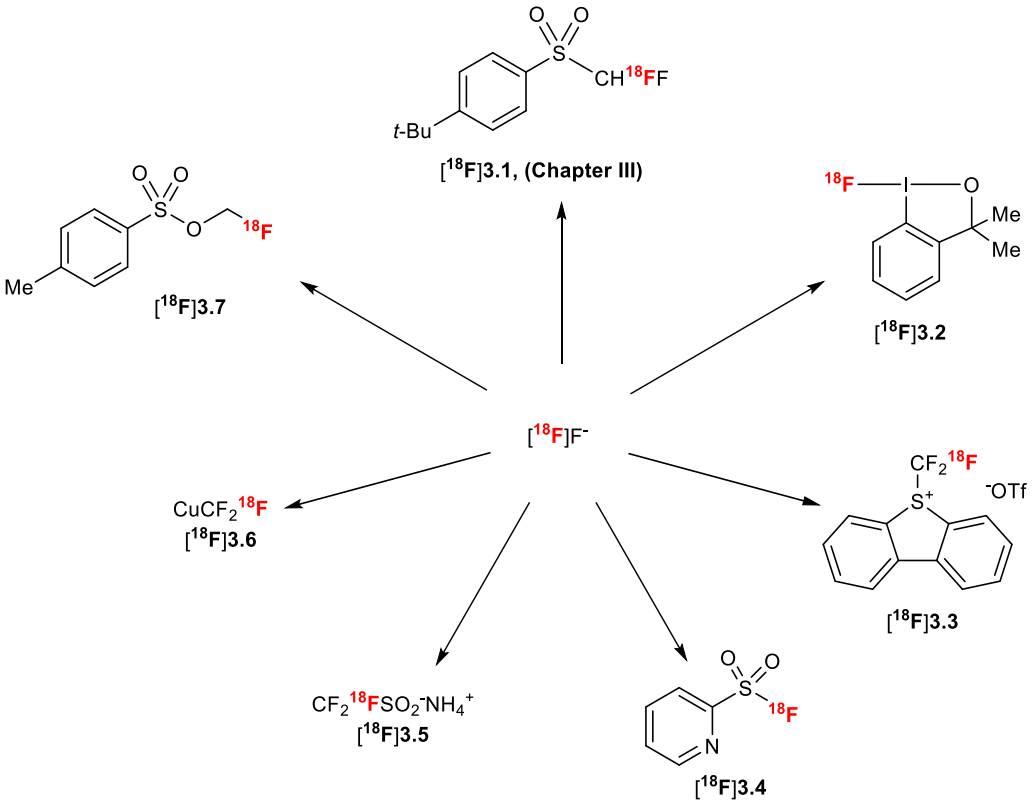

Scheme 3.1 Examples of ^{18}F-fluorinating reagents derived from [^{18}F]fluoride.

3.5.2 Production and Use of [^{18}F]F_2

Electrophilic fluorine-18 [^{18}F]F_2 is typically produced *via* two methods. The first involves the irradiation of Ne/F_2 mixture with deuterium (^{20}Ne(d,α)^{18}F) affording [^{18}F]F_2, whilst the second method proceeds *via* irradiation of [^{18}O]O_2 with protons (^{18}O(p,n)^{18}F) .[14,15] The latter of these two methods is used predominantly. In 1997, Bergman and Solin reported an indirect route to [^{18}F]F_2 using [^{18}F]F^-. In this work [^{18}F]F^- is produced *via* the ^{18}O(p,n)^{18}F nuclear reaction and subsequently azeotropically dried to yield a [^{18}F]KF/K_{222} complex. Addition of a methyl iodide solution yields [^{18}F]CH_3F. This resulting gas is purified by gas chromatography (GC) and passed through an electrical discharge chamber which contains neon and the carrier gas $^{19}F_2$. The electrical discharge triggers ^{18}F-^{19}F exchange, yielding [^{18}F]F_2 in MA up to 55 GBq µmol^{-1}.[16] The high reactivity and

often unselective nature of $[^{18}F]F_2$ with electron rich substrates, has encouraged radiochemists to develop $[^{18}F]F_2$-derived reagents with tamed reactivity and better selectivity profiles. Gouverneur and Solin reported the radiosynthesis of [^{18}F]NFSI and [^{18}F]Selectfluor bis(triflate) directly from $[^{18}F]F_2$. Other [^{18}F]N-F reagents derived from $[^{18}F]F_2$ include [^{18}F]*N*-fluoropyridinium triflate and [^{18}F]fluoro-2-pyridone as well as $[^{18}F]CF_3COF$, [^{18}F]AcOF and $[^{18}F]XeF_2$.[17] Due to the low MA associated with $[^{18}F]F_2$ and the fact that PET centres are often not equipped to produce $[^{18}F]F_2$, [^{18}F]fluoride or reagents derived thereof are preferentially used in F-18 radiochemistry.[18]

3.6 Fluorine-18: Application to PET and The Clinic

With more than 10,000 FDG scans performed daily worldwide, 2-[^{18}F]–fluorodeoxyglucose (FDG) is without a doubt the PET tracer most routinely used in the clinic. FDG, which is a glucose analogue bearing a fluorine-18 substituent instead of the hydroxy group positioned at the C2 in glucose, is a potent tracer for cancer imaging (**Figure 3.2**). Cancerous cells divide faster than healthy cells and therefore express the glucose transporter in higher concentrations, resulting in tumorous cells consuming more glucose than healthy cells. Analogous to glucose, cancerous cells consume more FDG than healthy cells. Once it enters the cell, FDG is phosphorylated. The presence of the fluorine atom in place of the hydroxyl moiety in FDG however prevents it from progressing to the next step in glycolysis, allowing it to localise within the cell.[19] This selective accumulation of FDG in cancerous cells makes it a powerful tool in the clinic to detect cancer or to study the evolution or efficacy of a given drug treatment.[4]

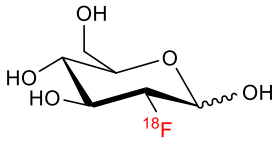

[18F]3.8

Figure 3.2 2-[18F]Fluoro-2-D-glucose ([18F]FDG).

Other notable F-18 labelled radiotracers used in the clinic include [18F]FDOPA which is used in the examination of patients with Parkinson's disease. Analogous to [18F]FDG and [18F]FDOPA, most clinical PET tracers have been labelled with fluorine-18 (**Figure 3.3**).[20]

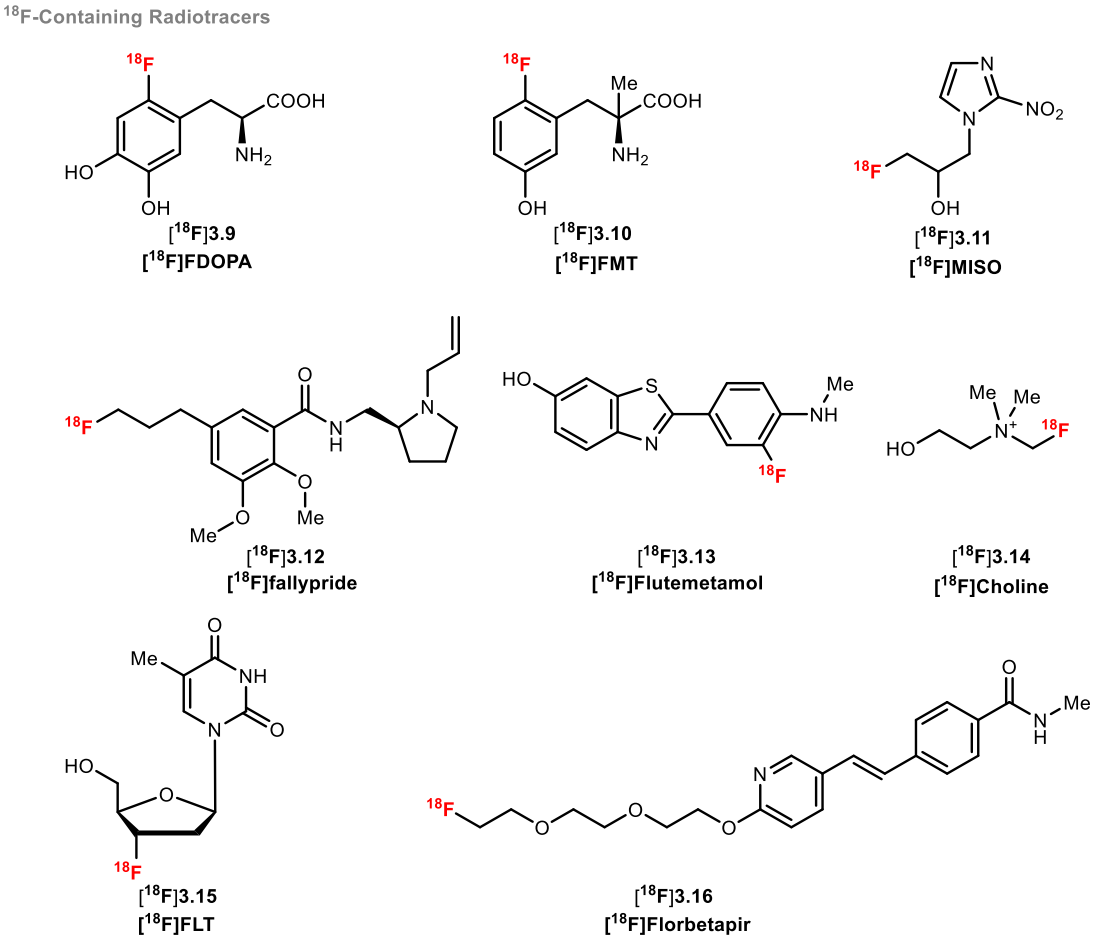

Figure 3.3 Commonly used fluorine-18 PET tracers in the clinic.

3.7 ^{18}F-Fluorination

3.7.1 Aliphatic ^{18}F-Fluorination

Nucleophilic substitution reactions are most commonly used for the radiofluorination of aliphatic motifs (typically *via* thermally induced bimolecular nucleophilic substitution (S_N2)). Precursors for such radiosyntheses are typically designed with an appropriate leaving group such as a halide or pseudohalide.[21] [^{18}F]FDG, the most widely used PET tracer in the clinic is prepared by direct aliphatic ^{18}F-fluorination of an acetate-protected mannose triflate or tosylate precursor.[22]

3.7.2 Aromatic ^{18}F-Fluorination

Analogous to aliphatic ^{18}F-fluorination reactions, the most commonly used method to access ^{18}F-substituted arenes is *via* S_NAr. Generally, such reactions facilitate high ^{18}F incorporation, however reactivity is limited to aromatic rings with electron withdrawing groups (NO_2, CF_3, CN etc.) *ortho* or *para* to a good leaving group (F, Br, OTf, $^+NMe_3$ etc.).[23,24] While generally robust, when such a strategy is applied to a tracer with greater complexity, the precursor is not always easy to access. The synthesis of 6-^{18}F-fluoro-L-DOPA is a prime example of this, where time-consuming optimisation was required.[25] In these instances, it is clear that late-stage methods to incorporate F-18 in the final step of a radiosynthesis are beneficial. The last decade has witnessed an upsurge in new radiofluorination methodologies which allow for the incorporation of F-18 in aromatic rings with varying electronics from a wide selection of precursors. Several reactions are available to access [^{18}F](hetero)arenes from [^{18}F]fluoride, with precursors including, arenes[26], (hetero)aryl halides[27], nitroarenes[28], trimethylammonium salts[29], sulfonium salts[30], sulfoxides[31], iodonium salts[32], iodonium ylides[33], stannanes[34], phenols[35,36],

sydnones[37,38], boronic esters[39] and pre-formed organometallic complexes of palladium[40] or nickel.[41] Since the suitability of each method is highly dependent on the structure of the substrate and accessibility of starting material, it is important that a wide toolbox of methods exists for radiochemists to choose from (**Scheme 3.2**).

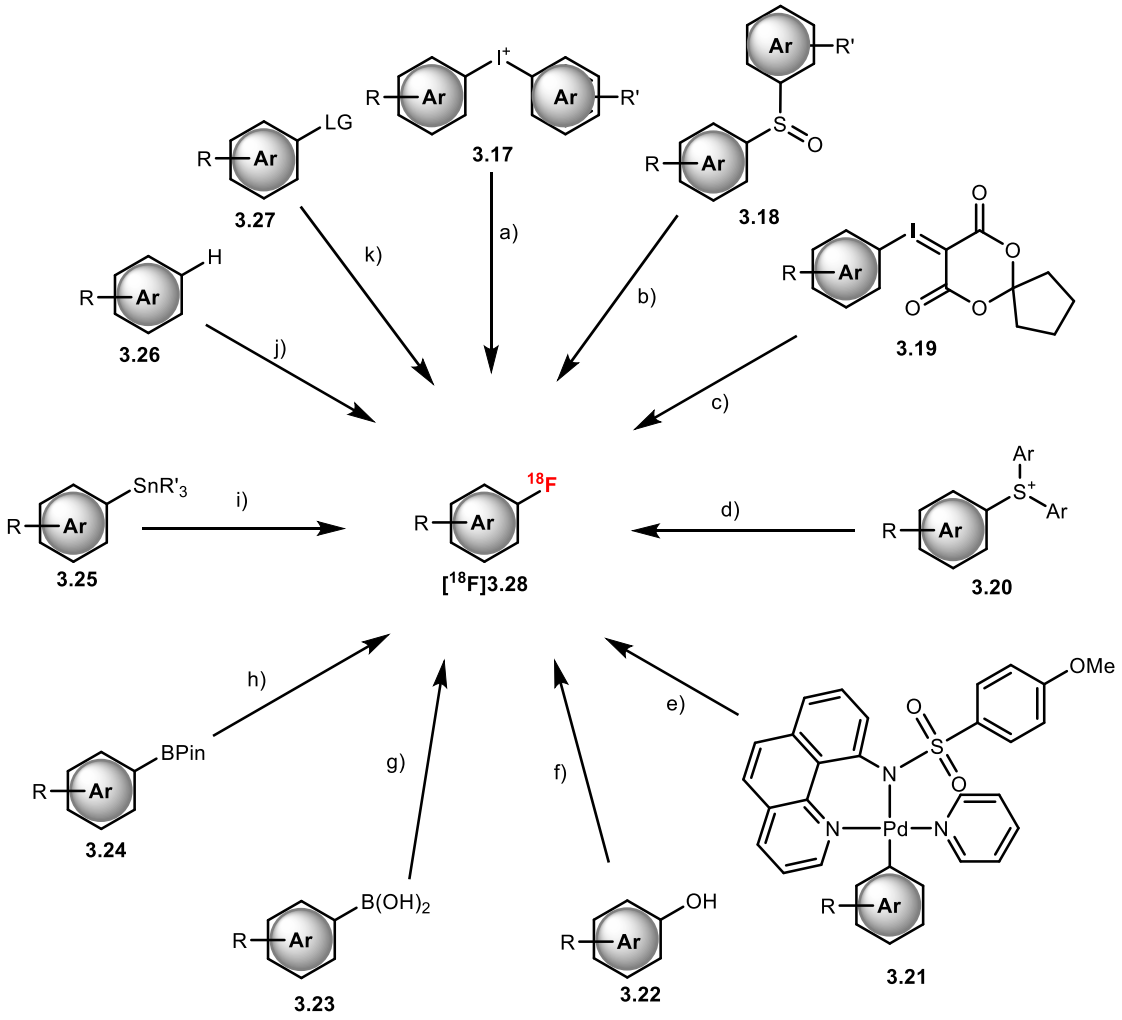

Scheme 3.2 Methods for the ^{18}F-fluorination of arenes and heteroarenes.

3.8 Methods to F-18 label Aromatic CF_3 groups

3.8.1 $ArCF_2{}^{18}F$ Derived From [^{18}F]fluoride

Despite (hetero)aryl and alkyl fluorides occupying a prominent space within the radiochemical literature, polyfluorinated motifs are also of interest due to their prevalence in drug manifolds. The first reported radiosynthesis of a ^{18}F-trifluoromethylated aromatic was accomplished through ^{19}F-^{18}F isotopic exchange with [^{18}F]KF/K_{222}. The low MA observed for the resulting products has encouraged radiochemists to develop alternative methods based on halogen exchange (halex) reactions.[42] (chlorodifluoromethyl)arene and (bromodifluoromethyl)arene substrates were identified as possible precursors in the presence of [^{18}F]KF/K_{222} at high temperatures (220 ˚C and 160 ˚C respectively) (**Scheme 3.3A** and **Scheme 3.3B**). The thermal activation used to induce ^{18}F incorporation however, led to decomposition of the starting materials, causing $^{19}F^-$ release which led to low MA of the isolated radiolabelled products.[43] Gouverneur and co-workers envisioned that milder conditions could be used to achieve halogen exchange. Using AgOTf as an additive, Gouverneur and co-workers were able to induce a halex nucleophilic ^{18}F-fluorination at 60 ˚C in DCE on bromodifluoromethyl building blocks using [^{18}F]KF/K_{222} as the F-18 source. Despite this advancement the MA of the radiolabelled products remained low (**Scheme 3.3C**).[44] In 2013, Gouverneur and co-workers developed a copper-mediated ^{18}F-trifluoromethylation of aryl iodides alleviating the need for pre-engineered substrates. The MA of the radiolabelled products in the range of 0.1 GBq µmol^{-1} was still not satisfactory.[45] In 2014, Vugts and co-workers expanded on this methodology, illustrating aryl boronic acids were suitable precursors for ^{18}F-trifluoromethylation. Furthermore,

they illustrated that the radiolabelled products could be obtained in higher MA (~100 GBq µmol^{-1}).[46]

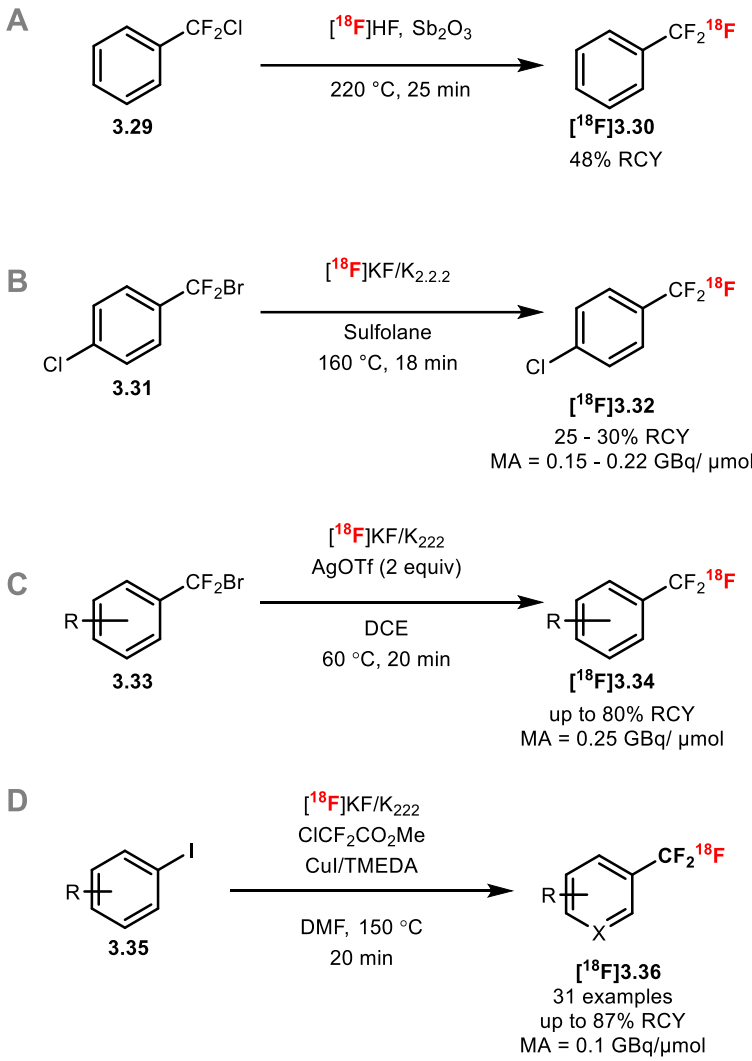

Scheme 3.3 ^{18}F-fluorination for the preparation of aryl-$CF_2{}^{18}F$ motifs.

More recently the emergence of the CF_2H group in drug discovery programs, has triggered the need to develop new technologies which allow this motif to be radiolabelled with F-18. In **Chapters IV and V** we disclose the development of two LSF strategies which allow facile radiolabelling of a variety of -CHF^{18}F groups through ^{18}F-fluorodecarboxylation and ^{18}F-difluoromethylation strategies respectively.

3.9 References

1. M. E. Phelps. *Proc. Natl. Acad. Sci., USA* 2000, **97**, 9226; b) S. M. Ametamey, M. Honer, P. A. Schubiger, *Chem. Rev.,* 2008, **108**, 1501; c) S. L. Pimlott, A. Sutherland, *Chem. Soc. Rev.,* 2011, **40**, 149; d) L. Zhu, K. Ploessl, H. F. Kung, *Chem. Soc. Rev.*, 2014, **43**, 6683; e) R. Chakravarty, H. Hong, W. Cai, *Mol. Pharmaceutics*, 2014, **11**, 3777.
2. S. Placzek, W. Zhao, H.-Y. Wey, T. M. Morin, J. M. Hooker, *Semin. Nucl. Med.,* 2016, **46**, 20.
3. P. M. Matthews, E. A. Rabiner, J. Passchier, R. N. Gunn, *Br. J. Clin. Pharmacol.,* 2012, **73**, 175.
4. P. W. Miller, N. J. Long, R. Vilar, A. D. Gee, *Angew. Chem. Int. Ed.,* 2008, **47**, 8998.
5. E. Aboagye, *Mol. Imaging Bio.*, 2005, **7**, 53.
6. M. Bergstom, A. Grahnen, B. Langstrom, *Eur. J. Clin. Pharmacol.*, 2003, **59**, 357.
7. K. Kaitin, J. Dimasi, *Clin. Pharamocol. Ther.,* 2011, **89**, 183.
8. J. Dimasi, H. Grabowski, R. Hansen, *N. Eng. J. Med.,* 2015, **372**, 1972.
9. H. H. Coenen, A. D. Gee, M. Adam, G. Antoni, C. S. Cutler, Y. Fujibayashi, J. M. Jeong, R. H. Mach, T. L. Mindt, V. W. Pike, A. D. Windhorst, *Nucl. Med. Biol.,* 2017, **55**, 5.
10. M. R. Kilbourn, J. T. Hood and M. J. Welch, *Int. J. Appl. Radiat. Isot.,* 1984, **35**, 599.
11. M. A. Avila-Rodriguez, J. S. Wilson and S. A. McQuarrie, *Appl. Radiat. Isot.,* 2008, **66**, 1775.
12. C. Zhan and D. A. Dixon, *J. Phys. Chem. A,* 2004, **108**, 2020.

13. (a) S. Verhoog, C. W. Kee, Y. Wang, T. Khotavivattana, T. C. Wilson, V. Kersemans, S. Smart, M. Tredwell, B. G. Davis and V. Gouverneur, *J. Am. Chem. Soc.,* 2018, **140**, 1572; (b) C. W. Kee, O. Tack, F. Guibbal, T. C. Wilson, P. G. Isenegger, M. Imiolek, S. Verhoog, M. Tilby, G. Boscutti and S. Ashworth, *J. Am. Chem. Soc.,* 2020, **142**, 1180; (c) H. Teare, E. G. Robins, A. Kirjavainen, S. Forsback, G. Sandford, O. Solin, S. K. Luthra and V. Gouverneur, *Angew. Chem. Int. Ed.* 2010, **49**, 6821; (d) H. Teare, E. G. Robins, E. Årstad, S. K. Luthra and V. Gouverneur, *Chem. Commun.,* 2007, 2330; (e) M. A. C. González, P. Nordeman, A. B. Gómez, D. N. Meyer, G. Antoni, M. Schou and K. J. Szabó, *Chem. Commun.,* 2018, **54**, 4286; (f) T. R. Neal, S. Apana and M. S. Berridge, , *Int. J. Rad. Appl. Instrum. [A].,* 2005, **48**, 557; (g) M. K. Nielsen, C. R. Ugaz, W. Li and A. G. Doyle, *J. Am. Chem. Soc.,* 2015, **137**, 9571.
14. G. Blessing, H. Coenen, K. Franken and S. Qaim, *Int. J. Rad. Appl. Instrum. [A].,* 1986, **37**, 1135.
15. R. Nickles, M. Daube and T. Ruth, *Int. J. Appl. Radiat. Isot.,* 1984, **35**, 117.
16. J. Bergman and O. Solin, *Nucl. Med. Biol.,* 1997, **24**, 677.
17. (a) R. Chirakal, G. Firnau, G. J. Schrobilgen, J. Mckay and E. Garnett, *Int. J. Appl. Radiat. Isot.,* 1984, **35**, 401; (b) M. Murakami, K. Takahashi, Y. Kondo, S. Mizusawa, H. Nakamichi, H. Sasaki, E. Hagami, H. Iida, I. Kanno and S. Miura, *J. Labelled Compd. Radiopharmaceut.,* 1988, **25**, 573; (c) R. Neirinckx, R. Lambrecht and A. Wolf, *Int. J. Appl. Radiat. Isotopes,* 1978, **29**, 323.
18. S. Preshlock, M. Tredwell, V. Gouverneur, *Chem. Rev.,* 2016, **116**, 719.
19. M. Pretze, C. Wangler and B. Wangler, *Biomed. Res. Int.,* 2014, **2014**, 674063.

20. A. Almuhaideb, N. Papathanasiou and J. Bomanji, *Ann. Saudi Med.,* 2011, **31**, 3.

21. L. Zheng and M. S. Berridge, *Appl. Radiat. Isotopes,* 2000, **52**, 55.

22. R. Chirakal, B. McCarry, M. Lonegran, G. Firnau and S. Garnett, *Appl. Radiat. Isotopes,* 1995, **46**, 149.

23. G. Angelini, M. Speranza, A. Wolf and C. Shiue, *J. Fluorine Chem.,* 1985, **27**, 177.

24. M. S. Haka, M. R. Kilbourn, G. Leonard Watkins and S. A. Toorongian, *J. Labelled Compd. Radiopharmaceut.,* 1989, **27**, 823.

25. C. Lemaire, L. Libert, X. Franci, J. Genon, S. Kuci, F. Giacomelli and A. Luxen, *J. Labelled Compd. Radiopharmaceut.,* 2015, **58**, 281.

26. (a) W. Chen, Z. Huang, N. E. S. Tay, B. Giglio, M. Wang, H. Wang, Z. Wu, D. A. Nicewicz and Z. Li, *Science,* 2019, **364**, 1170; (b) L. S. Sharninghausen, A. F. Brooks, W. P. Winton, K. J. Makaravage, P. J. Scott and M. S. Sanford, *J. Am. Chem. Soc.,* 2020, **142**, 7362; (c) S. J. Lee, K. J. Makaravage, A. F. Brooks, P. J. Scott and M. S. Sanford, *Angew. Chem. Int. Ed.,* 2019, **58**, 3119.

27. T. Irie, K. Fukushi, O. Inoue, T. Yamasaki, T. Ido and T. Nozaki, *Int. J. Appl. Radiat. Isot.,* 1982, **33**, 633.

28. C. Lemaire, M. Guillaume, L. Christiaens, A. Palmer and R. Cantineau, *Int. J. Rad. Appl. Instrum. [A].,* 1987, **38**, 1033.

29. Y. Seimbille, M. E. Phelps, J. Czernin and D. H. Silverman, *J. Label. Compd. Radiopharm.,* 2005, **48**, 829.

30. L. Mu, C. R. Fischer, J. P. Holland, J. Becaud, P. A. Schubiger, R. Schibli, S. M. Ametamey, K. Graham, T. Stellfeld and L. M. Dinkelborg, *Eur. J. Org. Chem.,* 2012, **2012**, 889.

31. J. Chun, C. L. Morse, F. T. Chin and V. W. Pike, *Chem. Commun.,* 2013, **49**, 2151.

32. N. Ichiishi, A. F. Brooks, J. J. Topczewski, M. E. Rodnick, M. S. Sanford and P. J. Scott, *Org. Lett.,* 2014, **16**, 3224.

33. B. H. Rotstein, N. A. Stephenson, N. Vasdev and S. H. Liang, *Nat. Commun.,* 2014, **5**, 1.

34. K. J. Makaravage, A. F. Brooks, A. V. Mossine, M. S. Sanford and P. J. Scott, *Org. Lett.,* 2016, **18**, 5440.

35. C. N. Neumann, J. M. Hooker and T. Ritter, *Nature,* 2016, **534**, 369.

36. Z. Gao, Y. H. Lim, M. Tredwell, L. Li, S. Verhoog, M. Hopkinson, W. Kaluza, T. L. Collier, J. Passchier, M. Huiban, V. Gouverneur, *Angew. Chem. Int. Ed.,* 2012, **51**, 6733.

37. M. K. Narayanam, G. Ma, P. A. Champagne, K. N. Houk and J. M. Murphy, *Angew. Chem. Int. Ed.* 2017, **56**, 13006.

38. H. Liu, D. Audisio, L. Plougastel, E. Decuypere, D. Buisson, O. Koniev, S. Kolodych, A. Wagner, M. Elhabiri and A. Krzyczmonik, *Angew. Chem. Int. Ed.,* 2016, **55**, 12073.

39. (a) M. Tredwell, S. M. Preshlock, N. J. Taylor, S. Gruber, M. Huiban, J. Passchier, J. Mercier, C. Genicot and V. Gouverneur, *Angew. Chem. Int. Ed.* **2014***, 53*, 7751; (b) S. Preshlock, S. Calderwood, S. Verhoog, M. Tredwell, M. Huiban, A. Hienzsch, S. Gruber, T. C. Wilson, N. J. Taylor, T. Cailly, M. Schedler, T. L. Collier, J. Passchier, R. Smits, J. Mollitor, A. Hoepping , M. Mueller , C. Genicot, J. Mercier and V. Gouverneur, *Chem. Commun.* **2016***, 52*, 8361;

40. E. Lee, A. S. Kamlet, D. C. Powers, C. N. Neumann, G. B. Boursalian, T. Furuya, D. C. Choi, J. M. Hooker and T. Ritter, *Science,* 2011, **334**, 639.

41. E. Lee, J. M. Hooker and T. Ritter, *J. Am. Chem. Soc.,* 2012, **134**, 17456.

42. T. Ido, T. Irie, Y. Kasida, *J. Label. Compd. Radiopharm.,* 1979, **16**, 153.

43. (a) G. Angelini, M. Speranza, C. Shiue, A. Wolf, *J. Chem. Soc., Chem. Commun.,* 1986, 924; (b) A. Hammadi, C. Crouzel, *J. Label. Compd. Radiopharm.,* 1993, **33**, 703

44. S. Verhoog, L. Pfeifer, T. Khotavivattana, S. Calderwood, T. L. Collier, K. Wheelhouse, M. Tredwell and V. Gouverneur, *Synlett,* 2016, **27**, 25.

45. M. Huiban, M. Tredwell, S. Mizuta, Z. Wan, X. Zhang, T. L. Collier, V. Gouverneur and J. Passchier, *Nat. Chem.,* 2013, **5**, 941.

46. D. van der Born, C. Sewing, J. D. Herscheid, A. D. Windhorst, R. V. Orru and D. J. Vugts, *Angew. Chem. Int. Ed.,* 2014, **53**, 11046.

Chapter 4: Synthesis of ^{18}F-difluoromethylarenes using aryl boronic acids, ethyl bromofluoroacetate and [^{18}F]fluoride

The work discussed in this chapter was published in *Chemical* Science.

Sap, J. B. I.; Wilson, T. C.; Kee, C. W.; Straathof, N. J.; am Ende, C. W.; Mukherjee, P.; Zhang, L.; Genicot, C.; Gouverneur, V. *Chem. Sci.* **2019***, 10*, 3237-3241.

Author contributions: Cross-coupling reaction optimisation was performed by Jeroen Sap with help from Dr. Choon Wee Kee. Reaction scope was performed by Jeroen Sap. F-19 decarboxylative fluorination experiments and mechanistic experiments were performed by Jeroen Sap. F-18 radiolabelling experiments were performed by Jeroen Sap, Dr. Thomas Wilson and Dr. Natan Straathof.

4.1 Prior Art: F-18 Radiolabelling of Difluoromethylarenes

With ample reports dedicated to the F-18 radiolabelling of arenes[1] and trifluoromethylarenes[2], it is perhaps surprising that the F-18 radiolabelling of difluoromethylarenes has received considerably less attention. It was not until 2013 that Gouverneur and co-workers reported the first radiosynthesis of [^{18}F]ArCF$_2$H. They illustrated that using a Ag(I) salt in the form of silver nitrate, and [^{18}F]F$_2$-derived [^{18}F]Selectfluor bis(triflate) they could access (*S*)-4-(fluoro(fluoro-^{18}F)methyl)-1,1'-biphenyl (**4.2**) from 2-([1,1'-biphenyl]-4-yl)-2-fluoroacetic acid (**4.1**) in 8.6 ± 2.6 % RCY and a M.A of 2.5 ± 0.2 GBq μmol^{-1} (**Scheme 4.1A**).[3] With this proof of concept in hand, Gouverneur and co-workers developed a more general technology which gave access to [^{18}F]ArCF$_2$H (**4.4**) featuring a Ag(I)-mediated halogen exchange reaction of electron-rich (chlorofluoromethyl)arenes (**4.3**) and [^{18}F]fluoride. Despite the use of [^{18}F]fluoride, the molar activity of the radiolabelled products remained low (0.03 GBq μmol^{-1}) (**Scheme 4.1B**).[4] In 2016, Ritter and co-workers disclosed a multi-step method to label [^{18}F]ArCF$_2$H (**4.6**) from aryl (pseudo)halides (**4.5**). Their ability to start from readily available starting materials and the use of cyclotron produced [^{18}F]fluoride was seen as advantageous. The procedure tolerates a wide range of functional groups such as halide, alcohol, aldehyde, ether, and ketone. The protocol compares favourably to the aforementioned methods which lack tolerance towards heterocycles and application to more complicated drug analogues and radiopharmaceuticals. Despite the clear advantages of Ritter's method, moderate M.A (2.9 GBq μmol^{-1}) and the requirement for a post-labelling basic hydrolysis step were seen as

disadvantageous (**Scheme 4.1C**).[5] The outlined methods all give access to [^{18}F]ArCF$_2$H, but the moderate-to-low MA observed may prevent clinical PET applications (**Scheme 4.1A-C**).[6] Inspired by the ^{19}F C-H fluorination methodology of Cai and Tang, which provides access to difluoromethylarenes from fluoromethylarenes through electrophilic C-H fluorination, Liang/Vasdev and co-workers reported an F-18 variant to access [^{18}F]ArCF$_2$H. Their method is comprised of two steps, the ^{18}F-fluorination of benzylic (pseudo)halides with [^{18}F]fluoride, followed by oxidative electrophilic fluorination of [^{18}F]ArCH$_2$F with sodium persulfate and ^{19}F selectfluor.[7,8] The intent of their strategy was to avoid undesired ^{18}F/^{19}F isotopic exchange which could lower the MA of the products. Liang and co-workers were successful and obtained 4-(difluoromethyl)-1,1'-biphenyl in high MA (22.2 GBq μmol^{-1}). The harsh conditions of the oxidative post-labelling C-H fluorination however limited the scope of their methodology to simple arene building blocks (**Scheme 4.1D**).[8] Despite these advances, a general route to [^{18}F](Het)ArCF$_2$H in high molar activity is still lacking especially for complex targets. Specifically, methods which employ cyclotron-produced [^{18}F]fluoride and easy to access starting materials such as aryl boron reagents in high MA are not available to radiochemists.

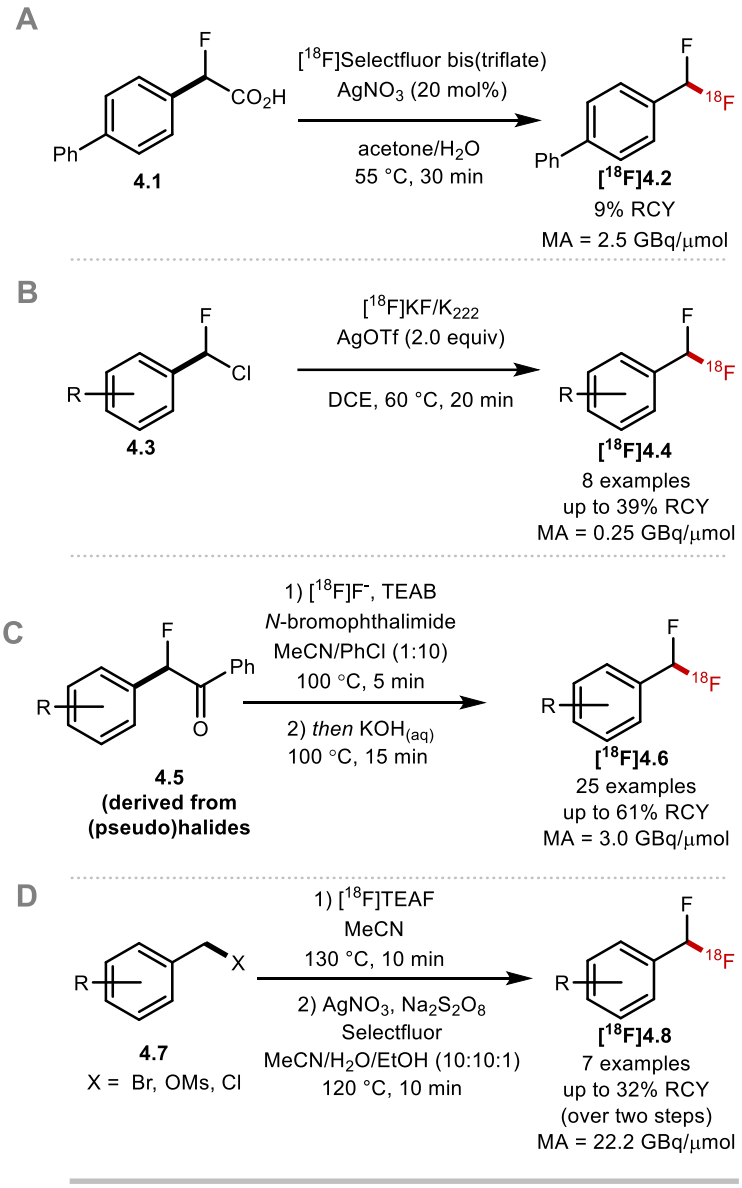

Scheme 4.1 Literature-known F-18 radiolabelling of difluoromethylarenes.

4.2 Initial Attempts at a One-Pot ^{18}F-Difluoromethylation From Aryl Boron Precursors

In order to augment the pool of available methods to label the [^{18}F](Het)ArCF$_2$H motif from [^{18}F]fluoride, we initially considered adapting known ^{19}F-difluoromethylation reactions operating *via* C–H functionalisation.[9] Whilst such strategies are ideal for (hetero)arenes with innate reactivity leading to site-selective ^{18}F-difluoromethylation,

substrates which are not reactive or too reactive would be unsuitable, thereby limiting the applicability of such a method for radioligand synthesis. We therefore opted to develop a method using pre-functionalised aryl boron reagents, which have already shown to be suitable precursors for ^{18}F-fluorination and ^{18}F-trifluoromethylation reactions (see **Chapter III**).[10,11] As such, extension of this approach to access [^{18}F](Het)ArCF_2H and its application to LSF was seen as a valuable addition to the current state of play.

Initial efforts to access [^{18}F](Het)ArCF_2H through a direct cross-coupling approach employing an aryl boron reagent, ethyl bromofluoroacetate and [^{18}F]fluoride were not fruitful (**Table 4.1**).

Table 4.1 Attempt at one-pot procedure with the aryl boron reagent, ethyl 1-fluoro-2-bromoacetate and ^{18}F-fluoride.

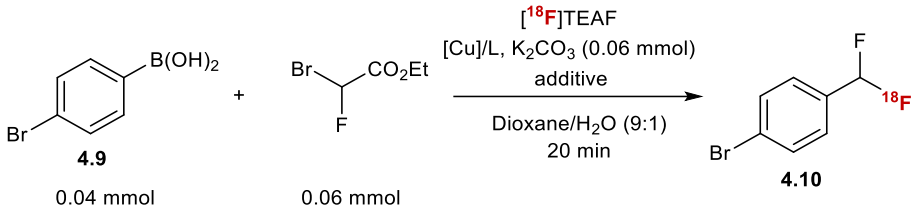

Entry	Cu-source (0.06 mmol)	Additive (mmol)	Temperature (˚C)	RCY (n =2)
1	CuI	TMEDA (0.1)	rt	0%
2	CuI	TMEDA (0.1)	rt	0%
3	$CuOTf_2(py)_4$	n/a	rt	0%
4	$CuOTf_2(py)_4$	n/a	rt	0%
5	(^{i}Pr)CuCl	n/a	rt	0%
6	(^{i}Pr)CuCl	n/a	rt	0%
7	CuI	TMEDA (0.1)	90	0%
8	CuI	TMEDA (0.1)	90	0%

4.3 Selection of Strategy

Due to a lack of ^{18}F-incorporation we opted to use the aryl boron reagent as a precursor to access to 2-fluoro-2-arylacetic acids which Gouverneur and co-workers demonstrated to be suitable for ^{18}F-fluorodecarboxylation. In addition to developing a method to access the radiolabelling precursors from aryl boron reagents, we also aimed at enabling ^{18}F-fluorodecarboxylation from [^{18}F]fluoride instead of using [^{18}F]F_2-derived [^{18}F]Selectfluor bis(triflate).

Inspired by the Ag(I)-mediated ^{18}F-fluorodecarboxylation towards [^{18}F]ArCF$_2$H (**Scheme 4.1A**) as well as a report from Groves and co-workers on the Mn-mediated fluorodecarboxylation of 2-arylacetic acid derivatives (**4.11**) (**Scheme 4.2A**)[12], we envisaged that the ^{18}F-fluorodecarboxylation of 2-fluoro-2-arylacetic acids with [^{18}F]fluoride could provide access to [^{18}F](Het)ArCF$_2$H in high MA (**Scheme 4.2B**).[3]

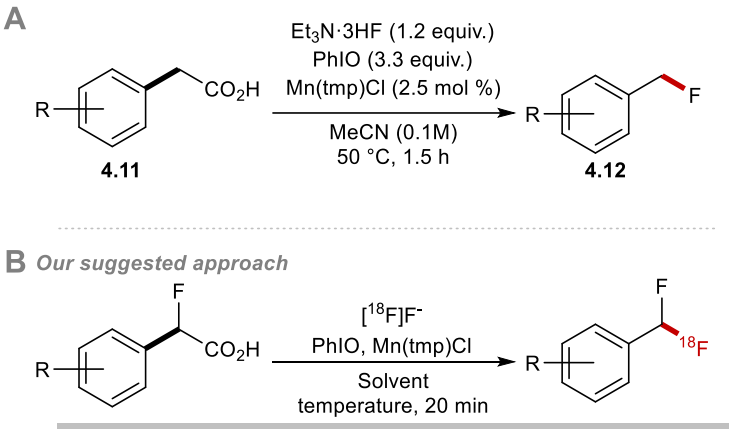

Scheme 4.2 A) Fluorodecarboxylation of 2-arylacetic acid derivatives, with nucleophilic fluoride. B) ^{18}F-fluorodecarboxylation of 2-fluoro-2-arylacetic acids with [^{18}F]fluoride.

In his report, Groves proposes that fluoride could readily displace chloride positioned axial in [Mn(tmp)Cl]. Under oxidative conditions, Mn(III) could form the Mn(V) oxo species which can trigger radical decarboxylation of a variety of carboxylic acids. The *in situ* generated Mn(IV) species could then induce radical recombination between a stabilised radical and a fluorine radical.[12] We were particularly inspired by this technology that uses fluoride. In order for the method to be widely adopted, a new technology which allows aryl boron reagents to be converted into 2-fluoro-2-arylacetic acids would be necessary. **Scheme 4.3** illustrates our reaction design to access ^{18}F-difluoromethylarenes; two stages consisting of cross coupling to access a library of 2-

fluoro-2-arylacetic acids, and the Mn-mediated ^{18}F-fluorodecarboxylation would need to be validated.

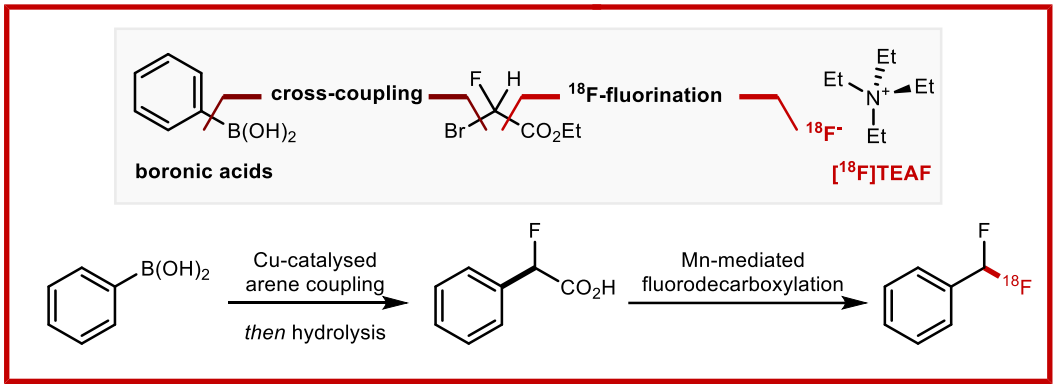

Scheme 4.3 Reaction design towards [^{18}F]ArCF$_2$H from aryl boronic acids.

4.4 Proof of Concept: Fluorodecarboxylation of 2-fluoro-2-Arylacetic Acids

First, we commenced our studies by investigating the ^{18}F-fluorodecarboxylation of 2-fluoro-2-arylacetic acids with [^{18}F]fluoride. Preliminary experiments were conducted with the model substrate 2-([1,1'-biphenyl]-4-yl)-2-fluoroacetic acid **4.1** and the non-radioactive and naturally occurring isotope of fluorine F-19. **4.1** was prepared directly from 2-([1,1'-biphenyl]-4-yl)acetic acid **4.13** applying the two-step process outlined in **Scheme 4.4.**

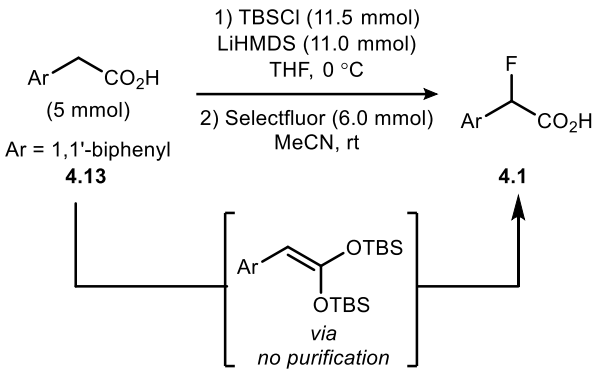

Scheme 4.4 Known synthesis of 2-fluoro-2-arylacetic acids.

When equimolar amounts of **4.1** and **4.13** were reacted with Mn(tmp)Cl (2.5 mol%), $Et_3N{\cdot}3HF$ (1.2 equiv) and iodosyl benzene (PhIO) (3.3 equiv) in MeCN at 50 ˚C, 4-(difluoromethyl)-1,1'-biphenyl (**4.2**) and 4-(fluoromethyl)-1,1'-biphenyl (**4.14**) were isolated in 44% and 20% yield, respectively (**Scheme 4.5**). This experiment illustrates the beneficial effect of fluorine-substitution at the benzylic carbon, which makes **4.1** more reactive towards fluorodecarboxylation than its non-fluorinated counterpart **4.13**. This reactivity preference could be explained by the increase in rate of formation of fluoromethyl radicals compared to their non-fluorinated counterparts. Given the literature precedence of Mn(tmp)Cl as a potent catalyst for C-H fluorination under similar conditions, we verified that product **4.2** did not form *via* C-H fluorination of **4.14**. When **4.14** was exposed to analogous reaction conditions, **4.2** was not observed. This experiment provides evidence that **4.2** is accessed through a fluorodecarboxylation pathway *in lieu* of a decarboxylation/C-H fluorination sequence.

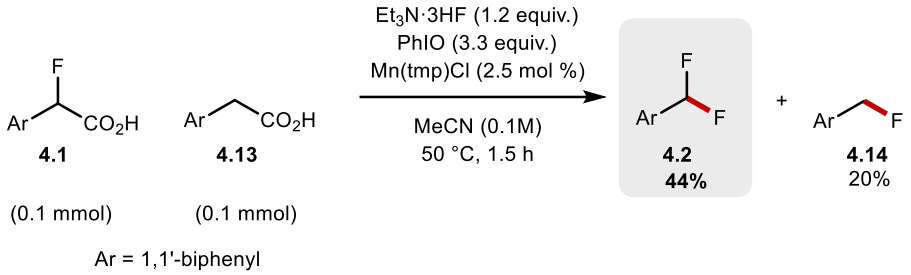

Scheme 4.5 Competition studies evaluating the effect of fluorine substitution on fluorodecarboxylation.

One of the limitations of the reaction conditions depicted in **Scheme 4.5** is the requirement of the harsh fluorinating agent $Et_3N{\cdot}3HF$, typically considered unsuitable for F-18 radiochemistry.[13] Furthermore, the reaction time of 1.5 hours is too long for radiochemistry applications. Finally, F-18 reactions are performed using sub-stoichiometric amounts of [^{18}F]fluoride (often sub-nanomolar concentrations), in contrast to F-19 reactions. For these reasons, we investigated whether fluorodecarboxylation of **4.1** was possible using a milder fluorinating reagent such as tetraethylammonium fluoride (TBAF) in sub-stoichiometric amounts (0.1 equiv) and under reduced reaction times (20 minutes). Pleasingly, when a ten-fold excess of **4.1** was treated with TBAF (0.1 equiv), PhIO (0.5 equiv) and Mn(tmp)Cl (0.2 equiv) in MeCN, **4.2** was obtained in 50% yield (determined by ^{19}F NMR based on TBAF consumption) (**Scheme 4.6**).

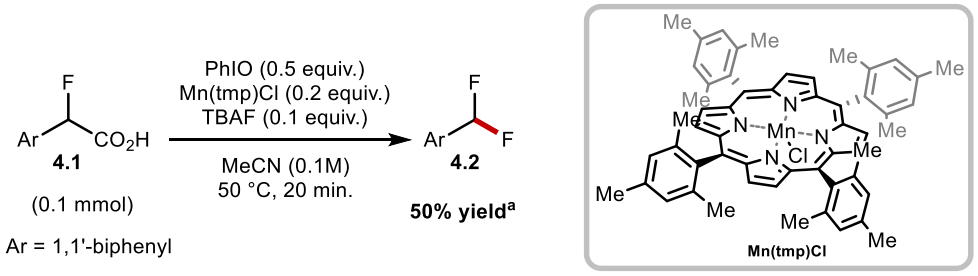

Scheme 4.6 Reaction with sub-stoichiometric fluoride.

In order to gain a deeper insight into the mechanism at play in this reaction, we examined whether pre-complexation of two equivalents 2-fluoro-2-arylacetic acids with a single equivalent of PhIO could generate an iodine(III) dicarboxylate intermediate. When two equivalents of 2-fluoro-2-(4-phenoxyphenyl)acetic acid (**4.15**) were pre-stirred with PhIO in MeCN, the corresponding iodine(III) dicarboxylate **4.16** was formed. Notably, the ^{1}H and ^{19}F NMR chemical shifts of the benzylic alpha proton and fluorine respectively changed as a result of the formation of **4.16**. In addition to the observed changes in chemical shift, diastereomeric doublets were observed in both ^{1}H and ^{19}F NMR spectra after iodine(III) dicarboxylate formation. These signals stem from the fact that iodine(III) dicarboxylate **4.16** has two stereogenic carbons (Ar**C**FHCO$_2$H) (**Scheme 4.7**).

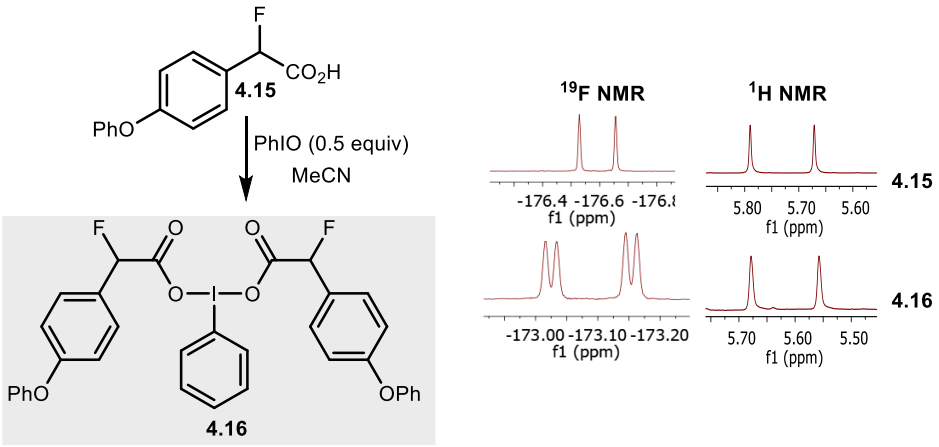

Scheme 4.7 Iodine(III) complex **4.16** formation.

Next, we investigated whether pre-forming the iodine (III) dicarboxylate complex of **4.17** prior to the addition of TBAF and Mn(tmp)Cl could improve conversion towards **4.2**. When **4.17** was made *in situ* from **4.1** and PhIO prior to the addition of TBAF and Mn(tmp)Cl, **4.2** was obtained in quantitative yield (**Scheme 4.8**). These preliminary data

boded well for F-18 labelling with [^{18}F]fluoride as the limiting reagent, and prompted the development of a robust protocol to access the necessary 2-fluoro-2-arylacetic acids from (hetero)aryl boron reagents.

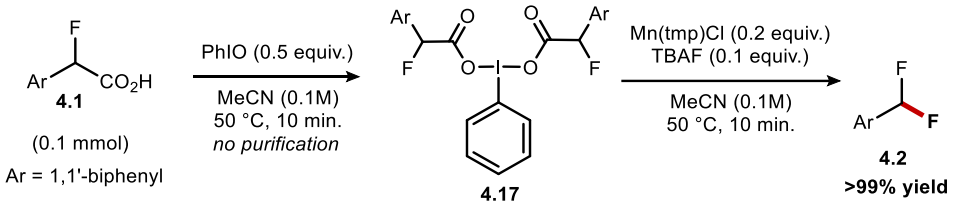

Scheme 4.8 Reaction of iodine(III) complex **4.17** with sub-stoichiometric fluoride. Yields of isolated products. Mn(tmp)Cl = Mn(III) meso-tetra(2,4,6-trimethylphenyl)porphyrin chloride. [a]Yields determined by quantitative ^{19}F NMR using α,α,α-trifluorotoluene as internal standard.

4.5 Prior Art: Access to The Starting Materials

Considering the paucity of methods available to access 2-fluoro-2-arylacetic acids, all requiring multi-step syntheses and starting from 2-arylacetic acid derivatives[13], our first objective was to develop a new protocol which would enable direct access to 2-fluoro-2-arylacetic acids from readily available precursors. This would allow for a more facile installation of this moiety in a LSF context. Given our previous success with (hetero)aryl boron reagents in radiochemistry, we selected these precursors for the optimisation of the cross-coupling reaction to access 2-fluoro-2-arylacetic acids.[11] To ensure the widespread utility of our method towards LSF as well as radiochemistry, we opted to use cheap, readily available and commercial starting materials. A one-pot cross-coupling reaction involving an aryl boron reagent and commercially available ethyl bromofluoroacetate followed by *in situ* hydrolysis in one-pot was envisaged as an attractive method towards 2-fluoro-2-arylacetic acids. We gave preference to a coupling methodology under Cu-catalysis instead of Pd[14] or Ni[15], a decision driven by guidelines

for residual metals in (radio)pharmaceuticals.[16] The cross-coupling towards 2-fluoro-2-arylacetic acetates has precedence in the literature (**Scheme 4.9**).[14,15] Therefore, a new robust method based on copper catalysis which could also provide *in situ* access to the corresponding 2-arylacetic acid derivative was deemed optimal. A final requirement we imposed on ourselves during the development of this reaction was to ensure that the aryl boron species was the limiting reagent. This was justified given the multi-step syntheses often required to access structurally diverse (hetero)aryl boron reagents, and the low cost of ethyl bromofluoroacetate.

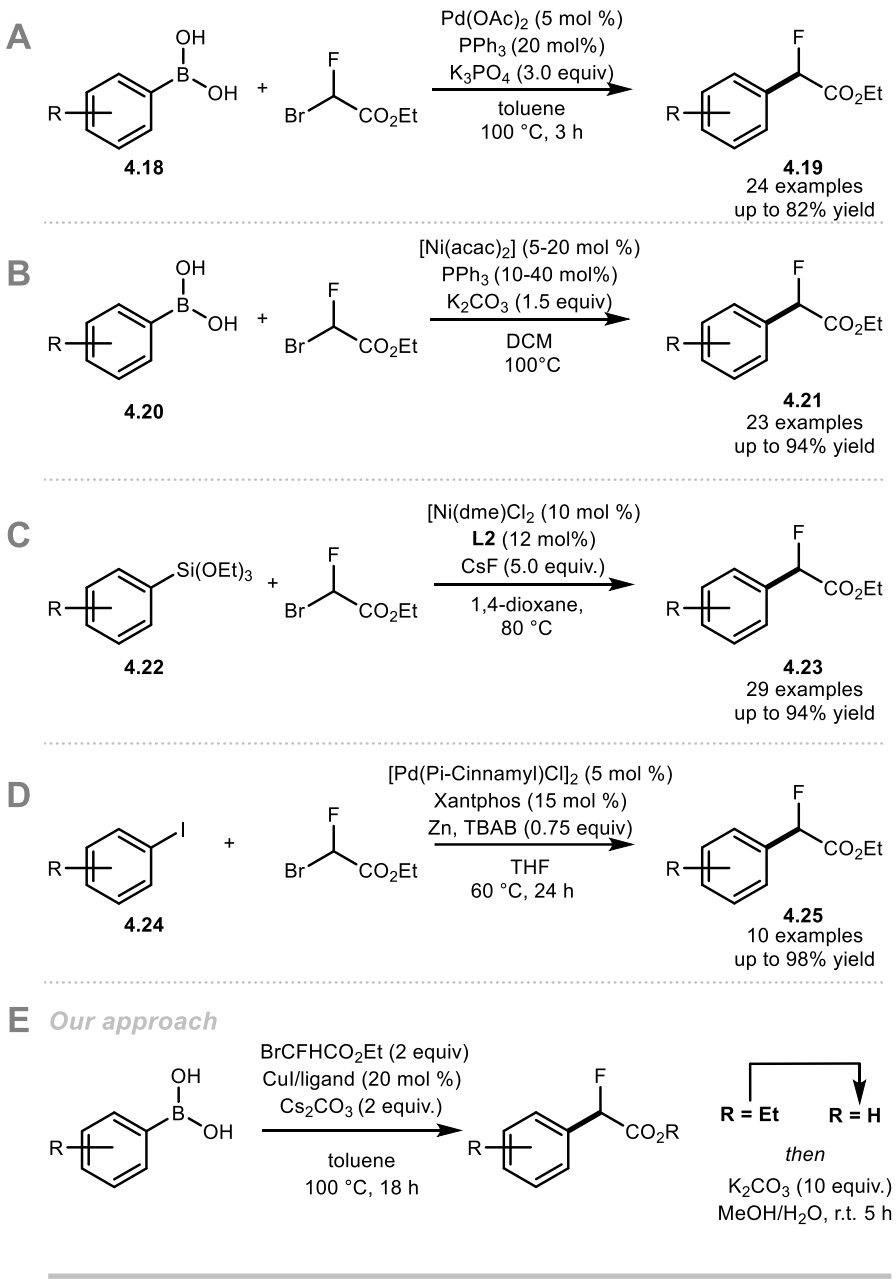

Scheme 4.9 Literature precedence cross-coupling methodologies towards 2-fluoro-2-arylacetic acetates.

4.6 Development of a General Copper Catalysed Cross-Coupling Reaction Towards 2-fluoro-2-Arylacetic Acids

Our studies commenced by reacting [1,10 -biphenyl]-4- ylboronic acid **4.26** (2.0 equiv) with commercially available ethyl bromofluoroacetate (1.0 equiv) in the presence of a catalytic amount of a Cu(I) source (CuI, 20 mol%) and 1,10-phenanthroline (**4.28**, 20

mol%), in a high boiling point solvent (dioxane, 0.2 M) under an atmosphere of nitrogen at 100 ˚C for 12 hours. These initial conditions afforded **4.27** in 7% yield as evidenced by presence of a doublet in ^{19}F NMR (-179.3 ppm, J_{H-F} = 47.6 Hz). (**Table 4.2**, entry 1). Substitution of **4.28** for 2,2':6',2''-terpyridine (**4.29**, 20 mol%) led to significantly improved conversion towards **4.27** (58%, **Table 4.2**, entry 2). When the stoichiometry of **4.26** and ethyl bromofluoroacetate was altered to 1.0 equivalent and 2.0 equivalents respectively, in the presence of 20 mol% of CuI and 20 mol% of 4,4',4''-tritert-butyl-2,2':6',2''-terpyridine (**4.30**) in toluene, **4.27** was isolated in 63% yield (**Table 4.2**, entry 3). Increasing the concentration of the reaction from 0.2 M to 0.4 M led to a further increase in yield of **4.27** (82%, Table 1, entry 4). The optimal protocol consists of treating **4.26** (1.0 equivalent) with ethyl bromofluoroacetate (2.0 equivalent), Cs_2CO_3 (2.0 equiv), CuI (20 mol %) and **4.30** (20 mol %) in toluene (0.4 M) at 100 ˚C. Next, we evaluated whether our procedure was amenable to a two-step-one pot process to directly access carboxylic acid **4.1** from boronic acid **4.26.** When applying a one-pot sequence involving cross-coupling followed by *in situ* hydrolysis with MeOH and aqueous K_2CO_3, **4.1** was isolated in 75% (**Table 4.2**, entry 5). Control reactions illustrated that in the absence of ligand and/or Cu(I)-source (**Table 4.2**, entries 6, 7), no product was detected. Substituting the CuI for a Cu(II) source (i.e. $CuCl_2$) led to no product formation (**Table 4.2**, entry 8). Similarly, no product was detected when the solvent was altered to DMF or DMSO (**Table 4.2**, entry 9). Bases other than Cs_2CO_3, for example K_2CO_3, CsF and K_3PO_4, Na_2CO_3 or RbF, all led to lower conversion towards **4.27** (**Table 4.2**, entries 10-14)**.**

Table 4.2 Optimisation of the Cu-catalysed cross-coupling of aryl boronic acid **4.26** with ethyl bromofluoroacetate towards ester **4.27** and the corresponding carboxylic acid **4.1**.

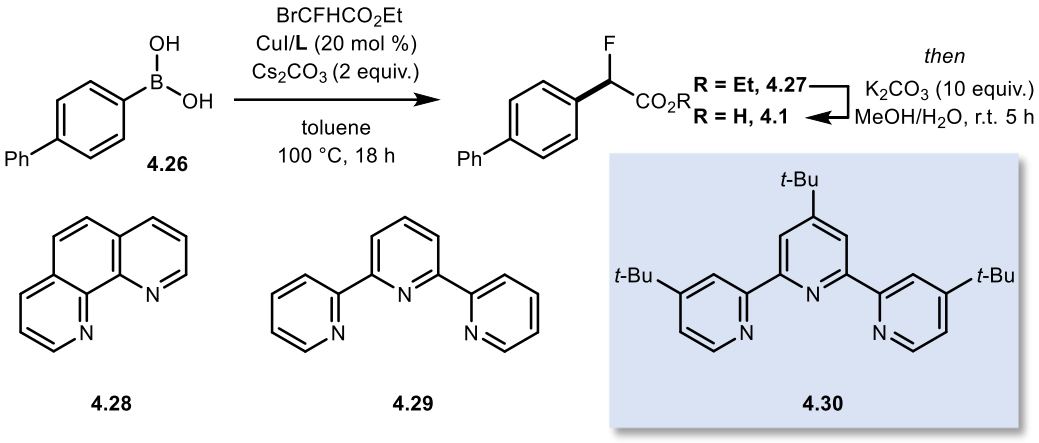

Entry	Solvent	Cu-Source	Ligand	Product	Yield[a]
1[b]	Dioxane (0.2 M)	CuI	4.28	4.27	7%
2[b]	Dioxane (0.2 M)	CuI	4.29	4.27	58%
3	Toluene (0.2 M)	CuI	4.30	4.27	63%
4[c]	**Toluene (0.4 M)**	**CuI**	**4.30**	**4.27**	**82%[d]**
5[c]	**Toluene (0.4 M)**	**CuI**	**4.30**	**4.1**	**75%[d,e]**
6[c]	Toluene (0.4 M)	CuI	-	4.27	0%
7[d]	Toluene (0.4 M)	-	-	4.27	0%
8[d]	Toluene (0.4 M)	$CuCl_2$	4.29	4.27	0%
9[d]	DMSO or DMF (0.2 M)	CuI	4.30	4.27	0%
10	Toluene (0.2 M)	CuI	4.30	4.27	54%[f]

11	Toluene (0.2 M)	CuI	4.30	4.27	64%[g]
12	Toluene (0.2 M)	CuI	4.30	4.27	39%[h]
13	Toluene (0.2 M)	CuI	4.30	4.27	32%[i]
14	Toluene (0.2 M)	CuI	4.30	4.27	56%[j]

[a]Screening reactions performed on 0.1 mmol scale. [b]Yield determined by ^{19}F-NMR using α, α, α -trifluorotoluene as internal standard. [c]2.0 equiv of **4.26** and 1.0 equiv. of ethyl bromofluoroacetate. [d]1.0 equiv. of **4.26**, and 2.0 equiv. of ethyl bromofluoroacetate. [e]Yield of isolated product. [f]K_2CO_3 (2 equiv) used in place of Cs_2CO_3. [g]CsF (2 equiv) used in place of Cs_2CO_3. [h]K_3PO_4 (2 equiv) used in place of Cs_2CO_3. [f]Na_2CO_3 (2 equiv) used in place of Cs_2CO_3. [f]RbF (2 equiv) used in place of Cs_2CO_3.

4.7 Scope and Limitations

The optimised reaction conditions set out for **4.1** (**Table 2.2**, entry 5) were used to determine the generality of our cross-coupling methodology towards a variety of (hetero)aryl boronic acids with varying substitution patterns (**Scheme 4.10**). All reactions were performed on a 0.3 mmol scale. The reaction proved broad in scope, tolerating a variety of functional groups. For example, substrates containing alkyl **4.31**–**4.33** and **4.47**–**4.49**, alkoxy **4.34**, **4.35**, trifluoromethyl **4.36**, bromo **4.44**, **4.45**, iodo **4.46**, and aldehyde **4.37** were all isolated in moderate to good yield (30%-74%), illustrating the tolerance towards both electron deficient and electron rich backbones. Substrates featuring heterocycles such as dibenzofuran **4.38**, pyridine **4.39**, triazole **4.40**, and pyrazoles **4.41**, **4.42** gave the desired products in 40% to 70% yield. Furthermore, this chemistry was applied to access **4.43**, a derivative of fenofibrate in 72% yield. Pleasingly our protocol was amenable to scale-up, with minimum effect on yield. **4.41** was isolated in 55% yield on 5 mmol scale.

Despite the successful application of our technology to a wide array of (hetero)aryl boronic acids, several substrates reacted poorly under the optimised reaction conditions. A common feature amongst these unsuccessful substrates was the presence of a coordinating nitrogen atom which presumably readily engages with the copper catalyst. Examples of low-yielding *N*-heterocycles include **4.51** (25% yield, determined by quantitative ^{19}F NMR yield), **4.53** and **4.55-4.58** (<10 % yield, determined by quantitative ^{19}F NMR yield). **4.52**, derived from thiophen-3-ylboronic acid, a sulfur-containing heterocycle was accessible in moderate yield (30%, determined by quantitative ^{19}F NMR yield). Crude mixtures of these poor performing substrates were analysed by GC-MS. The analysis of the reaction mixtures revealed substantial conversion towards homocoupling as well as protodeborylated and iodinated products. In most cases, the starting material was fully consumed. We speculate that the conversion towards **4.51** was higher than other *N*-heterocyclic substrates such as **4.53** and **4.55** due to the steric hindrance imposed by the CF_3-substituent at the 2' position which may prevent chelation of the substrate to copper.

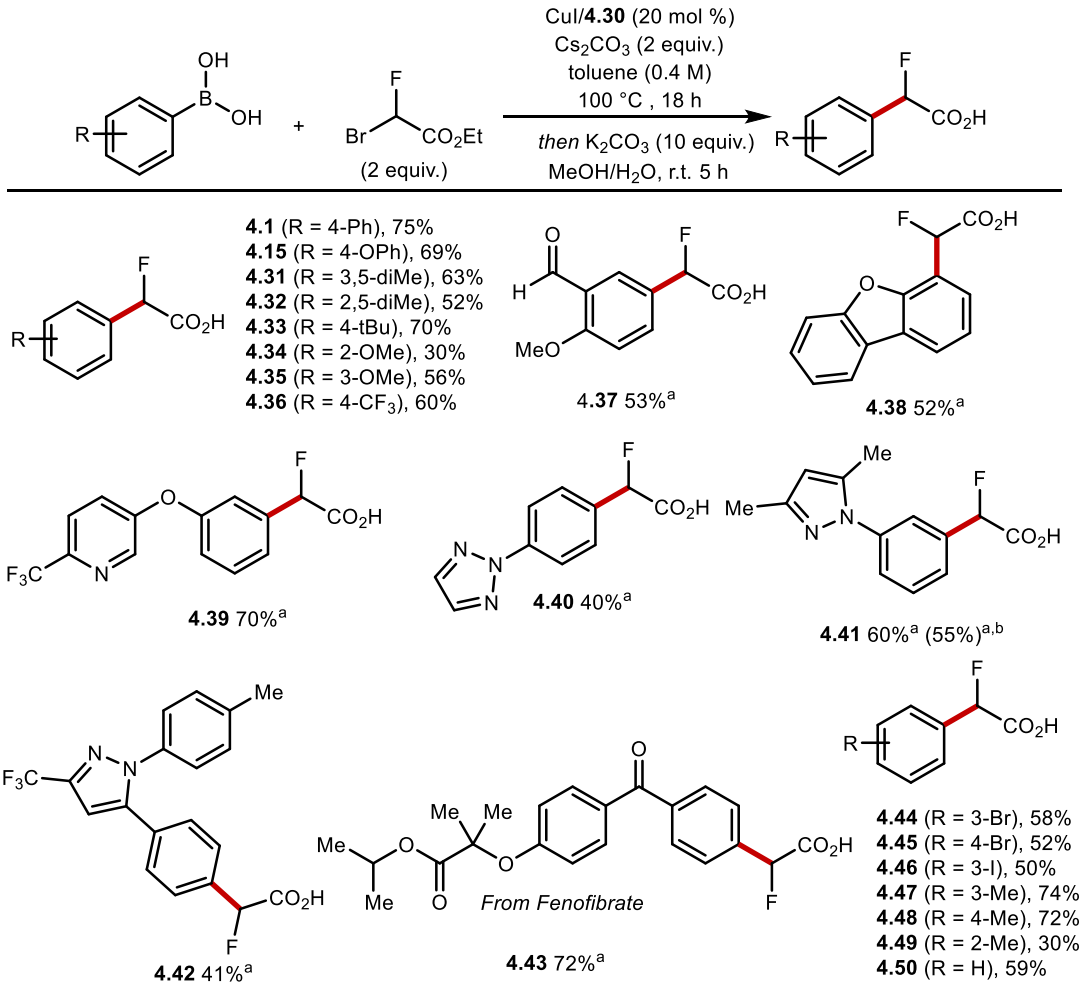

Scheme 4.10 Scope of Cu-catalysed cross-coupling. The reactions were performed on a 0.3 mmol scale. Conditions: CuI (20 mol %), **4.30** (20 mol %), aryl boronic acid (1.0 equiv), ethyl bromofluoroacetate (2.0 equiv), Cs_2CO_3 (2.0 equiv), toluene (0.4 M), 100 ˚C, 18 h then one pot hydrolysis with K_2CO_3 (10 equiv), MeOH/H_2O (1 : 1), 5 h. [a]Hydrolysis performed as a subsequent step with K_2CO_3 (5.0 equiv).[b] Reaction run on 5 mmol scale. All yields are of isolated products. [c]Yield determined by ^{19}F-NMR using α, α, α-trifluorotoluene as internal standard.

4.8 Cross-coupling: mechanistic investigations

Although the exact mechanism of our transformation remains unclear, we found experimentally that the addition of 1.5 equivalents of TEMPO to the reaction of **4.26** under the optimised conditions prevents the formation **4.27** (**Scheme 4.11**).

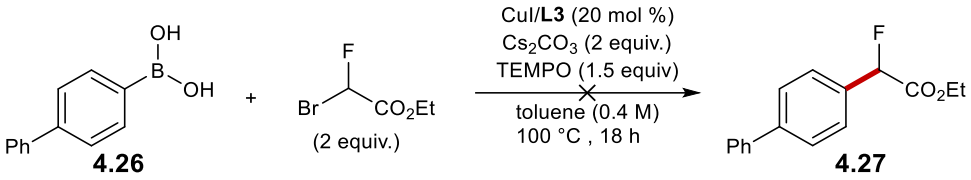

Scheme 4.11 TEMPO mechanistic experiment.

The improved conversion observed when using the *tert*-butyl substituted terpyridine ligand **4.30** versus **4.29** may be explained by its ability to shut down a reaction pathway which involves radical addition to the ligand itself, a commonly reported side-reaction in the literature. Based on results found in the literature[15] as well as our preliminary observations, a plausible mechanism based on a Cu^{I}/Cu^{III} catalytic cycle is proposed (**Scheme 4.12**). The suggested catalytic cycle commences with a pre-catalyst **4.59** which undergoes transmetallation with an equivalent of (hetero)aryl boronic acid (**4.60**) to generate a Cu^{I}-Ar species (**4.61**), under activation with Cs_2CO_3. Subsequently, **4.61** can activate the C-Br bond of ethyl bromofluoroacetate *via* a SET process, generating a fluoroalkyl radical and the Cu^{II} species **4.62**. Species **4.63** is then generated through an oxidative radical addition process. **4.63**, a Cu^{III} species then readily undergoes reductive elimination to furnish the desired ethyl 2-fluoro-2-arylacetate product (**4.64**), which if exposed to basic hydrolysis conditions yields the 2-fluoro-2-arylacetic acid product (**4.15**).

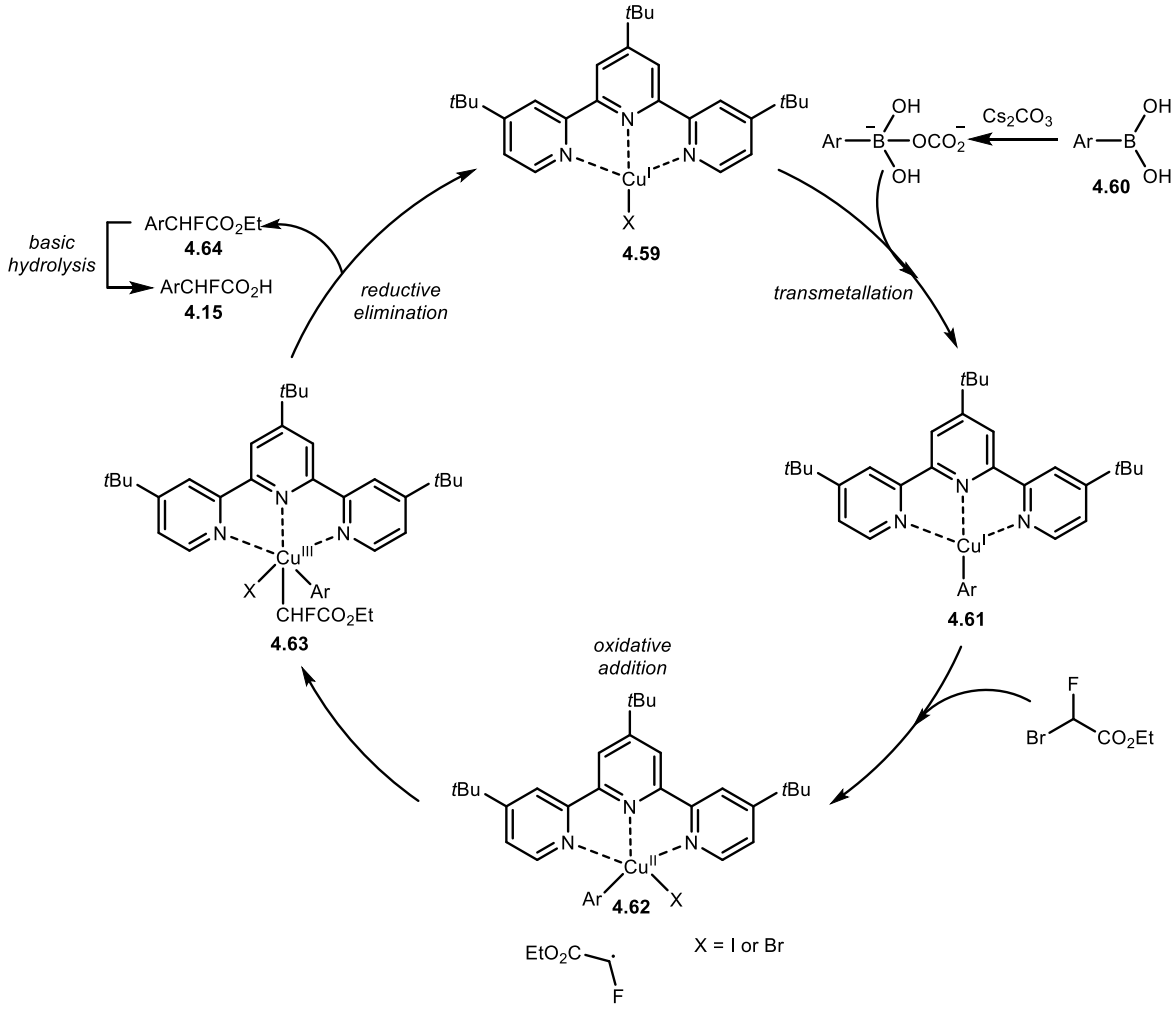

Scheme 4.12 Proposed catalytic cycle of copper cross-coupling reaction.

4.9 Optimisation of ^{18}F-Defluorocarboxylation

Having developed a new copper-catalysed cross-coupling technology towards 2-fluoro-2-arylacetic acids and having established that fluorodecarboxylation of these precursors is feasible using sub-stoichiometric quantities of a nucleophilic fluoride source, we were keen to translate this methodology to F-18 radiochemistry. The key ^{18}F-fluorodecarboxylation step was therefore studied next (**Table 4.3**)**.** We first investigated protocol A, which comprised of reacting in one-pot, **4.15** (0.11 mmol), PhIO (0.33 mmol), Mn(tmp)Cl (2 mg) and [^{18}F]tetraethylammonium fluoride ([^{18}F]TEAF) (20-30 MBq) in

MeCN (600 µL) at 50 ˚C. Under these conditions, only traces of **[^{18}F]4.65** (**Table 4.3,** entry 1) were obtained. Decreasing the loading of PhIO to 0.02 mmol and the solvent volume to 300 µL, **[^{18}F]4.65** was obtained in 6% ± 1% (n = 2) RCY (**Table 4.3**, entry 2). Altering the solvent to DMF led to similar results (**Table 4.3**, entry 3). When the loading of **4.15** was reduced, a significant increase in RCY was observed, 22% ± 7% (n = 2) (**Table 4.3**, entry 4). Pleasingly, when protocol B was applied, which consists of premixing **4.15** with PhIO, a process which generates complex **4.16**, prior to the addition of Mn(tmp)Cl (2 mg) and [^{18}F]TEAF (20–30 MBq), the RCY of **[^{18}F]4.65** was increased to 40% ± 10% (n = 10) (**Table 4.3**, entry 5). When the temperature was further increased to 100 ˚C, **[^{18}F]4.65** was not observed (**Table 4.3**, entry 6). In the absence of Mn(tmp)Cl, or when the axial Cl ligand was substituted for OTs (Mn(tmp)OTs), **[^{18}F]4.65** was not formed (**Table 4.3**, entries 7 and 8).

Table 4.3 ^{18}F-fluorodecarboxylation optimisation.

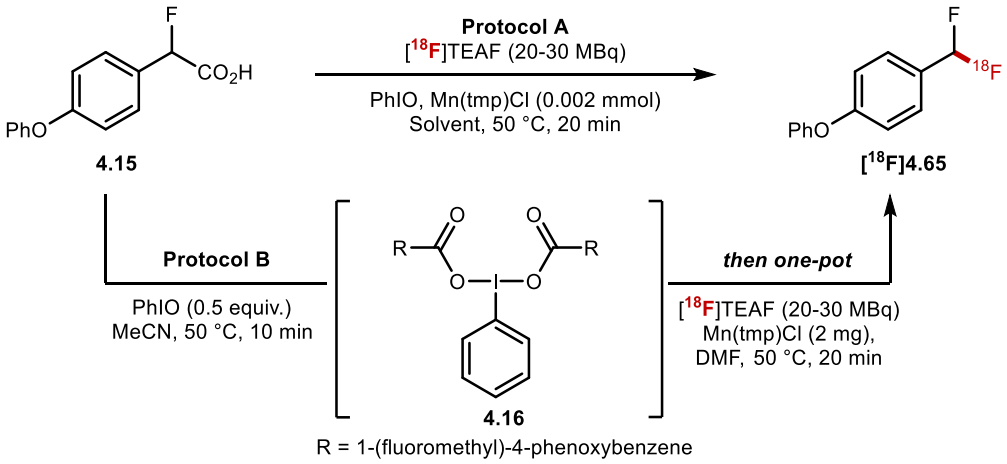

Entry	Starting Material (mmol)	Protocol	Solvent	PhIO (mmol)	RCY[a,b] (*n* = 2)
1	**4.15** 0.11	**A**	MeCN[c]	0.33	3% ± 1%
2	**4.15** 0.11	**A**	MeCN[d]	0.02	6% ± 1%
3	**4.15** 0.11	**A**	DMF[d]	0.02	7% ± 2%
4	**4.15** 0.055	**A**	DMF	0.02	22% ± 7%
5	**4.16 0.014**	**B**	**DMF[d,e]**	**n/a**	**40% ± 10%[f]**
6	**4.16** 0.014	**B**	DMF[d,e]	n/a	0%[g]
7	**4.16** 0.014	**A**	MeCN[d]	0.02	0%[h]
8	**4.16** 0.014	**B**	DMF[d,e]	n/a	0%[i]

[a]Radiochemical yield. [b]n = number of reactions. [c]600 µL of MeCN. [d]300 µL of MeCN. [e]MeCN removed at 100 ˚C after dispensing [^{18}F]TEAF. [f](n = 10). [g]Reaction temperature = 100 ˚C. [h]Catalyst is Mn(tmp)OTs. [i]No Mn Catalyst.

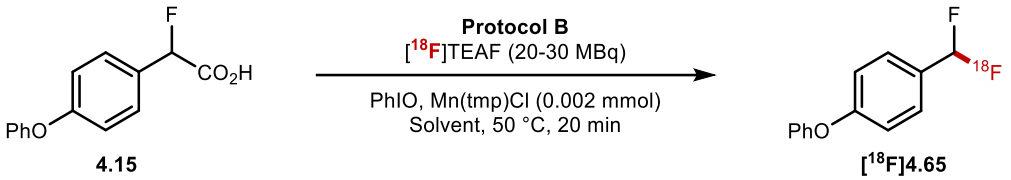

Reaction	Radio-TLC	Radiochemical Conversion
1	50%	50%
2	37%	37%
3	45%	45%
4	37%	37%
5	46%	46%
6	53%	53%
7	34%	34%
8	22%	22%
9	30%	30%
10	43%	43%
Radiochemical Conversion + Standard Deviation		**40% ± 10%**

Scheme 4.13 ^{18}F-fluorodecarboxylation of model substrate **4.15**.

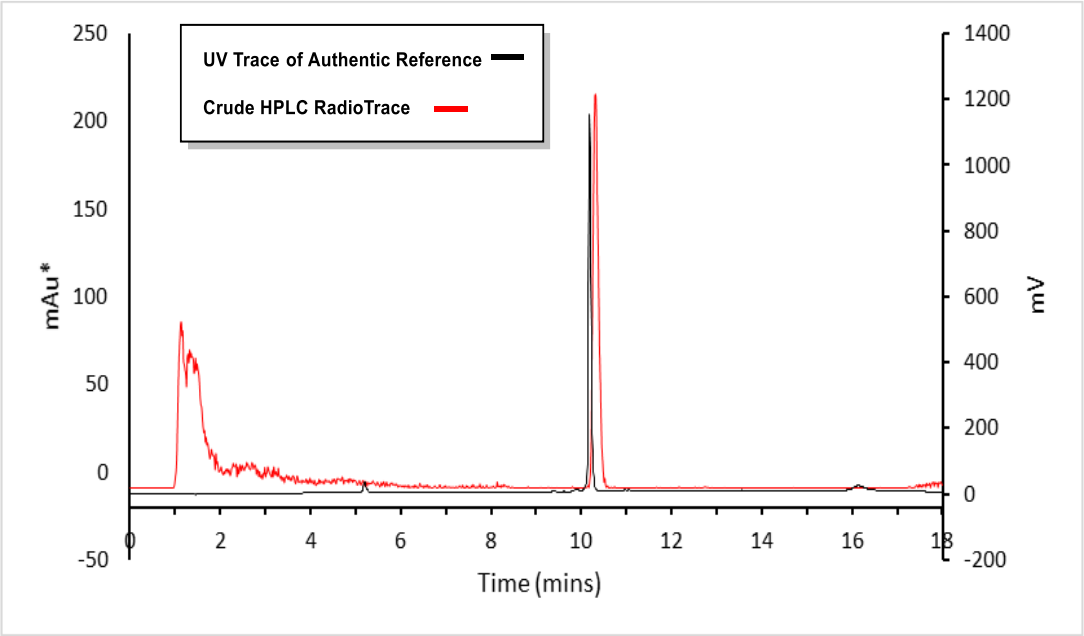

Figure 4.1 Crude mixture HPLC radiotrace overlaid with UV trace of authentic reference of **4.65**.

4.10 Scope of ^{18}F-Defluorocarboxylation

The conditions outlined in **Table 4.3**, entry 5 were applied to a selection of 2-fluoro-2-arylacetic acids using 20-30 MBq of [^{18}F]TEAF as the source of [^{18}F]fluoride (**Scheme 4.14**). Ether (**[^{18}F]4.68**, **[^{18}F]4.70**, **[^{18}F]4.71**, **[^{18}F]4.73** and **[^{18}F]4.81**), alkyl (**[^{18}F]4.66**, **[^{18}F]4.67**, and **[^{18}F]4.69**), aldehyde (**[^{18}F]4.68**), ketone (**[^{18}F]4.77**), pyridine (**[^{18}F]4.74**), triazole (**[^{18}F]4.75**), pyrazole (**[^{18}F]4.76** and **[^{18}F]4.78**), dibenzofuran (**[^{18}F]4.73**) moieties were all tolerated. Electron-rich substrates were found to be the most reactive resulting in higher RCYs. Fenofibrate-derived **[^{18}F]4.77** was successfully labelled in 23 ± 4% (n = 4) RCY. To illustrate the application of this F-18 methodology with more relevant bioactive molecular scaffolds, the F-18 analogue of COX-II inhibitor ZA140 **[^{18}F]4.82** was prepared in 15% ± 2% RCY (n = 3).

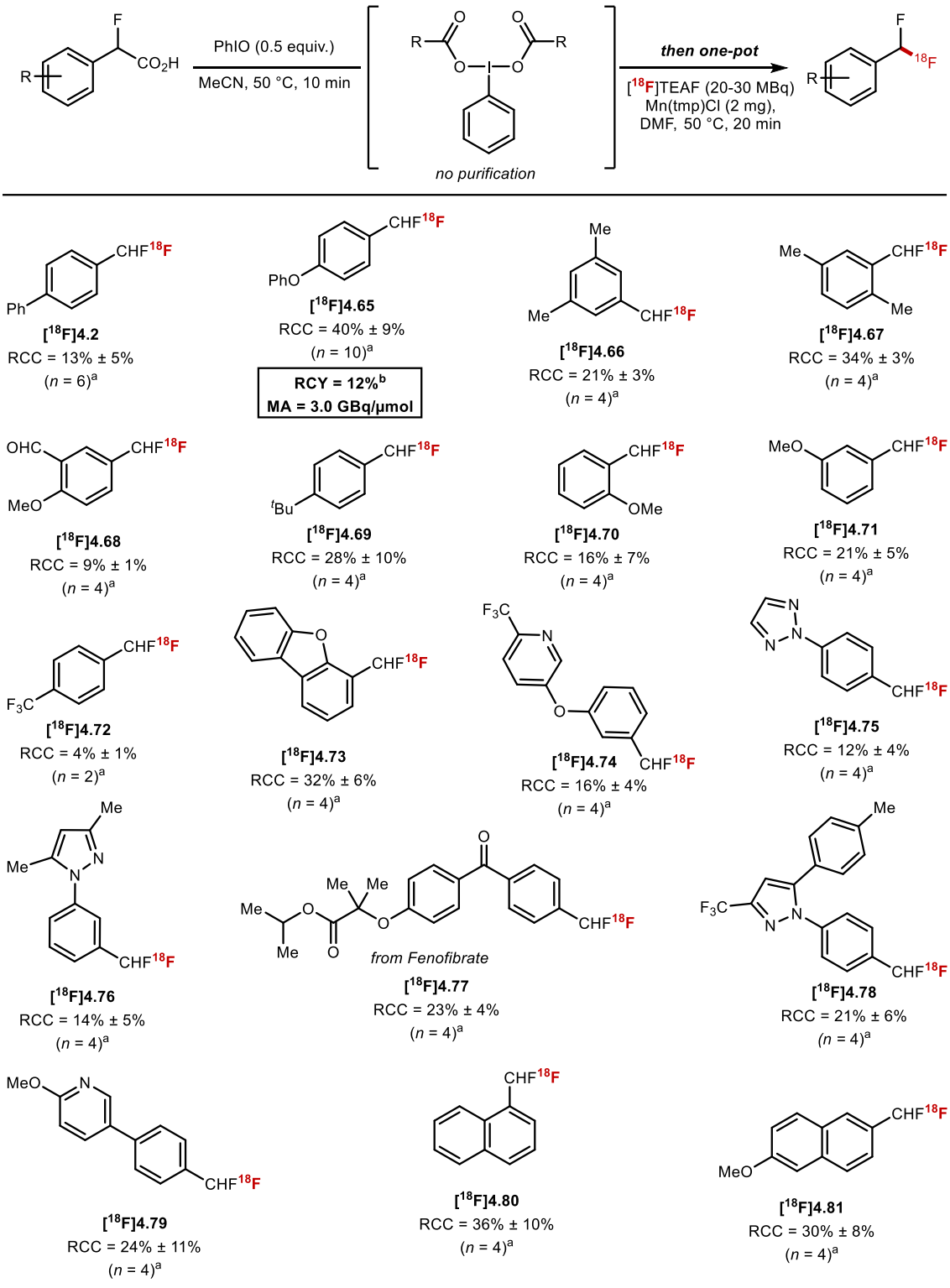

Scheme 4.14 Scope of ^{18}F-fluorodecarboxylation.

Next, we questioned whether [^{18}F](het)ArOCHF^{18}F could be within reach using a similar protocol). Prior to this discovery, the only known method to label this motif required multi-step synthesis of ArOCHFCl precursors which themselves were prepared from ArOCHFCO$_2$H.[17] Our ^{18}F-fluorodecarboxylation protocol afforded the OCHF^{18}F substituted analogue of estrone **[^{18}F]4.83** in 21% ± 6% RCY (n = 3) (**Scheme 4.15**). In both cases, **[^{18}F]4.82** and **[^{18}F]4.83** were obtained selectively, with no F-18 labelled by-products observed in the crude reaction mixture (**Figure 4.2** and **Figure 4.3**).

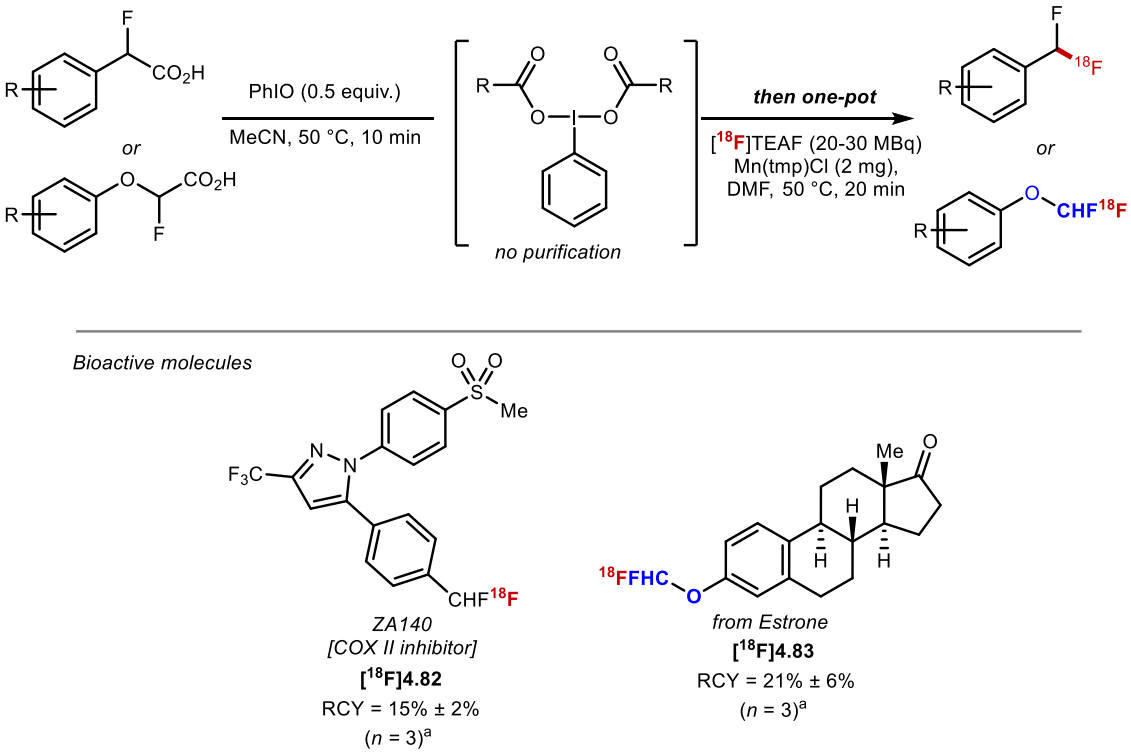

Scheme 4.15 ^{18}F-Fluorodecarboxylation of biologically relevant molecules.

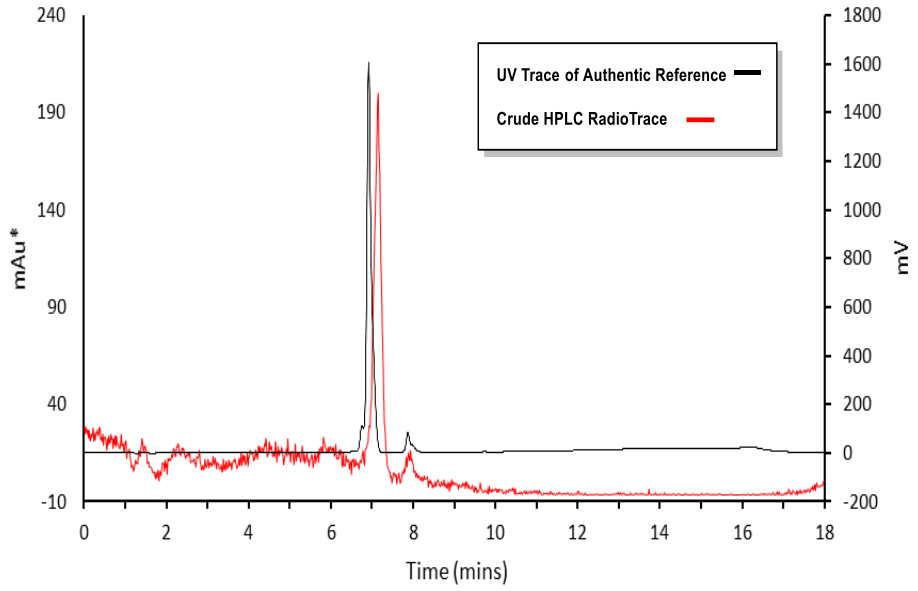

Figure 4.2 Crude mixture HPLC radiotrace overlaid with UV trace of authentic reference of **[^{18}F]4.82**.

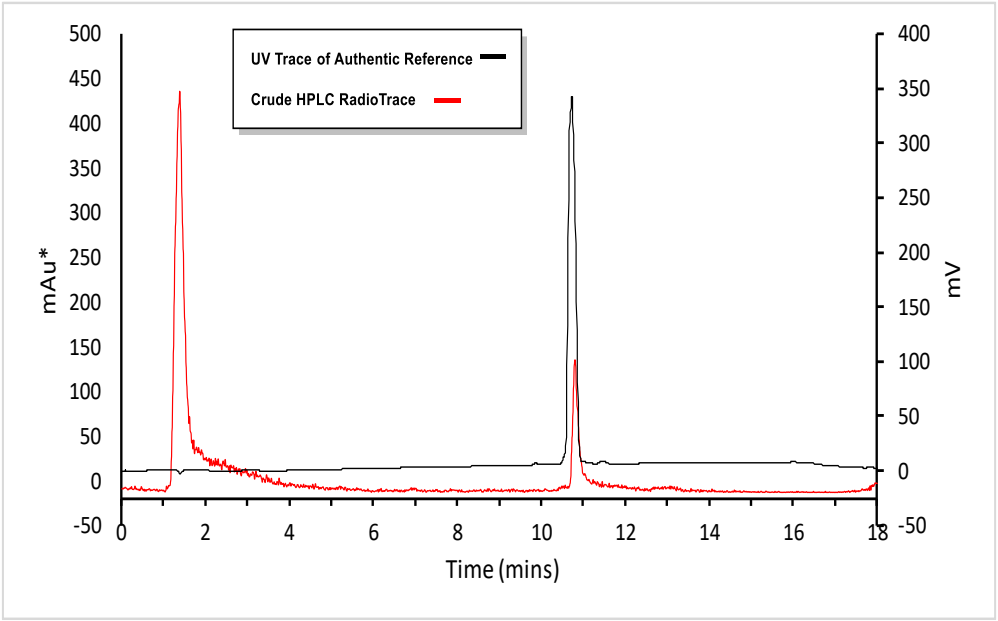

Figure 4.3 Crude mixture HPLC radiotrace overlaid with UV trace of authentic reference of **[^{18}F]4.83**.

Unfortunately, this method did not prove general, and only traces or low F-18 incorporation was observed for **[^{18}F]4.85**, **[^{18}F]4.86** and **[^{18}F]4.87**, indicating that further

development to access this motif is needed **(Scheme 4.16)**. One attributing factor of the low RCY could be the instability of the corresponding I(III) intermediate.

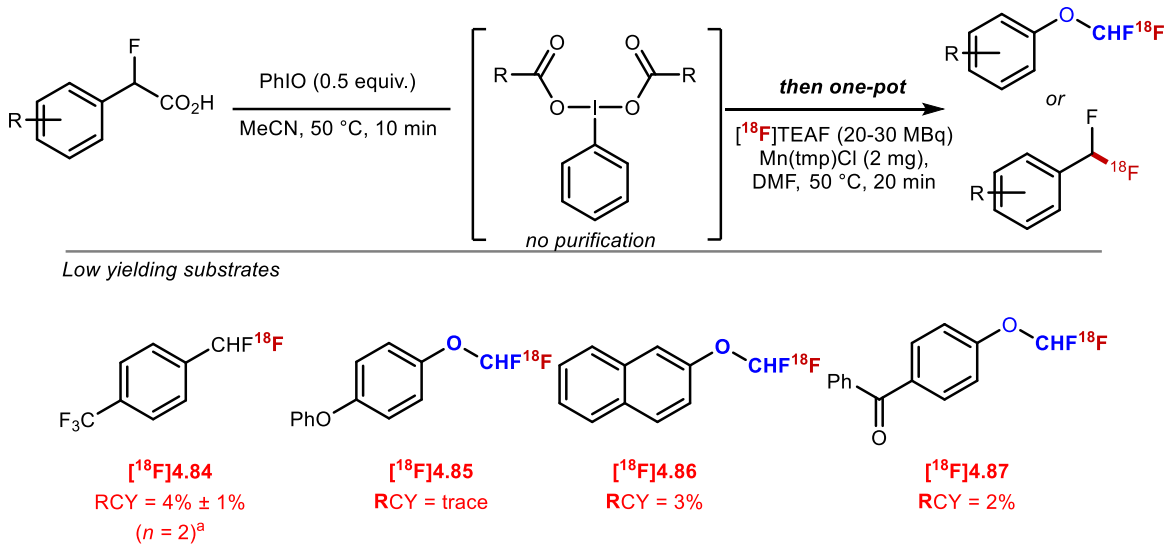

Scheme 4.16 ^{18}F-fluorodecarboxylation of low yielding substrates.

4.11 Scale-Up of ^{18}F-Fluorodecarboxylation Towards the Production of Clinically Relevant Doses.

The ^{18}F-fluorodecarboxylation reactions described thus far were all carried on a 20 – 30 MBq scale, often referred to as 'research mode' radiochemistry. The RCYs of these reactions are determined through analysis of the crude reaction mixture by both radioTLC and radioHPLC. This 'low-activity' scale was deemed appropriate for the initial reaction development and to determine overall functional group compatibility, all whilst minimizing exposure of the researchers to radiation. However, the production of PET radiotracers for clinical imaging requires higher doses (approximately 300 MBq of HPLC-purified tracer).[18] For reactions performed with 20-30 MBq, a 1.0 mL solution of [^{18}F]TEAF/$TEAHCO_3$ in MeCN is prepared by re-dissolving an azeotropically-dried [^{18}F]TEAF/$TEAHCO_3$. For each individual reaction a small aliquot (5 – 50 µL) is then

dispensed, containing only a small fraction of the original $TEAHCO_3$ (starting material in excess). In contrast, when a radiochemical reaction with F-18 is performed on GBq scale or 'batch scale', the entire azeotropically dried [^{18}F]TEAF/ $TEAHCO_3$ batch is used in a single reaction. In this case, one reaction contains the full amount of $TEAHCO_3$. These amounts are then within the same order of magnitude as the starting materials, and as such, can have a significant impact on the reaction. When we scaled up the ^{18}F-fluorodecarboxylation reaction from 20 Mbq to ~ 1.0 GBq of [^{18}F]fluoride, the RCY for **[^{18}F]4.65** dropped from 40% to 2%. We suspected that the increased concentration of tetraethylammonium bicarbonate ($TEAHCO_3$) could be the reason for the significant drop in RCY. In order to testify whether this hypothesis was correct, we performed next a spiking experiment. When performing the ^{18}F-fluorodecarboxylation reaction on a 20 MBq scale under our optimal conditions, but this time in the presence of $TEAHCO_3$ (9 mg), **[^{18}F]4.65** was obtained in an RCY of 4% instead of 40%. In order to circumvent the detrimental effect of $TEAHCO_3$ on larger dose reactions, we attempted to modify the elution procedure. Based on previous mechanistic studies from Groves and co-workers who illustrated the rapid exchange F/Cl halogen exchange Mn(tmp)OTs, it is likely that [^{18}F]fluoride could readily react with Mn(tmp)Cl to form *in situ* [^{18}F]Mn(tmp)F.[12] Given the low concentrations of [^{18}F]fluoride, we were hopeful that the elution of [^{18}F]fluoride directly from the QMA cartridge, was feasible by using an elution solution comprised solely of Mn(tmp)Cl and in the absence of $TEAHCO_3$. If successful, this would not only circumvent the need for $TEAHCO_3$, but also eliminate the tedious azeotropic drying step normally required after the elution of [^{18}F]fluoride.

Pleasingly, when [^{18}F]Fluoride was separated from ^{18}O-enriched-water using an anion exchange cartridge (Sep-Pak Accell Plus QMA Carbonate Plus Light Cartridge, 46 mg Sorbent per Cartridge, 40 µm particle size, Waters) and released with a solution of Mn(tmp)Cl (8 mg) in 600 µL of anhydrous MeOH, we were able to recover [^{18}F]fluoride

in the form of [^{18}F]Mn(tmp)F with an elution efficiency of 85%. With this new elution protocol in hand, we reinvestigated the reaction of **4.16** towards **[^{18}F]4.65** (**Table 4.4**). Improved conditions were found by changing the solvent from DMF to DCE as well as lowering the substrate loading to 0.007 mmol. Applying these changes, **[^{18}F]4.65** could be obtained in an RCY of 37% ± 0% (n = 2, **Table 4.4**, entry 7). Applying these new conditions, the ^{18}F-fluorodecarboxylation of **4.16** was performed with 841 MBq of starting [^{18}F]fluoride. **[^{18}F]4.65** was obtained in a decay corrected AY of 12% and a molar activity of 3.0 GBq µmol^{-1} after C18 SepPak cartridge purification in a total synthesis time of 30 minutes.

Table 4.4 Optimisation of ^{18}F-fluorodecarboxylation on 'batch' scale.

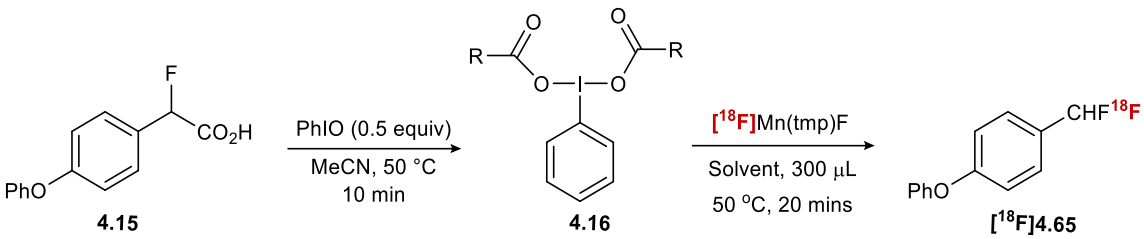

R = 2-fluoro-2-(4-phenoxyphenyl)

Entry	Substrate (mmol) (4.16)	Solvent	RCY (n = 2)
1	0.014	DMF	0%
2	0.014	MeCN	4% ± 1%
3	0.014	DCM	0%
4	0.014	DCE	25% ± 6%
5	0.056	DCE	3% ± 1%
6[a]	0.056	DCE	10% ± 1%
7	**0.007**	**DCE**	**37% ± 0%**

4.12 Molar Activity Measurement

The MA of **[^{18}F]4.65** was determined by HPLC (radiodetector and UV). A UV-calibration curve of **4.65** was constructed (**Figure 4.4**), which allowed the quantification of the MA, according to the calculations outlined below in equations 1 and 2.

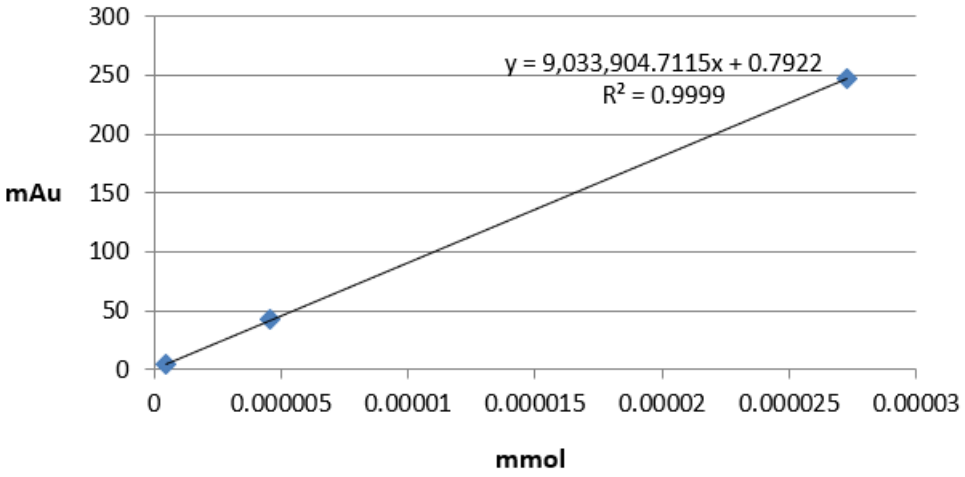

Run	MA (GBq µmol^{-1})	Activity (MBq)	mmol	Area (mAu)
First injection	**3.22**	3.07	9.52412E-07	8.604
Second injection	**2.77**	2.76	9.95915E-07	8.997

Figure 4.4 Molar activity measurement and calculation of **[^{18}F]4.65**.

First Injection

y = 9,033,904.7115x + 0.7922 (y = mAu, x = mmol)
Area measured from isolated sample: 8.604 mAu
Activity of isolated sample: 3.07 MBq = 3.07E-03 GBq
mmol of isolated sample = 8.604/9,033,904= 9.52412E-07 mmol
9.52412E-07 mmol = 9.52412E-04 µmol
MA = 0.00307/9.52412E-04= 3.22 GBqµmol^{-1}

Second Injection

y = 9,033,904.7115x + 0.7922 (y = mAu, x = mmol)

Area measured from isolated sample: 8.997 mAu

Activity of isolated sample: 2.76 MBq = 2.76E-03 GBq

mmol of isolated sample = 8.997/9,033,904= 9.95915E-07 mmol

9.95915E-07 mmol = 9.95915E-04 µmol

MA = 0.00276/9.95915E-04= 2.77 GBqµmol^{-1}

Average

MA = 3.0 GBq/µmol

4.12.1 Reasons for Moderate Molar Activity

The molar activity of 3.0 GBq µmol^{-1} was analogous to the one obtained by Ritter and co-workers in their radiosynthesis of ^{18}F-difluoromethylarenes from aryl(pseudo) halides, and implies that this methodology is best suited in the context of drug development studies.[5] Low to moderate MA values are commonly observed in the F-18 labelling of polyfluorinated motifs.[19]. We therefore investigated the impurity profile (through GC-MS) of the fluorodecarboxylation reaction of **4.15** and observed several by-products, most prominently 4-phenoxybenzoyl fluoride (**4.90**) and 4-phenoxybenzaldehyde (**4.91**). The identity of these side-products allowed us to propose reaction pathways for their formation (**Scheme 4.17)**. We postulate that in addition to the desired reaction pathway, **4.16** can undergo a radical rebound hydroxylation reaction, which has been studied extensively in the literature and suggested to readily occur from a Mn(IV) hydroxy species. The resulting product, fluoro (4-phenoxyphenyl)methanol (**4.89**), is known to be unstable in the literature, either undergoing oxidation to yield **4.90** or spontaneously undergoing defluorination to yield **4.91**.[20] Such processes release fluoride in solution. In the F-18 equivalent of this reaction,

the release of fluoride could exchange with *in situ* generated [^{18}F]Mn(tmp)F, ultimately resulting in dilution of the F-18 product. Future endeavours aiming to improve the MA of this transformation should therefore in the first instance focus on investigating methods to minimise undesired hydroxylation rebound pathway. It is likely that structural modifications of the tmp ligand could have a significant effect on the relative kinetics of fluorination and hydroxylation, and could therefore significantly affect the MA.

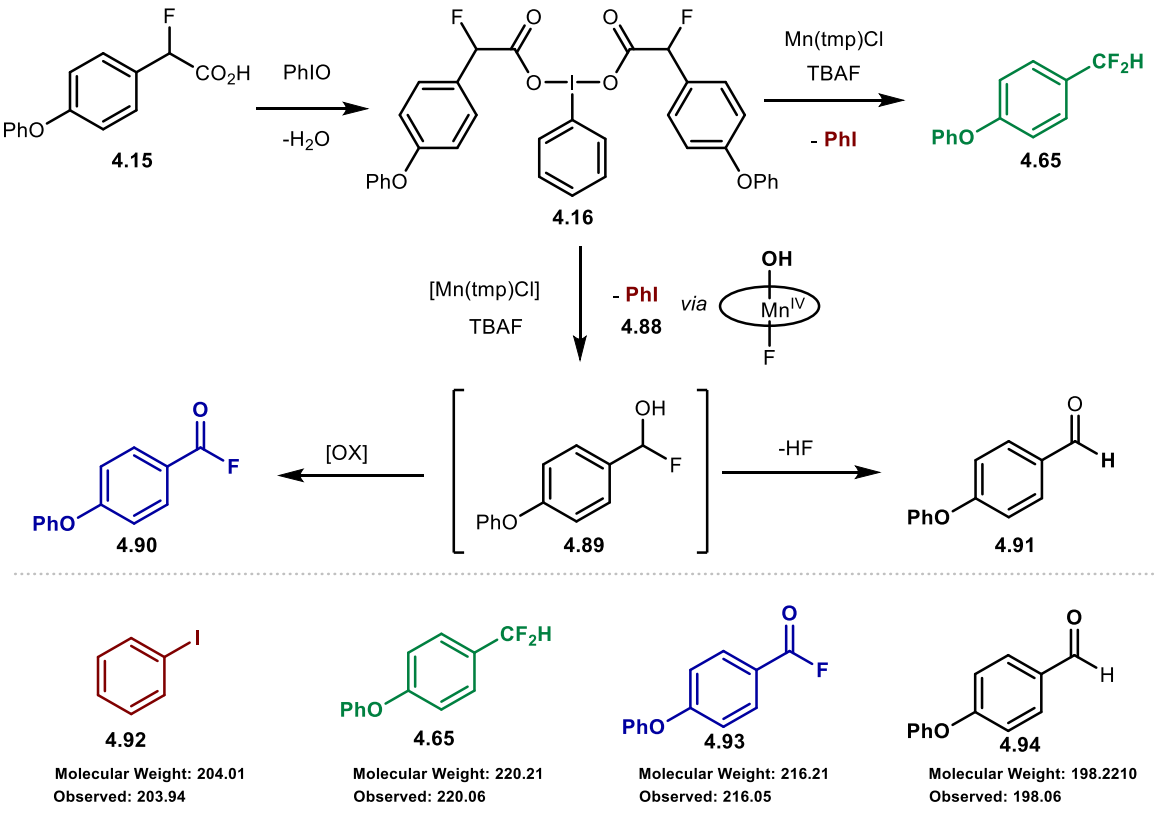

Scheme 4.17 Impurity profile of the fluorodecarboxylation reaction of **4.15**.

Finally, we studied the effect of the benzylic fluorine on the formation of the iodine(III) complex and the ^{18}F-fluorodecarboxylation step. We found that the fluorine substituent was advantageous for both steps (**Scheme 4.18A and B**). When a competition

experiment was performed with equimolar **4.95** and **4.17**, [^{18}F]TEAF, Mn(tmp)Cl at 50 ˚C in DMF, **[^{18}F]4.2** was the only product observed in the crude radiochemical reaction (**Scheme 4.18A)**. Furthermore, an additional competition experiment between **4.13** and **4.1** showed that iodine (III) complex **4.17** formed preferentially to **4.95**, albeit in moderate selectivity (**Scheme 4.18B**).

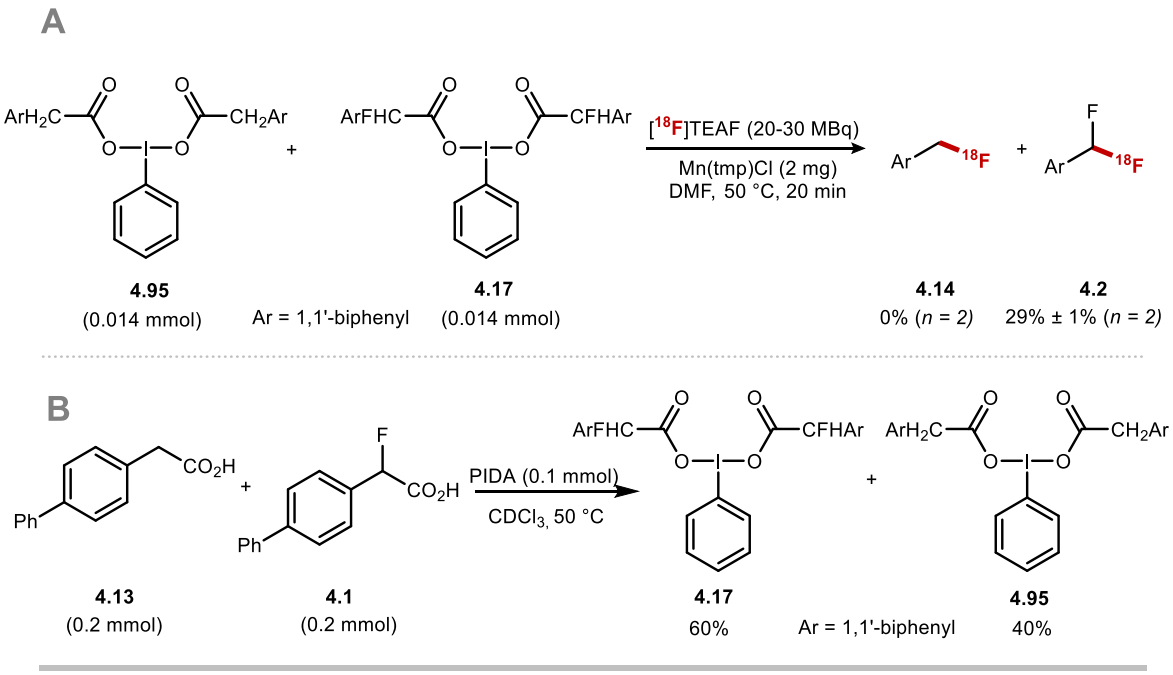

Scheme 4.18 A) Competition experiment subjecting equimolar amount of **4.95** and **4.17** to ^{18}F-fluorodecarboxylation. B) Competition experiment reacting equimolar amount of **4.13** and **4.1** with PIDA.

4.13 Proposed mechanism of ^{18}F-fluorodecarboxylation

We have established that iodine(III) carboxylate esters are intermediates in our fluorodecarboxylation reaction (**Scheme 4.7** and **Scheme 4.8**). We also identified the side products present in the crude reaction mixture (**Scheme 4.17**). This allowed us to postulate the reaction mechanism outlined in **Scheme 4.19**. We propose that the first step in the reaction mechanism involves axial ligand exchange between chloride and ^{18}F-

fluoride, resulting in **[^{18}F]4.97**. The second step involves activation of the carboxylic acid starting material (**4.98**). This activation can occur through two different pathways, the first of which involves the formation of an iodine(III) carboxylate ester which is able to oxidise (**[^{18}F]4.99**) to an Mn(IV) intermediate (**[^{18}F]4.102**) (**Pathway A**). Alternatively, **Pathway B** involves hydrogen abstraction from the hydroxy group of the carboxylic acid by an Mn(V) oxo species (**[^{18}F]4.99**). Both pathways generate radical intermediate **4.100** which spontaneously decarboxylates to form **4.101**. This fluorobenzylic radical is then able to react with in situ formed **[^{18}F]4.103** to afford the desired fluorodecarboxylated product **4.104** regenerating Mn(III) (**4.96**) in the process. Given that the reaction yields are significantly higher when pre-formed iodine(III) dicarboxylate ester is used in the reaction, we expect **Pathway A** to be the preferred reaction pathway.

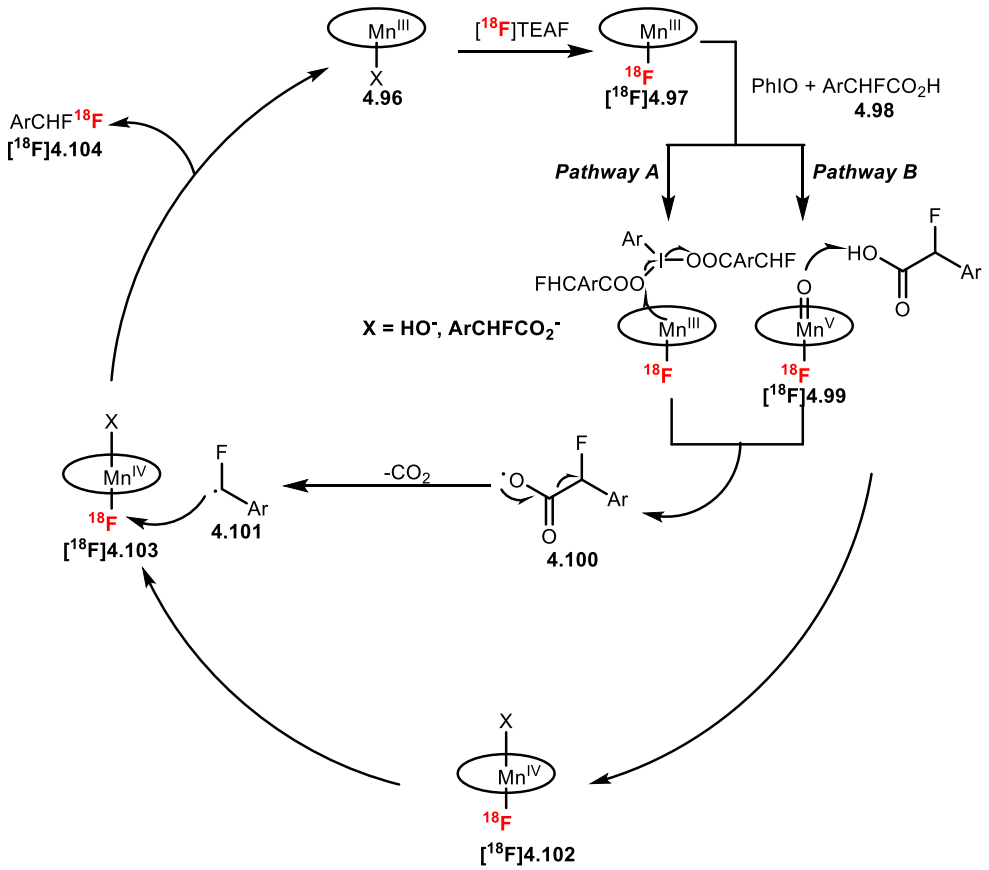

Scheme 4.19 Proposed mechanism of ^{18}F-fluorodecarboxylation.

4.14 Comparison of Our Technology to a Recently Disclosed ^{18}F-Difluoromethylation Protocol

After dissemination of the work disclosed in this chapter, Genicot and Luxen inspired by seminal work by Baran and Hu, reported the first ^{18}F-difluoromethylation protocol of *N*-heteroarenes.[9a,21,22] Unlike the previous reports as well as the one described in this chapter, Genicot and Luxen's technology allows for the direct installation of the CHF^{18}F group onto heteroarenes. Their strategy required the novel ^{18}F reagent, [^{18}F](difluoromethyl)sulfonyl)benzo[d]thiazole (**[^{18}F]4.106**) which was prepared in a two-step-one-pot protocol (^{18}F-fluorination followed by oxidation) from [^{18}F]fluoride. This reagent **[^{18}F]4.106** could be accessed in a RCY of 11.9% ± 1.4% and a MA of 75 GBq µmol^{-1} (decay corrected to E.O.B). ^{18}F-difluoromethylation with this reagent is applicable

to a wide selection of *N*-heteroaromatics (**4.107**), and occurred at the innately most reactive C-H bonds. The authors propose that the CHF^{18}F radical is formed via photocatalytic SET activation of **[^{18}F]4.106** (**Scheme 4.20**).

After this initial publication, the authors published a follow-up report, which automates the synthesis of **[^{18}F]4.106** and the subsequent ^{18}F-difluoromethylation steps.[23]

The work described in this chapter is distinct from the reports of Genicot and Luxen. One benefit of our method is the ability to use [^{18}F]fluoride directly after cyclotron production. Genicot and Luxen's method instead requires firstly the synthesis of **[^{18}F]4.106** from cyclotron-produced fluoride. Mechanistically, the methods are also distinct. While our method exploits aryl boron reagents, Genicot and Luxen's method relies on the innate reactivity of C-H bonds. With regards to scope, the two technologies are highly complementary. While our report works well on electron-rich arenes, Genicot and Luxen's method is best suited for electron deficient *N*-heteroarenes. Even though Genicot and Luxen's method does not require pre-installation of a reaction handle, as is the case for our method, their ^{18}F-difluoromethylation lacks regioselectivity, resulting in the formation of multiple F-18 labelled products. In contrast, our method shows complete site-selectivity at the position of boronic acid substitution, which aids purification.

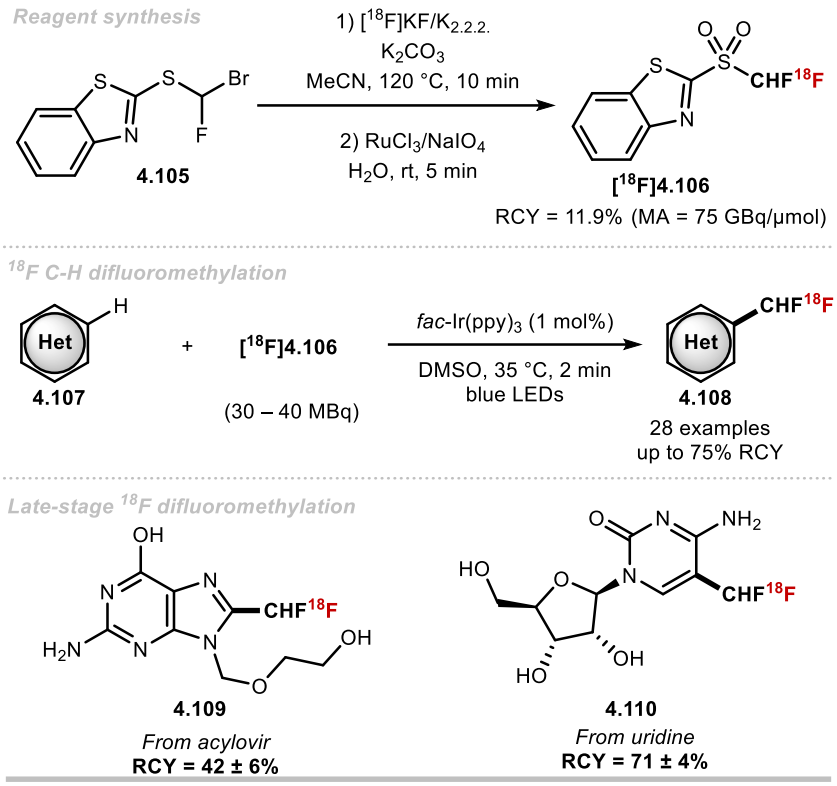

Scheme 4.20 ^{18}F-difluoromethylation of heteroarenes.

4.15 Conclusion

In conclusion, we have developed a novel approach to transform aryl boronic acids to ^{18}F-difluoromethylarenes. Prior to the labelling step, a cross-coupling between aryl boronic acids and commercially available ethyl bromofluoroacetate was accomplished under copper catalysis, followed by *in situ* hydrolysis. The radioisotope, F-18 was then subsequently introduced in the final step through a Mn-mediated ^{18}F-fluorodecarboxylation approach using cyclotron-produced [^{18}F]fluoride. Our study has unveiled three key features for the F-18 labelling step. First, the beneficial effect of fluorine substitution at the benzylic position of the carboxylic acid precursor. Secondly, we discovered through mechanistic experiments that formation of the hypervalent iodine complex prior to ^{18}F-fluorination led to higher RCYs. Finally, we established that

our Mn-mediated ^{18}F-fluorodecarboxylation enabled access to [^{18}F]ArOCF$_2$H in addition to [^{18}F]ArCF$_2$H.

4.16 Future work

Future developments should focus on expanding the current toolbox of available methods to access the [^{18}F]CF$_2$H motif. Specifically, the development of a ^{18}F-difluoromethylation method, which allows direct cross-coupling of aryl (pseudo)halides or aryl boron reagents would be welcomed by the community. This would be an obvious extension of the work disclosed in this chapter, circumventing the need for a two-step approach. Secondly, the development of a C-H ^{18}F-difluoromethylation protocol which goes beyond functionalisation of innately reactive sites, would be well received. Additionally, ^{18}F-difluoromethylation procedures which exploit reactive intermediates beyond [^{18}F]CF$_2$H radical, such as [^{18}F]difluorocarbene ([^{18}F]DFC) or [^{18}F]CF$_2$H anion should be considered. Such developments will help unlock novel radiochemical space of polyfluorinated F-18 motifs and further expand the existing chemical space of [^{18}F](het)ArOCF$_2$H. Finally, while current developments have focused on incorporating the [^{18}F]CF$_2$H motif onto (hetero)aromatics, methods to install this motif onto C$_{sp3}$ centres remain undisclosed. Given the prevalence of C$_{sp3}$-difluoromethylation protocols in the F-19 literature, translation of these methods to F-18 radiochemistry is likely to be possible after adequate optimisation.

4.17 References

1. M. Tredwell and V. Gouverneur, *Angew. Chem. Int. Ed.,* 2012, **51**, 11426.
2. (a) G. Angelini, M. Speranza, C. Shiue, A. Wolf, *J. Chem. Soc., Chem. Commun.,* 1986, 924; (b) A. Hammadi, C. Crouzel, *J. Label. Compd. Radiopharm.,* 1993, **33**, 703; (c) S. Verhoog, C. W. Kee, Y. Wang, T. Khotavivattana, T. C. Wilson, V. Kersemans, S. Smart, M. Tredwell, B. G. Davis and V. Gouverneur, *J. Am. Chem. Soc.,* 2018, **140**, 1572; (d) C. W. Kee, O. Tack, F. Guibbal, T. C. Wilson, P. G. Isenegger, M. Imiolek, S. Verhoog, M. Tilby, G. Boscutti and S. Ashworth, *J. Am. Chem. Soc.,* 2020, **142**, 1180..
3. S. Mizuta, I. S. Stenhagen, M. O'Duill, J. Wolstenhulme, A. K. Kirjavainen, S. J. Forsback, M. Tredwell, G. Sandford, P. R. Moore, M. Huiban, S. K. Luthra, J. Passchier, O. Solin and V. Gouverneur, *Org. Lett*., 2013, **15**, 2648.
4. S. Verhoog, L. Pfeifer, T. Khotavivattana, S. Calderwood, T. L. Collier, K. Wheelhouse, M. Tredwell and V. Gouverneur, *Synlett,* 2016, **27**, 25.
5. H. Shi, A. Braun, L. Wang, S. H. Liang, N. Vasdev and T. Ritter, *Angew. Chem., Int. Ed.,* 2016, **55**, 10786.
6. P. W. Miller, N. J. Long, R. Vilar and A. D. Gee, *Angew. Chem. Int. Ed.,* 2008, **47**, 8998.
7. J. J. Ma, W. Bin Yi, G.P. Lu, C. Cai, *Org. Biomol. Chem.* 2015, **13**, 2890.
8. G. Yuan, F. Wang, N. A. Stephenson, L. Wang, B. H. Rotstein, N. Vasdev, P. Tang and S. H. Liang, *Chem. Commun.,* 2017, **53**, 126.
9. (a) Y. Fujiwara, J. A. Dixon, R. A. Rodriguez, R. D. Baxter, D. D. Dixon, M. R. Collins, D. G. Blackmond and P. S. Baran., *J. Am. Chem. Soc.*, 2012, **134**, 1494; (b) T. T.

Tung, S. B. Christensen and J. Nielsen, *Chem. Eur. J.,* 2017, **23**, 18125; (c) R. Sakamoto, H. Kashiwagi and K. Maruoka, *Org. Lett.*, 2017, **19**, 5126.

10. L. Wang, J. Wei, R. Wu, G. Cheng, X. Li, J. Hu, Y. Hu and R. Sheng, *Org. Chem. Front.,* 2017, **4**, 214.
11. T. C. Wilson, T. Cailly and V. Gouverneur, *Chem. Soc. Rev.,* 2018, **47**, 6990.
12. X. Huang, W. Liu, J. M. Hooker and J. T. Groves, *Angew. Chem., Int. Ed.,* 2015, **54**, 5241.
13. F. Zhang and J. Z. Song, *Tetrahedron Lett.,* 2006, **47**, 7641.
14. (a) Y. Wu, H.-R. Zhang, Y.-X. Cao, Q. Lan and X.-S. Wang, *Org. Lett.,* 2016, **18**, 5564; (b) Y. M. Su, G. S. Feng, Z. Y. Wang, Q. Lan and X. S. Wang, *Angew. Chem., Int. Ed.,* 2015, **54**, 6003.
15. (a) C. Guo, X. Yue and F. L. Qing, *Synthesis*, 2010, **11,** 1837; T. Xia, L. He, Y. A. Liu, J. F. Hartwig and X. Liao, *Org. Lett.,* 2017, **19**, 2610.
16. Source: http://www.ich.org/products/guidelines/quality/article/quality-guidelines.html, accessed on 28/06/20.
17. T. Khotavivattana, S. Verhoog, M. Tredwell, L. Pfeifer, S. Calderwood, K. Wheelhouse, T. L. Collier and V. Gouverneur, *Angew. Chem., Int. Ed.,* 2015, **54**, 9991.
18. J. M. Martí-Climent, E. Prieto, V. Morán, L. Sancho, M. Rodríguez-Fraile, J. Arbizu, M. J. García-Velloso and J. A. Richter, *EJNMMI research,* 2017, **7**, 37.
19. M. Huiban, M. Tredwell, S. Mizuta, Z. Wan, X. Zhang, T. L. Collier, V. Gouverneur and J. Passchier, *Nat. Chem.,* 2013, **5**, 941.
20. Y. Pan, *ACS Med. Chem. Lett.* 2019, 10, **7**, 1016.

21. Rong, L. Deng, P. Tan, C. Ni, Y. Gu and J. Hu, *Angew. Chem., Int. Ed.,* 2016, **55**, 2743.

22. L. Trump, A. Lemos, B. Lallemand, P. Pasau, J. Mercier, C. Lemaire, A. Luxen and C. Genicot, *Angew. Chem. Int. Ed.* 2019, **58**, 13149.

23. L. Trump, A. Lemos, J. Jacq, P. Pasau, B. Lallemand, J. Mercier, C. Genicot, A. Luxen and C. Lemaire, *Org. Process Res. Dev.* 2020, **24**, 734.

Chapter 5: [^{18}F]Difluorocarbene Unlocks New and More Stable F-18 Motifs for Positron Emission Tomography

The work discussed in this chapter is to date unpublished.

Author contributions: [^{18}F]ArSO_2CF_2Cl synthesis was optimised by Jeroen Sap and Dr. Natan Straathof. [^{18}F]ArSO_2CF_2H synthesis was optimised by Jeroen Sap, Dr. Natan Straathof, and Claudio Meyer. Radiolabelling mechanistic experiments illustrating [^{18}F]ArSO_2CF_2H is a difluorocarbene reagent, were performed by Jeroen Sap and Claudio Meyer. Optimisation studies towards [^{18}F]ArOCF_2H, [^{18}F]ArSCF_2H, [^{18}F](het)ArNCF_2H were performed by Jeroen Sap and Claudio Meyer. F-18 competition experiments were performed by Jeroen Sap and Claudio Meyer.

5.1 Introduction: Thermodynamic and Metabolic Stability of Fluoroalkylated Motifs Used in PET

Today, methods for the preparation of structurally diverse radiotracers from [^{18}F]fluoride have relied on nucleophilic substitution of alkyl electrophiles, nucleophilic aromatic substitution (S_NAr), and more recently cross-coupling technologies.[1,2] Another compelling strategy to F-18 label substrates which bear innate nucleophilic handles such as (thio)phenols or *N*-heteroarenes exploit [^{18}F]fluoride-derived alkylating reagents, most commonly [^{18}F]fluoromethyl tosylate and [^{18}F]fluoromethyl iodide.[3] In contrast to the first category, which has witnessed continuous development throughout the last decade, innovation of the latter has lagged behind. Whilst ^{18}F-alkylation strategies are typically robust and high yielding from a radiochemistry standpoint, challenges remain due to the inherent instability of the resulting [^{18}F]fluoromethyl(thio)ethers.[4]

CyP450-mediated radiodefluorinations of [^{18}F]fluoromethyl(thio)ether radiotracers lead to metabolic degradation due to the release of [^{18}F]fluoride *in vivo* which accumulates in the skull and bones. If this happens, PET images provide false-positive information on bone imaging, and/or suffer from poor signal to background ratio. Common strategies to avoid radiodefluorination (*via* CyP450-oxidation or elimination) or considerably reduce it, include deuterium incorporation.[5]

An exemplary case study which illustrates the propensity of [^{18}F]fluoromethylethers to undergo undesirable radiodefluorination was performed on MeNER, a high-affinity ligand for norepinephrine transporter (NET). Initially, PET images were secured with [^{11}C]MeNER (**[^{18}F]5.2**), a radiotracer obtained by methylation with [^{11}C]MeOTf as the alkylating reagent (**Scheme 5.1**). One limitation of this radiotracer is the short half-life

of C-11 ($t_{1/2}$ = 20.4 min) responsible for the acquisition of poor PET images because *in vivo* binding did not proceed effectively within 90 minutes. As a result, [^{18}F]FMeNER (**[^{18}F]5.3**), a radiotracer which exhibited similar affinity for the receptor, but contains the longer-lived radioisotope (F-18) was synthesised. **[^{18}F]5.3** was prepared from the same precursor as **[^{18}F]5.2** with [^{18}F]fluoromethyl triflate as the F-18 alkylating reagent. Despite alleviating the half-life related problems associated with **[^{18}F]5.2**, PET images with **[^{18}F]5.3** showed increased bone uptake, a problem arising from *in vivo* radiodefluorination. To combat this pressing problem, the deuterated derivative [^{18}F]FMeNER-D_2 **[^{18}F]5.4** was prepared which successfully minimised radiodefluorination (**Scheme 5.2B**).[6]

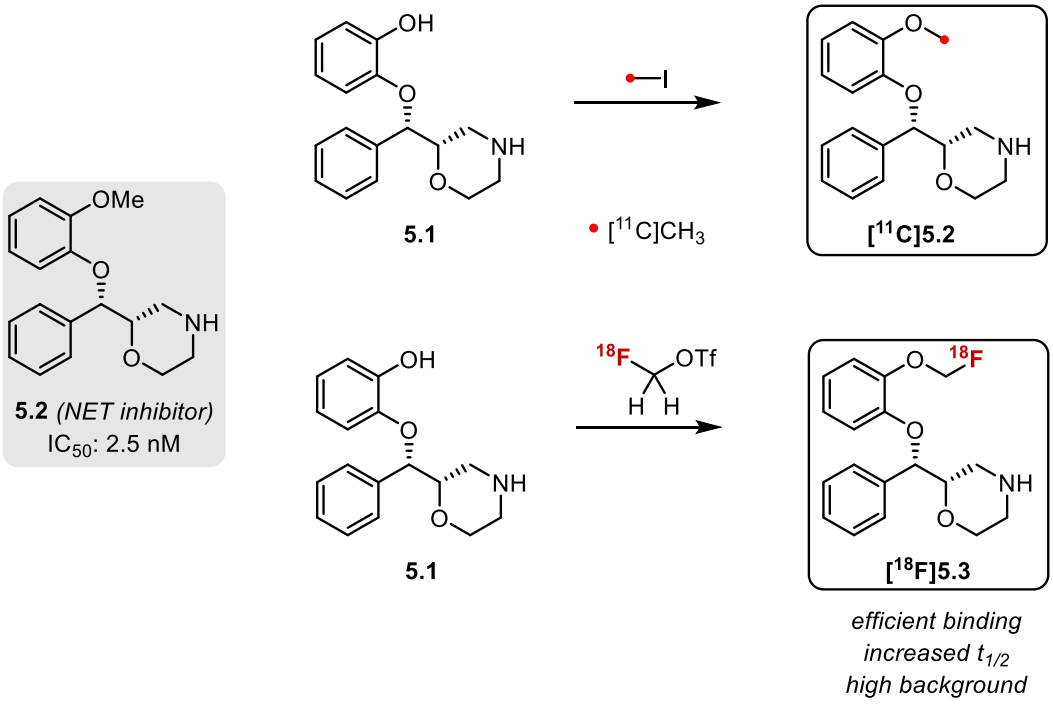

Scheme 5.1 C-11 and F-18 radiotracers of MeNER-D_2.

Another contributing factor to overall resistance to radiodefluorination is thermodynamic stability (**Scheme 5.2**). Typically, the overall stability increases with higher degrees of fluorination in the following order, $ArOCF_3$>$ArOCF_2H$>$ArOCH_2F$.[7] This trend is informative given that the radiochemical space of [^{18}F]$ArOCF_3$ and [^{18}F]$ArOCF_2H$ remains virtually unexplored.

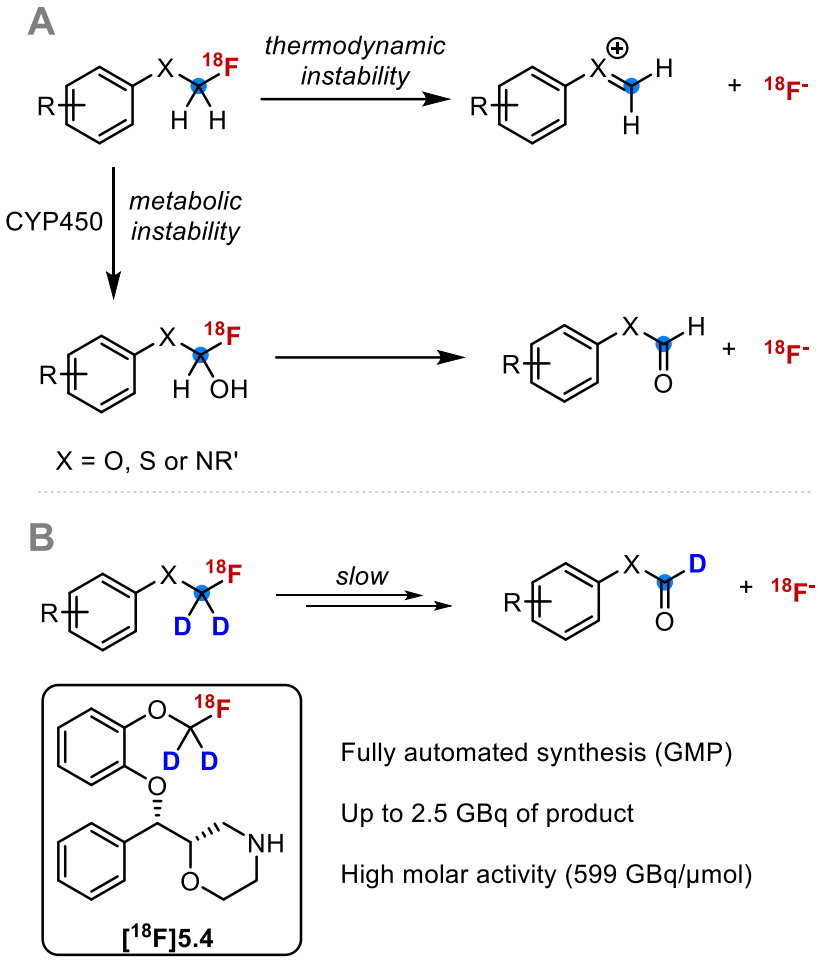

Scheme 5.2 A) Metabolic and thermodynamic stability of [^{18}F]$ArXCH_2F$ radiotracers. B) [^{18}F]FMeNER-D_2 as a more stable analogue towards radiodefluorination.

To minimise/prevent/avoid *in vivo* defluorination of fluoroalkylated tracers, radiochemists have employed tactics such as extending the length of fluoroalkyl chains or exchanging selected hydrogen atoms for deuterium (+cyclobutyl to avoid HF

elimination). Whilst in several cases, the *in vivo* properties of such tracers can be improved through these strategies, deuteration typically does not entirely suppress unwanted radiodefluorination (**Figure 5.1**). Furthermore, extension of the fluoroalkyl spacer, generates increased steric constraints, which may alter the properties of the radiotracer altogether.[5]

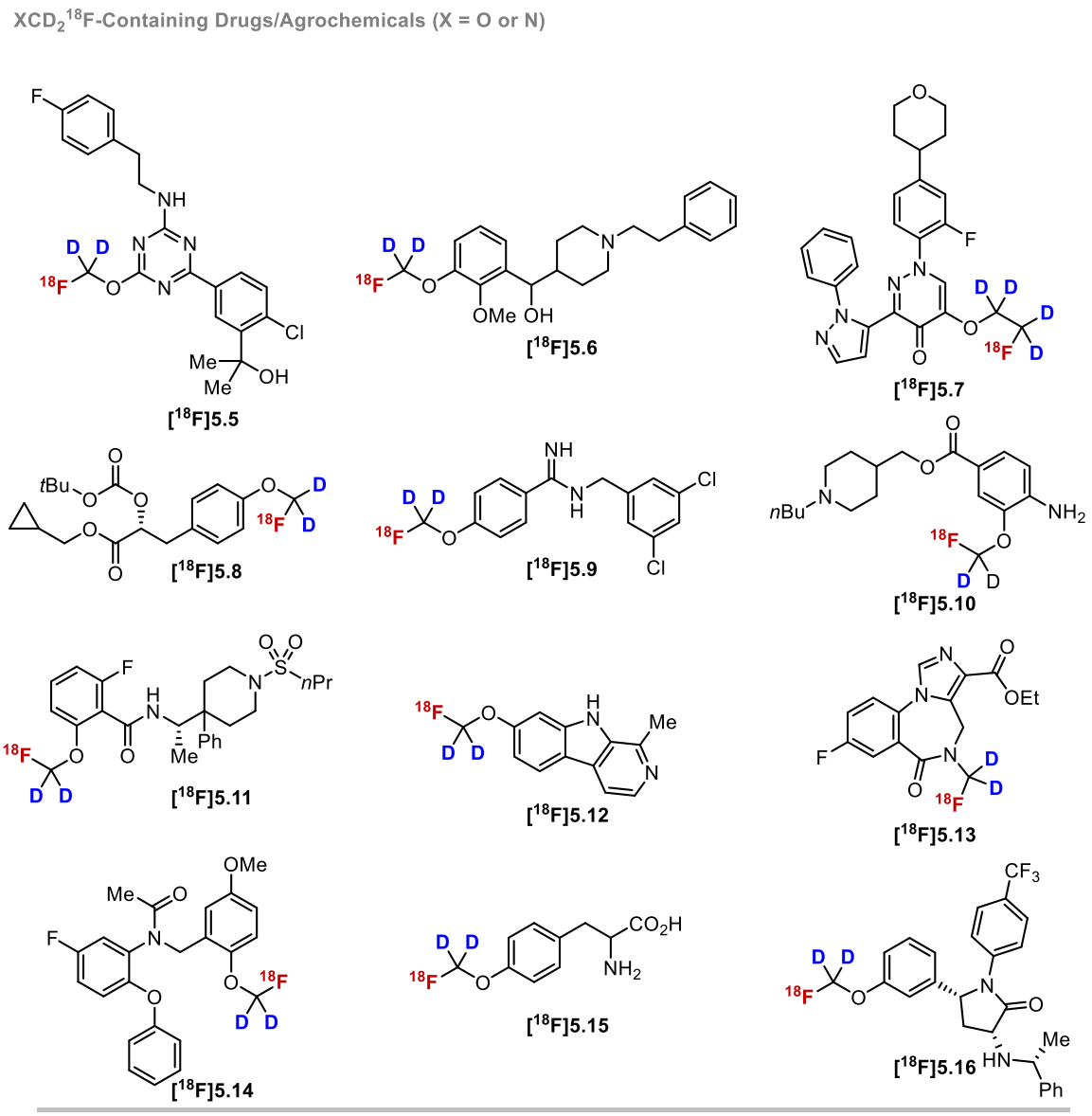

Figure 5.1 Deutero fluoroalkylated radiotracers which suffered detrimental radiodefluorination rescued in part by deuteration.

Whilst in F-19 chemistry difluoromethyl(thio)ethers have emerged as stable bioisosteres of methoxy groups, protecting drugs against undesired metabolism, ^{18}F-radiolabelling technologies to access these motifs remain underdeveloped, and the methods developed to date lack generality, and are not applicable to complex ^{18}F-labeled tracers (**Figure 5.2**).[7]

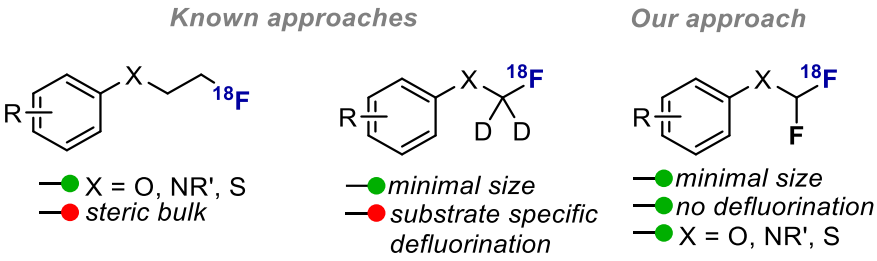

Figure 5.2 A) Routinely used strategies. B) Our approach.

5.2 Prior Art: F-18 Radiolabelling of [^{18}F]ArOCF$_2$H

In 2015, Gouverneur and co-workers hallmarked the first radiosynthesis of [^{18}F]ArOCF$_2$H (**[^{18}F]5.18**) through a silver-mediated ^{18}F-fluorination from the corresponding chloro-precursors (**5.17**) (**Scheme 5.3A**).[8] The main limitation of this method was the modest scope (limited to small building blocks) and low MA (0.1 – 0.2 GBq µmol^{-1}). The authors illustrated that this silver-mediated halogen exchange could be extended to access [^{18}F]ArOCF$_3$ and [^{18}F]ArSCF$_3$, and applied this technology to the radiosynthesis of 5-^{18}F-(trifluoromethyl)dibenzothiophenium trifluoromethanesulfonate ([^{18}F]Umemoto's reagent). From a LSF perspective, the multi-step syntheses required to access the necessary labelling precursors were proved challenging to implement especially for highly functionalized molecules. In **Chapter IV**, we illustrated that [^{18}F]ArOCF$_2$H (**[^{18}F]5.20**) is accessible from [^{18}F]fluoride through ^{18}F-fluorodecarboxylation. This

strategy however lacks generality, and likewise required time consuming synthesis of the necessary pre-functionalised precursors (**Scheme 5.3B**).[9]

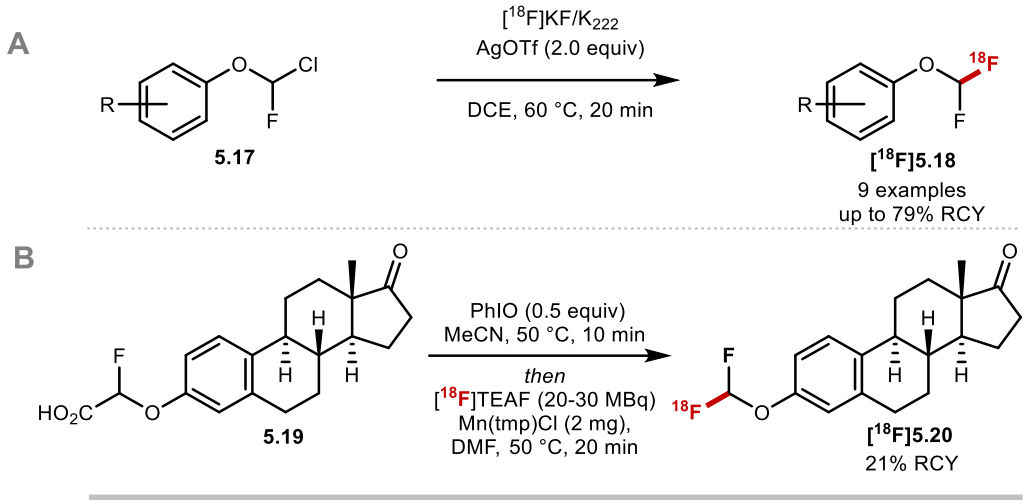

Scheme 5.3 State of the art: current methods to access [^{18}F]ArOCF$_2$H.

It is evident that there is a pressing need for new methods which provide access to [^{18}F]ArOCF$_2$H and other difluoromethylated PET motifs such as [^{18}F]ArSCF$_2$H and [^{18}F]NCF$_2$H (currently not within reach) directly accessible from innate reactive handles. Upon closer inspection of the literature, it was apparent that a universal method to access these motifs in a streamlined manner from readily available materials would require innovative radiochemistry to reach F-18 labelled difluorocarbene (DFC).

5.3 Commonly Used Difluorocarbene Reagents in Organic Synthesis

As illustrated in **Chapter I**, DFC is a reactive intermediate which has been used extensively for the difluoromethylation of (thio)phenols and *N*-heterocycles as well as the difluorocyclopropanation of alkenes and alkynes. The potential of DFC spans beyond these substrate classes, and has also witnessed utility in multi-component reactions and more recently metal-catalysed cross-coupling reactions. As a result of its versatility,

many DFC-releasing reagents have been developed over the last decade(s) (**Figure 5.3**). As discussed in **Chapter I**, these DFC reagents can release DFC either through activation by a base/nucleophile or through thermolysis. Depending on which mode of activation is used to generate DFC, the selectivity and product outcome of DFC reactions can be altered.

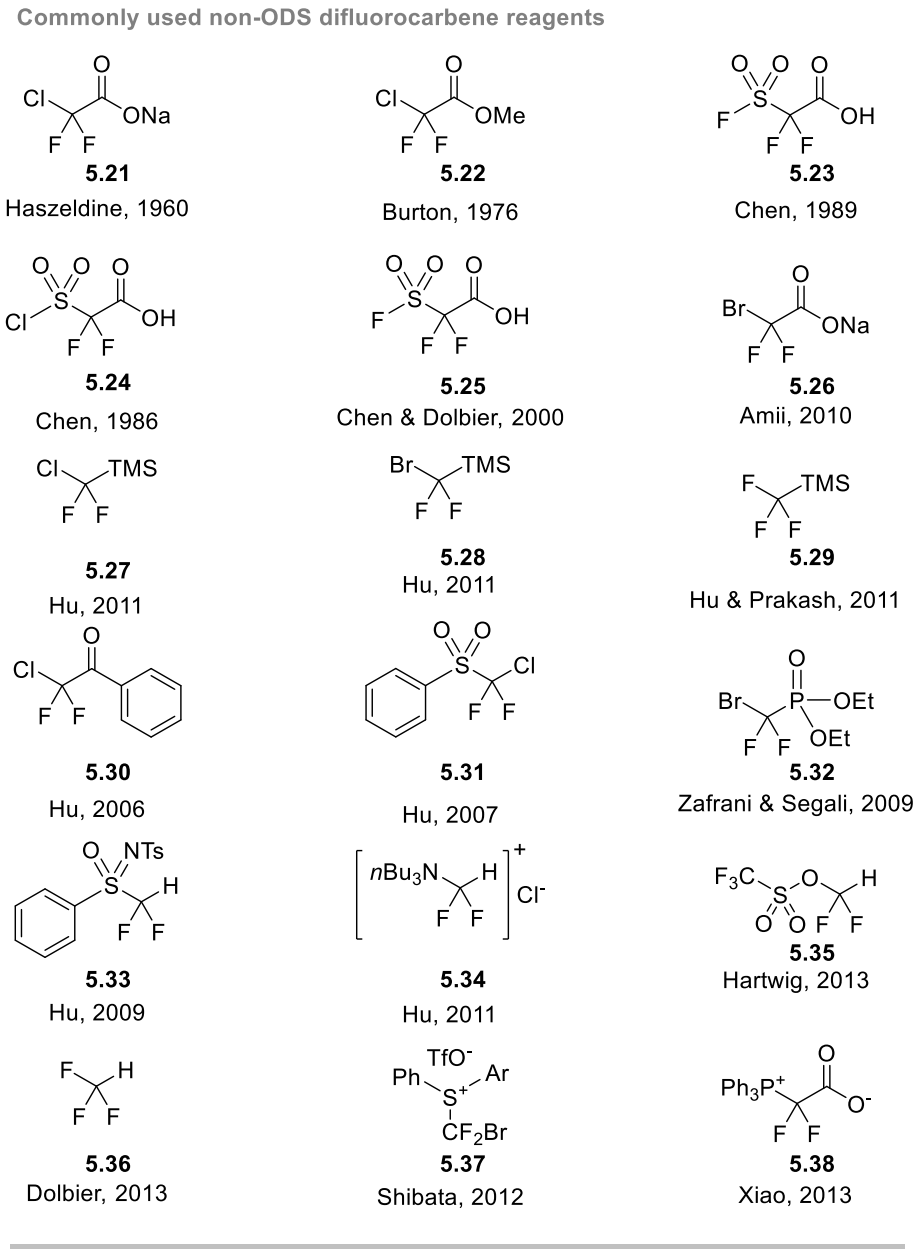

Figure 5.3 Structures of difluorocarbene sources used in recent organic synthesis.[10]

5.4 Difluorocarbene in F-18 Radiochemistry

The utility of DFC within the field of organic synthesis is well established, gauging an interest amongst radiochemists to exploit this reactive intermediate in radiochemistry. As early as 1991, Burton and co-workers reported the generation of $CuCF_3$ from chlorodifluoroacetate, and illustrated its application in transferring the CF_3 group to a selection of aryl iodides.[11] The authors proposed a mechanism whereby a Cu(I) salt induced DFC formation, which subsequently reacted with fluoride to generate the CF_3 anion. This anion was then trapped by a Cu(I) salt, generating $CuCF_3$ *in situ*.

In 2013, the Gouverneur group was able to translate this reaction to F-18 radiochemistry. They illustrated that a wide selection of (hetero)aryl iodides (**5.39**) were readily trifluoromethylated in good radiochemical yields using [^{18}F]KF and methyl chlorodifluoroacetate, a reagent acting as a ^{19}F-difluorocarbene (^{19}F-DFC) source. In addition to a large selection of heteroarenes, two biologically active molecules, fluoxetine and flutamide were readily trifluoromethylated in 37% ± 4% and 55% ± 3% RCY, respectively. One limitation of this methodology is the low molar activity (MA) observed for the F-18 labelled products. [^{18}F]1-nitro-4-(trifluoromethyl)benzene was isolated with a MA of 0.1 GBq/µmol (**Scheme 5.4A**).[12] This concept attracted the attention of many radiochemists (**Scheme 5.4B**)[13], unlocked various drug discovery programs, and paved the way to a new development in the Gouverneur's laboratory. [^{18}F]$CF_3SO_2NH_4$ (**[^{18}F]5.44**) was prepared by merging [^{18}F]Fluoride with a ^{19}F-DFC reagent and *N*-methylmorpholine·SO_2 (**5.43**) which enabled site-selective C–H ^{18}F-trifluoromethylation of unmodified peptides as large as insulin at tyrosine (**5.46**) or tryptophan residues (**5.47**) (**Scheme 5.4C**).[14] One stringent limitation of this

radiochemistry based on ^{19}F-DFC is the low MA of the corresponding products, an issue narrowing dramatically the range of applications for PET imaging studies. In 2015, the Liang group also exploited ^{19}F-DFC in the context of radiochemistry. They were successful in the ^{18}F-trifluoromethylthiolation of benzyl bromides (**5.49**) (**Scheme 5.4D**)[15] and α-bromo carbonyl compounds (**5.51**) (**Scheme 5.4E**).[16] In both instances, [^{18}F]fluoride was the fluoride source, PDFA was used as the ^{19}F-DFC reagent, and S_8 was the source of sulfur.

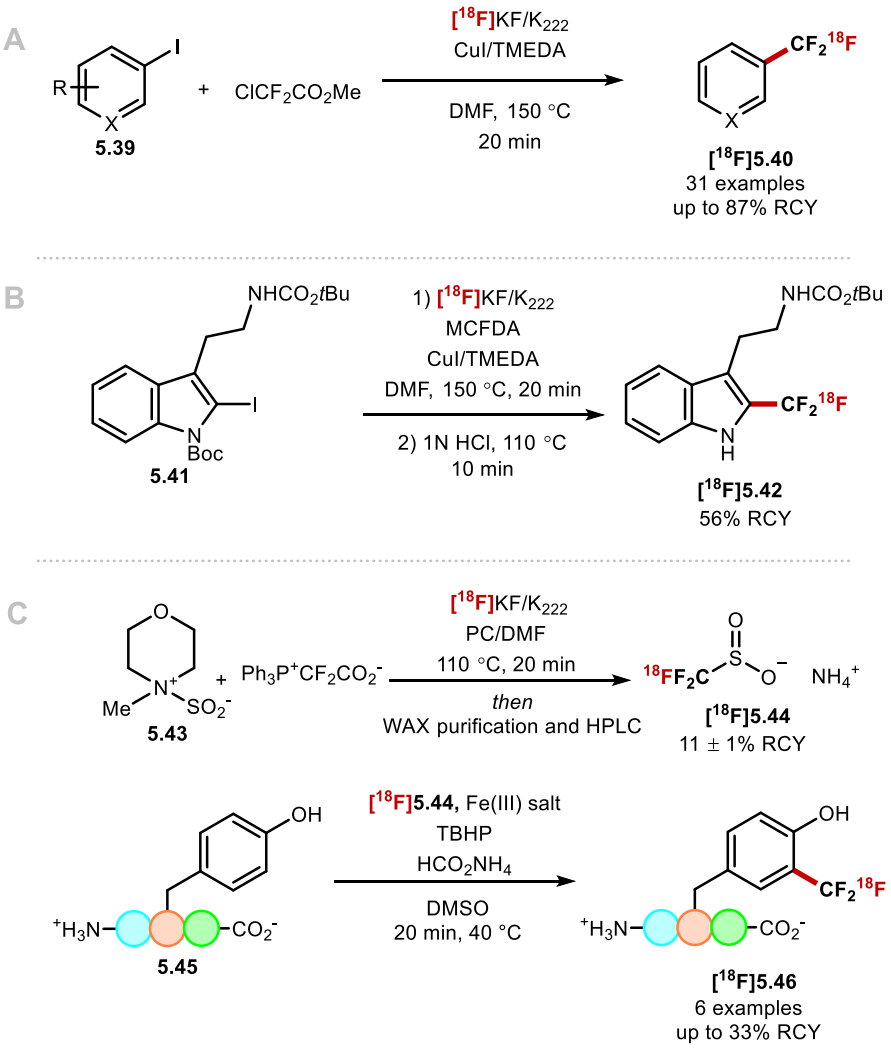

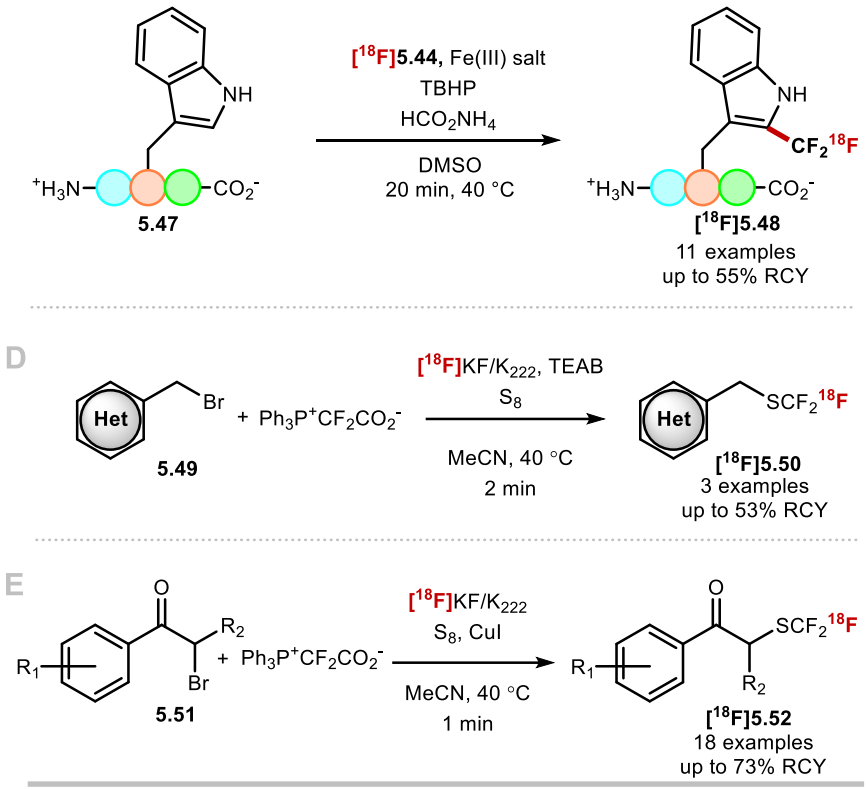

Scheme 5.4 State of the art: difluorocarbene in F-18 radiochemistry

For ^{18}F-difluoromethylation, one would require F-18 labelling DFC itself, which to the best of our knowledge has not been accomplished. While isotopic exchange of ^{19}F-DFC is a viable option, the expected low molar activity (MA) and unfavourable equilibrium in favour of $[^{18}F]CF_3^-$ (**Scheme 5.5A**) encouraged us to explore a reagent-based approach (**Scheme 5.5B**).

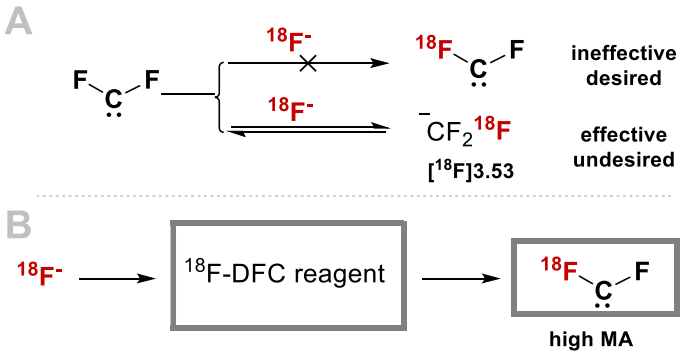

Scheme 5.5 A) Unproductive reaction pathways: reaction of [^{18}F]fluoride and ^{19}F-difluorocarbene. B) Reagent based approach toward ^{18}F-DFC.

We anticipated that an F-18 labelled DFC reagent could release ^{18}F-DFC in a controlled manner to access a variety of (heteroatom)-(X)CF_2H motifs of interest to the radiochemistry community. In F-19 chemistry, a given DFC reagent would likely be chosen based on its reactivity profile, selectivity and cost. Radiochemists however prioritise different factors such as ease of handling (non-volatile, non-gaseous), preparation, and purification. For this reason, we did not prioritise silane-based DFC reagents for F-18 labelling despite their popularity in F-19 mode. These reagents would likely be difficult to prepare from fluoride given the fluorophilicity of the silicon atom, and challenging to purify given their HPLC instability. We therefore opted to explore alternative DFC reagents (**Figure 5.3)**.

5.5 Preliminary Investigations to Label [^{18}F]Difluoromethyltriflate

During the early stages of this project, difluoromethyltriflate (HCF_2OTf) was viewed as a suitable DFC reagent for translation to F-18 radiochemistry. This reagent developed by Hartwig and co-workers has been extensively used in organic synthesis for the difluoromethylation of (thio)phenols, and was shown to be amenable to one-pot processes involving aryl boron reagents and arenes.[17] Moreover, the short reaction times of the corresponding difluoromethylation reactions (2 minutes) was viewed as attractive for radiochemistry. Based on literature precedents which illustrated the instability of the triflate salt of 5-(difluoromethyl)-5H-dibenzo[b,d]thiophen-5-ium (**5.55**), and its decomposition to HCF_2OTf (76% yield), we explored the possibility to apply a strategy analogous to the one used for the radiosynthesis of [^{18}F]Umemoto reagent (^{18}F-fluorination of a ArSCFHCl precursor, followed by oxidative ring closure)

(**Scheme 5.6A**).[18] For this purpose, we would employ [1,1'-biphenyl]-2-yl(chlorofluoromethyl)sulfane (**5.57**) as the labelling precursor. If successful, we envisioned that a one-pot strategy involving ^{18}F-fluorination followed by oxidative ring closure would provide direct access to [^{18}F]HCF_2OTf (**5.56**). Preliminary experiments with F-19 illustrated that **5.56** was accessible in 25% yield using a two-step-one-pot protocol involving fluorination of **5.57** with AgF (2.0 equiv) in DCE, followed by oxidative ring closure with Oxone/Tf_2O (3.0 equiv). Subsequent attempts to react this crude mixture with (thio)phenols under aqueous basic conditions (KOH, 12 equiv) were not fruitful (**Scheme 5.6B**). We investigated which impurity, if any, was inhibiting the difluoromethylation step of our reaction sequence. A spiking experiment was conducted with commercial **5.56** (1.0 equiv), 4-biphenylphenol (0.1 mmol) under aqueous basic conditions (12 equiv). To this reaction mixture was added one equivalent of trifluoromethanesulfonic acid (TfOH) a by-product generated in the oxidative ring closure step). Analysis of the crude reaction mixture by quantitative ^{19}F NMR, illustrated that no difluoromethylated product was formed (**Scheme 5.6C**).

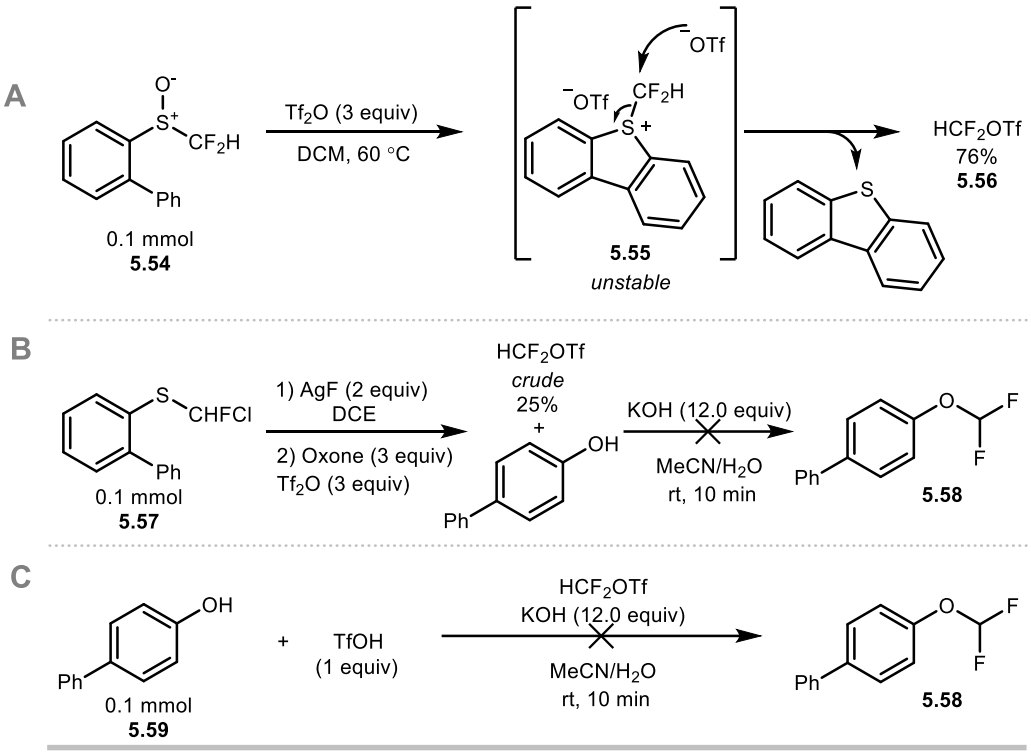

Scheme 5.6 A) Planned route to **5.56**. B) Attempted telescoped synthesis of **5.58** from a crude mixture of HCF_2OTf. C) Difluoromethylation spiking experiment of **5.59** with TfOH.

Given the challenges associated with removing TfOH in a radiochemistry setting, as well as the low boiling point of **5.56** (49 ˚C) and its instability on reverse-phase HPLC, we explored alternative DFC reagents for F-18 radiolabelling.

5.6 Radiosynthesis of [^{18}F]1-(Tert-butyl)-4-((chlorodifluoromethyl)sulfonyl)benzene

In our search for an alternative ^{18}F-DFC reagent, we were inspired by a report from Genicot, Luxen and co-workers (see **Chapter IV**). The authors disclosed the radiosynthesis of [^{18}F](difluoromethyl)sulfonyl)benzo[d]thiazole with application to the C-H ^{18}F-difluoromethylation of heteroarenes.[19] Building on this precedent, we opted to prepare [^{18}F]chlorodifluoromethyl phenyl sulfone (**[^{18}F]5.61)**, a known ^{19}F-DFC reagent first prepared by Hu and co-workers.[20] Previous knowledge from our group on the silver

mediated radiosynthesis of [^{18}F]ArSCF$_3$ from ArSCF$_2$Br, and the work of Luxen and Genicot proved useful.[19,21] Either a two-step protocol (involving ^{18}F-fluorination, followed by chlorination) or a three-step protocol (involving ^{18}F-fluorination, oxidation and chlorination) were considered to access **[^{18}F]5.61** (**Scheme 5.7**).

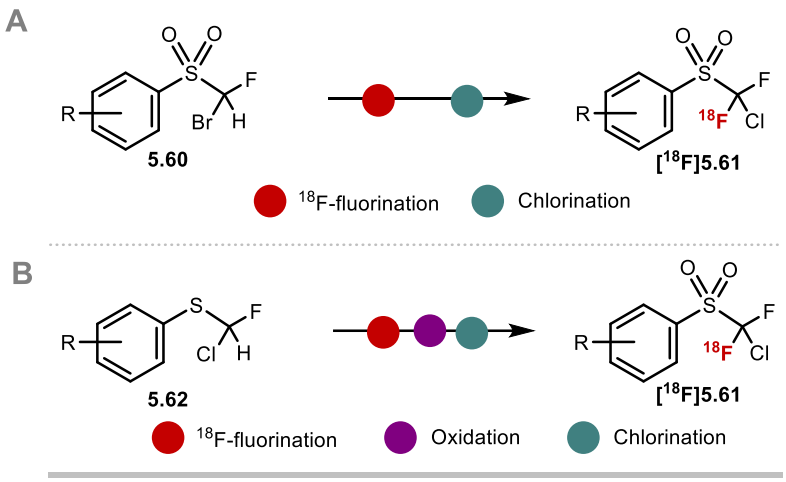

Scheme 5.7 Reaction strategy blueprint A) Two-step radiosynthesis of (chlorodifluoromethyl)sulfone B) Three-step radiosynthesis of (chlorodifluoromethyl)sulfone.

We first investigated the plausibility of the two-step approach outlined in **Scheme 5.7A**. Using ((bromo)fluoromethyl)sulfonyl)benzene as model substrate, ^{18}F-fluorination towards **[^{18}F]5.61** was investigated. Several conditions known to be effective for halogen exchange processes were screened, including silver and silver-free based approaches (**Table 5.1**, entries 1-5). None of these approaches led to F-18 incorporation, and in all cases, [^{18}F]fluoride was recovered quantitatively.

Table 5.1 ^{18}F-fluorination of ((bromofluoromethyl)sulfonyl)benzene.

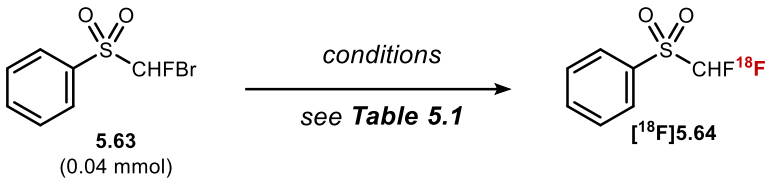

5.63
(0.04 mmol)

[^{18}F]5.64

Entry	Conditions	RCY *(n = 2)*
1	[^{18}F]AgF/KOTf/diCy-18-crown-6, DCE, 65˚C, 20 mins	0%
2	[^{18}F]KF/K_{222}, Acetone 60°C, 20 mins	0%
3	[^{18}F]KF/K_{222}, DABCO (0.06 mmol) DMSO, 120°C, 20 mins	0%
4	[^{18}F]KF/K_{222}, DMF 150°C, 20 mins	0%
5	[^{18}F]KF/K_{222}, *t*BuOH, 80°C, 20 mins	0%

Given the unsuccessful attempts to access **[^{18}F]5.64** through [^{18}F]fluorination of **5.63**, we explored the possibility of accessing **[^{18}F]5.61** through a three-step protocol. In the context of F-18 radiolabeling, such a strategy which involves two post ^{18}F-labelling and multiple purification steps is far from optimal but would allow rapid assessment of whether access to ^{18}F-DFC is at all feasible.

The ^{18}F-fluorination step of this radiosynthesis was investigated first. ArSCFHCl with varying ring para-substituents (-*t*Bu, -Cl, -NO_2) were elected as precursors. These

precursors (0.04 mmol) were reacted with [^{18}F]AgF/KOTf/diCy-18-crown-6 (20-30 MBq) in DCE (0.3 mL) at 60 °C for 20 minutes. (4-(tert-butyl)phenyl)(chlorofluoromethyl)-sulfane (**5.65**) was the best substrate (RCY = 88 ± 3% (n = 4)) performing better than **5.66** (RCY = 40 ± 8% (n = 4)) and **5.67** (RCY = 31 ± 5% (n = 4)). Given that **5.65** gave higher RCYs for the F-18 labelling step, this precursor was chosen for subsequent studies.

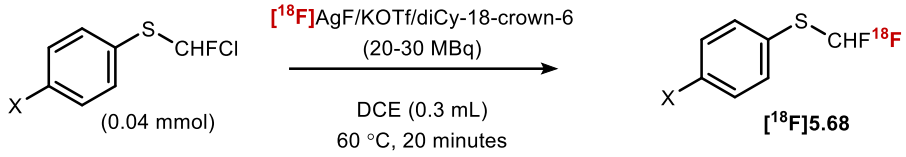

X = ^{t}Bu **(5.65)** => RCY = 88 ± 3% (n = 4)

X = Cl **(5.66)** => RCY = 40 ± 8% (n = 4)

X = NO_2 **(5.67)** => RCY= 31 ± 5% (n = 4)

Scheme 5.8 ^{18}F-fluorination of ArSCHFCl with varying ring substituents.

Optimisation of the oxidation step led to the discovery that $RuCl_3$ (20 mol%, 2 mg)/$NaIO_4$ (0.16 mmol, 52 mg) in 1:1 MeCN/H_2O (0.5 mL) readily oxidised **[^{18}F]5.65** to the corresponding sulfone (**[^{18}F]5.69**) at room temperature (RCY (95 ± 2% (n=2))). Semi-prep purification and subsequent reformulation yielded [^{18}F](difluoromethyl)phenyl sulfone (**[^{18}F]5.69**) in an AY of 12% ± 2% (n = 4). We next reacted **[^{18}F]5.69** with NaOCl, which provided access to [^{18}F]1-(tert-butyl)-4-((chlorodifluoromethyl)sulfonyl)benzene **[^{18}F]5.70** in 20% RCY calculated from **[^{18}F]5.69**, and an overall AY of ~1% from [^{18}F]fluoride. The use of other chlorinating reagents such as $SOCl_2$ or NCS were not fruitful to improve the RCY of the chlorination step.

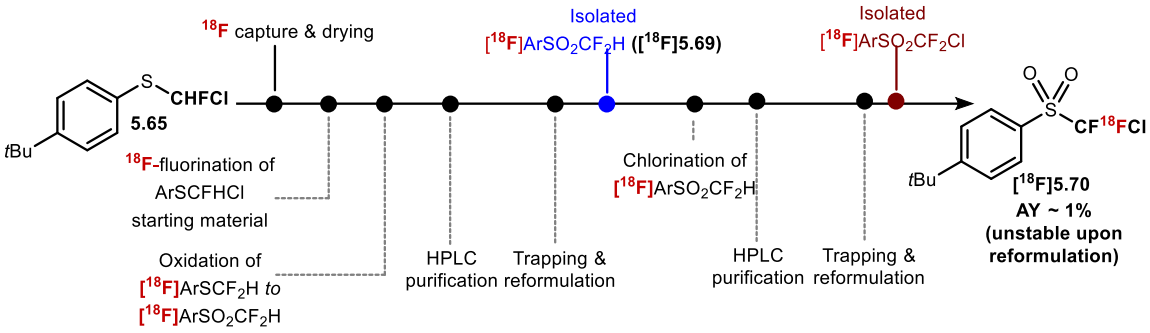

Scheme 5.9 Step-by-step sequence of the radiosynthesis for [^{18}F]1-(tert-butyl)-4-((chlorodifluoromethyl)sulfonyl)benzene.

5.7 [^{18}F]1-(Tert-butyl)-4-((chlorodifluoromethyl)sulfonyl)benzene as a ^{18}F-DFC reagent

Using the conditions outlined in **Scheme 5.10 (5.59)**, [1,1'-biphenyl]-4-ol successfully reacted with **[^{18}F]5.70** to afford the difluoromethylated product [^{18}F]5.58 in RCY = 40% ± 5% *(n = 2)*, hallmarking the first synthesis and application of a ^{18}F-DFC reagent.

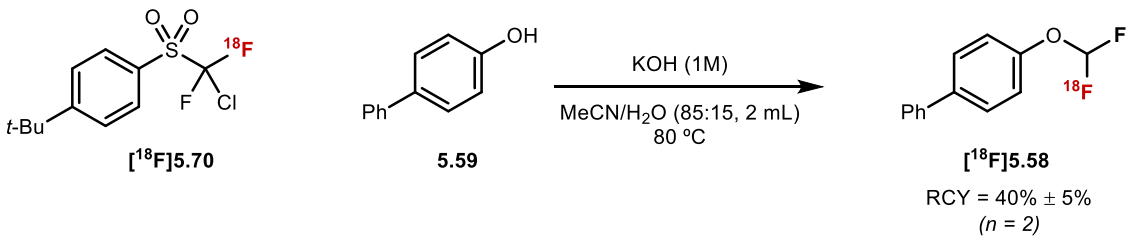

Scheme 5.10 Difluoromethylation of [1,1'-biphenyl]-4-ol with [^{18}F]1-(tert-butyl)-4-((chlorodifluoromethyl)sulfonyl)benzene.

With this result in hand, it was important to improve the AY of **[^{18}F]5.70**. Given the low conversion of the chlorination step of our radiosynthesis, we attempted to perform the chlorination step without HPLC purification of **[^{18}F]5.69**. This modification would not only reduce the overall synthesis time of our radiosynthesis, but also minimise any activity losses attributed to HPLC purification and reformulation sequences. Attempts to perform the chlorination post-labelling step on a crude mixture of **[^{18}F]5.69** were not

fruitful. Decomposition of **[^{18}F]5.70** upon reformulation as well as the low AY, encouraged us to consider alternative DFC reagents for F-18 labelling.

5.8 Radiosynthesis of [^{18}F]1-(Tert-butyl)-4-((difluoromethyl)sulfonyl)benzene

In search for an alternative [^{18}F]DFC reagent which was chemically more stable, we considered a report from Hine and Porter published in 1960, which described the release of DFC from $PhSO_2CF_2H$ (**5.64**) under basic conditions.[22] **5.64** is commonly reported as a nucleophilic difluoromethylating reagent, but its reactivity as DFC reagent has not been explored.[23] Given that we had previously illustrated that **[^{18}F]**1-(tert-butyl)-4-((difluoromethyl)sulfonyl)benzene **[^{18}F]5.69** was accessible in good AY en route to **[^{18}F]5.70**, and more importantly was stable after reformulation, its reactivity as a DFC reagent was worth investigating. At first instance, it was important to establish if this reagent was suitable for the difluoromethylation of phenols. Furthermore, given that most difluoromethylation protocols use an excess of DFC reagent, we had to verify whether **5.64** could be used in sub-stoiochmetric quantities. When 10 equivalent of phenol (**5.71**) and KOH were reacted with **5.64** in a MeCN/H_2O mixture at 50 ˚C for four hours, (difluoromethoxy)benzene was isolated in 23% yield. To further evaluate whether **5.64** was acting as a DFC reagent, we examined the difluorocyclopropanation of 1,1-diphenylethylene (**5.74**). Mechanistically, such a reaction would most likely proceed through a difluorocarbene pathway. Pleasingly, when **5.74** was reacted with **5.64** under basic conditions at 200 ˚C in propylene carbonate (P-C), (2,2-difluorocyclopropane-1,1-diyl)dibenzene was observed by quantitative ^{19}F NMR (**5.75**, 19%) (**Scheme 5.11**). With these experiments we proved that **5.64** can release DFC.

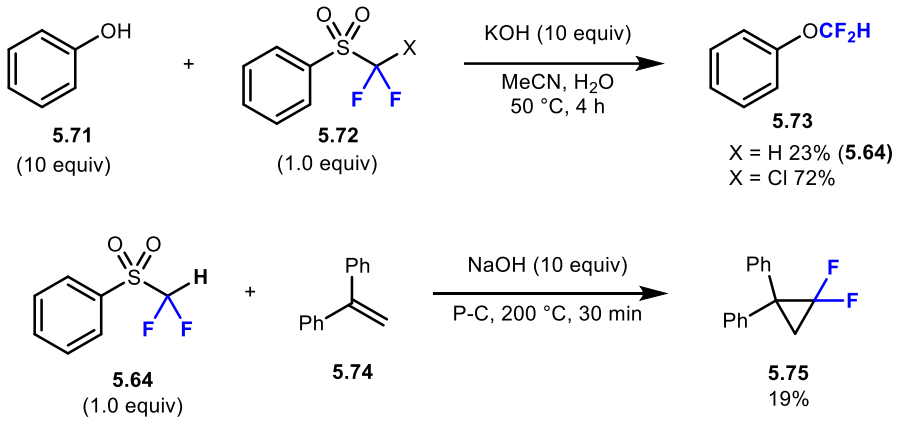

Scheme 5.11 Proof of concept: difluoromethylation of phenol and difluorocyclopropanation of ethene-1,1-diyldibenzene.

Next we further optimised the radiosynthesis of **[^{18}F]5.69**. The sequence involves the formation of [^{18}F]AgF from [^{18}F]KF, ^{18}F-fluorination, and a post-labelling oxidation step as outlined below.

<u>Optimal procedure:</u> [^{18}F]KF/diCy-18-cr-6 capture. ^{18}F-Fluoride was separated from ^{18}O-enriched-water using an anion exchange cartridge (Waters Sep-Pak AccellPlus QMA Carbonate Plus Light Cartridge, activated with H_2O (10.0 mL) prior to use) and released with a solution of diCy-18-cr-6 (14 mg), $K_2C_2O_4$ (4 mg) and K_2CO_3 (0.2 mg) in MeCN/H_2O (1 mL, 4:1, v/v). The solution was dried by azeotropic using dry MeCN (200 µL) under a flow of N_2 at 105 °C (temperature: 105 °C)

[^{18}F]AgF synthesis ([^{18}F]AgF/KOTf/diCy-18-cr-6). To the v-vial containing dried [^{18}F]KF/diCy-18-cr-6 (*vide infra*) was added a solution of *fresh white grains* of AgOTf (21 mg, 80 µmol) in dry MeCN (dry, 0.5 mL) and the solvent was removed by heating at 105 °C (temperature: 105 °C) under a stream of nitrogen (Q = 1.0 L·min^{-1}, *maximum drying time should be 5 minutes*) (*a colour change could be observed to dark red*). After this,

the reaction vial was cooled down prior to the next reaction. A dark red/brown solid was obtained and used for the next step.

Synthesis of **[^{18}F]5.69** step 1: After Cooling 65 ˚C, a solution of (4-(tert-butyl)phenyl)(chlorofluoromethyl)sulfane (11.8 mg, 0.04 mmol) in DCE (300 µL) was added. The resulting brown suspension was allowed to stir at 65 °C for 20 minutes, after which it was allowed to cool to room temperature prior to use in the next step.

Synthesis of **[^{18}F]5.69** step 2: To a v-vial containing the crude reaction mixture in DCE solvent was added $RuCl_3xH_2O$ (20 mol%, 2 mg) and $NaIO_4$ (0.16 mmol, 52 mg) in MeCN/H_2O (1:1, v/v, 0.5 mL). This mixture was stirred at 25 °C (temperature: 36 °C) for 5 minutes, diluted with a solution consisting of water (4.2 mL) and EtOH (0.3 mL) and trapped on a C18 plus cartridge (conditioned 10 mL MeOH, then 10 mL H_2O). **[^{18}F]5.69** was eluted with MeCN (1.0 mL) and loaded onto the HPLC sample-loop for preparative HPLC purification (using isocratic 65% MeCN in 25 mM ammonium formate buffer, Q = 4 mL/min, t_R(**[^{18}F]5.69**) = ~ 8-12 minutes). The ^{18}F-product was collected into H_2O (20 mL), which was then eluted over a C18 Plus cartridge (pre-conditioned with 10 mL MeOH and10 mL of H_2O). HPLC-pure **[^{18}F]5.69** was then released from the C18 Plus cartridge with MeCN (1.0 mL) into a v-vail and used in subsequent ^{18}F-difluoromethylation reactions.

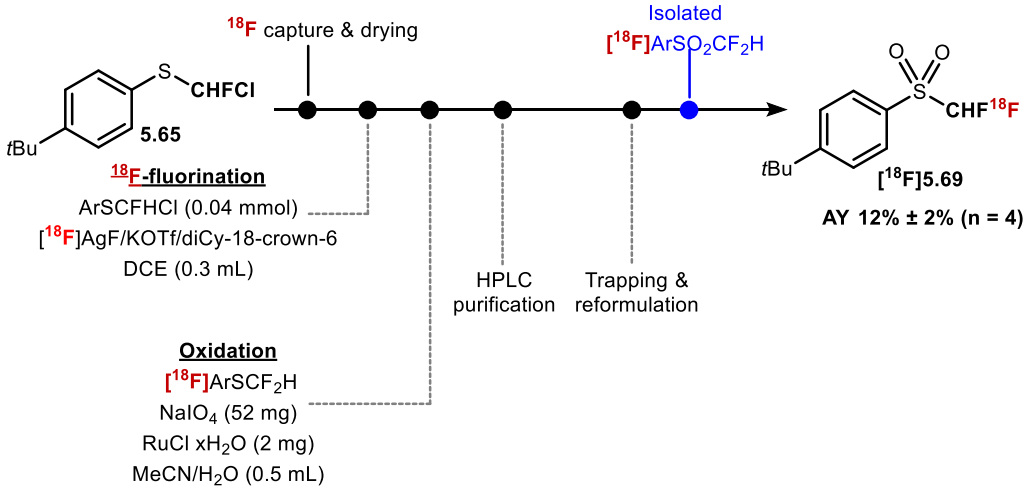

Scheme 5.12 Radiosynthesis for [^{18}F]1-(tert-butyl)-4-((difluoromethyl)sulfonyl)benzene.

Having demonstrated that **[^{18}F]5.69** can release **[^{18}F]DFC**, we next confirmed whether this novel DFC ^{18}F-reagent could react with **5.74** to access **[^{18}F]5.75**. On a 0.1 mmol scale, using 0.5 equivalents of NaOH at 200 ˚C in P-C, **[^{18}F]5.75** was accessible in 36% RCY. Decreasing the temperature to 150 ˚C shut down the reaction completely (**Table 5.2**, entry 2). Increasing the substrate loading to 0.2 mmol resulted in decreased RCY (22%, **Table 5.2**, entry 3).

Table 5.2 ^{18}F-difluorocyclopropanation of 1,1-diphenylethylene

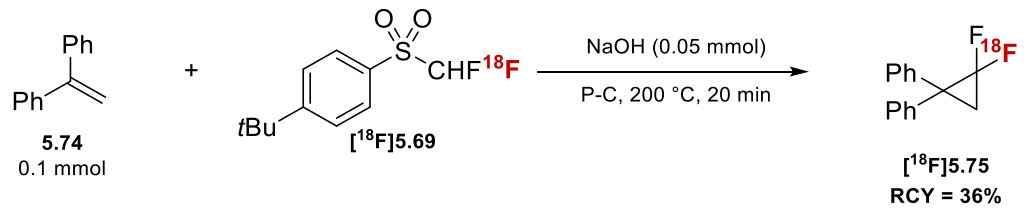

Entry	Substrate	Solvent (µL)	NaOH	Temp (˚C)	RCY
1	0.1 mmol	P-C (300 µL)	0.05 mmol	200	36%

2	0.2 mmol	P-C (300 µL)	0.05 mmol	150	0%
3	0.2 mmol	P-C (300 µL)	0.05 mmol	200	22%

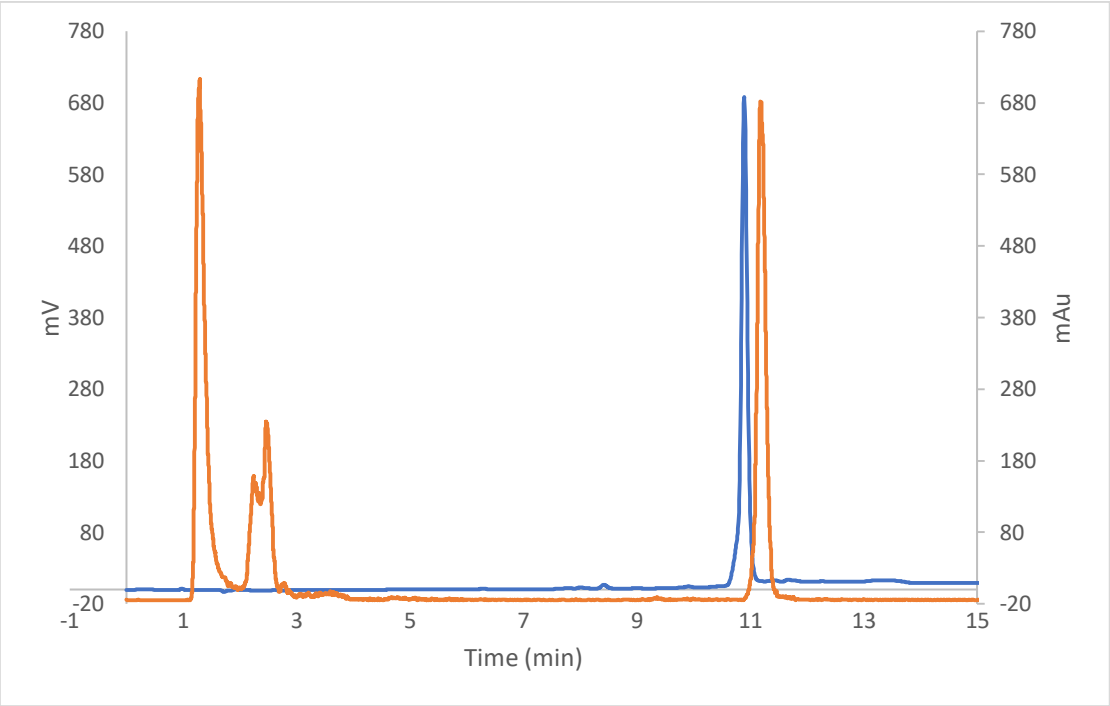

Figure 5.4 HPLC radio-trace of **[^{18}F]5.75** (orange) overlaid with HPLC UV-trace (λ = 220 nm) of ^{19}F reference compound (**5.75**, blue).

Having demonstrated that **[^{18}F]5.69** is a ^{18}F-DFC reagent, we focused on identifying milder reaction conditions for the ^{18}F-difluoromethylation of (thio)phenols. When **5.59** (0.1 mmol) was treated with **[^{18}F]5.69** in a mixture of aqueous KOH and acetonitrile at 80 ˚C), the corresponding difluoromethyl ether **[^{18}F]5.58** was formed in 58% RCY (**Table 5.3**, entry 1). Doubling substrate concentration increased the RCY to 71% ± 9% (n = 5) (**Table 5.3**, entry 2). When the amount of potassium hydroxide was decreased to 50 µL (25% aqueous), or increased to 150 µL (25% aqueous), **[^{18}F]5.58** was obtained in lower RCY (**Table 5.3**, entries 3-4). Changing the solvent to DMSO had also a detrimental effect on the reaction outcome (**Table 5.3**, entry 5). Furthermore, when the reaction was

performed in absence of water, the desired product was not observed (**Table 5.3**, entry 6). Additional attempts aimed at lowering substrate loading led to a lower radiochemical yield of **[^{18}F]5.58** (**Table 5.3**, entry 7).

Table 5.3 Optimisation: ^{18}F-difluoromethylation of 4-biphenylphenol.

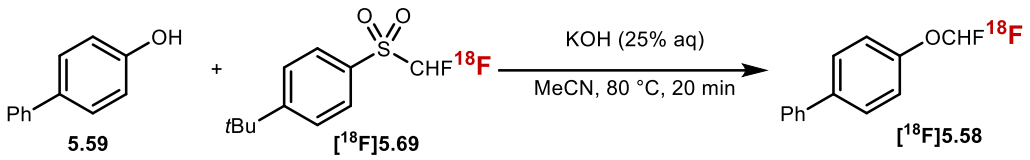

Entry	Substrate	Solvent	KOH (25% aq.)	Temp (˚C)	RCY
1	0.1 mmol	MeCN (600 µL)	100 µL	80	58%
2	**0.2 mmol**	**MeCN (600 µL)**	**100 µL**	**80**	**71% ± 9% (n = 5)**
3	0.2 mmol	MeCN (600 µL)	50 µL	80	*Trace*
4	0.2 mmol	MeCN (600 µL)	150 µL	80	59%
5	0.2 mmol	DMSO (600 µL)	100 µL	80	25%
6	0.2 mmol	MeCN (600 µL)	Neat (3 mg)	80	0%
7	0.1 mmol	MeCN (300 µL)	50 µL	80	52%

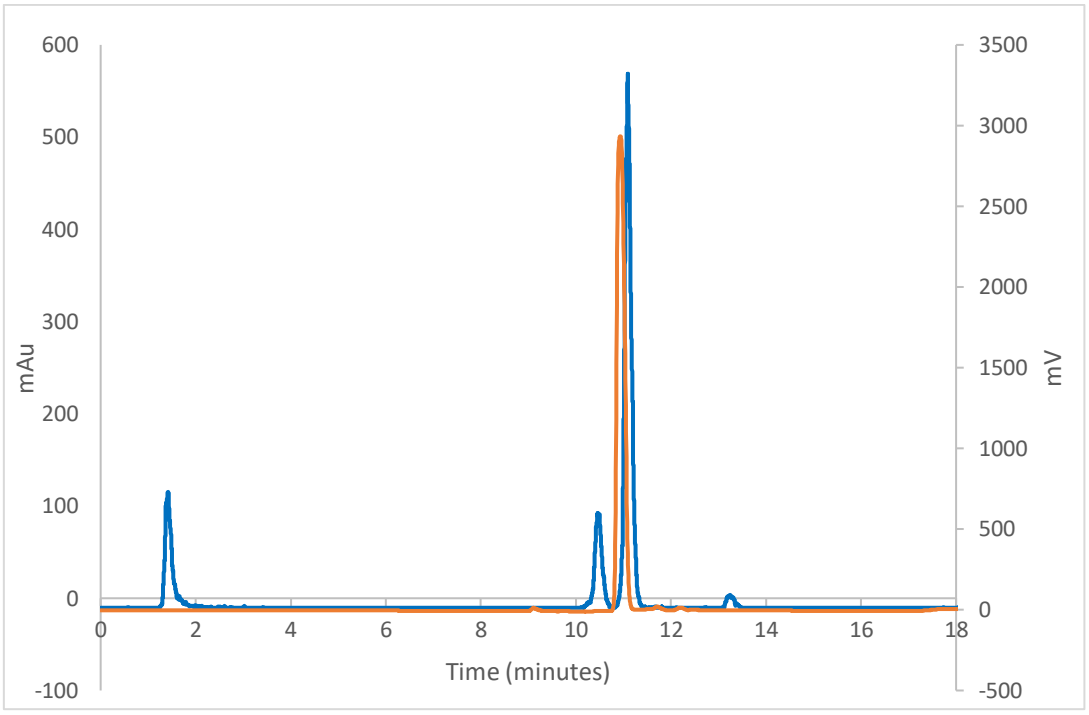

Figure 5.5 HPLC radio-trace of **[^{18}F]5.58** (blue) overlaid with HPLC UV-trace (λ = 220 nm) of ^{19}F reference compound (**5.58**, orange).

Next we illustrated that under analogous conditions (**Table 5.3**, entry 2), 4-nitrobenzenethiol (**5.76**) readily reacted to afford [^{18}F](difluoromethyl)(4-nitrophenyl)sulfane (**[^{18}F]5.77**) in good RCY (57% ± 4% (n = 2)) (**Scheme 5.12**).

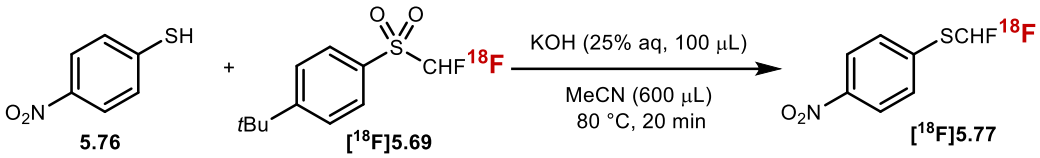

Scheme 5.12 ^{18}F-difluoromethylation of 4-nitrobenzenethiol.

We next turned our attention to the ^{18}F-difluoromethylation of *N*-heterocycles such as benzimidazole **5.78**. This substrate was subjected to the reactions conditions optimised for the ^{18}F-difluoromethylation of (thio)phenols, leading to [^{18}F]1-(difluoromethyl)-1H-benzo[d]imidazole **[^{18}F]5.79** in good 48 ± 4% RCY. When the solvent was changed to DMF (0.3 mL) with sodium hydride (0.2 mmol) used as base, **[^{18}F]5.79** was obtained in an improved RCY of 61 ± 16% (n = 3) (**Table 5.4**, entry 9).

Table 5.4 Optimisation: ^{18}F-difluoromethylation of benzimidazole.

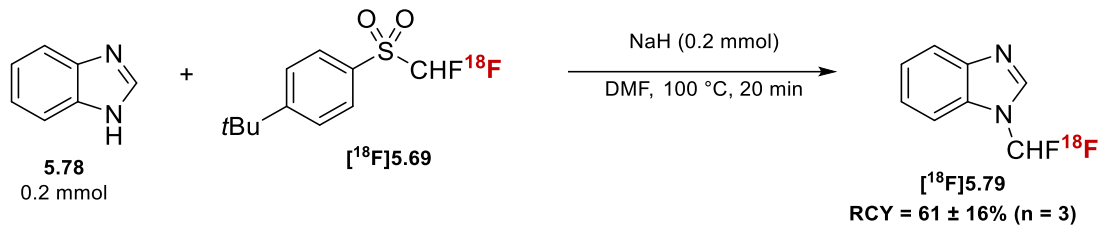

5.78
0.2 mmol

[^{18}F]5.69

[^{18}F]5.79
RCY = 61 ± 16% (n = 3)

Entry	Substrate	Solvent	Base (mmol)	Temp (˚C)	RCY
1	0.1 mmol	DMF (300 µL)	NaOH (0.1)	80	5%
2	0.2 mmol	DMF (300 µL)	NaOH (0.1)	80	7%
3	0.2 mmol	DMF (300 µL)	NaH (0.2)	80	4%
4	0.2 mmol	DMF (300 µL)	NaH (0.2)	80	14%
5	0.2 mmol	DMF (300 µL)	NaH (0.2)	100	58%
6	0.2 mmol	DMF (300 µL)	NaH (0.2)	70	4%
7	0.2 mmol	DMF (600 µL)	NaH (0.2)	80	7%
8	0.2 mmol	DMF (600 µL)	NaH (0.2)	90	64%
9	**0.2 mmol**	**DMF (600 µL)**	**NaH (0.2)**	**100**	**61 ± 16% (n = 3)**
10	0.2 mmol	DMF (600 µL)	NaOH (0.1)	100	17%

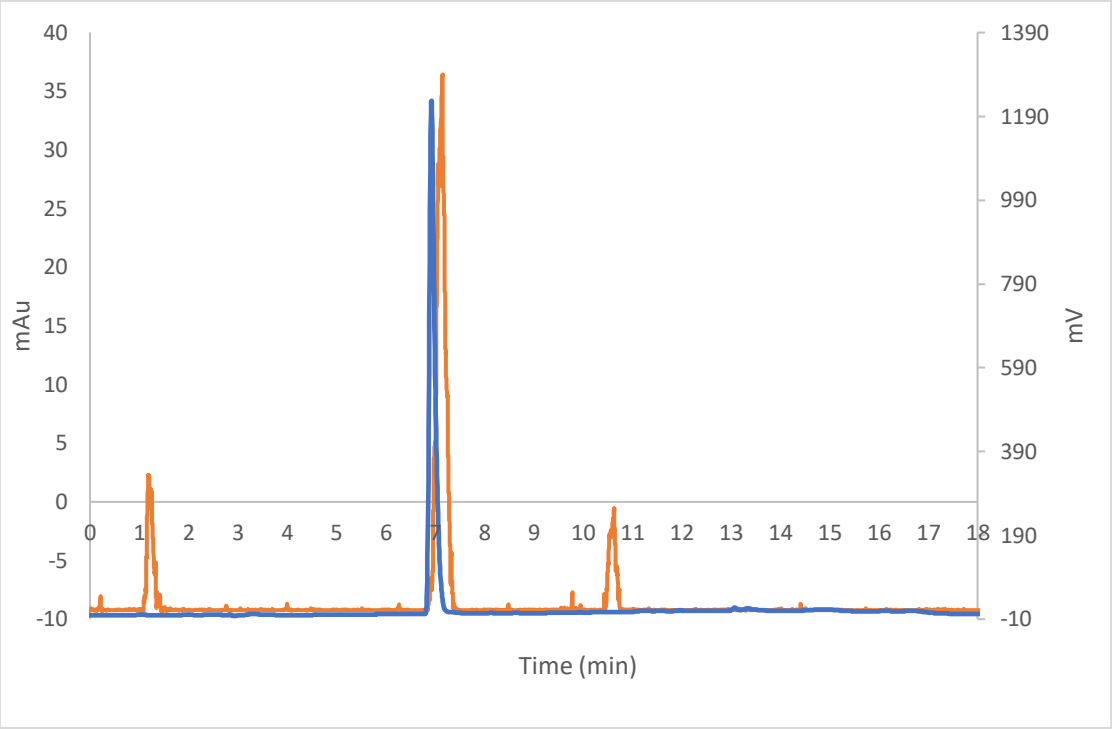

Figure 5.6 HPLC radio-trace of **[^{18}F]5.79** (orange) overlaid with HPLC UV-trace (λ = 220 nm) of ^{19}F reference compound (**5.79**, blue).

Thiabendazole (**5.80**), an antifungal agent was chosen as model compound to explore whether our optimized conditions can be applied to a bioactive molecule. Applying the conditions of **Table 5.4** (entry 9), thiabendazole underwent ^{18}F-difluoromethylation providing access to [^{18}F]4-(1-(difluoromethyl)-1H-benzo[d]imidazol-2-yl)thiazole (**[^{18}F]5.81**) in modest RCY (10% ± 3% (n = 2)); significant amount of unreacted **[^{18}F]5.69** remained. When the reaction conditions were altered changing the temperature from 100 ˚C to 140 ˚C, the RCY increased to 73% (**Scheme 5.13**).

5.80
0.2 mmol

[^{18}F]5.69

[^{18}F]5.81
RCY = 73%

Scheme 5.13 ^{18}F-difluoromethylation of thiabendazole.

Inspired by a recent report from Hartwig and co-workers, we investigated a one-pot procedure from readily available boronic acids. When boronic acid **5.82** (0.2 mmol) was first treated with urea hydroperoxide (0.2 mmol) and without further purification subsequently reacted under the standard reaction conditions, **[^{18}F]5.58** was obtained in 40% RCY (n = 1) (**Scheme 5.14**). This one-pot procedure from aryl boron precursors was seen as advantageous, given the propensity of methods to install such a motif in a late-stage fashion and its applicability to F-18 radiochemistry.

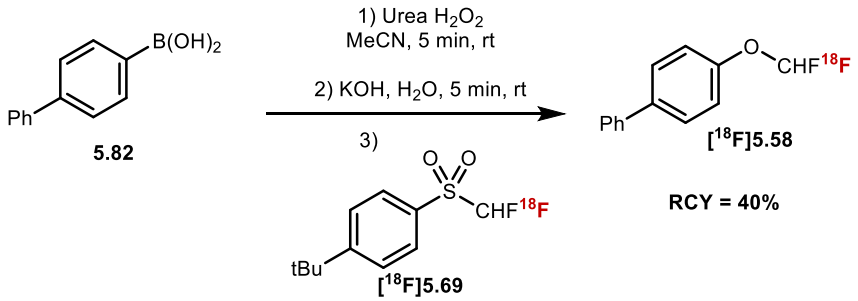

Scheme 5.14 One-pot sequence ^{18}F-difluoromethylation of [1,1'-biphenyl]-4-ylboronic acid.

5.9 Competition Experiments:

Given the absence of knowledge on DFC reactivity in the context of F-18 radiochemistry, we studied its reactivity towards competing sites of insertion, and whether these additional sites could compete for DFC insertion. Evaluation of the relative reactivity profiles of ^{18}F-DFC derived from **[^{18}F]5.69** through simple competition experiments would provide insightful information for end-users who intend to apply the methodology to complex scaffolds. Competition experiments were conducted between **5.59** and **5.78** in order to determine which functionality N-H or O-H would more readily react. Under the standard reaction conditions both substrates underwent ^{18}F-difluoromethylation (~ 1:1 ratio of **[^{18}F]5.59:[^{18}F]5.78** (**Scheme 5.15A)**. An additional competition experiment

between **5.83** and **5.85** revealed that under the standard reaction conditions, phenols react selectively suggesting that aliphatic alcohols will not require protection for radiotracers containing both aryl and alkyl alcohols (**Scheme 5.15B**).

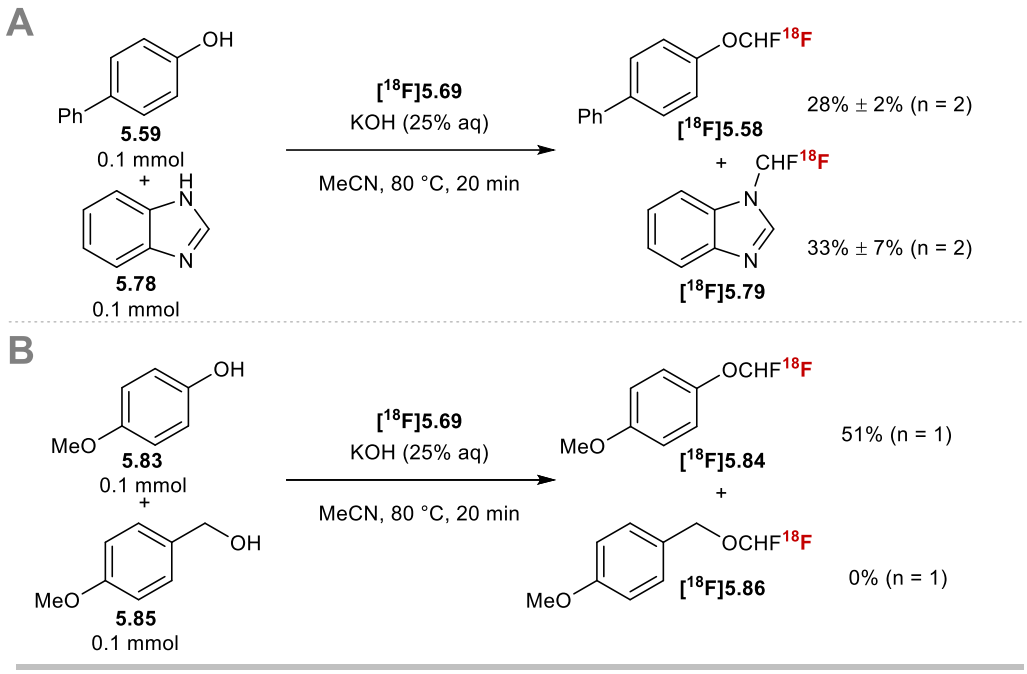

Scheme 5.15 Competitions experiments.

5.10 [^{18}F]1-(tert-butyl)-4-((difluoromethyl)sulfonyl)benzene as a Nucleophilic Difluoromethylating Reagent

Having demonstrated the successful radiosynthesis of **[^{18}F]5.69** and its application as a ^{18}F-DFC reagent, we next considered its use for nucleophilic ^{18}F-difluoromethylation. Given the precedence of **5.69** as a nucleophilic difluoromethylating reagent in the F-19 literature, translation to F-18 radiochemistry would provide unprecedented access to sp^3-substituted [^{18}F]CF_2H products such as [^{18}F]difluoromethyl alcohols.[23] The model substrate acetophenone **5.87** (0.04 mmol) was initially treated with **[^{18}F]5.69** (20 – 30 MBq) and LiHMDS in THF (0.1 mL, 1M solution) at -78 °C with no success (**Table 5.5**, entry 1). When a mixed solvent system comprised of THF and DMA (9:1, 0.3

mL) was used, the desired difluoromethyl(sulfonylaryl) adduct **[^{18}F]5.88** was formed in 12% RCY. Altering the solvent system to a mixture of THF with DMI (9:1, 0.3 mL) significantly improved the yield leading to **[^{18}F]5.88** in high RCY (84 ± 8%, n = 16) (**Table 5.5**, entry 5).

Table 5.5 ^{18}F-difluoromethylation of acetophenone: Optimisation of step 1.

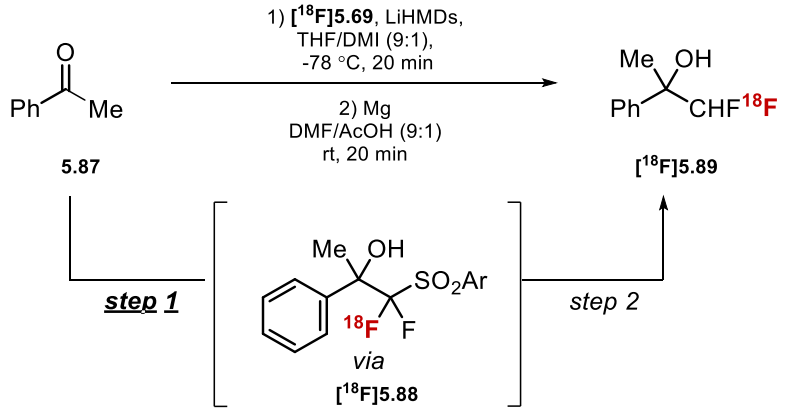

Entry	Conditions step 1	RCY (step 1)
1	LiHMDS (0.1 mmol), THF, -78 °C	0%
2	LiHMDS, THF/DMF (9:1), -78 °C	0%
3	LiHMDS, THF/DMA (9:1), -78 °C	12%
4	LiHMDS, THF/HMPA (9:1), -78 °C	0%
5	**LiHMDS, THF/DMI (9:1), -78 °C**	**84 ± 8% (n = 16)**

For the deprotection step (step 2), addition of Mg^0 (0.8 mmol) in DMF/AcOH (9:1, v/v, 0.3 mL) to C-18 purified reaction mixture led to the desulfonylated product in 27% RCY (**Table 5.6**, entry 2). The conversion was increased to 70% by increasing the temperature of the reaction to 80 ˚C (**Table 5.6**, entry 3). When the reaction mixture was heated at 100 ˚C, no product was detected (**Table 5.6**, entry 4).

Table 5.6 Optimisation of step 2 of ^{18}F-difluoromethylation of acetophenone

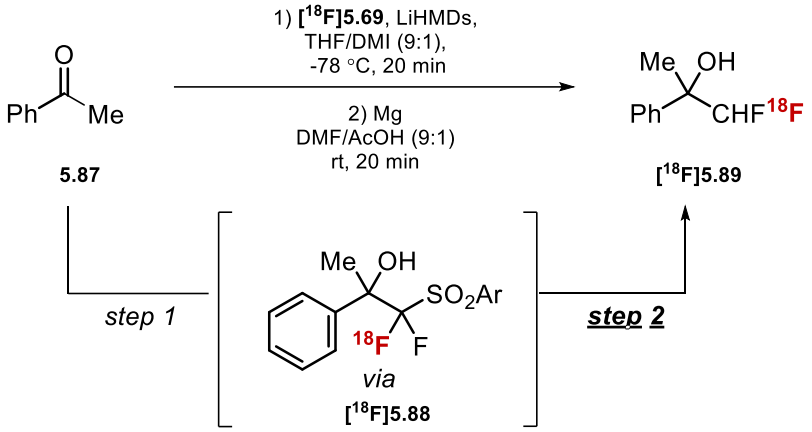

Entry	Conditions step 2	RCC (step 2)
1	Mg^0, NaOAc, DMF/AcOH (9:1), r.t.	RCC = 0%
2[b]	Mg^0, NaOAc, DMF/AcOH (9:1), r.t.	RCC = 27%
3[b]	**Mg^0, DMF/AcOH (9:1), 80 °C**	**RCC = 70%**
4[b]	Mg^0, DMF/AcOH (9:1), 100 °C	RCC = t.b.c.

[a]Reaction performed in one-pot. [b]Reaction mixture crude was trapped on a C18 cartridge and released with DMF/AcOH (9:1) prior step 2.

5.11 Conclusion

In conclusion, we have developed the first protocol enabling access to ^{18}F-DFC, an ^{18}F-isotopologue of a highly versatile reactive intermediate in fluorine chemistry. We have developed the synthesis of the first ^{18}F-DFC reagent **[^{18}F]5.69** which was accomplished through a two-step-one-pot protocol involving halogen exchange ^{18}F-fluorination and oxidation. With **[^{18}F]5.69** in hand, we illustrated this ^{18}F reagent is capable of controlled ^{18}F-DFC insertion into a variety of X-H (X = O, S, N) bonds. We also found that aryl difluoromethylether **[^{18}F]5.58** is accessible from an aryl boronic acid in a one-pot fashion involving oxidation to the corresponding phenol followed by in situ ^{18}F-difluoromethylation. In view of the number of reactions relying on DFC-type reagents, access to the first ^{18}F-DFC reagent **[^{18}F]5.69** will likely have a considerable impact on the radiochemical space which is being explored for PET applications. Specifically, it can access more stable analogues of ^{18}F radiotracers which are traditionally prepared by ^{18}F-alkylation strategies.

5.12 Future Work

Having illustrated the first synthesis of a ^{18}F-DFC reagent and showcased its utility in the ^{18}F-difluoromethylation of phenols, thiophenols, *N*-heterocycles and the ^{18}F-difluorocyclopropanation of alkenes, the next step will be to investigate the generality of our reaction scope. We also propose to investigate whether our methodology will tolerate more complex manifolds.

While Genicot and Luxen have shown that heteroarenes are amenable to direct radical C-H ^{18}F-difluoromethylation using [^{18}F](difluoromethyl)sulfonyl)benzo[d]thiazole under

photoredox activation, this reaction is limited in scope and in many cases lacks regioselectivity as controlled solely by the substrates innate reactivity.[19] On the contrary the ^{18}F-difluoromethylation of arenes remains unsolved. Given that several reports have recently proposed the reactivity of metal difluorocarbene complexes e.g [Pd=CF_2] to achieve direct difluoromethylation of aryl boron reagents, we will investigate whether the direct ^{18}F-difluoromethylation of aryl boron reagents is feasible with our ^{18}F-DFC reagent. Mechanistically, this Pd(II)-dependent process involves nucleophilic addition of the aryl boron reagent onto [Pd=CF_2] followed by protonation of the resulting [PdCF_2Ar] complex. Other metals which can form [M=CF_2] will be considered as necessary.

5.13 References

1. M. Tredwell and V. Gouverneur, *Angew. Chem. Int. Ed.,* 2012, **51**, 11426.
2. (a) P. W. Miller, N. J. Long, R. Vilar and A. D. Gee, *Angew. Chem., Int. Ed.,* 2008, **47**, 8998; (b) Z. Gao, Y. H. Lim, M. Tredwell, L. Li, S. Verhoog, M. Hopkinson, W. Kaluza, T. L. Collier, J. Passchier, M. Huiban and V. Gouverneur, *Angew. Chem., Int. Ed.,* 2012, **51**, 6733; (c) B. H. Rotstein, N. A. Stephenson, N. Vasdev and S. H. Liang, *Nat. Commun.,* 2014, **5**, 4365; (d) E. L. Cole, M. N. Stewart, R. Littich, R. Hoareau and P. J. H. Scott, *Curr. Top. Med. Chem.,* 2014, **14**, 875; (e) M. Tredwell, S. M. Preshlock, N. J. Taylor, S. Gruber, M. Huiban, J. Passchier, J. Mercier, C. Genicot and V. Gouverneur, *Angew. Chem., Int. Ed.*, 2014, **53**, 7751; (f) A. V. Mossine, A. F. Brooks, K. J. Makaravage, J. M. Miller, N. Ichiishi, M. S. Sanford and P. J. H. Scott, *Org. Lett.,* 2015, **17**, 5780; (g) C. N. Neumann, J. M. Hooker and T. Ritter, *Nature*, 2016, **534**, 369; (h) S. Preshlock, M. Tredwell and V. Gouverneur, *Chem. Rev.,* 2016, **116**, 719; (i) M. K.

Narayanam, G. Ma, P. A. Champagne, K. N. Houk and J. M. Murphy, *Angew. Chem., Int. Ed.,* 2017, **56**, 13006.

3. (a) S. Merchant, L. Allott, L. Carroll, V. Tittrea, S. Kealey, T. H. Witney, P. W. Miller, G. Smith and E. O. Aboagye, *RSC Adv.,* 2016, **6**, 57569; (b) T. Venkatachalam, D. Stimson, K. Frisch, G. Pierens, R. Bhalla and D. Reutens, *Appl. Radiat. Isot.,* 2019, **152**, 172; (c) G. Smith, Y. Zhao, J. Leyton, B. Shan, M. Perumal, D. Turton, E. Årstad, S. K. Luthra, E. G. Robins and E. O. Aboagye, *Nucl. Med. Biol.,* 2011, **38**, 39.
4. Y. Pan, *ACS Med. Chem. Lett.* 2019, 10, **7**, 1016.
5. M. Kuchar and C. Mamat, *Molecules,* 2015, **20**, 16186.
6. C. Rami-Mark, M. Zhang, M. Mitterhauser, R. Lanzenberger, M. Hacker and W. Wadsak, *Nucl. Med. Biol.,* 2013, **40**, 1049.
7. L. Xing, D. C. Blakemore, A. Narayanan, R. Unwalla, F. Lovering, R. A. Denny, H. Zhou and M. E. Bunnage, *ChemMedChem,* 2015, **10**, 715.
8. T. Khotavivattana, S. Verhoog, M. Tredwell, L. Pfeifer, S. Calderwood, K. Wheelhouse, T. Lee Collier and V. Gouverneur, *Angew. Chem. Int. Ed.* 2015, **54**, 9991.
9. J. B. Sap, T. C. Wilson, C. W. Kee, N. J. Straathof, C. W. am Ende, P. Mukherjee, L. Zhang, C. Genicot and V. Gouverneur, *Chem. Sci.,* 2019, **10**, 3237.
10. C. Ni and J. Hu, *Synthesis,* 2014, **46**, 842.
11. J. G. MacNeil Jr and D. J. Burton, *J. Fluorine Chem.,* 1991, **55**, 225
12. M. Huiban, M. Tredwell, S. Mizuta, Z. Wan, X. Zhang, T. L. Collier, V. Gouverneur and J. Passchier, *Nat. Chem.,* 2013, **5**, 941.

13. H. Y. Kim, J. Y. Lee, Y. Lee and J. M. Jeong, *J. Labelled Compd. Radiopharmaceut.,* 2019, **62**, 566

14. C. W. Kee, O. Tack, F. Guibbal, T. C. Wilson, P. G. Isenegger, M. Imiołek, S. Verhoog, M. Tilby, G. Boscutti,S. Ashworth, J. Chupin, R. Kashani, A. W. J. Poh, J. K. Sosabowski, S. Macholl, C. Plisson, B. Cornelissen, M. C. Willis, J. Passchier, B. G. Davis and V. Gouverneur, *J. Am. Chem. Soc.,* 2020, **142**, 1180

15. J. Zheng, L. Wang, J. Lin, J. Xiao and S. H. Liang, *Angew. Chem. Int. Ed.,* 2015, **54**, 13236

16. J. Zheng, R. Cheng, J. Lin, D. Yu, L. Ma, L. Jia, L. Zhang, L. Wang, J. Xiao and S. H. Liang, *Angew. Chem. Int. Ed.,* 2017, **56**, 3196.

17. P. S. Fier and J. F. Hartwig, *Angew. Chem. Int. Ed.,* 2013, **52**, 2092.

18. G. S. Prakash, C. Weber, S. Chacko and G. A. Olah, *Org. Lett.,* 2007, **9**, 1863

19. (a) L. Trump, A. Lemos, B. Lallemand, P. Pasau, J. Mercier, C. Lemaire, A. Luxen and C. Genicot, *Angew. Chem. Int. Ed.* 2019, **58**, 13149; (b) L. Trump, A. Lemos, J. Jacq, P. Pasau, B. Lallemand, J. Mercier, C. Genicot, A. Luxen and C. Lemaire, *Org. Process Res. Dev.* 2020, **24**, 734.

20. 1 J. Zheng, Y. Li, L. Zhang, J. Hu, G. J. Meuzelaar and H. Federsel, *Chem. Commun.,* 2007, 5149.

21. J. Wu, Q. Zhao, T. C. Wilson, S. Verhoog, L. Lu, V. Gouverneur and Q. Shen, *Angew. Chem. Int. Ed.,* 2019, **58**, 2413.

22. J. Hine and J. J. Porter, *J. Am. Chem. Soc.,* 1960, **82**, 6178.

23. G. S. Prakash, J. Hu, Y. Wang and G. A. Olah, *Eur. J. Org. Chem.,* 2005, **2005**, 2218

24. J. W. Lyga and R. M. Patera, *J. Fluorine Chem.,* 1998, **92**, 141

Chapter 6: Experimental and Analysis

6.1 General Experimental Information

Unless stated otherwise all chemicals were used as received. Solvents were purchased from Sigma-Aldrich, Honeywell or Fisher. Chemicals were purchased from Acros, Alfa Aesar, Fisher, Fluorochem or Sigma-Aldrich and used as received without further purification.

All NMR spectra were recorded on Bruker DPX200, AV400 and AV500 spectrometers. Proton and carbon-13 NMR spectra are reported as chemical shifts (δ) in parts per million (ppm) relative to the solvent peak. Fluorine-19 NMR spectra are referenced relative to an internal standard ($CFCl_3$). Coupling constants (J) are reported in units of hertz (Hz). The following abbreviations are used to describe multiplicities; s (singlet), d (doublet), t (triplet), q (quartet), m (multiplet), br. (broad).

High resolution mass spectra (HRMS) were recorded on a Bruker Micro TOF spectrometer using positive electrospray ionization (ESI^+), on a Micromass GCT spectrometer using filed ionization (FI+) or chemical ionization (CI^+), or on a Waters GCT Classic GCMS using electron impact ionisation (EI).

Gas chromatography low resolution mass spectra (GC-MS) were recorded on a GC/MS Waters GCT

Infrared spectra were recorded either as the neat compound or in a solution using a Bruker Tensor 27 FT-IR spectrometer. Absorptions are reported in wavenumbers (cm^{-1}).

Melting points of solids were measured on a Griffin apparatus and are uncorrected.

Thin-layer chromatography (TLC) was carried out on Merck Kiesegel 60 F254 plates. Silica gel column chromatography was performed over Merck silica gel C60 (40-60 µm).

Preparative HPLC was performed with a using a Synergi C-18 HYDRO-RP prep column.

Reactions were carried out in a home-made photobox made of carboard, fitted with a UFO Blue (460-470 nm) LED Grow Light 'Morbo' – 50 Watt, a continuous nitrogen flow was used to cool the box and maintain room temperature. High throughput screening reactions were performed in a Lumidox photoredox 96-well plate (30mA/470 nm light).

6.2 General Radiochemical Information

[^{18}F]Fluoride was produced by Alliance Medical (UK) via the ^{18}O(p,n)^{18}F reaction and delivered as [^{18}F]fluoride in ^{18}O-enriched-water. Radiosynthesis and azeotropic drying was performed on a NanoTek microfluidic device (Advion).

Whilst working in SOMIL, **at least two trained researchers (including myself) were present work was carried out in a safe manner.** When carrying out small-scale aliquot reactions, two researchers worked together in order to optimise the use of [^{18}F]fluoride. Reactions were carried out in duplicate (n = 2), from which a mean RCY was quantified. Each reaction underwent a sequence of steps:

1. Reagents were weighed out into reaction v-vial.

2. Dispensing aliquot of [^{18}F]fluoride into vial.

3. Adding solvent and placing the reaction vial into heating block.

4. Removing reaction from heating block and quenching.

5. Preparing samples for radio-TLC and radio-HPLC analysis.

6. Injecting radio-HPLC sample.

7. Running radio-TLC plate and analysing using moving bed detector.

For chapter IV all radiolabelling work was conducted by Jeroen Sap + one of Dr. Thomas Wilson or Dr. Natan Straathof. **For chapter V initial radiolabelling work towards [^{18}F]5.70 was performed by Jeroen Sap + Dr. Natan Straathof, all other radiolabelling experiments were performed by Jeroen Sap + Claudio Meyer.**

6.3 Mechanistic Experiments Chapter II

TEMPO trapping experiment:

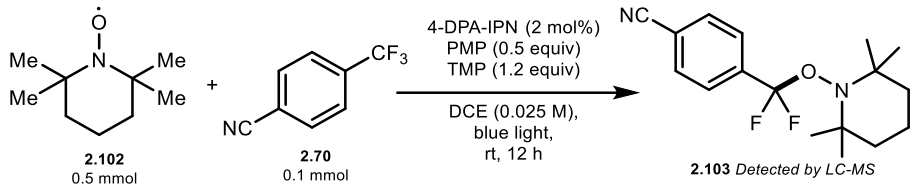

Scheme 6.1 Tempo trapping experiment.

To an oven-dried 8 mL screw top reaction tube, equipped with a stirring bar, was added 4-DPA-IPN (2 mg, 0.0025 mmol, 2.5 mol%). To this reaction tube was added, 4-(trifluoromethyl)benzonitrile (0.1 mmol, 1.0 equiv) and 4-hydroxythiophenol (0.6 mmol, 6.0 equiv). Hereafter, 2,2,6,6-tetramethylpipyridine (0.12 mmol, 1.2 equiv) and 1,2,2,6,6-pentamethylpipyridine (0.05 mmol, 0.5 equiv) were added via micro-syringe followed by TEMPO (0.5 mmol, 5.0 equiv). The reaction tube was capped and filled with DCE (4 mL, 0.025 M). The mixture was sparred with nitrogen for 2 minutes (*a slight increase in fluorescents of the reaction mixture was observed*) and then placed 5 cm away from a Blue LED array (455 nm), stirred and irradiated for 12 hours. Reaction temperature was maintained within 25 ± 1 °C. After this an internal standard was added (0.1 mmol of 4-fluoroanisole) to the crude reaction mixture, diluted with *d*-solvent and analysed by ^{19}F-NMR and LC-MS.

Alkene trapping experiment:

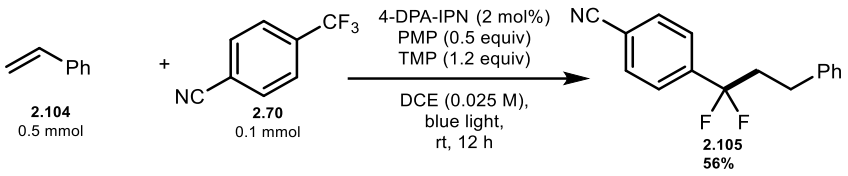

Scheme 6.2 Alkene trapping experiment.

To an oven-dried 8 mL screw top reaction tube, equipped with a stirring bar, was added 4-DPA-IPN (2 mg, 0.0025 mmol, 2.5 mol%). To this reaction tube was added, 4-(trifluoromethyl)benzonitrile (0.1 mmol, 1 equiv.) and 4-hydroxythiophenol (0.6 mmol, 6.0 equiv.). Hereafter, 2,2,6,6-tetramethylpipyridine (0.12 mmol, 1.2 equiv.) and 1,2,2,6,6-pentamethylpipyridine (0.05 mmol, 0.5 equiv.) were added via micro-syringe followed by styrene (0.5 mmol, 5.0 equiv.). The reaction tube was capped and filled with 1,2-dichloroethane (4 mL, 0.025 M). The mixture was sparred with nitrogen for 1 minute (*a slight increase in fluorescents of the reaction mixture was observed*) and then placed 5 cm away from a Blue LED array (455 nm), stirred and irradiated for 12 hours. Reaction temperature was maintained within 25 ± 1 °C. After this an internal standard was added (0.1 mmol of 4-fluoroanisole) to the crude reaction mixture, diluted with *d*-solvent and analysed by ^{19}F-NMR and GC-MS. Under the described conditions (low concentration of 0.025 M), it is unlikely that an oligomer species would form, the dimer or trimer species were not observed by GC-MS.

Deuteration experiment:

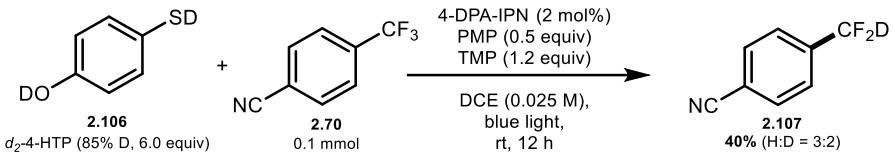

Scheme 6.3 Deuteration experiment.

To an oven-dried 8 mL screw top reaction tube, equipped with a stirring bar, was added 4-DPA-IPN (2 mg, 0.0025 mmol, 2.5 mol%). To this reaction tube was added, 4-(trifluoromethyl)benzonitrile (0.1 mmol, 1 equiv.) and d_2-4-HTP (85% D) (0.3 mmol, 3.0 equiv.). Hereafter, 2,2,6,6-tetramethylpipyridine (0.12 mmol, 1.2 equiv.) and 1,2,2,6,6-pentamethylpipyridine (0.05 mmol, 0.5 equiv.) were added via micro-syringe. The reaction tube was capped and filled with 1,2-dichloroethane (4 mL, 0.025 M). The mixture was sparred with nitrogen for 1 minute (*a slight increase in fluorescents of the reaction mixture was observed*) and then placed 5 cm away from a Blue LED array (455 nm), stirred and irradiated for 12 hours. Reaction temperature was maintained within 25 ± 1 °C. After this an internal standard was added (0.1 mmol of 4-fluoroanisole) to the crude reaction mixture, diluted with *d*-solvent and analysed by ^{19}F-NMR.

Stern-Volmer Experiments <u>(experiments performed with Claudio Meyer)</u>:

Stern-Volmer studies were conducted using 4-DPA-IPN as the photocatalyst. Standard solutions of quenching mixtures containing photocatalyst and 4-hydroxythiophenol + TMP, PMP, TMP, 4-(trifluoromethyl)benzonitrile, cesium formate and $(TMS)_3SiH$ were measured to illustrate potential photocatalyst excited state quenching. Prior to the measurement, all solutions were degassed thoroughly by bubbling argon through the reaction mixture for 5 minutes, followed by irradiation of the sample with a blue light

(455 nm) for 2 minutes. The mixtures were then analysed using a Horiba Fluorolog-3. Samples were irradiated at 430 nm and emission was measured from 450-650 nm.

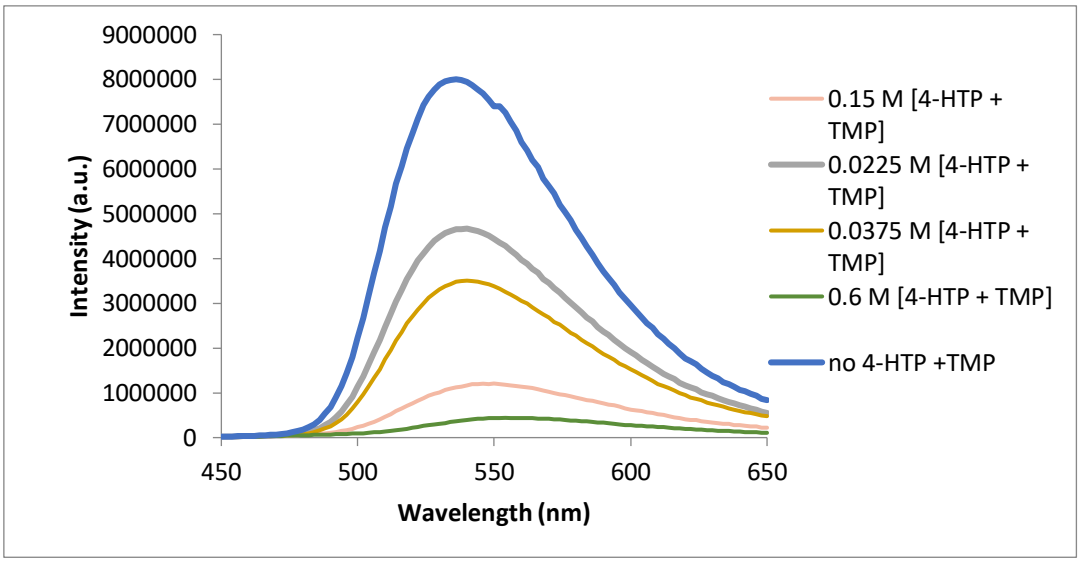

Figure 6.1 Emission profile of 4-DPA-IPN with 4-hydroxythiophenol/TMP (1:1) in DCE.

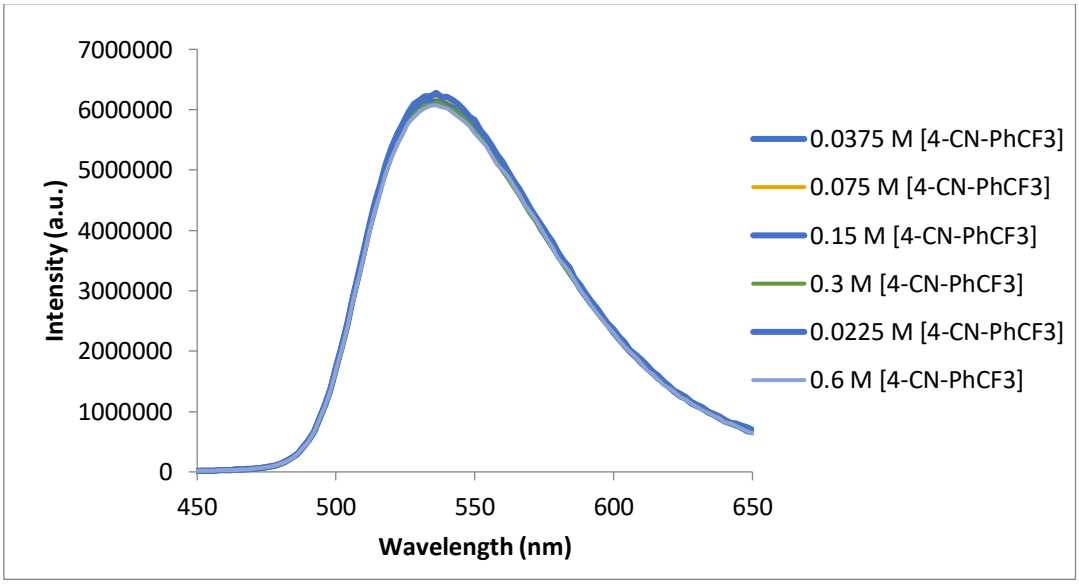

Figure 6.2 Emission profile of 4-DPA-IPN with 4-(trifluoromethyl)benzonitrile in DCE.

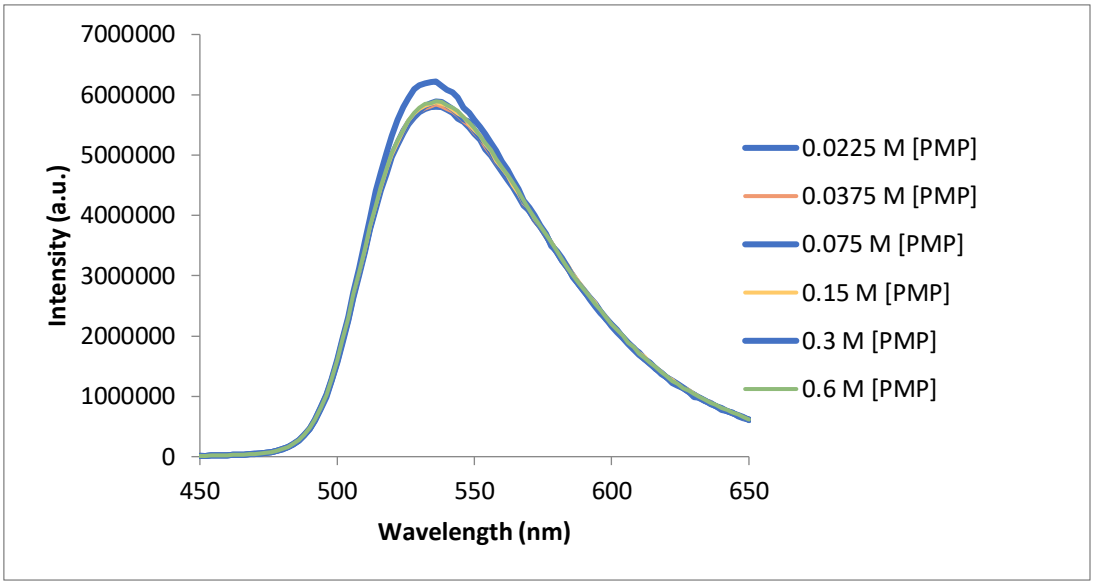

Figure 6.3 Emission profile of 4-DPA-IPN with PMP in DCE.

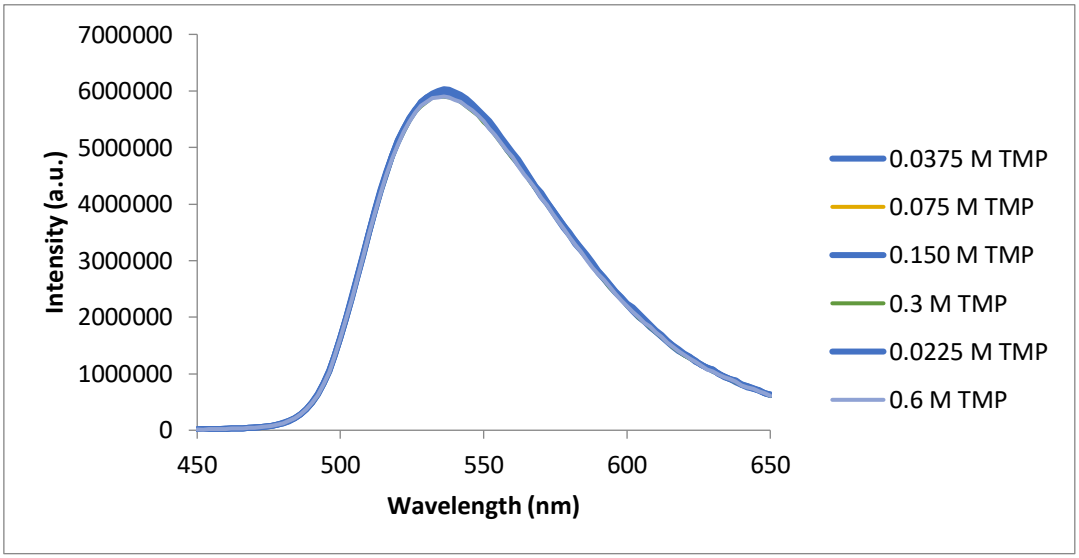

Figure 6.4 Emission profile of 4-DPA-IPN with TMP in DCE.

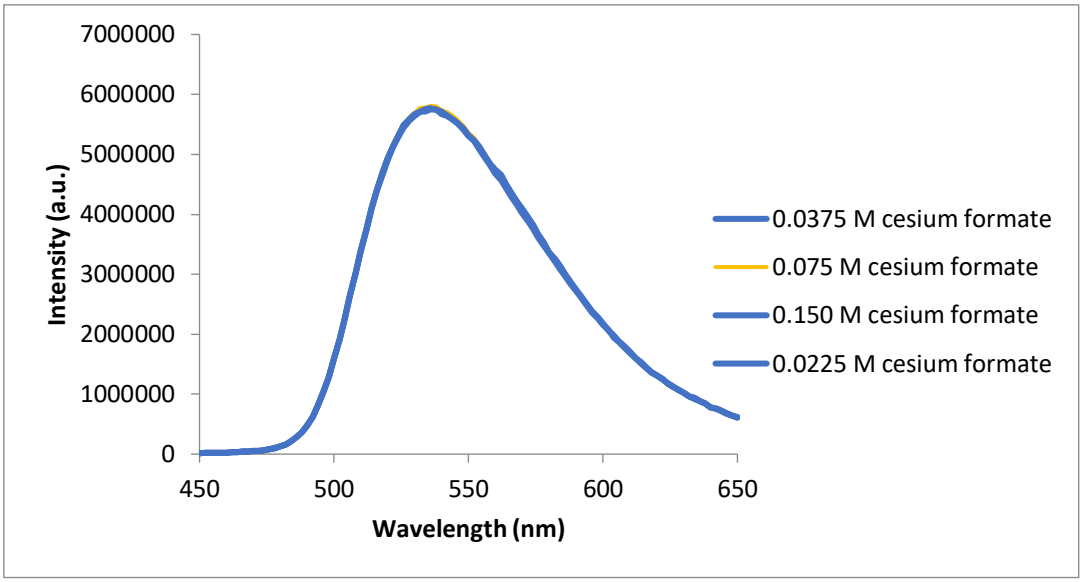

Figure 6.5 Emission profile of 4-DPA-IPN with cesium formate in DCE.

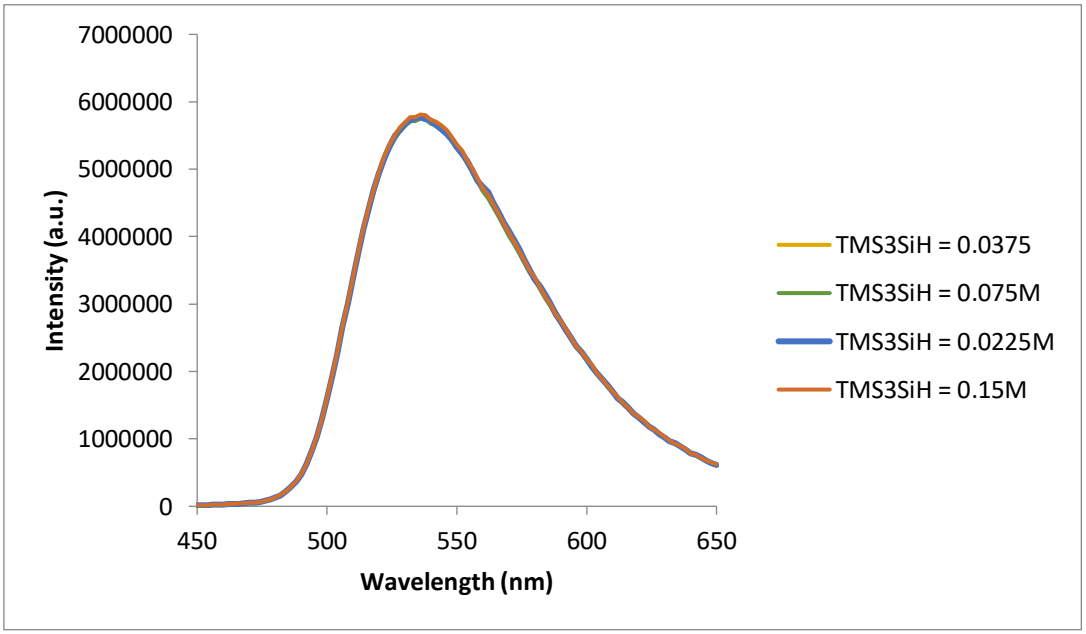

Figure 6.6 Emission profile of 4-DPA-IPN with $(TMS)_3SiH$ in DCE.

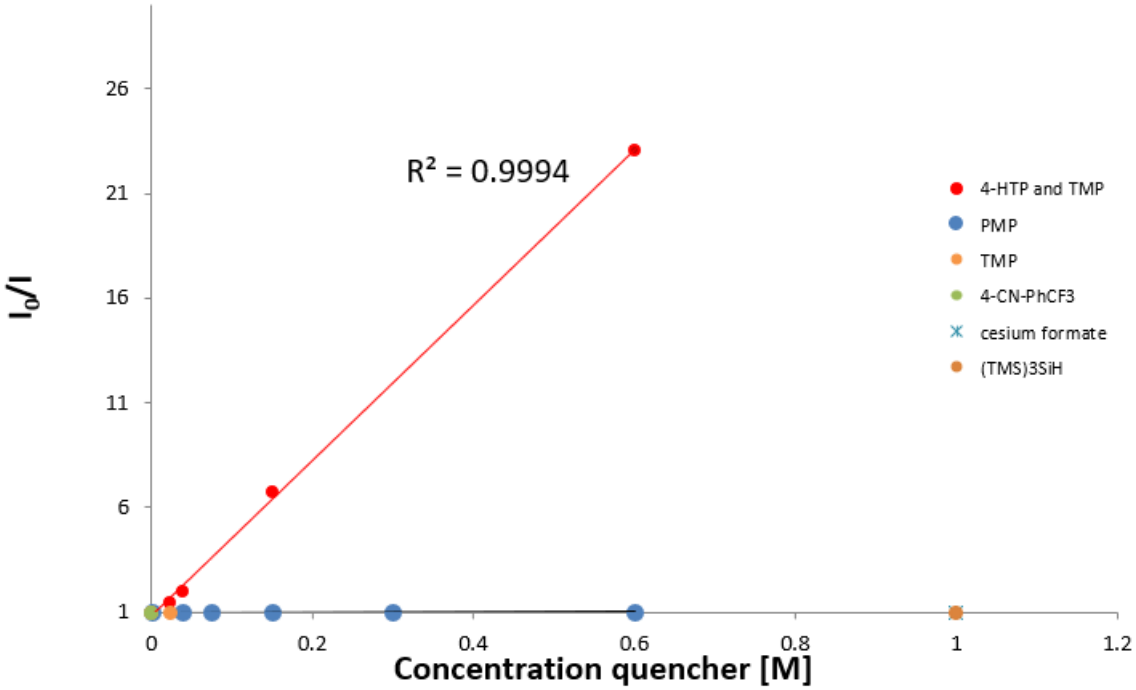

Figure 6.7 Stern-Volmer plot.

Proposed Mechanism

Explanation: Based on both the TEMPO trapping experiment as well as the experiment with styrene as an additive, we can conclude that the reaction proceeds through a radical mechanism. We propose that our photocatalyst is excited by blue light. Stern-Volmer quenching studies then confirmed that 4-hydroxythiophenolate is acting as the reductive excited state quencher in our reaction mixture, reducing the excited photocatalyst from PC* to PC^{n-1}. Its reduced state allows the photocatalyst to do a single electron transfer to our trifluoromethylarene starting material (**2.70**). This generates a radical anion which can undergo mesolytic cleavage (**2.111**), eliminating F^- resulting in a difluoromethylarene radical (**2.112**). Deuteration experiments then illustrated that 4-hydroxythiophenol can participate in a hydrogen atom transfer process to afford the desired difluoromethylarene product (**2.71**). The role of the bases (TMP and PMP) in our reaction mixture are presumably to deprotonate 4-hydroxythiophenol. A secondary

function of the bases might be to mop up any HF that is generated as the reaction proceeds.

6.4 Control Experiments Chapter II

Hydrodefluorination of 3-(4-acetamidophenoxy)-N-(4-cyano-3-(trifluoromethyl)phenyl)-2-hydroxy-2-methylpropanamide under other reported hydrodefluorination conditions

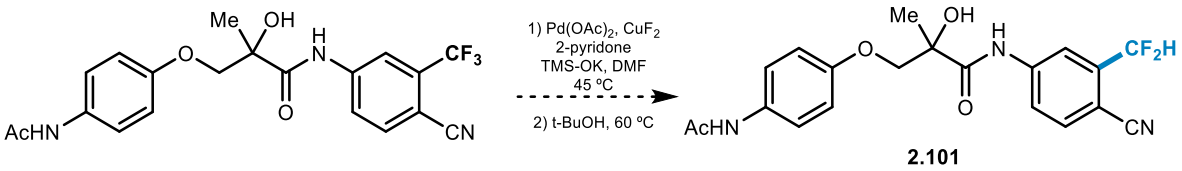

Scheme 6.4 Control experiment under reported conditions.

Following the optimised procedure of Lalic and co-workers[2], the desired mono hydrodefluorinated product was not observed. Starting material could be recovered quantitively.

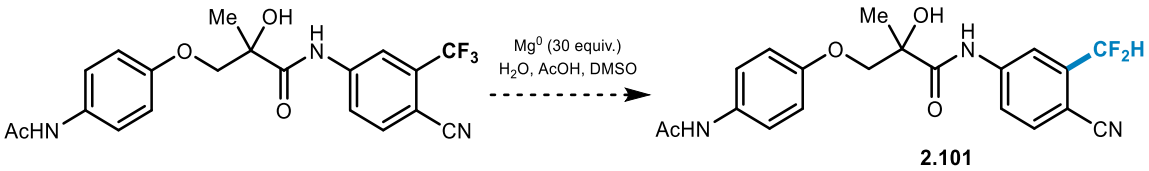

Scheme 6.5 Control experiment under reported conditions.

Following the optimised procedure of Prakash and co-workers[3], the desired mono hydrodefluorinated product was not observed. Starting material could be recovered quantitively.

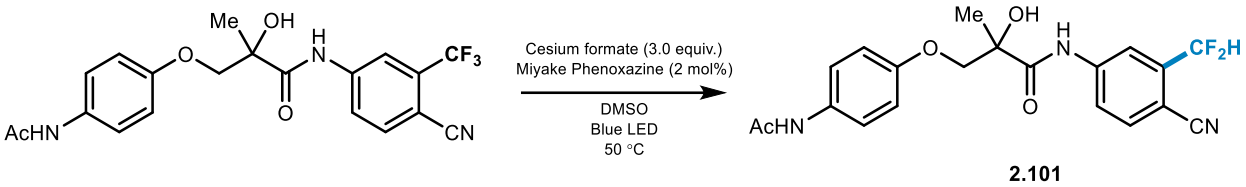

2.101

4% ^{19}F Quantitative NMR yield
selectivity (2:1) CF_2H:CH_2F

Scheme 6.6 Control experiment under reported conditions.

Following the optimised procedure of Jui and co-workers[4], the desired mono hydrodefluorinated product was observed in 4% (2:1) measured by quantitative ^{19}F NMR yield, using 4-fluoroanisole as an internal standard. Low conversion, mostly unreacted starting material.

6.5 Experimental Procedures and Characterisation for Compounds in Chapter II

All CF_3 precursors were bought from commercial vendors, except for those whom the synthesis is described below in (**General Procedure A**).

N-[4-Cyano-3-(trifluoromethyl)phenyl]-2-methyloxirane-2-carboxamide (CAS: 90357-51-0) which was used to make the starting materials and is commercially available and was purchased from Biosynth® Carbosynth (50 $ for 25 g).

General Procedure A

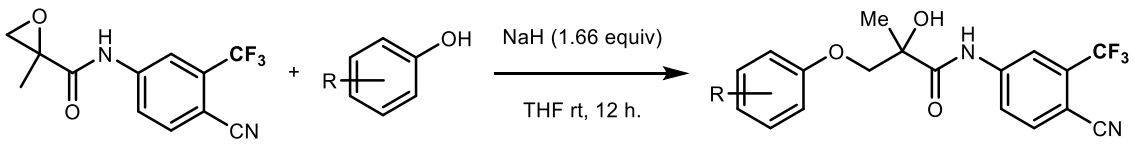

Scheme 6.7 Synthesis of CF_3 precursors.

To a mixture of NaH (60% in mineral oil, 0.1 g, 2.46 mmol, 1.66 equiv) in anhydrous THF (4 mL) at 0 °C under N_2 atmosphere was added a solution of phenol (2.22 mmol, 1.55

equiv) in 2 mL of anhydrous THF. This mixture was stirred at rt for 20 min. A solution of commercially available N-(4-cyano-3-(trifluoromethyl)phenyl)-2-methyloxirane-2-carboxamide (0.4 g, 1.48 mmol) in anhydrous THF (6 mL) was added slowly. The reaction mixture was stirred at rt. overnight. The mixture was then diluted with ethyl acetate (60 mL), washed with brine (30 mL) and water (60 mL), dried over $MgSO_4$ and concentrated *in vacuo*. The crude residue was then purified by flash column chromatography. This procedure was adapted from a known literature procedure.[5]

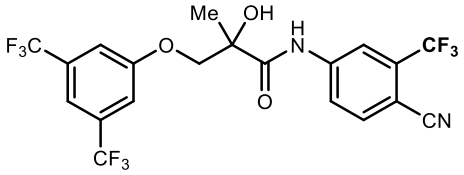

3-(3,5-bis(trifluoromethyl)phenoxy)-N-(4-cyano-3-(trifluoromethyl)phenyl)-2-hydroxy-2-methylpropanamide was prepared using General Procedure A using N-(4-cyano-3-(trifluoromethyl)phenyl)-2-methyloxirane-2-carboxamide and 3,5-bis(trifluoromethyl)phenol.

^{1}H NMR (500 MHz, Chloroform-*d*) δ 9.14 (s, 1H), 8.12 (d, *J* = 2.1 Hz, 1H), 7.97 (dd, *J* = 8.5, 2.1 Hz, 1H), 7.81 (d, *J* = 8.4 Hz, 1H), 7.51 (s, 1H), 7.34 (s, 2H), 4.56 (d, *J* = 9.0 Hz, 1H), 4.11 (d, *J* = 9.0 Hz, 1H), 3.33 (s, 1H), 1.64 (s, 3H).

^{19}F NMR (471 MHz, Chloroform-*d*) δ -62.25 (s), -63.08 (s).

^{13}C NMR (126 MHz, Chloroform-*d*) δ 172.2, 158.4, 141.5, 136.1, 134.4 (q, *J* = 32.9 Hz), 133.3 (q, *J* = 33.6 Hz), 124.2, 122.5 (q, *J* = 273.3 Hz), 122.0, 117.5 (q, *J* = 5.0 Hz), 115.7 (p, *J* = 3.8 Hz), 115.6, 115.3 (q, *J* = 3.7 Hz), 105.0 (t, *J* = 2.3 Hz), 76.0, 73.2, 23.2.

HRMS (ESI) *m/z* calculated for $[M - H]^-$ 499.0710 Found, 499.0715.

IR (cm^{-1}): 3312, 2120, 1950, 1637, 1610, 1531, 1443, 1321.

Mp: 128 – 131 °C.

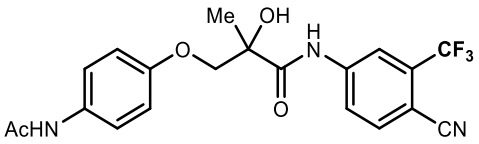

3-(4-acetamidophenoxy)-*N*-(4-cyano-3-(trifluoromethyl)phenyl)-2-hydroxy-2-methylpropanamide was prepared using General Procedure A, using N-(4-cyano-3-(trifluoromethyl)phenyl)-2-methyloxirane-2-carboxamide and N-(4-hydroxyphenyl)acetamide.

^{1}H NMR (400 MHz, DMSO-d_6) δ 10.57 (s, 1H), 9.77 (s, 1H), 8.57 (d, *J* = 2.2 Hz, 1H), 8.32 (dd, *J* = 8.6, 2.1 Hz, 1H), 8.09 (d, *J* = 8.6 Hz, 1H), 7.56 – 7.39 (m, 2H), 7.05 – 6.75 (m, 2H), 6.26 (s, 1H), 4.19 (d, *J* = 9.5 Hz, 1H), 3.95 (d, *J* = 9.6 Hz, 1H), 2.00 (s, 3H), 1.44 (s, 3H).

^{19}F NMR (377 MHz, DMSO-d_6) δ -61.16 (s).

^{13}C NMR (101 MHz, DMSO-d_6) δ 175.1, 168.2, 154.7, 143.7, 136.7, 133.3, 132.0 (q, *J* = 31.5 Hz), 123.1, 123.0 (q, *J* = 273.6 Hz), 120.9, 117.8 (q, *J* = 5.3 Hz), 116.3, 115.1, 102.4, 75.3, 74.3, 24.2, 23.5.

HRMS (ESI) *m/z* calculated for $[M + H]^+$ 422.1328 Found, 422.1330

IR (cm^{-1}): 3332, 2098, 1970, 1621, 1615, 1521, 1430, 1221.

Mp: 135– 138 °C

General procedure B

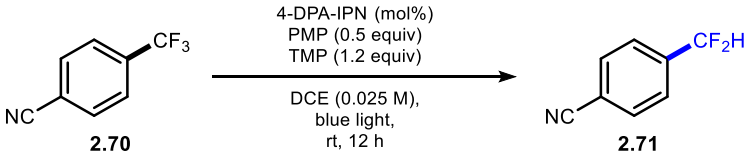

Scheme 6.7 General procedure B towards **2.71**

Stock solutions were prepared of the desired additives (starting materials, HAD, base, etc.) in DCE. Unless stated otherwise, to an oven-dried 8 mL screw top reaction tube, equipped with a stirring bar, was added 4-DPA-IPN (0.25 mol% - 2.5 mol%). To this reaction tube was added, CF_3-arene (0.1 mmol, 1.0 equiv.) and 4-hydroxythiophenol (0.6 mmol, 6.0 equiv.). Hereafter, 2,2,6,6-tetramethylpipyridine (0.12 mmol, 1.2 equiv.) and 1,2,2,6,6-pentamethylpipyridine (0.05 mmol, 0.5 equiv.) were added via micro-syringe. The reaction tube was capped and filled with 1,2-dichloroethane (4 mL, 0.025 M). The mixture was sparred with nitrogen for 2 minutes (*a slight increase in fluorescents of the reaction mixture was observed*) and then placed 5 cm away from a Blue LED array (455 nm), stirred and irradiated for 12 hours at room temperature. Reaction temperature was maintained within 25 ± 1 °C during the reaction by nitrogen circulation inside the photo-box. All reactions were run in duplicate and purified on 0.2 mmol scale. First, the solvent was removed under reduced pressure. The crude mixture was then purified through a silica plug, followed by semi-prep HPLC.

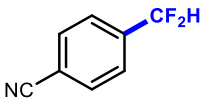

4-(difluoromethyl)benzonitrile (2.71). Compound was prepared following *General*

Procedure B. Compound was isolated by flash chromatography (pentane/Et_2O gradient), followed by Prep-HPLC (gradient 35% MeCN in 65% H_2O to 95% MeCN in 5% H_2O) on a C18 HPLC column. The title compound was obtained as a colorless oil. (**Yield = 60%**). Spectral data was consistent with literature.[6]

^{1}H-NMR: (400 MHz, Chloroform-*d*) δ 7.78 (dq, *J* = 7.8, 0.9 Hz, 2H), 7.71 – 7.57 (m, 2H), 6.70 (t, *J* = 55.8 Hz, 1H).

^{19}F-NMR: (376 MHz, Chloroform-*d*) δ -113.21 (d, *J* = 55.9 Hz).

^{13}C-NMR (101 MHz, Chloroform-*d*) δ): 138.5 (t, *J* = 23.3 Hz), 132.8, 126.7 (t, *J* = 6.3 Hz), 118.2, 115.5, 112.9 (t, *J* = 240.4 Hz).

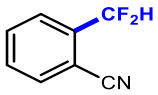

2-(difluoromethyl)benzonitrile (2.86). Compound was prepared following *General Procedure B*. Compound was isolated by flash chromatography (pentane/Et_2O gradient), followed by Prep-HPLC (gradient 35% MeCN in 65% H_2O to 95% MeCN in 5% H_2O) on a C18 HPLC column. The title compound was obtained as a pale yellow oil. (**Yield = 63%**). Spectral data was consistent with literature.[7]

^{1}H-NMR: (400 MHz, Chloroform-*d*) δ 7.80-7.69 (m, 3H), 7.65-7.59 (m, 1H), 6.92 (t, *J* = 54.5 Hz, 1H)

^{19}F-NMR: (376 MHz, Chloroform-*d*) δ -112.2 (d, *J* = 54.5 Hz, 2F).

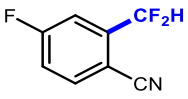

2-(difluoromethyl)-4-fluorobenzonitrile (2.87). Compound was prepared following *General Procedure B*. Compound was isolated by flash chromatography (pentane/Et_2O gradient), followed by Prep-HPLC (gradient 35% MeCN in 65% H_2O to 95% MeCN in 5% H_2O) on a C18 HPLC column. The title compound was obtained as a clear wax. (**Yield = 88%**).

^{1}H NMR (500 MHz, Chloroform-*d*) δ 7.90 – 7.74 (m, 1H), 7.49 (dd, *J* = 8.4, 2.6 Hz, 1H), 7.33 (td, *J* = 8.7, 2.3 Hz, 1H), 6.93 (t, *J* = 54.4 Hz, 1H).

^{13}C NMR (126 MHz, Chloroform-*d*) δ 165.0 (d, *J* = 259.3 Hz), 140.0 (td, *J* = 23.8, 8.3 Hz), 135.9 (d, *J* = 9.2 Hz), 118.9 (dt, *J* = 22.5, 1.8 Hz), 115.0, 114.6 (dt, *J* = 24.8, 6.1 Hz), 111.3 (t, *J* = 241.5 Hz), 107.4 – 106.4 (m).

^{19}F-NMR (^{1}H decoupled): (471 MHz, Chloroform-*d*) δ -99.96 (s), -112.98 (s)

HRMS: GC-MS (EI) *m/z* calculated for $C_8H_4F_3N$ $[M]^+$ 171.0296, found, 171.0294.

IR (cm^{-1}): 3065, 2937, 2842, 2360, 2237, 2129, 1683, 1614, 1596, 1499, 1438, 1316, 1130.

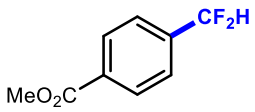

Methyl 4-(difluoromethyl)benzoate (2.88). Compound was prepared following *General Procedure B*. Compound was isolated by flash chromatography (pentane/Et_2O gradient), followed by Prep-HPLC (gradient 35% MeCN in 65% H_2O to 95% MeCN in 5% H_2O) on a C18 HPLC column. The title compound was obtained as a white solid. (**Yield = 30%**). Spectral data was consistent with literature.[8]

^{1}H-NMR: (400 MHz, Chloroform-*d*) δ 8.04 (dq, *J* = 7.8, 0.9 Hz, 2H), 7.61 – 7.44 (m, 2H), 6.61 (t, *J* = 56.1 Hz, 1H), 3.86 (s, 3H).

^{19}F-NMR: (376 MHz, Chloroform-*d*) δ -112.27 (d, *J* = 56.1 Hz).

^{13}C NMR: (101 MHz, Chloroform-*d*) δ 166.2, 138.4 (t, *J* = 22.4 Hz), 132.3 (t, *J* = 1.9 Hz), 129.9, 125.6 (t, *J* = 6.0 Hz), 114.0 (t, *J* = 239.8 Hz), 52.4.

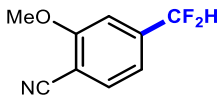

4-(difluoromethyl)-2-methoxybenzonitrile (2.89). Compound was prepared following *General Procedure B* using 2.5 mol% of 4-DPA-IPN. Compound was isolated by flash chromatography (20% DCM in pentane), followed by Prep-HPLC (gradient 35% MeCN in 65% H_2O to 95% MeCN in 5% H_2O) on a C18 HPLC column. The title compound was obtained as a white solid. (**Yield = 42%**).

^{1}H NMR (500 MHz, Chloroform-*d*) δ 7.66 (d, *J* = 7.8 Hz, 1H), 7.15 (d, *J* = 8.0 Hz, 1H), 7.12 (s, 1H), 6.66 (t, *J* = 55.9 Hz, 1H), 4.00 (s, 3H).

^{13}C NMR (126 MHz, Chloroform-*d*) δ 161.9, 140.7 (t, *J* = 22.7 Hz), 134.7, 118.4 (t, *J* = 6.3 Hz), 116.0, 113.7 (t, *J* = 243.0 Hz), 108.7 (t, *J* = 6.1 Hz), 104.7, 56.8.

^{19}F-NMR: (376 MHz, Chloroform-*d*) δ -113.03 (d, *J* = 56.0 Hz).

IR (cm^{-1}): 2219, 1643, 1641, 1530, 1470, 1320, 1164, 1079.

HRMS (ESI) *m/z* calculated for $C_9H_7F_2NO$ $[M + Na]^+$ 206.0393, found, 206.0396.

Mp: Decomposition

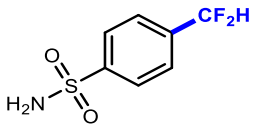

4-(difluoromethyl)benzenesulfonamide (2.90). Compound was prepared following *General Procedure B*. Compound was isolated by flash chromatography (20% DCM in pentane), followed by Prep-HPLC (gradient 35% MeCN in 65% H_2O to 95% MeCN in 5% H_2O) on a C18 HPLC column. The title compound was obtained as a white solid. (**Yield = 30%**).[9]

^{1}H NMR (400 MHz, DMSO-d_6) δ 7.97 (d, *J* = 8.2 Hz, 2H), 7.78 (d, *J* = 8.2 Hz, 2H), 7.53 (s, 2H), 7.15 (t, *J* = 55.4 Hz, 1H).

^{19}F NMR (376 MHz, DMSO-d_6) δ -111.4 (d, *J* = 55.7 Hz, 2F)

^{13}C NMR (101 MHz, DMSO-d_6) δ 147.1, 136.1 (t, *J* = 22.8 Hz), 126.2 (t, *J* = 5.5 Hz), 126.3, 114.2 (t, *J* = 236.3 Hz).

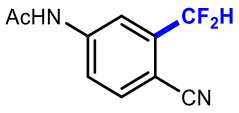

N-(4-cyano-3-(difluoromethyl)phenyl)acetamide (2.91). Compound was prepared following *General Procedure B.* Compound was isolated by flash chromatography (15% Et_2O in DCM), followed by Prep-HPLC (gradient 35% MeCN in 65% H_2O to 95% MeCN in 5% H_2O) on a C18 HPLC column. The title compound was obtained as a clear wax. (**Yield = 60%**).

^{1}H NMR (400 MHz, Chloroform-*d*) δ 7.92 (d, *J* = 8.4 Hz, 1H), 7.82 (d, *J* = 2.1 Hz, 1H), 7.71 (d, *J* = 8.5 Hz, 1H), 7.45 (s, 1H), 6.88 (t, *J* = 54.6 Hz, 1H), 2.25 (s, 3H).

^{19}F NMR (376 MHz, Chloroform-*d*) δ -112.45 (d, *J* = 54.3 Hz).

^{13}C NMR (101 MHz, Chloroform-*d*) δ 168.7, 142.5, 138.3 (t, *J* = 23.1 Hz), 134.8, 121.3, 116.7 (t, *J* = 6.2 Hz), 116.0, 112.1 (t, *J* = 240.8 Hz), 105.3, 25.0.

HRMS (ESI) *m/z* calculated for $[M + Na]^+$ 233.0502, found, 233.0504.

IR (cm^{-1}): 3538, 3321, 3064, 2235, 1694, 1597, 1542, 1498, 1429, 1374.

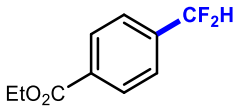

Ethyl 4-(difluoromethyl)benzoate (2.92). Compound was prepared following *General Procedure B*. Compound was isolated by flash chromatography (pentane/Et_2O gradient), followed by Prep-HPLC (gradient 35% MeCN in 65% H_2O to 95% MeCN in 5% H_2O) on a C18 HPLC column. The title compound was obtained as a colourless oil. (**Yield = 40%**). Spectral data was consistent with literature.[7]

^{1}H-NMR: (400 MHz, Chloroform-*d*) δ 8.13 (d, *J* = 8.1 Hz, 2H), 7.57 (d, *J* = 8.1 Hz, 2H), 6.70 (t, *J* = 56.2 Hz, 1H), 4.42 (q, *J* = 7.0 Hz, 2H), 1.42 (t, *J* = 7.0 Hz, 3H).

^{19}F-NMR: (376 MHz, Chloroform-*d*) δ -112.2 (d, *J* = 56.2 Hz, 2F).

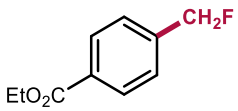

Ethyl 4-(fluoromethyl)benzoate. Compound was prepared following *General Procedure B* using 2.5 mol% 4-DPA-IPN. Compound was isolated by flash chromatography (pentane/Et_2O gradient), followed by Prep-HPLC (gradient 35% MeCN in 65% H_2O to 95% MeCN in 5% H_2O) on a C18 HPLC column. The title compound was obtained as a colourless oil. (**Yield = 40%**). Spectral data was consistent with literature.[10]

^{1}H-NMR: (400 MHz, Chloroform-*d*) δ 8.05 (d, *J* = 7.7 Hz, 2H), 7.42 (d, *J* = 7.4 Hz, 2H), 5.45 (d, *J* = 47.0 Hz, 2H), 1.39 (t, *J* = 7.1 Hz, 3H).

^{19}F-NMR: (376 MHz, Chloroform-*d*) δ -212.6 (t, *J* = 47.0 Hz, 1F).

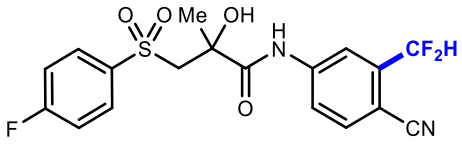

N-(4-cyano-3-(difluoromethyl)phenyl)-3-((4-fluorophenyl)sulfonyl)-2-hydroxy-2-methylpropan-amide (2.96). Compound was prepared following *General Procedure B*. Compound was isolated by a short plug of SiO_2 (2% Et_2O in DCM) followed by trituration in Et_2O. Prep-HPLC (gradient 35% MeCN in 65% H_2O to 85% MeCN in 15% H_2O) on a C18 HPLC column, the title product was obtained as a white solid. (**Yield = 43%**).

^{1}H NMR (400 MHz, DMSO-d_6) δ 10.23 (s, 1H), 8.28 (s, 1H), 8.08 – 8.02 (m, 1H), 7.99 – 7.91 (m, 3H), 7.40 (t, *J* = 9.0 Hz, 2H), 7.31 (t, *J* = 53.7 Hz, 1H), 6.36 (s, 1H), 3.95 (d, *J* = 14.8 Hz, 1H), 3.73 (d, *J* = 14.8 Hz, 1H), 1.42 (s, 3H).

^{19}F NMR: (376 MHz, DMSO-d_6) δ -105.56 (m), -112.34 (d, *J* = 54.7 Hz).

^{13}C NMR (101 MHz, DMSO-d_6) δ 174.0, 165.3 (d, *J* = 252.1 Hz), 143.5, 137.7 (d, *J* = 3.0 Hz), 137.3 (t, *J* = 22.3 Hz), 135.5, 131.8 (d, *J* = 9.9 Hz), 122.3, 118.2 (t, *J* = 7.5 Hz), 116.9, 116.5 (d, *J* = 22.7 Hz), 113.6 (t, *J* = 238.0 Hz), 103.3 (t, *J* = 4.7 Hz), 73.6, 63.9, 27.6.

HRMS (ESI) *m/z* calculated for $C_{18}H_{14}F_3N_2O_4S$ $[M - H]^-$ 411.0632, found, 411.06277.

IR (cm^{-1}): 3337, 3115, 2230, 1978, 1687, 1612, 1591, 1453, 1326, 1128.

Mp: 189 – 191 °C

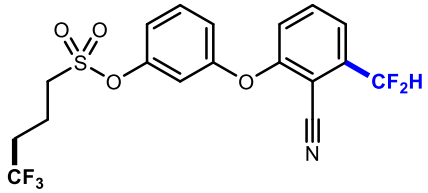

3-(2-cyano-3-(difluoromethyl)phenoxy)phenyl 4,4,4-trifluorobutane-1-sulfonate (2.97). Compound was prepared following *General Procedure B*. The title compound was unstable upon isolation. NMR yield based on quantitative fluorine NMR, using 4-fluoroanisole as an internal standard gave 63% (7:1). Product identity was confirmed by HRMS and chemoselectivity was confirmed by quantitative ^{19}F NMR.

HRMS (ESI) *m/z* calculated for $C_{18}H_{14}F_5NNaO_4S$ $[M + Na]^+$ 458.0461, found, 458.0465.

^{19}F-NMR: (376 MHz, Chloroform-*d*) δ-66.17 (s, 3F), -112.48 (d, *J* = 54.6 Hz, 2F).

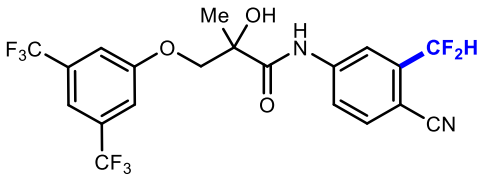

3-(3,5-bis(trifluoromethyl)phenoxy)-N-(4-cyano-3-(difluoromethyl)phenyl)-2-hydroxy-2-methylpropanamide (2.98). Compound was prepared following *General Procedure B*. Compound was isolated by column silica gel chromatography (DCM) followed by Prep-HPLC (gradient 35% MeCN in 65% H_2O to 95% MeCN in 5% H_2O) on a C18 HPLC column, the title product was obtained as a white solid. (**Yield = 53%**).

^{1}H NMR (400 MHz, Chloroform-*d*) δ 9.06 (s, 1H), 8.01 – 7.93 (m, 2H), 7.75 (d, *J* = 8.3 Hz, 1H), 7.53 (s, 1H), 7.35 (s, 2H), 6.90 (t, *J* = 54.5 Hz, 1H), 4.57 (d, *J* = 8.9 Hz, 1H), 4.11 (d, *J* = 9.0 Hz, 1H), 3.19 (s, 1H), 1.64 (s, 3H).

^{13}C NMR (101 MHz, Chloroform-*d*) δ 170.8, 157.2, 140.5, 137.2 (t, *J* = 23.2 Hz), 133.6, 132.1 (q, *J* = 33.6 Hz), 122.0 (q, *J* = 272.6 Hz), 120.2, 115.9 (t, *J* = 6.3 Hz), 114.8 – 114.5 (m), 114.1, 110.8 (t, *J* = 241.0 Hz), 104.7, 74.8, 72.0, 28.7, 22.1.

^{19}F NMR (376 MHz, Chloroform-*d*) δ -63.06 (s), -112.47 (d, *J* = 54.6 Hz).

HRMS (ESI) *m/z* calculated for $C_{20}H_{13}F_8N_2O_3$ $[M - H]^-$ 481.07929, found, 481.08083.

IR (cm^{-1}): 3344, 2981, 2233, 1690,1522, 1376, 1276, 1125.

Mp: 126 – 130 °C

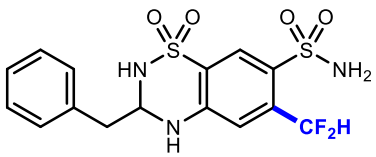

3-benzyl-6-(difluoromethyl)-3,4-dihydro-2H-benzo[e][1,2,4]thiadiazine-7-sulfonamide 1,1-dioxide (2.99). Compound was prepared following *General Procedure B*. Due to the little material at hand, NMR yield based on quantitative fluorine NMR is

given, using 4-fluoroanisole as an internal standard yielded 56% (4:1). Product identity was confirmed by HRMS and ^{19}F NMR

HRMS (ESI) *m/z* calculated for $C_{15}H_{15}F_2N_3O_4S_2$ $[M + H]^+$ 404.05448 found, 404.05440.

^{19}F-NMR: (376 MHz, DMSO-d_6) δ-114.48 (d, *J* = 54.4 Hz, 2F).

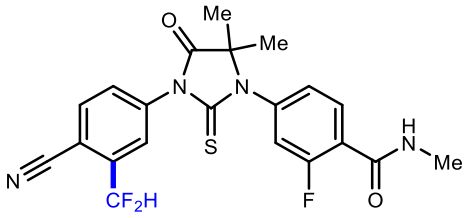

4-(3-(4-cyano-3-(difluoromethyl)phenyl)-5,5-dimethyl-4-oxo-2-thioxoimidazolidin-1-yl)-2-fluoro-N-methylbenzamide (2.100). Compound was prepared following *General Procedure B*. Compound was isolated by column silica gel chromatography (5% EtOAc in DCM) followed by Prep-HPLC (gradient 35% MeCN in 65% H_2O to 95% MeCN in 5% H_2O) on a C18 HPLC column, the title product was obtained as a white solid. (**Yield = 40%**).

^{1}H NMR (500 MHz, Chloroform-*d*) δ 8.28 (t, *J* = 8.4 Hz, 1H), 7.96 – 7.84 (m, 2H), 7.73 (ddd, *J* = 8.3, 2.1, 1.1 Hz, 1H), 7.26 – 7.24 (m, 1H), 7.16 (dd, *J* = 11.7, 2.0 Hz, 1H), 6.98 (t, *J* = 54.4 Hz, 1H), 6.72 (s, 1H), 3.07 (d, *J* = 4.9 Hz, 3H), 1.61 (s, 6H).

^{19}F NMR (376 MHz, Chloroform-*d*) δ -110.96 (m), -112.89 (d, *J* = 54.4 Hz).

^{13}C NMR (126 MHz, Chloroform-*d*) δ 180.0, 174.5, 162.7 (d, *J* = 3.3 Hz), 160.4 (d, *J* = 250.3 Hz), 139.1 (d, *J* = 10.8 Hz), 137.8 (t, *J* = 23.7 Hz), 137.2, 134.0, 133.4 (d, *J* = 3.4 Hz), 131.3, 126.8 (t, *J* = 6.1 Hz), 126.2 (d, *J* = 3.2 Hz), 122.6 (d, *J* = 12.1 Hz), 117.9 (d, *J* = 26.5 Hz), 115.1, 111.6 (t, *J* = 241.0 Hz), 111.1 (t, *J* = 5.1 Hz), 66.6, 27.0, 23.9.

HRMS (ESI) *m/z* calculated for $C_{21}H_{18}F_3N_4O_2S$ $[M + H]^+$ 447.1097, found, 447.1098.

IR (cm^{-1}): 3410, 2940, 2228, 1648, 1539, 1492, 1212.

Mp: 194 – 196 °C

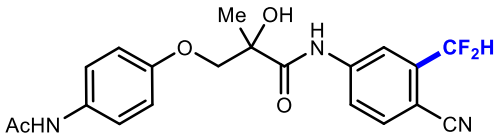

3-(4-acetamidophenoxy)-N-(4-cyano-3-(difluoromethyl)phenyl)-2-hydroxy-2-methylpropanamide (2.101). Compound was prepared following *General Procedure B*. Compound was isolated by column silica gel chromatography (5% EtOAc in DCM) followed by Prep-HPLC (gradient 35% MeCN in 65% H_2O to 85% MeCN in 15% H_2O) on a C18 HPLC column, the title product was obtained as a white solid. (**Yield = 60%**).

^{1}H NMR (500 MHz, Chloroform-*d*) δ 9.15 (s, 1H), 7.97 (s, 1H), 7.93 (d, *J* = 8.4 Hz, 1H), 7.71 (d, *J* = 8.5 Hz, 1H), 7.39 – 7.29 (m, 2H), 7.21 (s, 1H), 6.88 (d, *J* = 54.7 Hz, 1H), 6.85 – 6.80 (m, 2H), 4.40 (d, *J* = 9.1 Hz, 1H), 3.94 (d, *J* = 9.1 Hz, 1H), 3.71 (s, 1H), 2.15 (s, 3H), 1.57 (s, 3H).

^{19}F NMR (^{1}H decoupled) (376 MHz, Chloroform-*d*) δ -112.37 (s)

^{13}C NMR (126 MHz, Chloroform-*d*) δ 172.8, 168.4, 154.6, 141.8, 138.1 (t, *J* = 23.1 Hz), 134.6, 132.0, 121.9, 121.3, 116.9 (t, *J* = 6.2 Hz), 115.8, 115.2, 112.0 (t, *J* = 240.8 Hz), 105.3 (t, *J* = 5.0 Hz), 75.8, 72.8, 24.4, 23.0.

HRMS (ESI) *m/z* calculated for $C_{20}H_{20}F_2N_3O_4$ $[M + H]^+$ 404.14164, found, 404.14160.

IR (cm^{-1}): 3313, 2936, 2361, 2231, 1665, 1610, 1508, 1325, 1131, 1049.

Mp: 134–136 °C

6.6 Reaction in Flow Chapter II

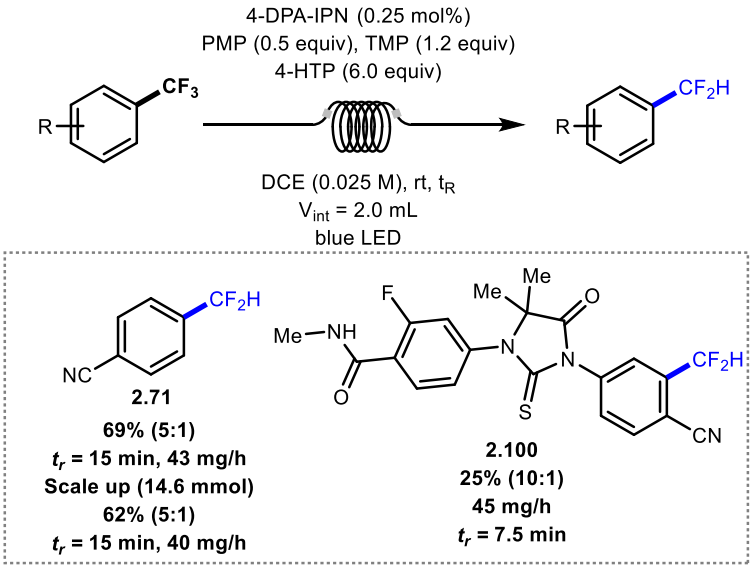

Scheme 6.8 Photoredox hydrodefluorination under continuous-flow conditions; the internal volume of the capillary (V_{int}) was 2.0 mL, t_R = residence time. Yields of isolated products.

The first reactions were performed in a microflow system made of a perfluoroalkoxyalkane (PFA) capillary with an internal volume of 2 mL. First reactions were performed on 0.2 mmol scale using 4.0 mL of reaction mixture. The reaction towards **2.71** was run for 15 minutes residence time (30 minutes reaction time). The reaction towards **2.100** was run for 7.5 minutes residence time (15 minutes reaction time), flow rates of 0.133 µL/min and 0.266 µL/min were used respectively. Analogous conditions for **2.71** (same concentration) were used in the scale up reaction, allowing 1.4 g of **2.71** to be isolated in 62% yield after 12 hours.

6.7 Robustness Screening Experiments Chapter II (reactions performed with Dr. Thomas Knauber)

Reactions were performed in a Lumidox photoredox 96-well plate and the scale of each reaction was 2.5 µmol. All screening reactions were run using a 30mA/470 nm light. The stirring rate was 1150 rpm. A stock solution of reaction mixture was prepared in a nitrogen filled glovebox and an aliquot (25 µL) was added in each vial. The additives were ordered pre-weighed from our neat store (Pfizer). The vials were transferred into the glovebox and DCE was added. Aliquots (25 µL) of the resulting stock solutions were added to the corresponding vials. All conversions are respective to n-tetradecane as internal standard. Note that all conversion are not corrected with response factors and the reference reaction gave an uncorrected yield of 20% for the desired product (compared to 60% isolation on 0.20 mmol scale). In all cases additives were added to the model reaction where 4-(trifluoromethyl)benzonitrile is the model substrate. Some of the additives were not available and are labelled in grey (these reactions were not performed). In the cases where additives were not fully soluble in DCE, they were added as a suspension. Samples of crude mixtures were analyzed by GC-FID/MS (see **Scheme 2.20** and **2.21** for further details).

6.8 References

1. (a) K. Chen, N. Berg, R. Gschwind and B. König, *J. Am. Chem. Soc.,* 2017, **139**, 18444;

(b) H. Wang and N. T. Jui, *J. Am. Chem. Soc.,* 2018, **140**, 163.

2. H. Dang, A. M. Whittaker and G. Lalic, *Chem. Sci.,* 2016, **7**, 505.

3. S. B. Munoz, C. Ni, Z. Zhang, F. Wang, N. Shao, T. Mathew, G. A. Olah and G. S. Prakash, *Eur. J. Org. Chem.,* 2017, **2017**, 2322.

4. D. B. Vogt, C. P. Seath, H. Wang and N. T. Jui, *J. Am. Chem. Soc.,* 2019, **141**, 13203.

5. S. Ferla, M. Bassetto, F. Pertusati, S. Kandil, A. D. Westwell, A. Brancale and C. McGuigan, *Bioorg. Med. Chem. Lett.,* 2016, **26**, 3636

6.9 Synthetic Procedures and Characterisation of Compounds Chapter IV:

General Procedure (GP) 1: Synthesis of α-aryl-α-fluoroacetic acids.

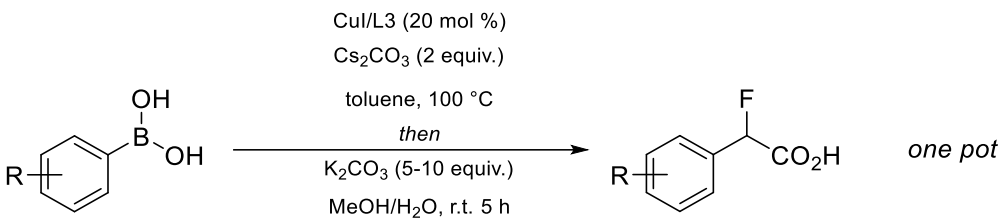

Scheme 6.9 Synthesis of α-aryl-α-fluoroacetic acids.

To a flame-dried pear-shaped round bottomed flask were added CuI (20 mol%), 4,4',4''-tri-*tert*-butyl-2,2':6',2''-terpyridine (20 mol%), boronic acid (1 equiv.) and Cs_2CO_3 (2 equiv.), followed by argon degassed toluene (1.5 mL). The reaction mixture is stirred for 18 hours at 100 °C. The reaction mixture is cooled to r.t, solvent removed under reduced pressure. The resulting suspension was then dissolved in a 2:1 MeOH and aqueous K_2CO_3 (10 equiv.) mixture before it was left to stir at r.t until all the ester had been consumed (determined by TLC). MeOH was then removed under reduced pressure. The aqueous suspension was then washed with Et_2O (3 x 10 mL), acidified using HCl (5 M) to pH = 2. The aqueous layer was then extracted with Et_2O (3 x 10 mL) and washed with Brine (2 x 10 mL). The organic extracts were then dried over $MgSO_4$ and concentrated under vacuum and washed with pentane, resulting in an off-white solid. The resulting crude 2-fluoro-2-phenylacetic acids were then subjected to column chromatography (gradient of hexane/ethyl acetate with acetic acid (1%) to ethyl acetate/MeOH with acetic acid (1%)). *Note: Alternatively, the α-(hetero)aryl-α-fluoroacetates can be purified via column*

chromatography and then hydrolysed without subsequent column chromatography of the carboxylic acid (GP 2).

General Procedure (GP) 2: Synthesis of α-(hetero)aryl-α-fluoroacetate and subsequent hydrolysis

Scheme 6.10 Synthesis of α-(hetero)aryl-α-fluoroacetate and subsequent hydrolysis.

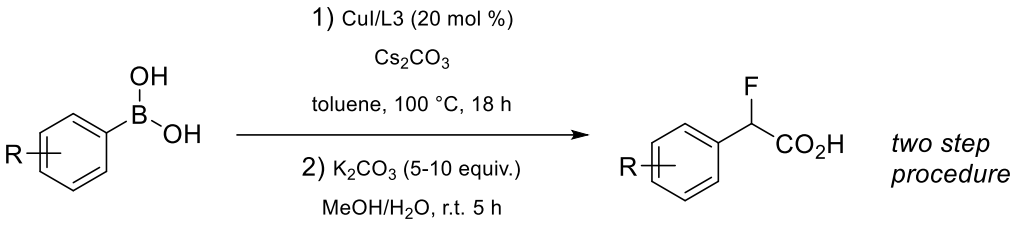

To a flame-dried pear-shaped round bottomed flask were added CuI (20 mol%), 4,4',4''-Tri-*tert*-butyl-2,2':6',2''-terpyridine (20 mol%), boronic acid (1 equiv.) and Cs_2CO_3 (2 equiv.). followed by argon degassed toluene (1.5 mL). The reaction mixture is stirred for 18 hours at 100 °C. The mixture is cooled to r.t, solvent removed under reduced pressure. The residue is then diluted with EtOAc and filtered through a plug of celite. EtOAc is then removed under reduced pressure. The resulting oil is purified by silica gel chromatography (EtOAc/Hexane), resulting in a clear colourless oil. This oil was then dissolved in a 2:1 MeOH and aqueous K_2CO_3 (5 equiv.) mixture before it was left to stir at r.t until all the ester had been consumed (determined by TLC). The resulting mixture was then acidified using HCl (5 M) to pH = 2. The aqueous layer was then extracted with Et_2O (3 x 10 mL) and washed with Brine (2 x 10 mL). The organic extracts were dried using $MgSO_4$ and were then concentrated under vacuum and washed with pentane.

General Procedure (GP) 3: Synthesis of (difluoromethyl)arenes reference compounds

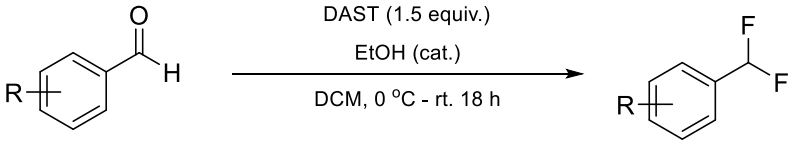

Scheme 6.11 Synthesis of (difluoromethyl)arenes reference compounds.

A flame-dried two-necked round-bottomed flask was charged with a stir-magnetic stir bar and a starting material (if solid). To this flask was added anhydrous DCM and a drop of EtOH. The resulting mixture was cooled to 0 °C and DAST (1.5 equiv.) was added dropwise. The resulting mixture was stirred at 0 °C for a further 10 minutes before it was allowed to warm to r.t. The resulting reaction mixture was stirred until TLC showed all starting material had been consumed. The reaction mixture was then quenched with $NaHCO_3$ until gas evolution stopped and then purified by column chromatography (eluent: *n*-pentane/DCM). *Note: electron rich title compounds such as 1-(difluoromethyl)-2-methoxybenzene and 1-(difluoromethyl)-4-phenoxybenzene are unstable when neat in standard glassware. When removing solvent these compounds should be transferred into a falcon tube and stored in a freezer. In case of decomposition, the compound will turn deep purple, but can be recovered if it is passed through a plug of silica.*

General Procedure (GP) 4: Synthesis of (difluoromethyl)arenes reference compounds

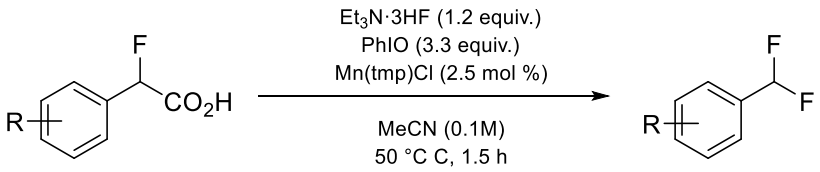

Scheme 6.12 Synthesis of (difluoromethyl)arenes reference compounds.

An oven-dried, 5 mL Schlenk flask equipped with a stir bar was placed under an atmosphere of N_2. Mn(tmp)Cl Catalyst (2.5 mol%) substrate (0.1 mmol) and DCE were then added, followed by $Et_3N{\cdot}3HF$ (1.2 equiv.). The reaction mixture was then heated to 50 °C. Under a stream of N_2, iodosylbenzene (3.3 equiv.) was added slowly to the reaction mixture in solid form over a period of 1.5 hours. After the addition of iodosylbenzene, the reaction was stirred until completion.

Synthesis of α-aryl-α-fluoroacetic acids

2-([1,1'-Biphenyl]-4-yl)-2-fluoroacetic acid (4.1)[2]

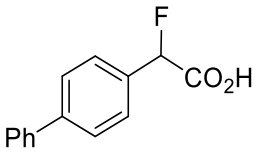

The title compound was prepared following GP1 using [1,1'-biphenyl]-4-ylboronic acid (59.4 mg, 0.3 mmol), ethyl bromofluoroacetate (67.2 µL, 0.6 mmol), Cs_2CO_3 (196 mg, 0.6 mmol), CuI (11.4 mg, 20 mol%) and 4,4′,4″-tri-*tert*-butyl-2,2′:6′,2″-terpyridine (24.1 mg, 20 mol%). The title compound (51.8 mg, 75% yield) was isolated as a white solid.

Physical appearance: White solid (yield: 75%). **^{1}H NMR** (400 MHz, DMSO-d_6) δ 7.74 (d, *J* = 7.8 Hz, 2H), 7.70 – 7.66 (m, 2H), 7.56 – 7.52 (m, 2H), 7.48 (dd, *J* = 8.4, 6.9 Hz, 2H), 7.42

– 7.37 (m, 1H), 6.04 (d, *J* = 47.5 Hz, 1H). **^{13}C NMR** (101 MHz, DMSO-d_6) δ 170.2 (d, *J* = 27.4 Hz), 141.7 (d, *J* = 2.3 Hz), 140.0, 134.6 (d, *J* = 19.6 Hz), 129.5, 128.3, 128.0 (d, *J* = 6.0 Hz), 127.5, 127.3, 89.8 (d, *J* = 183.2 Hz); **^{19}F NMR** (376 MHz, DMSO-d_6) δ -175.73 (d, *J* = 47.5 Hz). The physical data were identical in all respects to those previously reported.[2]

2-Fluoro-2-(4-phenoxyphenyl)acetic acid (4.15)

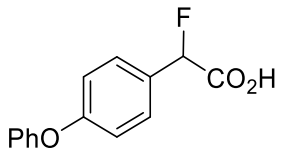

The title compound was prepared following General Procedure GP1 using (4-phenoxyphenyl)boronic acid (64.2 mg, 0.3 mmol), ethyl bromofluoroacetate (67.2 µL, 0.6 mmol), Cs_2CO_3 (196 mg, 0.6 mmol), CuI (11.4 mg, 20 mol%) and 4,4′,4″-tri-*tert*-butyl-2,2′:6′,2″-terpyridine (24.1 mg, 20 mol%). The title compound (51.0 mg, 69% yield) was isolated as a white solid.

Physical appearance: White solid (yield: 69%). **Mp:** 86 – 88 °C; **^{1}H NMR** (400 MHz, $CDCl_3$) δ: 7.45 (d, *J* = 9.4 Hz, 1H), 7.42 – 7.34 (m, 2H), 7.23 – 7.12 (m, 1H), 7.10 – 6.99 (m, 5H), 5.82 (d, *J* = 47.4 Hz, 1H); **^{13}C NMR** (101 MHz, $CDCl_3$) δ: 173.45 (d, *J* = 28.6 Hz), 159.25 (d, *J* = 2.4 Hz), 156.33, 130.08, 128.72 (d, *J* = 5.6 Hz), 127.74, 124.22, 119.76, 118.69, 88.59 (d, *J* = 186.4 Hz); **^{19}F NMR** (376 MHz, $CDCl_3$) δ: -177.21 (d, *J* = 47.7 Hz); Found, 245.06156; **IR** (film, cm^{-1}) υ 3038, 2917, 1768, 1589, 1243; **HRMS** (ESI) *m/z* calculated for $C_{14}H_{10}FO_3$ $[M - H]^-$ 245.06195, found, 245.06156.

2-(3,5-Dimethylphenyl)-2-fluoroacetic acid (4.31)

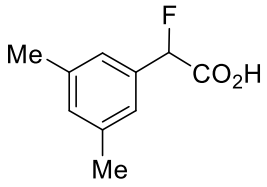

The title compound was prepared following General Procedure GP1 using (3,5-dimethylphenyl)boronic acid (45.0 mg, 0.3 mmol), ethyl bromofluoroacetate (67.2 µL, 0.6 mmol), Cs_2CO_3 (196 mg, 0.6 mmol), CuI (11.4 mg, 20 mol%) and 4,4′,4″-tri-*tert*-butyl-2,2′:6′,2″-terpyridine (24.1 mg, 20 mol%). The title compound (34.4 mg, 63% yield) was isolated as a white solid.

Physical appearance: White solid (yield: 63%). **Mp:** 68 – 70 °C; **^{1}H NMR** (400 MHz, $CDCl_3$) *δ*: 7.04 – 6.96 (m, 3H), 5.67 (d, 1H, *J* = 48.9 Hz), 2.26 (s, 6H). **^{13}C NMR** (101 MHz, $CDCl_3$) *δ*: 173.37 (d, *J* = 27. 8 Hz), 138.70, 133.21 (d, *J* = 20.3 Hz), 131.65 (d, *J* = 2.4 Hz), 124.50 (d, *J* = 5.9 Hz), 88.99 (d, *J* = 186.0 Hz), 21.23. **^{19}F NMR** (376 MHz, $CDCl_3$) *δ:* -179.17 (d, *J* = 47.4 Hz). **IR** (film, cm^{-1}) υ. 2919, 2166, 1725, 1066. **HRMS** (ESI) *m/z* calculated for $C_{10}H_{10}FO_2$ $[M - H]^-$ 181.06703, found, 181.06673.

2-(2,5-Dimethylphenyl)-2-fluoroacetic acid (4.32)

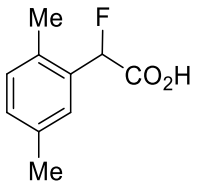

The title compound was prepared following General Procedure GP1 (3-iodophenyl)boronic acid (74.4 mg, 0.3 mmol), ethyl bromofluoroacetate (67.2 µL, 0.6

mmol), Cs_2CO_3 (196 mg, 0.6 mmol), CuI (11.4 mg, 20 mol%) and 4,4′,4″-tri-*tert*-butyl-2,2′:6′,2″-terpyridine (16.6 mg, 20 mol%). The title compound (42.0 mg, 52% yield) was isolated as a white solid.

Physical appearance: White solid (yield: 52%). **Mp**: 85 – 88 °C; **^{1}H NMR** (400 MHz, $CDCl_3$) *δ*: 7.22 (d, 1H, *J* = 10.9 Hz), 7.10 (s, 2H), 5.98 (d, 1H, *J* = 47.2 Hz), 2.38 (s, 3H), 2.31 (s, 3H); **^{13}C NMR** (101 MHz, $CDCl_3$) *δ:* 174.49 (d, *J* = 28.7 Hz), 136.13, 133.41 (d, *J* = 3.9 Hz), 131.68 (d, *J* = 19.1 Hz), 130.93, 130.72 (d, *J* = 2.5 Hz), 127.76 (d, *J* = 6.7 Hz), 86.64 (d, *J* = 185.6 Hz), 20.88, 18.68; **^{19}F NMR** (376 MHz, $CDCl_3$) *δ:* -180.02 (d, *J* = 47.2 Hz); **IR** (film, cm^{-1}) υ. 3024, 2929, 2845, 1708, 1243; **HRMS** (ESI) *m/z* calculated for $C_{10}H_{10}FO_2$ [M – H]$^-$ 181.06703, found, 181.06680.

2-(4-(*tert*-Butyl)phenyl)-2-fluoroacetic acid (4.33)[3]

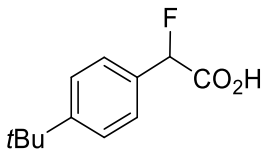

The title compound was prepared following General Procedure GP1 using (4-(tert-butyl)phenyl)boronic acid (53.4 mg, 0.3 mmol), ethyl bromofluoroacetate (67.2 µL, 0.6 mmol), Cs_2CO_3 (196 mg, 0.6 mmol), CuI (11.4 mg, 20 mol%) and 4,4′,4″-tri-*tert*-butyl-2,2′:6′,2″-terpyridine (24.1 mg, 20 mol%). The title compound (44.2 mg, 70% yield) was isolated as a white solid.

Physical appearance: White solid (yield: 70%). **^{1}H NMR** (400 MHz, $CDCl_3$**)** *δ*: 7.41 – 7.29 (m, 4H), 5.73 (d, *J* = 47.9 Hz, 1H), 1.25 (s, 9H); **^{13}C NMR** (101 MHz, $CDCl_3$) *δ*: 173.9 (d, *J* = 27.8 Hz), 153.3 (d, *J* = 2.0 Hz), 130.4 (d, *J* = 20.5 Hz), 126.6 (d, *J* = 5.7 Hz), 125.9, 88.7 (d,

J = 185.4 Hz), 34.8, 31.2; **^{19}F NMR** (376 MHz, $CDCl_3$) δ -179.1 (d, *J* = 48.2 Hz). The physical data were identical in all respects to those previously reported.[3]

2-Fluoro-2-(2-methoxyphenyl)acetic acid (4.34)[3]

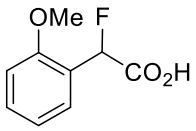

The title compound was prepared following General Procedure GP1 using (2-methoxyphenyl)boronic acid (45.6 mg, 0.3 mmol), ethyl bromofluoroacetate (67.2 µL, 0.6 mmol), Cs_2CO_3 (196 mg, 0.6 mmol), CuI (11.4 mg, 20 mol%) and 4,4′,4″-tri-*tert*-butyl-2,2′:6′,2″-terpyridine (16.6 mg, 20 mol%). The title compound (38.1 mg, 30% yield) was isolated as a white solid.

Physical appearance: White solid (yield: 30%). **^{1}H NMR** (400 MHz, $CDCl_3$) *δ*: 7.36 (t, *J* = 7.8 Hz, 1H), 7.05 (m, 1H), 7.02 (m, 1H), 6.99-6.94 (m, 1H), 5.84 (d, *J* = 46.9 Hz, 1H), 3.88 (s, 3H); **^{13}C NMR** (101 MHz, $CDCl_3$) *δ:* 173.66 (d*, J* = 28.8 Hz), 157.64 (d, *J* = 3.0 Hz), 132.17 (d, *J* = 2.8 Hz), 129.80 (d, *J* = 5.3 Hz), 122.62 (d, *J* = 19.2 Hz), 121.47 (d, *J* = 1.6 Hz), 111.81 (d, *J* = 1.0 Hz), 85.31 (d, *J* = 183.7 Hz), 56.27; **^{19}F NMR** (376 MHz, $CDCl_3$) *δ:* -178.49 (d, *J* = 46.4 Hz). The physical data were identical in all respects to those previously reported.[3]

1-(1-Fluoro-2-hydroperoxy-2l2-ethyl)-3-methoxybenzene (4.35)[2]

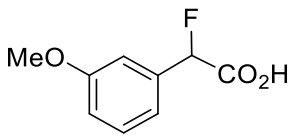

The title compound was prepared following General Procedure GP1 using (3-methoxyphenyl)boronic acid (45.6 mg, 0.3 mmol), ethyl bromofluoroacetate (67.2 µL, 0.6 mmol), Cs_2CO_3 (196 mg, 0.6 mmol), CuI (11.4 mg, 20 mol%) and 4,4',4''-tri-*tert*-butyl-2,2':6',2''-terpyridine (24.1 mg, 20 mol%). The title compound (32.6 mg, 56% yield) was isolated as a white solid.

Physical appearance: White solid (yield: 56%). **^{1}H NMR** (400 MHz, $CDCl_3$**)** δ: 7.52 (bs, 1H), 7.30 – 7.21 (m, 1H), 7.02 – 6.91 (m, 2H), 6.88 (ddt, *J* = 8.3, 2.3, 1.0 Hz, 1H), 5.72 (d, *J* = 47.9 Hz, 1H), 3.75 (s, 3H); **^{13}C NMR** (100 MHz, $CDCl_3$) δ: 173.6 (d, *J* = 27.5 Hz), 159.9, 134.8 (d, *J* = 20.4 Hz), 130.00, 118.9 (d, *J* = 6.2 Hz) 115.7 (d, *J* = 1.4 Hz), 111.8 (d, *J* = 6.3 Hz), 88.6 (d, *J* = 186.8 Hz), 55.3; **^{19}F NMR** (376 MHz, $CDCl_3$) δ -181.19 (d, *J* = 48.2 Hz). The physical data were identical in all respects to those previously reported.[2]

1-(1-Fluoro-2-hydroperoxy-2l2-ethyl)-4-(trifluoromethyl)benzene (4.36)

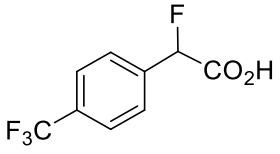

The title compound was prepared following General Procedure GP1 using (4-(trifluoromethyl)phenyl)boronic acid (57.0 mg, 0.3 mmol), ethyl bromofluoroacetate (67.2 µL, 0.6 mmol), Cs_2CO_3 (196 mg, 0.6 mmol), CuI (11.4 mg, 20 mol%) and 4,4',4''-tri-

tert-butyl-2,2′:6′,2″-terpyridine (24.1 mg, 20 mol%). The title compound (40.0 mg, 60% yield) was isolated as a yellow solid.

Physical appearance: Yellow solid (yield: 60%). **Mp:** 80 – 83 °C; **^{1}H NMR** (400 MHz, $CDCl_3$) δ: 7.66 – 7.51 (m, 4H), 5.83 (d, *J* = 47.1 Hz, 1H); **^{13}C NMR** (101 MHz, $CDCl_3$) *δ*: 173.2 (d, *J* =27.3 Hz), 133.5 – 131.1 (m), 127.7, 126.7 (d, *J* = 6.7 Hz), 125.9 (q, *J* = 3.8 Hz), 88.0 (d, *J* = 178.2 Hz); **^{19}F NMR** (376 MHz, $CDCl_3$) δ: -62.9 (s), -185.2 (d, *J* = 47.2 Hz); **IR** (neat, cm^{-1}) υ 2853, 1739, 1418, 1321, 1119, 1066. **HRMS** (ESI) *m/z* calculated for $C_9H_5F_4O_2$ $[M - H]^-$, 221.02312. found, 221.02290.

Ethyl 2-fluoro-2-(3-formyl-4-methoxyphenyl)acetate

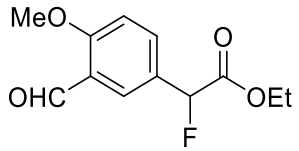

The title compound was prepared following General Procedure GP2 (3-formyl-4-methoxyphenyl)boronic acid (111.1 mg, 0.3 mmol), ethyl bromofluoroacetate (67.2 µL, 0.6 mmol), Cs_2CO_3 (196 mg, 0.6 mmol), CuI (11.4 mg, 20 mol%) and 4,4′,4″-tri-*tert*-butyl-2,2′:6′,2″-terpyridine (16.6 mg, 20 mol%).

Physical appearance: Colourless Oil. **^{1}H NMR** (400 MHz, $CDCl_3$) δ 10.45 (s, 1H), 7.91 (t, *J* = 2.0 Hz, 1H), 7.67 (ddd, *J* = 8.7, 2.5, 1.0 Hz, 1H), 7.05 (d, *J* = 8.6 Hz, 1H), 5.74 (d, *J* = 47.5 Hz, 1H), 4.33 – 4.16 (m, 2H), 3.96 (s, 3H), 1.25 (t, *J* = 7.1 Hz, 3H). **^{13}C NMR** (101 MHz, $CDCl_3$) δ 188.99, 168.25 (d, *J* = 27.9 Hz), 162.51 (d, *J* = 2.0 Hz), 134.05 (d, *J* = 5.4 Hz), 127.48 (d, *J* = 5.7 Hz), 126.84 (d, *J* = 21.5 Hz), 124.73, 112.29, 88.53 (d, *J* = 185.8 Hz), 61.97, 55.93, 14.04. **^{19}F NMR** (376 MHz, $CDCl_3$) δ -177.89 (d, *J* = 47.6 Hz). **IR** (neat, cm^{-1})

υ. 2921, 2159, 1978, 1758, 1644. **HRMS** (ESI) *m/z* calculated for $C_{12}H_{14}FO_4$ $[M + H]^+$, 241.0876, found, 241.0875.

2-Fluoro-2-(3-formyl-4-methoxyphenyl)acetic acid (4.37)

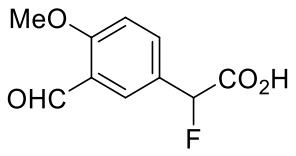

Physical appearance: yellow solid (yield: 53% based on two steps). **Mp**: Decomposes between 120 – 150 °C; **^{1}H NMR** (400 MHz, $CDCl_3$) δ 7.61 (s, 1H), 7.39 – 7.30 (m, 1H), 7.12 – 6.92 (m, 3H), 5.80 (d, *J* = 47.5 Hz, 1H), 3.83 (s, 3H); **^{13}C NMR** (101 MHz, $CDCl_3$) δ 173.58 (d, *J* = 27.9 Hz), 159.89, 134.77 (d, *J* = 20.5 Hz), 130.00, 118.91 (d, *J* = 6.3 Hz), 115.71 (d, *J* = 2.0 Hz), 111.84 (d, *J* = 6.6 Hz), 88.67 (d, *J* = 187.2 Hz), 55.37; **^{19}F NMR** (376 MHz, $CDCl_3$) δ -181.18 (d, *J* = 47.5 Hz); **IR** (film, cm^{-1}) υ. 2918, 2850, 1756, 1643, 1604, 1256, 1223; **HRMS** (ESI) *m/z* calculated for $C_{10}H_8FO_4$ $[M – H]^-$, 211.04121, Found, 211.04101.

2-(Dibenzo[b,d]furan-4-yl)-2-fluoroacetic acid (4.38)

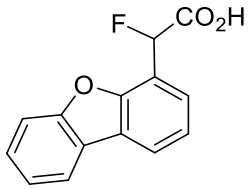

The title compound was prepared following General Procedure GP1 using dibenzo[b,d]furan-4-ylboronic acid (63.6 mg, 0.3 mmol), ethyl bromofluoroacetate (67.2 µL, 0.6 mmol), Cs_2CO_3 (196 mg, 0.6 mmol), CuI (11.4 mg, 20 mol%) and 4,4′,4″-tri-*tert*-butyl-2,2′:6′,2″-terpyridine (24.1 mg, 20 mol%). The title compound (38.1 mg, 52% yield) was isolated as a white solid.

Physical appearance: White solid (yield: 52%). **Mp**: 96 – 98 °C; **^{1}H NMR** (400 MHz, DMSO-d_6) δ: 13.70 (bs, 1H), 8.36 – 8.21 (m, 2H), 7.80 (d, *J* = 8.2 Hz, 1H), 7.69 – 7.43 (m, 4H), 6.51 (d, *J* = 48.2 Hz, 1H); **^{13}C NMR** (101 MHz, DMSO-d_6) δ: 169.6 (d, *J* = Hz), 155.9, 153.4 (d, *J* = 2.9 Hz), 128.6, 127.4 (d, *J* = 5.0 Hz Hz), 124.8, 123.9 (d, *J* = 0.9 Hz), 123.7, 123.2 (d, *J* = 2.8 Hz) 121.9, 119.6 (d, *J* = 20.1 Hz), 112.3, 85.1 (d, *J* = 179.4 Hz); **^{19}F NMR** (376 MHz, DMSO-d_6) δ: -176.0 (d, *J* = 48.5 Hz); **IR** (film, cm^{-1}) υ 3041, 1734, 1591, 1450, 743; **HRMS** (ESI) *m/z* calculated for $C_{14}H_8FO_3$ $[M - H]^-$, 243.04630. Found, 243.04589.

Ethyl 2-fluoro-2-(3-((5-(trifluoromethyl)pyridin-2-yl)oxy)phenyl)acetate

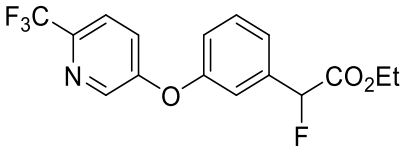

The title compound was prepared following General Procedure GP2 using (3-((5-(trifluoromethyl)pyridin-2-yl)oxy)phenyl)boronic acid (84.9 mg, 0.3 mmol), ethyl bromofluoroacetate (67.2 µL, 0.6 mmol), Cs_2CO_3 (196 mg, 0.6 mmol), CuI (11.4 mg, 20 mol%) and 4,4′,4″-tri-*tert*-butyl-2,2′:6′,2″-terpyridine (24.1 mg, 20 mol%).

Physical appearance: Yellow oil. **^{1}H NMR** (400 MHz, $CDCl_3$) δ 8.44 (dq, *J* = 2.8, 0.9 Hz, 1H), 7.96 – 7.91 (m, 1H), 7.48 (td, *J* = 7.9, 0.9 Hz, 1H), 7.40 – 7.35 (m, 1H), 7.32 – 7.29 (m, 1H), 7.21 (ddt, *J* = 8.1, 2.2, 1.0 Hz, 1H), 7.05 (dt, *J* = 8.6, 0.7 Hz, 1H), 5.81 (d, *J* = 47.6 Hz, 1H), 4.34 – 4.18 (m, 2H), 1.28 (t, *J* = 7.1 Hz, 3H); **^{13}C NMR** (101 MHz, $CDCl_3$) δ 168.09 (d, *J* = 27.0 Hz), 165.39 (d, *J* = 1.0 Hz), 153.39, 145.41 (q, *J* = 4.4 Hz), 136.83 (q, *J* = 3.2 Hz), 136.15 (d, *J* = 20.9 Hz), 124.97, 123.36 (d, *J* = 6.6 Hz), 122.55 (d, *J* = 1.9 Hz), 122.27, 121.86 (q, *J* = 34.3 Hz), 119.56 (d, *J* = 6.8 Hz), 111.57, 88.72 (d, *J* = 187.0 Hz), 62.03, 14.03; **^{19}F**

NMR (376 MHz, $CDCl_3$) δ -61.71, -182.11 (d, *J* = 47.6 Hz); **IR** (film, cm^{-1}) υ 3005, 1751, 1280, 1126, 1064; **HRMS** (ESI) *m/z* calculated for $C_{16}H_{14}F_4NO_3$ $[M + H]^+$ 344.09043, Found, 344.09054.

2-Fluoro-2-(3-((5-(trifluoromethyl)pyridin-2-yl)oxy)phenyl)acetic acid (4.39)

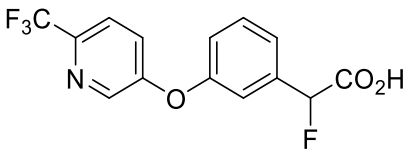

Physical appearance: White Solid (Yield = 70% based on two steps). **^{1}H NMR** (400 MHz, Methanol-d_4) δ 8.39 (s, 1H), 7.95 (d, *J* = 10.8 Hz, 1H), 7.67 – 7.52 (m, 4H), 6.88 (d, *J* = 8.6 Hz, 1H), 5.89 (d, *J* = 47.9 Hz, 1H), 3.95 (s, 3H). **^{13}C NMR** (101 MHz, $CDCl_3$) δ 170.27 (d, *J* = 27.5 Hz), 164.26, 152.25, 145.91 – 142.06 (m), 136.23 (q, *J* = 3.1 Hz), 134.61 (d, *J* = 20.8 Hz), 129.28, 123.81, 122.60 (d, *J* = 6.4 Hz), 121.77 (d, *J* = 1.7 Hz), 121.34 – 120.82 (m), 118.59 (d, *J* = 6.7 Hz), 110.83, 87.17 (d, *J* = 188.1 Hz), 28.68.**^{19}F NMR** (376 MHz, $CDCl_3$) δ -61.68 (s) -182.15 (d, *J* = 47.7 Hz); **IR** (film, cm^{-1}) υ 3735, 2361, 2341, 1748, 1329. **HRMS** (ESI) *m/z* calculated for $C_{14}H_8F_4NO_3$ $[M – H]^-$, 316.05913. Found, 316.05911.

Ethyl 2-(4-(2H-1,2,3-triazol-2-yl)phenyl)-2-fluoroacetate

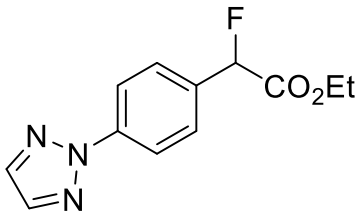

The title compound was prepared following General Procedure GP2 using (4-(2H-1,2,3-triazol-2-yl)phenyl)boronic acid (56.7 mg, 0.3 mmol), ethyl bromofluoroacetate (67.2 µL,

0.6 mmol), Cs_2CO_3 (196 mg, 0.6 mmol), CuI (11.4 mg, 20 mol %) and 4,4′,4″-tri-*tert*-butyl-2,2′:6′,2″-terpyridine (16.6 mg, 20 mol %).

Physical appearance: Colourless oil. **^{1}H NMR** (400 MHz, Methanol-d_4) δ 8.17 – 8.10 (m, 2H), 7.93 (s, 2H), 7.65 – 7.59 (m, 2H), 5.98 (d, *J* = 47.2 Hz, 1H), 4.40 – 4.10 (m, 2H), 1.23 (t, *J* = 7.1 Hz, 3H). **^{13}C NMR** (101 MHz, Methanol-d_4) δ 170.00 (d, *J* = 28.0 Hz), 137.32, 135.39 (d, *J* = 20.6 Hz), 129.14 (d, *J* = 6.2 Hz), 120.04, 89.90 (d, *J* = 183.6 Hz), 62.99, 14.31. **^{19}F NMR** (376 MHz, Methanol-d_4) δ -180.95 (d, *J* = 47.2 Hz). **IR** (neat, cm^{-1}) υ 1935, 1556, 1138, 1096; **HRMS** (ESI) *m/z* calculated for $C_{12}H_{13}FN_3O_2$ $[M + H]^+$ for 250.09863, Found, 250.09874.

2-(4-(2H-1,2,3-Triazol-2-yl)phenyl)-2-fluoroacetic acid (4.40)

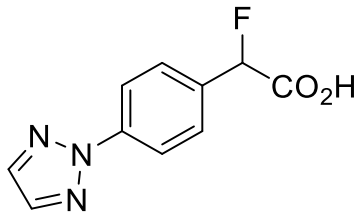

Physical appearance: White solid (yield: 40%, based on two steps). **Mp:** 140 – 142 °C; **^{1}H NMR** (500 MHz, Acetonitrile-d_3) δ 8.30 (d, *J* = 8.0 Hz, 2H), 8.09 (s, 2H), 7.82 – 7.75 (m, 2H), 6.12 (d, *J* = 47.2 Hz, 1H); **^{13}C NMR** (101 MHz, Methanol-d_4) δ 170.41 (d, *J* = 27.4 Hz), 140.35, 135.86, 134.42 (d, *J* = 20.7 Hz), 127.67 (d, *J* = 5.8 Hz), 118.57, 88.45 (d, *J* = 182.8 Hz); **^{19}F NMR** (470 MHz, Acetonitrile-d_3) δ -178.45 (d, *J* = 47.2 Hz); **IR** (neat, cm^{-1}) υ 2849, 1736, 1118, 1066; **HRMS** (ESI) *m/z* calculated for $C_{10}H_7FN_3O_2$ $[M - H]^-$, 220.05278, Found, 220.05232.

Ethyl 2-(3-(3,5-dimethyl-1H-pyrazol-1-yl)phenyl)-2-fluoroacetate

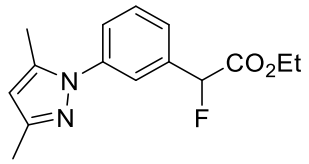

The title compound was prepared following General Procedure GP2 using (3-(3,5-dimethyl-1H-pyrazol-1-yl)phenyl)boronic acid (64.8 mg, 0.3 mmol), ethyl bromofluoroacetate (67.2 µL, 0.6 mmol), Cs_2CO_3 (196 mg, 0.6 mmol), CuI (11.4 mg, 20 mol %) and 4,4′,4″-tri-*tert*-butyl-2,2′:6′,2″-terpyridine (16mg, 20 mol %).

Physical appearance: Colourless oil. **^{1}H NMR** (500 MHz, $CDCl_3$) δ 7.56 (dt, *J* = 2.5, 1.2 Hz, 1H), 7.53 – 7.47 (m, 2H), 7.48 – 7.43 (m, 1H), 6.02 (s, 1H), 5.83 (d, *J* = 47.5 Hz, 1H), 4.33 – 4.17 (m, 2H), 2.34 – 2.28 (m, 6H), 1.27 (t, *J* = 7.1 Hz, 3H). **^{13}C NMR** (126 MHz, $CDCl_3$) δ 168.53 (d, *J* = 27.2 Hz), 149.78, 140.71, 139.86, 135.71 (d, *J* = 20.7 Hz), 129.92, 125.97 (d, *J* = 1.9 Hz), 125.38 (d, *J* = 6.4 Hz), 123.06 (d, *J* = 6.7 Hz), 107.80, 89.21 (d, *J* = 186.9 Hz), 62.45, 14.45, 13.90, 12.86. **^{19}F NMR** (470 MHz, $CDCl_3$) δ -181.63 (d, *J* = 47.6 Hz). **IR** (film, cm^{-1}) υ 1935, 1710, 1201; **HRMS** (ESI) *m/z* calculated for $C_{15}H_{17}FN_2O_2$ $[M + H]^+$ for 277.13468, Found, 277.13473.

2-(3-(3,5-Dimethyl-1H-pyrazol-1-yl)phenyl)-2-fluoroacetic acid (4.41)

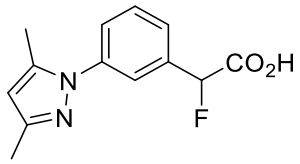

Physical appearance: White solid (yield: 60%, based on two steps). **Mp**: 122 – 125 °C; **^{1}H NMR** (400 MHz, Methanol-d_4) δ 7.61 – 7.53 (m, 3H), 7.51 (d, *J* = 2.6 Hz, 1H), 6.09 (1, 1H), 5.97 (d, *J* = 47.6 Hz, 1H), 2.28 (s, 3H), 2.25 (s, 3H); **^{13}C NMR** (101 MHz, Methanol-d_4) δ 170.18 (d, *J* = 26.8 Hz), 149.30, 140.51, 139.63, 136.58 (d, *J* = 20.7 Hz), 129.38, 126.70 – 125.12 (m), 122.97, 106.80, 88.39 (d, *J* = 183.4 Hz), 11.76, 10.76; **^{19}F NMR** (376 MHz, Methanol-d_4) δ -181.91 (d, *J* = 47.7 Hz); **IR** (film, cm^{-1}) υ 2917, 2849, 1745, 1148; **HRMS** (ESI) *m/z* calculated for $C_{13}H_{14}FN_2O_2$ $[M + H]^+$, 249.10338, Found, 249.10327.

Ethyl 2-fluoro-2-(4-(5-(p-tolyl)-3-(trifluoromethyl)-1H-pyrazol-1-yl)phenyl)acetate

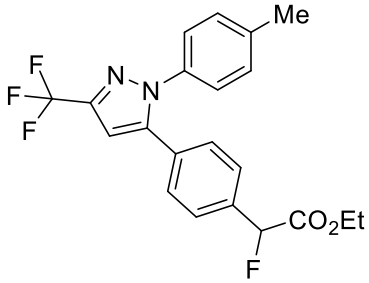

The title compound was prepared following General Procedure GP2 (4-(1-(p-tolyl)-3-(trifluoromethyl)-1H-pyrazol-5-yl)phenyl)boronic acid (104 mg, 0.3 mmol), ethyl bromofluoroacetate (67.2 µL, 0.6 mmol), Cs_2CO_3 (196 mg, 0.6 mmol), CuI (11.4 mg, 20 mol%) and 4,4′,4″-tri-*tert*-butyl-2,2′:6′,2″-terpyridine (16.6 mg, 20 mol%).

Physical appearance: Colourless Oil. **^{1}H NMR** (500 MHz, $CDCl_3$) δ 7.52 – 7.47 (m, 2H), 7.42 – 7.37 (m, 2H), 7.17 (d, *J* = 8.1 Hz, 2H), 7.14 – 7.12 (m, 2H), 6.75 (s, 1H), 5.82 (d, *J* = 47.6 Hz, 1H), 4.27 (qq, *J* = 10.8, 7.1 Hz, 2H), 2.39 (s, 3H), 1.28 (t, *J* = 7.1 Hz, 3H); **^{13}C NMR** (126 MHz, $CDCl_3$) δ 167.99 (d, *J* = 27.2 Hz), 144.92, 144.26 – 142.70 (m), 140.22 (d, *J* = 2.4 Hz), 139.37, 134.30 (d, *J* = 20.9 Hz), 129.53, 128.68, 127.28 (d, *J* = 6.4 Hz), 125.60, 124.69 – 117.40 (m), 105.69 (d, *J* = 2.4 Hz), 88.64 (d, *J* = 186.8 Hz), 62.09, 29.72, 21.32, 14.03; **^{19}F NMR** (470 MHz, $CDCl_3$) δ -62.33, -181.94 (d, *J* = 48.7 Hz); **IR** (film, cm^{-1}) υ 2985, 1759, 1235, 1131; **HRMS** (ESI) *m/z* calculated for $C_{21}H_{19}F_4N_2O_2$ $[M + H]^+$, 407.13772, Found, 407.13719

2-Fluoro-2-(4-(5-(p-tolyl)-3-(trifluoromethyl)-1H-pyrazol-1-yl)phenyl)acetic acid (4.42)

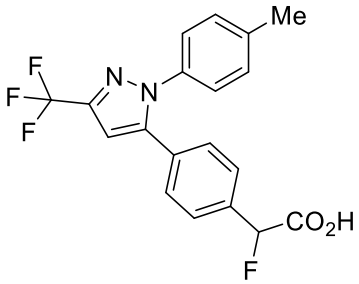

Physical appearance: White solid (yield: 41%, based on two steps). **Mp**: 148 – 152 °C. **^{1}H NMR** (400 MHz, Methanol-d_4) δ 7.46 – 7.40 (m, 2H), 7.31 – 7.24 (m, 2H), 7.09 – 7.02 (m, 4H), 6.77 (s, 1H), 5.82 (d, *J* = 47.6 Hz, 1H), 2.23 (s, 3H); **^{19}F NMR** (376 MHz, Methanol-d_4) δ -63.77, -181.72 (d, *J* = 47.9 Hz); **^{13}C NMR** (101 MHz, Methanol-d_4) δ 170.12 (d, *J* = 27.1 Hz), 145.49, -142.98 (q, *J* = 38.5 Hz), 139.96 (d, *J* = 2.3 Hz), 139.38, 135.72 (d, *J* = 20.6 Hz), 129.09, 128.59, 127.23 (d, *J* = 6.2 Hz), 125.92, 125.58, 121.31 (q, *J* = 290.3 Hz), 105.0, 88.30 (d, *J* = 183.4 Hz), 19.86; **IR** (film, cm^{-1}) υ 2918, 2360, 1748, 1510, 1475, 1456; **HRMS** (ESI) *m/z* calculated for $C_{19}H_{14}F_4N_2O_2$ $[M + H]^+$, 379.10642, Found, 379.10639.

2-Fluoro-2-(4-(4-((1-isopropoxy-2-methyl-1-oxopropan-2-yl)oxy)benzoyl)phenyl)acetic acid (4.43)

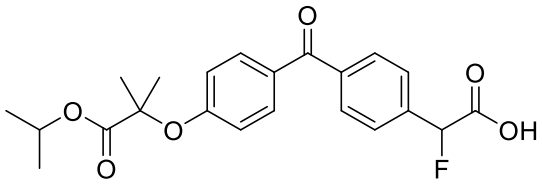

The title compound was prepared following General Procedure GP2 using (4-(4-((1-isopropoxy-2-methyl-1-oxopropan-2-yl)oxy)benzoyl)phenyl)boronic acid (111.1 mg, 0.3 mmol), ethyl bromofluoroacetate (67.2 µL, 0.6 mmol), Cs_2CO_3 (196 mg, 0.6 mmol), CuI (11.4 mg, 20 mol%) and 4,4′,4″-tri-*tert*-butyl-2,2′:6′,2″-terpyridine (16.6 mg, 20 mol%). The title compound (60.4 mg, 72% yield) was isolated as a brown solid.

Physical appearance: brown solid (yield: 72%). **Mp**: 140 – 142 °C; **^{1}H NMR** (400 MHz, $CDCl_3$) *δ*: 7.69 (dd, *J* = 8.4, 4.2 Hz, 4H), 7.52 (d, *J* = 7.9 Hz, 2H), 6.78 (d, *J* = 8.4 Hz, 2H), 5.82 (d, *J* = 47.5 Hz, 1H), 5.00 (m, 1H), 1.59 (s, 6H), 1.13 (d, *J* = 6.2 Hz, 6H); **^{13}C NMR** (101 MHz, $CDCl_3$) *δ:* 195.41, 173.17, 171.80 (d, *J* = 28.9 Hz), 160.05, 139.18, 137.31 (d, *J* = 20.4 Hz), 132.32, 130.09, 129.87, 126.27 (d, *J* = 6.6 Hz), 117.24, 88.35 (d, *J* = 188.8 Hz), 79.48, 69.49, 25.36, 21.51; **^{19}F NMR** (376 MHz, $CDCl_3$) *δ:* -183.28 (d, *J* = 47.8 Hz); **IR** (film, cm^{-1}) υ. 2985, 2361, 1718, 1558, 1503, 1252, 1146, 680; **HRMS** (ESI) *m/z* calculated for $[M + H]^+$, 403.15514, Found, 403.15535.

2-(3-Bromophenyl)-2-fluoroacetic acid (4.44)

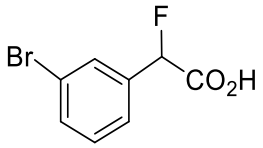

The title compound was prepared following General Procedure GP1 using (3-bromophenyl)boronic acid (60.2 mg, 0.3 mmol), ethyl bromofluoroacetate (67.2 µL, 0.6 mmol), Cs_2CO_3 (196 mg, 0.6 mmol), CuI (11.4 mg, 20 mol%) and 4,4′,4″-tri-*tert*-butyl-2,2′:6′,2″-terpyridine (16.6 mg, 20 mol%). The title compound (35.0 mg, 58% yield) was isolated as a brown solid.

Physical appearance: Brown Solid (yield: 58%). **Mp**: 81 – 83 °C; **^{1}H NMR** (400 MHz, $CDCl_3$**)** *δ*: 10.10 (bs, 1H), 7.56 (d, *J* = 2.0 Hz, 1H), 7.47 (dd, *J* = 8.0, 2.0 Hz, 1H), 7.34 (dd, *J* = 7.8, 1.5 Hz, 1H), 7.21 (t, *J* = 7.9 Hz, 1H), 5.71 (d, *J* = Hz, H); **^{13}C NMR** (100 MHz, $CDCl_3$) *δ*: 173.7 (d, *J* =27.3 Hz), 135.4 (d, *J* = 21.2 Hz), 133.0 (d, *J* = 2.1 Hz), 130.5, 129.5 (d, *J* =7.1 Hz), 125.1 (d, *J* = 6.0 Hz), 122.9, 87.3 (d, *J* = 178.3 Hz); **^{19}F NMR** (376 MHz, $CDCl_3$) δ -183.16 (d, *J* = 47.1 Hz); **IR** (film, cm^{-1}) υ 3035, 1759, 1689, 156, 818; **HRMS** (ESI) *m/z* calculated for $C_8H_5BrFO_2$ $[M - H]^-$, 230.94624. Found, 230.94586.

2-(4-Bromophenyl)-2-fluoroacetic acid (4.45)[3]

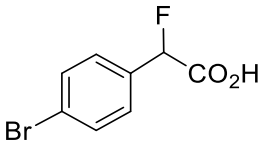

The title compound was prepared following General Procedure GP1 using (4-bromophenyl)boronic acid (60.3 mg, 0.3 mmol), ethyl bromofluoroacetate (67.2 µL, 0.6 mmol), Cs_2CO_3 (196 mg, 0.6 mmol), CuI (11.4 mg, 20 mol%) and 4,4′,4″-tri-*tert*-butyl-

2,2′:6′,2″-terpyridine (24.1 mg, 20 mol%). The title compound (36.3 mg, 52% yield) was isolated as a brown solid.

Physical appearance: Brown solid (yield: 52%). **^{1}H NMR** (400 MHz, $CDCl_3$**)** δ: 10.44 (bs, 1H), 7.58 (d, *J* = 8.2 Hz, 2H), 7.38 (d, *J* = 8.2 Hz, 2H), 5.80 (d, *J* = 47.2 Hz, 1H); **^{13}C NMR** (100 MHz, $CDCl_3$) δ: 173.8 (d, *J* = 27.4 Hz), 132.4 (d, *J* = 21.1 Hz), 132.1, 128.2 (d, *J* = 6.1 Hz), 124.3 (d, *J* = 2.9 Hz), 88.2 (d, *J* = 175.4 Hz); **^{19}F NMR** (376 MHz, $CDCl_3$) δ -182.3 (d, *J* = 47.2 Hz). The physical data were identical in all respects to those previously reported.[3]

2-Fluoro-2-(3-iodophenyl)acetic acid (4.46)

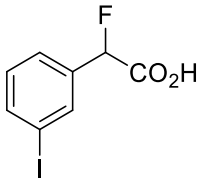

The title compound was prepared following General Procedure GP1 (3-iodophenyl)boronic acid (74.4 mg, 0.3 mmol), ethyl bromofluoroacetate (67.2 µL, 0.6 mmol), Cs_2CO_3 (196 mg, 0.6 mmol), CuI (11.4 mg, 20 mol%) and 4,4′,4″-tri-*tert*-butyl-2,2′:6′,2″-terpyridine (16.6 mg, 20 mol%). The title compound (42.0 mg, 50% yield) was isolated as a white solid.

Physical appearance: White Solid (yield: 50%). **Mp**: 102 – 104 °C; **^{1}H NMR** (400 MHz, Methanol-d_4) δ 7.83 (s, 1H), 7.77 (d, *J* = 8.7 Hz, 1H), 7.48 (d, *J* = 6.8 Hz, 1H), 7.19 (t, *J* = 7.8 Hz, 1H), 5.83 (d, *J* = 47.6 Hz, 1H). **^{13}C NMR** (101 MHz, Methanol-d_4) δ 171.6 (d, *J* = 27.4 Hz), 139.7, 138.8 (d, *J* = 20.6 Hz), 136.7 (d, *J* = 6.4 Hz), 127.1 (d, *J* = 6.1 Hz), 89.5 (d, *J* = 183.2 Hz); **^{19}F NMR** (376 MHz, Methanol-d_4) δ -181.77 (d, *J* = 47.8 Hz); **IR** (film, cm^{-1})

υ 3021, 2613, 1689, 1766, 1703; **HRMS** (ESI) *m/z* calculated for $C_8H_5FIO_2$ $[M - H]^-$ for 278.93237, Found, 278.93228.

2-Fluoro-2-(m-tolyl)acetic acid (4.47)[4]

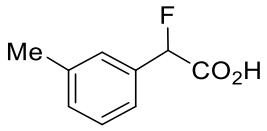

The title compound was prepared following General Procedure GP1 using m-tolylboronic acid (40.8 mg, 0.3 mmol), ethyl bromofluoroacetate (67.2 µL, 0.6 mmol), Cs_2CO_3 (196 mg, 0.6 mmol), CuI (11.4 mg, 20 mol%) and 4,4′,4″-tri-*tert*-butyl-2,2′:6′,2″-terpyridine (24.1 mg, 20 mol%). The title compound (36.3 mg, 74% yield) was isolated as a white solid.

Physical appearance: White solid (yield: 74%). **^{1}H NMR** (400 MHz, $CDCl_3$**)** *δ*: 10.16 (bs, 1H), 7.26 – 7.12 (m, 4H), 5.70 (d, *J* = 48.8 Hz, 1H), 2.30 (s, 3H); **^{13}C NMR** (100 MHz, $CDCl_3$) *δ*: 174.4 (d, *J* = 28.1 Hz), 138.8, 133.3 (d, *J* = 20.1 Hz), 130.8 (d, *J* = 2.4 Hz), 128.8, 127.3 (d, *J* = 6.1 Hz), 123.9 (d, *J* = 6.3 Hz), 88.9 (d, *J* = 186.2 Hz), 21.4; **^{19}F NMR** (376 MHz, $CDCl_3$) δ -180.3 (d, *J* = 48.9 Hz). The physical data were identical in all respects to those previously reported.[4]

2-Fluoro-4-(p-tolyl)acetic acid (4.48)[4]

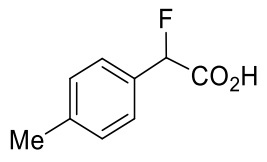

The title compound was prepared following General Procedure GP1 using p-tolylboronic acid (40.8 mg, 0.3 mmol), ethyl bromofluoroacetate (67.2 µL, 0.6 mmol), Cs_2CO_3 (196 mg, 0.6 mmol), CuI (11.4 mg, 20 mol%) and 4,4′,4″-tri-*tert*-butyl-2,2′:6′,2″-terpyridine (24.1 mg, 20 mol%). The title compound (36.3 mg, 72% yield) was isolated as a white solid.[3]

Physical appearance: White solid (yield: 72%). **^{1}H NMR** (400 MHz, $CDCl_3$**)** δ: 7.11 (d, 2H), 7.30 (d, 2H), 5.45 (d, *J* = 47.6 Hz, 1H), 2.15 (s, 3H); **^{19}F NMR** (376 MHz, $CDCl_3$) δ: 178.4 (d, *J* = 47.4 Hz); The physical data were identical in all respects to those previously[4]

2-Fluoro-2-(o-tolyl)acetic acid (4.49)[5]

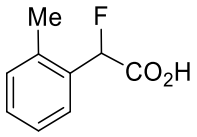

The title compound was prepared following General Procedure GP1 using o-tolylboronic acid (40.8 mg, 0.3 mmol), ethyl bromofluoroacetate (67.2 µL, 0.6 mmol), Cs_2CO_3 (196 mg, 0.6 mmol), CuI (11.4 mg, 20 mol%) and 4,4′,4″-tri-*tert*-butyl-2,2′:6′,2″-terpyridine (24.1 mg, 20 mol%). The title compound (15.1 mg, 30% yield) was isolated as a white solid.

Physical appearance: White solid (yield: 30%). **^{1}H NMR** (400 MHz, $CDCl_3$**)** δ: 7.18-7.28 (m, 4H), 5.48 (d, *J* = 48.2 Hz, 1H,), 2.28 (t, 3H); **^{19}F NMR** (376 MHz, $CDCl_3$) δ: 178.8 (d, *J* = 48.4 Hz). The physical data were identical in all respects to those previously reported.[5]

2-Fluoro-2-phenylacetic acid (4.50)[2]

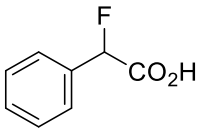

The title compound was prepared following General Procedure GP1 using phenylboronic acid (36.6 mg, 0.3 mmol), ethyl bromofluoroacetate (67.2 µL, 0.6 mmol), Cs_2CO_3 (196 mg, 0.6 mmol), CuI (11.4 mg, 20 mol%) and 4,4′,4″-tri-*tert*-butyl-2,2′:6′,2″-terpyridine (24.1 mg, 20 mol%). The title compound (27.3 mg, 59% yield) was isolated as a white solid.

Physical appearance: White solid (yield: 59%). **^{1}H NMR** (400 MHz, $CDCl_3$**)** δ: 8.67 (bs, 1H), 7.46 – 7.31 (m, 5H), 5.75 (d, *J* = Hz, 1H); **^{13}C NMR** (100 MHz, $CDCl_3$) δ: 173.8 (d, *J* = 27.8 Hz), 133.4 (d, *J* = 20.6 Hz), 130.0 (d *J* = 2.2 Hz), 128.9, 126.7 (d, *J* = 5.9 Hz), 88.8 (d, *J* = 186.8 Hz); **^{19}F NMR** (376 MHz, $CDCl_3$) δ -180.8 (d, *J* = 47.5 Hz). The physical data were identical in all respects to those previously reported.[2]

Ethyl 2-diazo-2-(4-(6-methoxypyridin-3-yl)phenyl)acetate

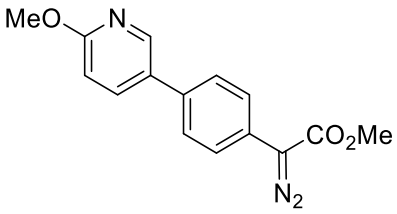

To a mixture of methyl 2-(4-(6-methoxypyridin-3-yl)phenyl)acetate (10 mmol, 1 equiv.) and *p*-ABSA (12 mmol, 1.2 equiv.) in anhydrous MeCN (30 mL), DBU (14 mmol, 1.4 equiv.) was added at 0^{o}C. Th reaction mixture was stirred at r.t overnight. Upon the complete consumption of the starting materials, the reaction mixture was diluted with distilled water (20 mL), followed by extraction with Et_2O (3 × 10 mL). After washing with

10% NH_4Cl solution (3×10 mL) and brine (3×10 mL), the combined organic extracts were dried over $MgSO_4$, concentrated and chromatographed EtOAc:Hexane (10:90) to yield the diazoester.

Physical appearance: Orange solid. **Mp:** 135 – 137 °C; **^{1}H NMR** (400 MHz, $CDCl_3$**)** δ: 8.39 (dd, *J* = 2.7, 0.8 Hz, 1H), 7.79 (dd, *J* = 8.6, 2.6 Hz, 1H), 7.56 (bs, 4H), 6.82 (dd, *J* = 8.6, 0.7 Hz, 1H), 3.98 (s, 3H), 3.89 (s, 3H). **^{13}C NMR** (100 MHz, $CDCl_3$) δ: 165.5, 163.7, 144.8, 137.2, 135.4, 129.3, 127.1, 124.5, 124.5, 110.9, 53.6, 52.1. **IR** (film, cm^{-1}) υ 3012, 2951, 2094, 1686, 1160, 815. **HRMS** (ESI) *m/z* calculated for $C_{15}H_{14}N_3O_3$ $[M + H]^+$, 284.10297 Found, 284.10294.

Methyl 2-fluoro-2-(4-(6-methoxypyridin-3-yl)phenyl)acetate

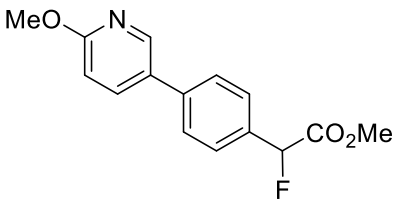

In a 20 mL falcon tube was charged with methyl 2-diazo-2-(4-(6-methoxypyridin-3-yl)phenyl)acetate (0.3 mmol) in 2mL of DCM and cooled to 0^{o}C. HF pyridine (70 %) (0.36 mmol) was then added slowly. The reaction was temperature was raised to r.t after gas evolution. The reaction was monitored by TLC until completion. The reaction was then quenched with $NaHCO_3$ and the organic layer was extracted with DCM (3 x 5 mL). The organic layer was dried over $MgSO_4$, concentrated and chromatographed EtOAc:Hexane (10:90).

Physical appearance: White solid. **Mp:** 64 – 65 °C; **^{1}H NMR** (400 MHz, $CDCl_3$**)** δ: 8.32 (dd, *J* = 2.6, 0.8 Hz, 1H), 7.71 (dd, *J* = 8.6, 2.6 Hz, 1H), 7.54 – 7.43 (m, 4H), 6.76 (dd, *J* = 8.6, 0.7 Hz, 2H), 5.76 (d, *J* = 48.2 Hz, 1H), 3.92 (s, 3H), 3.74 (s, 3H); **^{13}C NMR** (100 MHz, $CDCl_3$) δ: 168.9 (d, *J* = 27.2 Hz), 163.9, 145.1, 139.4 (d, *J* = 3.2 Hz), 137.4, 133.1 (d, *J* =20.0 Hz), 129.2, 127.3 (d, *J* = 6.2 Hz), 127.1, 111.0, 89.1 (d, *J* = 184.3 Hz), 53.6, 52.8; **^{19}F NMR** (376 MHz, $CDCl_3$) δ -179.9 (d, *J* = 48.2 Hz); **IR** (film, cm^{-1}) υ 3014, 2949, 1498, 1195, 822; **HRMS** (ESI) *m/z* calculated for $C_{15}H_{15}FNO_3$ $[M + H]^+$, 276.10305. Found, 276.10293.

2-Fluoro-2-(4-(6-methoxypyridin-3-yl)phenyl)acetic acid

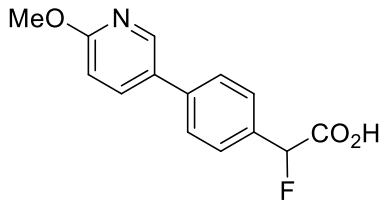

In a 50 mL round bottom flask, methyl 2-fluoro-2-(4-(6-methoxypyridin-3-yl)phenyl)acetate (5 mmol, 1.0 equiv.) was added to a mixture of MeOH (15 mL, 0.3 M) and 1 M K_2CO_3 aq. (15 mL) and stirred at r.t until TLC showed consumption of starting material. The reaction was then poured into 1 M HCl aq. to acidify to pH 5, and the aqueous phase was extracted with Et_2O (3 × 10 mL), washed with brine (10 mL), dried over $MgSO_4$. The resulting gum was then washed with pentane, until a white free-flowing white solid formed.

Physical appearance: White solid (yield: 45% (over 3 steps)). **Mp:** 150 – 153 °C; **^{1}H NMR** (400 MHz, Methanol-d_4) δ: 8.44 – 8.38 (m, 1H), 7.97 (dd, *J* = 8.7, 2.5 Hz, 1H), 7.66 (d, *J* = 8.0 Hz, 2H), 7.58 (d, *J* = 8.0 Hz, 2H), 6.90 (d, *J* = 8.6 Hz, 1H), 5.91 (d, *J* = 48.7 Hz, 1H), 3.97 (s, 3H); **^{13}C NMR** (100 MHz, Methanol-d_4) δ: 170.8 (d, *J* = 27.9 Hz), 163.9, 144.5, 138.7

(d, *J* = 2.1 Hz), 134.3 (d, *J* = 20.1 Hz), 127.2 (d, *J* = 6.1 Hz), 126.5, 110.4, 88.8 (d, *J* = 180.2 Hz), 52.8; **^{19}F NMR** (376 MHz, Methanol-d_4) -179.6 (d, *J* = 47.9 Hz); **IR** (film, cm^{-1}) υ 2360, 1736, 1607, 1041, 825; **HRMS** (ESI) *m/z* calculated for $C_{14}H_{13}FNO_3$ $[M + H]^+$ 262.08740 Found, 262.08731.

2-Fluoro-2-(6-methoxynaphthalen-2-yl)acetic acid

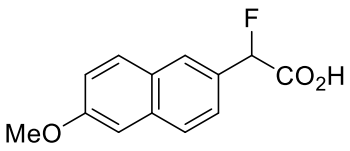

An oven-dried Schlenk tube containing a magnetic stir bar was charged with $Pd(OAc)_2$ (5.6 mg, 0.025 mmol, 5 mol%), PPh_3 (26.2 mg, 0.10 mmol, 20 mol%), boronic acid (1.0 mmol, 2.0 equiv.), and $K_3PO_4 \cdot 3\ H_2O$ (400 mg, 1.5 mmol, 3.0 equiv.). The Schlenk tube was sealed with a rubber septum and then evacuated and backfilled with N_2 three times. Toluene (5.0 mL) was added through the septum via syringe and the resulting mixture was stirred at r.t for 5 min. Ethyl *α*-bromo-*α*-fluoroacetate (92.5 mg, 0.50 mmol, 1.0 equiv.) was then added dropwise via syringe. The Schlenk tube was sealed and the mixture was heated at 100 °C with vigorous stirring for 3 h. The mixture was then allowed to cool to r.t and quenched with H_2O (10 mL). The layers were separated and the aqueous phase was extracted with EtOAc (3 × 5 mL). The combined organic phases were washed with brine (20 mL), dried with $MgSO_4$, filtered, and concentrated. The crude product was purified by flash chromatography (silica gel (Pentane–EtOAc, 50:1) to give the title the ester product. The ester was then dissolved in a 2:1 MeOH and aqueous K_2CO_3 (5-10 equiv.) mixture before it was left to stir at r.t until all the ester had been consumed (determined by TLC). The resulting mixture was then acidified using HCl (5 M) to pH = 2. The aqueous layer was then extracted with Et_2O (3 x 20 mL) and washed with Brine (2 x 20 mL). The organic extracts were dried using $MgSO_4$ and were then concentrated under vacuum and washed with pentane, resulting in the title compound as a white solid.

Physical appearance: White solid (yield: 50% over two steps). **Mp**: 150 – 152 °C; **^{1}H NMR** (400 MHz, Methanol-d_4**)** δ: 7.78 (t, J = 2.0 Hz, 1H), 7.70 (t, J = 9.4 Hz, 2H), 7.40 (dd, J = 8.5, 1.8 Hz, 1H), 7.16 (d, J = 2.5 Hz, 1H), 7.07 (dd, J = 8.9, 2.5 Hz, 1H), 5.86 (d, 1H, J = 47.8 Hz), 3.82 (s, 3H); **^{13}C NMR** (100 MHz, Methanol-d_4) δ: 158.58, 135.19 (d, J = 1.8 Hz) 130.03 (d, J = 20.4 Hz), 129.29, 128.44, 127.12, 126.40 (d, J = 6.8 Hz) 123.95 (d, J = 5.1 Hz), 119.09, 105.32, 89.35 (d, J = 181.3 Hz) 54.39. **^{19}F NMR** (376 MHz, Methanol-d_4) δ: -177.22 (d, J = 48.0 Hz); **IR** (film, cm^{-1}) υ.3157, 1764, 1703, 1606. 1267, 1234, 1051, 1029, 815; **HRMS** (ESI) *m/z* calculated for $C_{13}H_{10}FO_3$ $[M - H]^-$ for 233.06195, Found, 233.06185.

2-Fluoro-2-(naphthalen-1-yl)acetic acid[3]

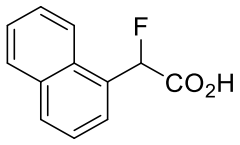

Step 1: A flame dried flask containing a solution of arylacetic acid (559 mg, 3.0 mmol, 1.0 equiv.) and TBSCl (1.04 g, 6.90 mmol, 2.3 equiv.) in THF (0.50 M) was cooled to 0 °C. LiHMDS (1.0 M in THF; 2.2 equiv.) was added slowly and the resulting mixture was stirred at 0 °C for 15 min and then warmed to r.t. It was then stirred at r.t over night before volatiles were removed in vacuo. The crude was taken up in hexane and solid LiCl was filtered off. The filtrate was washed with hexane and the combined organic fractions were concentrated to dryness in vacuo.

Step 2: The residue was dissolved in MeCN (0.50 M) and slowly added to a solution of Selectfluor (2.30 g, 6.50 mmol, 1.3 equiv.) in MeCN (30 mL) at r.t. After stirring for 15 min at r.t the reaction mixture was poured into aq. HCl (1.0 M, 10 mL/mmol acid). This

solution was extracted with Et_2O (2x) and the combined Et_2O layers were then extracted with NaOH (1.0 M; 2x). The combined aqueous layers were washed with Et_2O (2x), acidified with HCl (6.0 M) until pH = 1 and extracted with Et_2O (3x). The combined organic fractions were dried over $MgSO_4$ and concentrated to dryness in vacuo to give the desired aryl(fluoro)acetic acid. The title compound (817 mg, 80%) as a white solid.

Physical appearance: White solid (yield: 80%). **^{1}H NMR** (400 MHz, $CDCl_3$): δ = 9.55 (br s, 1H), 8.17 (d, *J* = 8.2 Hz, 1H), 7.96 -7.89 (m, 2H), 7.64 (d, *J* = 7.2 Hz, 1H), 7.61 -7.52 (m, 2H), 7.52 -7.47 (m, 1H), 6.42 (d, *J* = 46.8 Hz, 1H); **^{13}C NMR** (101 MHz, $CDCl_3$): δ = 174.3 (d, *J* = 28.6 Hz), 133.9, 130.8 (d, *J* = 2.2 Hz), 130.5 (d, *J* = 1.5 Hz), 129.3 (d, *J* = 18.3 Hz), 128.9, 127.2, 126.9 (d, *J* = 8.1 Hz), 126.3, 125.0, 123.5 (d, *J* = 1.5 Hz), 88.0 (d, *J* = 186.3 Hz); **^{19}F NMR** (376 MHz, $CDCl_3$): δ = -178.7 (d, *J* = 46.3 Hz); The physical data were identical in all respects to those previously reported.[3]

Ethyl 2-fluoro-2-(4-(1-(4-(methylsulfonyl)phenyl)-3-(trifluoromethyl)-1H-pyrazol-5-yl)phenyl)acetate

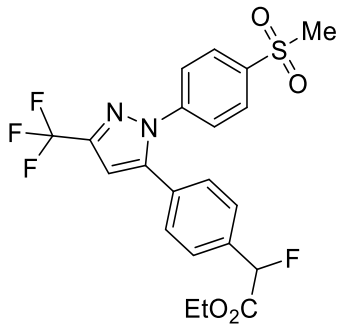

To a dry screw-cap tube equipped with a magnetic stirrer, 30 mg of 1-(4-(methylsulfonyl)phenyl)-1H-pyrazole (0.13 mmol, 1.1 equiv.), 1.5 mg of $Pd(OAc)_2$ (0.006 mmol, 5 mol%), 5 mg of L-proline (0.012 mmol, 10 mol%), 18 mg of K_2CO_3 (0.18 mmol,

1.5 equiv.), 17 mg of Ag_2CO_3 (0.06 mmol, 0.5 equiv.) and 4 mg of PivOH (0.04 mmol, 30 mol%) were added. After 3 cycles of vacuum/nitrogen, ethyl 2-fluoro-2-(4-iodophenyl)acetate (0.12 mmol, 1.0 eq.) and DMA (2 mL) were added. The tube was closed and stirred at 100 °C overnight. The reaction was cooled, diluted with a solution of saturated LiCl and extracted with Et_2O (3 x 10 mL), dried over $MgSO_4$. Solvent was removed under reduced pressure and the corresponding crude compound was purified using column chromatography (hexane/EtOAc = 7:3).

Physical appearance: Colourless oil (yield: 43%). **^{1}H NMR** (500 MHz, $CDCl_3$) δ 8.00 – 7.96 (m, 2H), 7.58 – 7.52 (m, 4H), 7.34 – 7.30 (m, 2H), 6.84 (s, 1H), 5.84 (d, *J* = 47.5 Hz, 1H), 4.36 – 4.25 (m, 2H), 3.10 (s, 3H), 1.31 (t, *J* = 7.1 Hz, 3H); **^{13}C NMR** (126 MHz, $CDCl_3$) δ 167.91 (d, *J* = 26.8 Hz), 144.98 – 144.30 (m), 144.24, 143.15, 140.19, 135.84 (d, *J* = 20.6 Hz), 129.68, 129.16, 128.70, 127.15 (d, *J* = 6.5 Hz), 125.73, 120.86 (q, *J* = 269.3 Hz), 107.13, 88.65 (d, *J* = 187.3 Hz), 62.22, 44.49, 14.09; **^{19}F NMR** (376 MHz, $CDCl_3$) δ -62.55 (s), -182.97 (d, *J* = 47.7 Hz). **IR** (film, cm^{-1}) υ 2985, 1756, 1151, 1096; **HRMS** (ESI) *m/z* calculated for: $C_{21}H_{18}F_4N_2O_4SNa$ $[M + Na]^+$, 493.08156, found, 493.08145.

2-Fluoro-2-(4-(1-(4-(methylsulfonyl)phenyl)-3-(trifluoromethyl)-1H-pyrazol-5-yl)phenyl)acetic acid

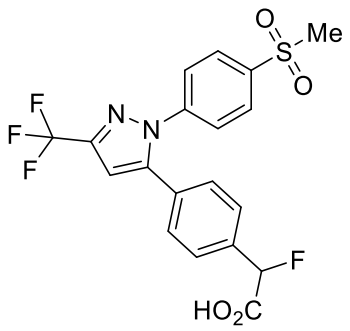

Ethyl 2-fluoro-2-(4-(1-(4-(methylsulfonyl)phenyl)-3-(trifluoromethyl)-1H-pyrazol-5-yl)phenyl)acetate (42 mg, 0.1 mmol, 1 equiv.) was dissolved in a 2:1 MeOH and aqueous K_2CO_3 (5 equiv.) (5 mL) mixture before it was left to stir at r.t until all the ester had been consumed (determined by TLC). The resulting mixture was then acidified using HCl (5 M) to pH = 2. The aqueous layer was then extracted with Et_2O (3 x 5 mL) and washed with Brine (2 x 5 mL). The organic extracts were dried using $MgSO_4$ and were then concentrated under vacuum and washed with pentane, resulting in the titled compound in 76% yield.

Physical appearance: White solid (yield 76%). **Mp =** 158 °C. **^{1}H NMR** (400 MHz, Methanol-d_4) δ 7.97 – 7.85 (m, 2H), 7.55 – 7.46 (m, 2H), 7.42 (dd, *J* = 8.2, 1.2 Hz, 2H), 7.32 – 7.20 (m, 2H), 5.79 (d, *J* = 47.7 Hz, 1H), 3.06 (s, 3H); **^{13}C NMR** (101 MHz, Methanol-d_4) δ 170.22 (d, *J* = 26.8 Hz), 144.89, 143.97 (t, *J* = 38.5 Hz), 143.08, 140.71, 136.65 (d, *J* = 20.5 Hz), 129.61 (d, *J* = 2.1 Hz), 129.11, 128.41, 126.96 (d, *J* = 6.1 Hz), 125.94, 122.52, 119.86, 106.43, 88.50 (d, *J* = 183.4 Hz), 42.77; **^{19}F NMR** (376 MHz, Methanol-d_4) δ -63.94,

-181.97 (d, *J* = 48.4 Hz). **IR** (film, cm^{-1}) υ 2919, 2361, 1749, 1136, 1095. **HRMS** (ESI) *m/z* calculated for $C_{19}H_{14}F_4N_2O_4SNa$ $[M + Na]^+$, 465.05026, found, 465.05000.

Synthesis of (difluoromethyl)arenes.

4-(Difluoromethyl)-1,1'-biphenyl (4.2)[3]

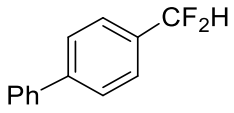

The title compound was prepared following General Procedure GP3 using 4-(difluoromethyl)-1,1'-biphenyl (55 mg, 0.3 mmol), DAST (73 mg, 0.45 mmol) and ethanol (few drops), in DCM (0.5 M). The title compound (48 mg, 78% yield) was isolated as a white solid.

Physical appearance: White solid (yield: 78 %). **^{1}H NMR** (400 MHz, $CDCl_3$**)** *δ*: 7.68 (d, *J* = 8.0 Hz, 2H), 7.64 – 7.55 (m, 4H), 7.47 (dd, *J* = 8.4, 6.8 Hz, 2H), 7.44 – 7.34 (m, 1H), 6.70 (t, *J* = 56.2 Hz, 1H); **^{19}F NMR** (376 MHz, $CDCl_3$) *δ* -110.35 (d, *J* = 55.9 Hz). The physical data were identical in all respects to those previously reported.[3]

1-(Difluoromethyl)-4-phenoxybenzene (4.65)[6]

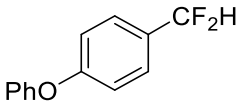

The title compound was prepared following General Procedure GP3 using 4-phenoxybenzaldehyde (59 mg, 0.3 mmol), DAST (73 mg, 0.45 mmol) and ethanol (few drops), in DCM (0.5 M). The title compound (28 mg, 43% yield) was isolated as a colourless oil.

Physical appearance: Colourless Oil (yield: 43%). **^{1}H NMR** (400 MHz, $CDCl_3$**)** δ: 7.39 (d, *J* = 8.2 Hz, 2H), 7.30 (t, *J* = 7.7 Hz, 2H), 7.09 (t, *J* = 7.4 Hz, 1H), 6.97 (d, *J* = 8.1 Hz, 4H), 6.55 (t, *J* = 58.3 Hz, 1H); **^{13}C NMR** (100 MHz, $CDCl_3$) δ: 159.6, 156.2, 130.0, 128.9 (t, *J* = 22.4 Hz) 127.3 (t, *J* = 6.1 Hz), 124.1, 119.6, 118.2, 114.6 (t, *J* = 235.8 Hz); **^{19}F NMR** (376 MHz, $CDCl_3$) δ: -109.0 (d, *J* = 56.4 Hz). The physical data were identical in all respects to those previously reported.[6]

1-(Difluoromethyl)-3,5-dimethylbenzene (4.66)[7]

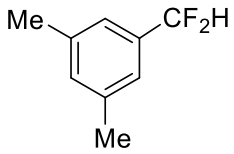

The title compound was prepared following General Procedure GP3 using 3,5-dimethylbenzaldehyde (40 mg, 0.3 mmol), DAST (73 mg, 0.45 mmol) and ethanol (few drops), in DCM (0.5 M). The title compound (25 mg, 54%) was isolated as a yellow oil

Physical appearance: Yellow Oil (yield: 54%). **^{1}H NMR** (400 MHz, $CDCl_3$) δ 7.12 (d, *J* = 5.4 Hz, 3H), 6.58 (t, *J* = 56.6 Hz, 1H), 2.37 (s, 6H); **^{19}F NMR** (376 MHz, $CDCl_3$) δ -110.17 (d, *J* = 56.6 Hz); **^{13}C NMR** (101 MHz, $CDCl_3$) δ 138.44, 132.27 (t, *J* = 2.1 Hz), 123.20 (t, *J* = 6.0 Hz), 114.99 (t, *J* = 238.4 Hz), 21.23. The physical data were identical in all respects to those previously reported.[7]

2-(Difluoromethyl)-1,4-dimethylbenzene (4.67)[6]

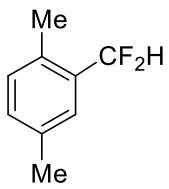

The title compound was prepared following General Procedure GP3 using 3,5-dimethylbenzaldehyde (40 mg, 0.3 mmol), DAST (73 mg, 0.45 mmol) and ethanol (few drops), in DCM (0.5 M). The title compound (20 mg, 43%) was isolated as yellow oil.

Physical appearance: Yellow oil (yield: 43%). **^{1}H NMR** (400 MHz, $CDCl_3$) δ 7.35 (s, 1H), 7.23 – 7.17 (m, 1H), 7.14 (d, *J* = 7.8 Hz, 1H), 6.76 (t, *J* = 55.6 Hz, 1H), 2.42 (s, 3H), 2.39 (s, 3H); **^{13}C NMR** (101 MHz, $CDCl_3$) δ 135.61, 133.01 (t, *J* = 4.6 Hz), 131.99 (t, *J* = 20.6 Hz), 131.21 (d, *J* = 2.2 Hz), 130.97, 126.35 (t, *J* = 7.3 Hz), 114.53 (t, *J* = 237.7 Hz), 20.91, 17.99. **^{19}F NMR** (376 MHz, $CDCl_3$) δ -112.87 (d, *J* = 56.0 Hz); The physical data were identical in all respects to those previously reported.[6]

1-(*tert*-Butyl)-4-(difluoromethyl)benzene (4.69)[6]

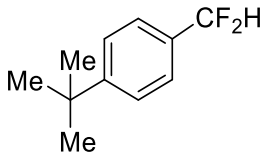

The title compound was prepared following General Procedure GP3 using 4-(tert-butyl)benzaldehyde (49 mg, 0.3 mmol), DAST (73 mg, 0.45 mmol) and ethanol (few drops), in DCM (0.5 M). The title compound (29 mg, 52%) was isolated as a colourless oil.

Physical appearance: Colourless oil (yield: 52%). **^{1}H NMR** (400 MHz, $CDCl_3$) δ 7.58 – 7.41 (m, 4H), 6.66 (t, *J* = 56.6 Hz, 1H), 1.36 (s, 9H); **^{19}F NMR** (376 MHz, $CDCl_3$) δ -109.87 (d, *J* = 56.6 Hz). The physical data were identical in all respects to those previously reported.[6]

1-(Difluoromethyl)-2-methoxybenzene (4.70)[3]

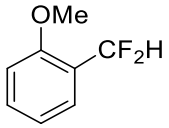

The title compound was prepared following General Procedure GP3 using 2-methoxybenzaldehyde (41 mg, 0.3 mmol), DAST (73 mg, 0.45 mmol) and ethanol (few drops), in DCM (0.5 M). The title compound (19 mg, 40%) was isolated as a yellow oil.

Physical appearance: Yellow oil (yield: 40%). **^{1}H NMR** (400 MHz, $CDCl_3$): δ = 7.59 (d, *J* = 7.3 Hz, 1H), 7.45 (t, *J* = 7.4 Hz, 1H), 7.06 (t, *J* = 7.4 Hz, 1H), 6.99 (t, *J* = 55.8 Hz, 1H), 6.96 (d, *J* = 8.5 Hz, 1H), 3.88 (s, 3H); **^{13}C NMR (**101 MHz, $CDCl_3$): δ =157.2 (t, *J* = 6.0 Hz), 131.9 (t, *J* = 1.8 Hz), 126.1 (t, *J* = 6.0 Hz), 122.6 (t, *J* = 22.2 Hz), 120.5, 111.6 (t, *J* = 234.9 Hz), 110.8, 55.5; **^{19}F NMR** (376 MHz, $CDCl_3$): δ = -115.3 (d, *J* = 55.9 Hz). The physical data were identical in all respects to those previously reported.[3]

1-(Difluoromethyl)-3-methoxybenzene (4.71)[3]

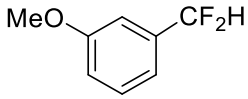

The title compound was prepared following General Procedure GP3 using 3-methoxybenzaldehyde (41 mg, 0.3 mmol), DAST (73 mg, 0.45 mmol) and ethanol (few drops), in DCM (0.5 M). The title compound (24 mg, 50%) was isolated as a colourless oil.

Physical appearance: Colourless Oil **(**yield = 50%) **^{1}H NMR** (400 MHz, $CDCl_3$) δ: δ = 7.38 (t, *J* = 7.9 Hz, 1H), 7.10 (d, *J* = 7.6 Hz, 1H), 7.06 (s, 1H), 7.03 (d, *J* = 8.4 Hz, 1H), 6.63 (t, *J* =

56.5 Hz, 1H), 3.85 (s, 3H); **^{13}C NMR** (101 MHz, $CDCl_3$): δ = 159.8, 135.7 (t, *J* = 22.0 Hz), 129.8, 117.8 (t, *J* = 6.2 Hz), 116.6 (t, *J* = 1.8 Hz), 114.6 (t, *J* = 239.2 Hz), 110.7 (t, *J* = 5.9 Hz), 55.3; **^{19}F NMR** (376 MHz, $CDCl_3$): δ = -110.7 (d, *J* = 55.9 Hz). The physical data were identical in all respects to those previously reported.[3]

1-(Difluoromethyl)-4-(trifluoromethyl)benzene (4.72)[6]

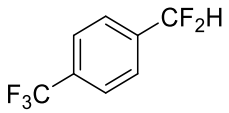

The title compound was prepared following General Procedure GP3 using 4-(trifluoromethyl)benzaldehyde (52 mg, 0.3 mmol), DAST (73 mg, 0.45 mmol) and ethanol (few drops), in DCM (0.5 M). The title compound (36 mg, 61%) was isolated as a colourless oil.

Physical appearance: Colourless oil (yield: 61%) **^{1}H NMR** (400 MHz, $CDCl_3$) δ 7.65 (d, *J* = 8.1 Hz, 2H), 7.56 (d, *J* = 8.1 Hz, 2H), 6.62 (t, *J* = 56.0 Hz, 1H); **^{13}C NMR** (101 MHz, $CDCl_3$) δ 137.79 (d, *J* = 1.4 Hz), 132.85 (d, *J* = 32.7 Hz), 126.08 (t, *J* = 6.1 Hz), 125.78 (q, *J* = 3.8 Hz), 122.61 (q, *J* = 271.5 Hz), 113.70 (t, *J* = 240.0 Hz); **^{19}F NMR** (376 MHz, $CDCl_3$) δ -63.04 (s), -112.37 (d, *J* = 55.8 Hz); The physical data were identical in all respects to those previously reported.[6]

5-(Difluoromethyl)-2-methoxybenzaldehyde (4.68)

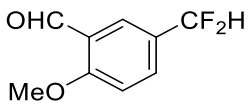

To a mixture of 2-bromo-4-(difluoromethyl)-1-methoxybenzene (450 mg, 1.9 mmol) in THF (20 mL) at -78 °C was added *n*BuLi (1.03 mL, 2.47 mmol, 2.4 M in hexanes). The mixture was stirred at -78 °C for 30 min and then DMF (208 mg, 2.85 mmol) was added. The mixture was stirred at -78 °C for an additional 30 min and then quenched with saturated NH_4Cl (20 mL). The mixture was extracted with EtOAc (2x) and the combined organic layers were washed with brine (2x), dried over anhydrous Na_2SO_4, filtered and concentrated under reduced pressure. The crude residue was purified by silica gel flash chromatography eluting with petroleum ether/ethyl acetate to yield the title compound as a white solid (150 mg, 42% yield).

Physical appearance: White solid (yield: 42%). **^{1}H NMR** (400 MHz, $CDCl_3$) δ 10.40 (s, 1H), 7.89 (dt, *J* = 2.5, 1.2 Hz, 1H), 7.65 (ddt, *J* = 8.8, 2.3, 1.1 Hz, 1H), 7.01 (d, *J* = 8.7 Hz, 1H), 6.56 (t, *J* = 56.4 Hz, 1H), 3.91 (s, 3H); **^{13}C NMR** (101 MHz, $CDCl_3$) δ 188.87, 163.17, 132.82 (t, *J* = 5.4 Hz), 127.04, 126.39 (t, *J* = 6.3 Hz), 124.62, 116.47, 114.10, 112.14, 111.73, 56.00. **^{19}F NMR** (376 MHz, $CDCl_3$) δ -109.59 (d, *J* = 56.7 Hz). **IR** (film, cm^{-1}) υ 1980, 1461, 1257, 1180.

4-(Difluoromethyl)dibenzo[b,d]furan (4.73)[6]

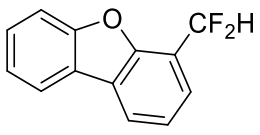

The title compound was prepared following General Procedure GP3 using dibenzo[b,d]furan-4-carbaldehyde (59 mg, 0.3 mmol), DAST (73 mg, 0.45 mmol) and ethanol (few drops), in DCM (0.5 M). The title compound (29 mg, 45%) was isolated as a colourless oil.

Physical appearance: Colourless oil (yield: 45%). **^{1}H NMR** (400 MHz, $CDCl_3$**)** δ: 7.91 (d, 1H, *J* = 7.6 Hz), 7.83 (d, 1H), 7.55 (dd, 1H, *J* = 7.6 Hz, *J* = 1.1 Hz), 7.53 (d, 1H *J* = 7.6 Hz), 7.47 – 7.30 (td, 1H, *J* = 8.3 Hz, *J* = 1.1 Hz), 7.33 – 7.21 (m, 1H), 7.11 (t, 1H, *J* = Hz); **^{19}F NMR** (376 MHz, $CDCl_3$) δ: -113.01 (d, *J* = 54.9 Hz); **^{13}C NMR** (100 MHz, $CDCl_3$) δ: 156.33, 153.03 (t, *J* = 5.2 Hz), 127.83, 125.17, 123.72 (t, *J* = 6.2 Hz), 123.37, 123.25, 123.10 (t, *J* = 1.6 Hz), 122.74, 120.79, 118.47 (t, *J* = 23.3 Hz), 111.95, 111.91 (t, *J* = 236.6 Hz). The physical data were identical in all respects to those previously reported.[6]

2-(3-(Difluoromethyl)phenoxy)-5-(trifluoromethyl)pyridine (4.74)

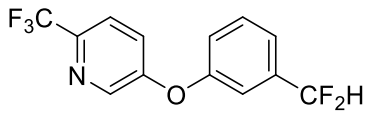

To trifluoromethyl)pyridin-2-yl)oxy)benzaldehyde (0.3 g, 1.12 mmol) in CH_2Cl_2 (4 mL) was added Deoxo-Fluor (497 mg, 2.25 mmol) and heated at 40 °C for 16 hours. Starting material aldehyde remained and therefore the reaction mixture was charged with additional Deoxo-Fluor (497 mg, 2.25 mmol) and heated at 40 °C for 6 hours, followed by an additional addition of Deoxo-Fluor (497 mg, 2.25 mmol) and heating at 40 °C for 16 hours. Saturated $NaHCO_3$ was added and the mixture was extracted with CH_2Cl_2 (2x) and the combined organic fraction was concentrated under reduced pressure. The crude residue was purified by silica gel flash chromatography eluting with petroleum ether/ethyl acetate, followed by purification by preparative reverse-phase HPLC (Column: Gemini-C18, 100*21.2 mm 5 µm; Mobile phase: MeCN-H_2O (0.1% FA); Gradient: 55% to 65%; Flow rate: 25 ml/min) to yield the title compound as a yellow oil (108 mg, 33% yield).

Physical appearance: Yellow oil (yield: 33%). **^{1}H NMR** (400 MHz, $CDCl_3$) *δ*: 8.35 (dt, *J* = 2.6, 1.0 Hz, 1H), 7.85 (dd, *J* = 8.6, 2.5 Hz, 1H), 7.45 (t, *J* = 7.9 Hz, 1H), 7.32 (dp, *J* = 7.8, 1.2 Hz, 1H), 7.21 – 7.17 (m, 1H), 6.98 (dt, *J* = 8.7, 0.8 Hz, 1H), 6.59 (t, *J* = 56.4 Hz, 1H); **^{13}C NMR** (101 MHz, $CDCl_3$) δ 165.32, 153.36, 145.40 (q, *J* = 4.4 Hz), 136.90 (q, *J* = 3.2 Hz), 136.20 (t, *J* = 22.7 Hz), 130.22, 123.88 (t, *J* = 1.8 Hz), 123.50 (q, *J* = 271.6 Hz), 122.56 (t, *J* = 6.2 Hz), 118.83 (t, *J* = 6.2 Hz), 116.36, 113.98, 111.61 (d, *J* = 3.1 Hz); **^{19}F NMR** (376 MHz, $CDCl_3$) *δ*: -61.71, -111.43 (d, *J* = 56.4 Hz); **IR** (film, cm^{-1}) υ 2916, 1448, 1395, 1030. **HRMS** (ESI) *m/z* calculated for $C_{13}H_9F_5NO$ $[M + Na]^+$ 290.05988 Found, 290.05998.

2-(4-(Difluoromethyl)phenyl)-2H-1,2,3-triazole (4.75)

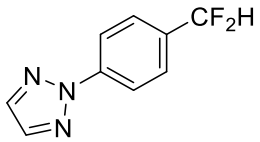

To a mixture of 4-(2*H*-1,2,3-triazol-2-yl)benzaldehyde (400 mg, 2.3 mmol) in CH_2Cl_2 (10 mL) was added EtOH (21.3 mg, 0.462 mmol) and Deoxo-Fluor (869 mg, 3.93 mmol) and heated at 40 °C for 18 hours. The reaction mixture was washed with water and brine, dried over anhydrous Na_2SO_4, filtered and concentrated under reduced pressure. The crude residue was purified by silica gel flash chromatography eluting with petroleum ether/ethyl acetate to yield the title compound as a white solid (131 mg, 29% yield).

Physical appearance: White solid (yield: 29%). **^{1}H NMR** (400 MHz, $CDCl_3$) δ 8.12 (d, *J* = 7.9, 2H), 7.78 (s, 2H), 7.57 (t, *J* = 8.7 Hz, 2H), 6.63 (s, 1H); **^{13}C NMR** (101 MHz, $CDCl_3$) δ 136.05, 133.37, 126.82 (t, *J* = 6.1 Hz), 119.04, 114.20 (t, *J* = 239.1 Hz). **^{19}F NMR** (376 MHz, $CDCl_3$) δ -110.77 (d, *J* = 56.3 Hz).

1-(3-(Difluoromethyl)phenyl)-3,5-dimethyl-1H-pyrazole (4.76)

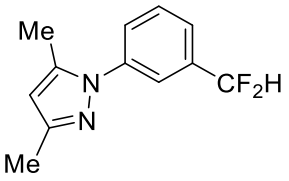

To a mixture of 3-(3,5-dimethyl-1*H*-pyrazol-1-yl)benzaldehyde (200 mg, 1 mmol) in CH_2Cl_2 (10 mL) was added EtOH (9.2 mg, 0.20 mmol) and Deoxo-Fluor (376 mg, 1.70 mmol) and heated at 40 °C for 18 hours. The reaction mixture was washed with water and brine, dried over anhydrous Na_2SO_4, filtered and concentrated under reduced pressure. The crude residue was purified by silica gel flash chromatography eluting with petroleum ether/ethyl acetate to yield the titled compound as a yellow oil (88 mg, 40% yield).

Physical appearance: Yellow oil (yield: 40%). **^{1}H NMR** (400 MHz, $CDCl_3$) δ 7.57 – 7.51 (m, 1H), 7.49 – 7.37 (m, 3H), 6.60 (t, *J* = 56.3 Hz, 1H), 5.94 (s, 1H), 2.24 (d, *J* = 0.8 Hz, 3H), 2.22 (s, 3H); **^{19}F NMR** (376 MHz, $CDCl_3$) δ -111.30 (d, *J* = 56.2 Hz); **^{13}C NMR** (101 MHz, $CDCl_3$) δ 149.53, 140.35, 139.49, 135.48 (t, *J* = 22.7 Hz), 129.49, 126.46 (t, *J* = 1.9 Hz), 124.05 (t, *J* = 6.0 Hz), 121.79 (t, *J* = 6.3 Hz), 117.62 – 110.90 (m), 107.56, 13.49,12.46; **IR** (film, cm^{-1}) υ 2982, 1452, 1275, 1059, 1024. **HRMS** (ESI) *m/z* calculated for $C_{12}H_{13}F_2N_2$ $[M + H]^+$, 223.10413, Found 223.10418.

Isopropyl 2-(4-(4-(difluoromethyl)benzoyl)phenoxy)-2-methylpropanoate (4.77)[8]

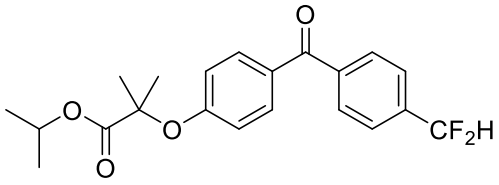

The title compound was prepared following General Procedure GP 4 using isopropyl 2-(4-(4-(difluoromethyl)benzoyl)phenoxy)-2-methylpropanoate (37.6 mg, 0.1 mmol, 1.0 equiv.), Mn(tmp)Cl (2.5 mol%), PhIO (0.33 mmol, 3.3 equiv.) $Et_3N{\cdot}3HF$ (0.12 mmol, 1.2 equiv.) and DCE (1 mL) and purified using column chromatography (DCM/*n*-pentane)

Physical appearance: White solid (yield: 22%). **^{1}H NMR** (400 MHz, $CDCl_3$) δ 7.77 (d, *J* = 7.9 Hz, 2H), 7.71 (d, *J* = 8.5 Hz, 2H), 7.56 (d, *J* = 7.6 Hz, 2H), 6.85 (d, *J* = 8.5 Hz, 2H), 6.67 (t, *J* = 56.2 Hz, 1H), 5.56-4.36 (m, 1H), 1.62 (s, 6H), 1.18 (d, *J* = 6.1 Hz, 6 H); **^{19}F NMR** (376 MHz, $CDCl_3$) δ -111.64 (d, *J* = 56.1 Hz). The physical data were identical in all respects to those previously reported.[8]

5-(4-(Difluoromethyl)phenyl)-2-methoxypyridine (4.79)

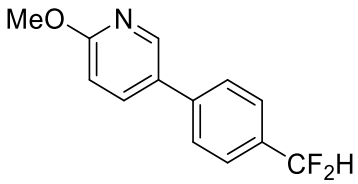

The title compound was prepared following General Procedure GP 4 using 2-fluoro-2-(4-(6-methoxypyridin-3-yl)phenyl)acetic acid (26.1 mg, 0.1 mmol, 1.0 equiv.), Mn(tmp)Cl (2.5 mol%), PhIO (0.33 mmol, 3.3 equiv.) $Et_3N{\cdot}3HF$ (0.12 mmol, 1.2 equiv.) and DCE (1 mL) and purified using column chromatography (DCM/*n*-pentane)

Physical appearance: White Solid (yield: 21%). **Mp**: 59 – 62 °C; **^{1}H NMR** (400 MHz, Methanol-d_4) δ 8.47 – 8.27 (m, 1H), 7.96 (dd, *J* = 8.7, 2.6 Hz, 1H), 7.70 (d, *J* = 8.6 Hz, 2H), 7.61 (d, *J* = 8.2 Hz, 2H), 6.89 (d, *J* = 8.6 Hz, 1H), 6.80 (t, *J* = 52.6 Hz, 1H), 3.95 (s, 3H); **^{13}C NMR** (101 MHz, Methanol-d_4) δ 165.56, 146.12, 141.49, 139.13, 135.22 (t, *J* = 22.4 Hz), 130.64, 129.53 – 125.64 (m), 116.36 (t, *J* = 236.6 Hz), 111.94, 54.31; **^{19}F NMR** (376 MHz, Methanol-d_4) δ -111.83 (d, *J* = 56.3 Hz); **IR** (film, cm^{-1}) υ 3010, 1402, 1256, 1120. **HRMS** (ESI) *m/z* calculated for $C_{13}H_{12}F_2NO$ $[M + H]^+$, 236.08924, Found, 236.08813.

2-(Difluoromethyl)-6-methoxynaphthalene (4.81)[9]

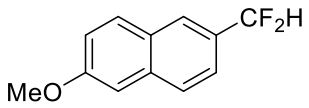

A dried Schlenk tube was charged with (0.2 mmol), PDFA (356 mg, 1.0 mmol), 1,3-Cyclopendione (19.6 mg, 0.2 mmol), $Ca(OH)_2$ (59.3 mg, 0.8 mmol), $Pd(PPh_3)_4$ (46.2 mg, 0.04 mmol), H_2O (9 mg, 0.5 mmol) and p-xylene (2 mL). The mixture was stirred at 90 °C for 3 h under N_2 atmosphere. After being cooled to room temperature, the mixture was subjected to flash column chromatography (petroleum ether / dichloromethane) to afford the pure product as a white solid.

Physical appearance: White solid (yield: 42%). ^{1}H **NMR** (200 MHz, $CDCl_3$) δ 7.95 – 7.76 (m, 3H), 7.57 (dd, *J* = 8.5, 1.8 Hz, 1H), 7.26 – 7.15 (m, 2H), 6.78 (t, *J* = 56.5 Hz, 1H), 3.95 (s, 3H); **^{19}F NMR** (376 MHz, $CDCl_3$) δ -109.13 (d, *J* = 56.5 Hz). The physical data were identical in all respects to those previously reported.[9]

1-(Difluoromethyl)naphthalene (4.80)[6]

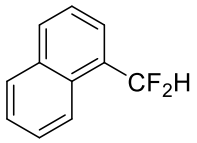

The title compound was prepared following General Procedure GP3 using 1-naphthaldehyde (47 mg, 0.3 mmol). DAST (73 mg, 0.45 mmol) and ethanol (few drops), in DCM (0.5 M). The title compound (27 mg, 55%) was isolated as a white solid.

Physical appearance: White solid (yield: 55%). **^{1}H NMR** (400 MHz, $CDCl_3$) δ 8.09 (d, *J* = 8.2 Hz, 1H), 7.88 (d, *J* = 8.3 Hz, 1H), 7.85 – 7.81 (m, 1H), 7.65 – 7.57 (m, 1H), 7.56 – 7.39 (m, 3H), 7.05 (s, 1H); **^{19}F NMR** (376 MHz, $CDCl_3$) δ -110.88 (d, *J* = 55.4 Hz). The physical data were identical in all respects to those previously reported.[6]

5-(4-(Difluoromethyl)phenyl)-1-(4-(methylsulfonyl)phenyl)-3-(trifluoromethyl)-1H-pyrazole (4.82)[8]

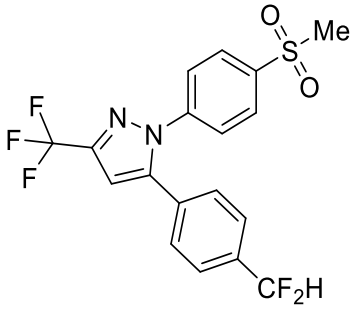

Synthesised according to a reported procedure.[8]

Physical appearance: Colourless oil (yield: 20%). **^{1}H NMR** (400 MHz, $CDCl_3$) δ 8.02 – 7.96 (m, 2H), 7.61 – 7.52 (m, 4H), 7.40 – 7.34 (m, 2H), 6.86 (s, 1H), 6.70 (t, 1H), 3.10 (s, 3H);

^{19}F NMR (376 MHz, $CDCl_3$) δ -62.55, -111.83 (d, *J* = 56.3 Hz). The physical data were identical in all respects to those previously reported.[8]

(8R,9S,13S,14S)-3-(Difluoromethoxy)-13-methyl-6,7,8,9,11,12,13,14,15,16-decahydro-17H-cyclopenta[a]phenanthren-17-one (4.83)[10]

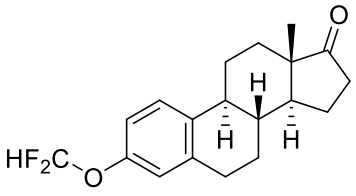

In a 10 mL round-bottomed flask was placed estrone (136 mg, 0.5 mmol, 1.0 equiv.), acetonitrile (1.0 mL) and 6M aqueous KOH (1.0 mL). The mixture was stirred rapidly at r.t and HCF_2OTf (0.21 mL, 1.5 mmol, 3.0 equiv.) was added at once at 0 °C. The mixture was stirred vigorously for 2 minutes, warmed to r.t and stirred for a further 20 minutes. The reaction was diluted with H_2O (10 mL) and extracted with ether (2 x 10 mL). The combined organic layers were dried over $MgSO_4$, concentrated, and purified by silica gel chromatography.

Physical appearance: White solid (yield: 43%). **^{1}H NMR** (400 MHz, $CDCl_3$) δ 7.29 (d, *J* = 8.4 Hz, 2H), 6.93 (d, *J* = 8.5, 1H), 6.88 (s , 1H), 6.50 (t, *J* = 74.3 Hz, 1H), 2.94 (dd, *J* = 9.0, 4.3 Hz, 2H), 2.58 – 2.47 (m, 1H), 2.42 – 2.37 (m, 1H), 2.27 (t, *J* = 10.6 Hz, 1H), 2.1 (ddd, *J* = 23.7, 13.3, 5.8 Hz, 2H), 1.98 (d, *J* = 10.4 Hz, 1H), 1.70 – 1.41 (m, 7H), 0.94 (s, 3H).**^{19}F NMR** (376 MHz, $CDCl_3$) δ -80.36 (d, *J* = 74.6 Hz). The physical data were identical in all respects to those previously reported.[10]

Preparation of Boronic Acid Precursors

Boronic acid precursors used in the synthesis towards **[^{18}F]4.77**, **[^{18}F]4.78** and **[^{18}F]4.79** were kindly donated by Pfizer inc.

(4-(4-((1-isopropoxy-2-methyl-1-oxopropan-2-yl)oxy)benzoyl)phenyl)boronic acid

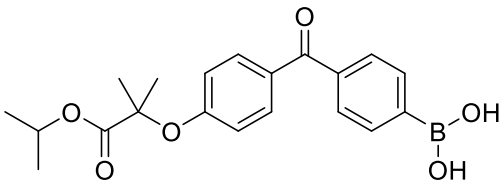

Prepared according to a known literature procedure[11]

^{1}H NMR (400 MHz, DMSO-d_6) δ 8.30 (s, 2H), 7.94 (d, *J* = 7.6 Hz, 2H), 7.76 – 7.69 (m, 2H), 7.67 – 7.60 (m, 2H), 6.94 – 6.87 (m, 2H), 5.04 – 4.93 (m, 1H), 1.61 (s, 6H), 1.16 (d, *J* = 6.3 Hz, 6H). **HRMS** (ESI, m/z) calcd [M - H]$^-$ for 369.15149, Found, 369.15117. The physical data were identical in all respects to those previously reported.[11] **Note: if ^{1}H NMR is taken in $CDCl_3$ peaks corresponding to the boroxine trimer may be observed!**

(4-(1-(p-tolyl)-3-(trifluoromethyl)-1H-pyrazol-5-yl)phenyl)boronic acid

Prepared according to a known literature procedure[12]

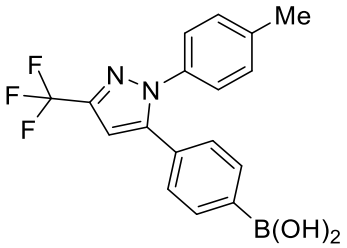

^{1}H NMR (400 MHz, DMSO-d_6) δ 7.76 (d, *J* = 8.4 Hz, 2H), 7.21 (d, *J* = 8.4 Hz, 2H), 7.07-7.15 (m, 5H), 2.21 (s, 3H); **LRMS**: (ESI$^+$, m/z) 347.1 ([M+H]$^+$, 100%). The physical data were

identical in all respects to those previously reported.[12] **Note: if ^{1}H NMR is taken in $CDCl_3$ peaks corresponding to the boroxine trimer may be observed!**

***In Situ* Preparation of Iodine(III) dicarboxylates**

In each radiochemical reaction, α-aryl-α-fluoroacetic acid and iodosylbenzene were pre-stirred in acetonitrile, solvent was removed under vacuum *a priori* to ^{18}F being dispensed into the reaction vial. To prove that iodine(III) dicarboxylate intermediate is formed during the pre-stirring step, the model radiochemistry substrate 2-fluoro-2-(4-phenoxyphenyl)acetic acid Iodine(III) dicarboxylate was fully characterised. For other substrates where appropriate, the Iodine (III) dicarboxylate intermediate complex formation was confirmed by ^{1}H NMR and ^{19}F NMR to prove a similar reaction mechanism. Notable shifts of both the benzylic alpha proton and fluorine were observed in ^{1}H and ^{19}F NMR respectively. Iodine(III) dicarboxylates diastereoisomer have peaks which stem from the stereogenic centre of the benzylic Ar-**C**FHCO_2H carbon which were made in a racemic fashion **(Scheme SI-8).**

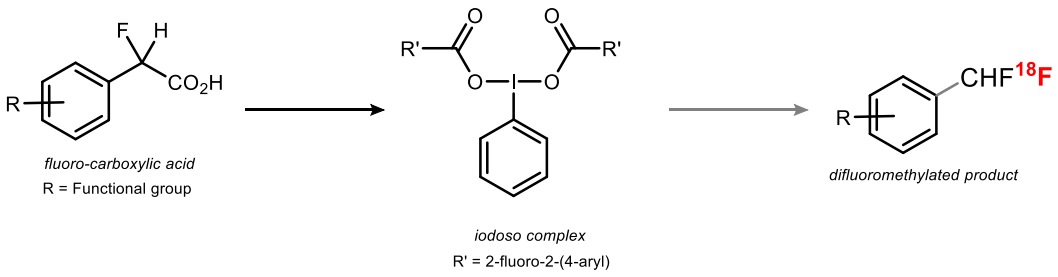

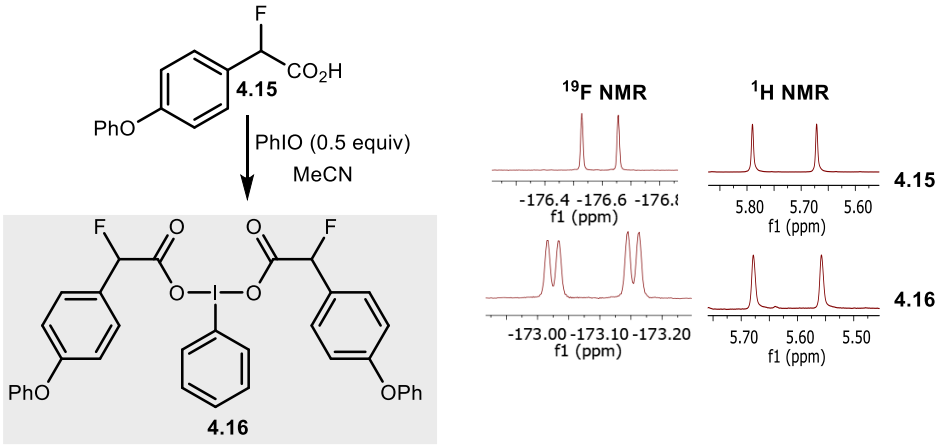

Scheme 6.13 Synthesis of Iodine(III) dicarboxylates.

Phenyl-l3-iodanediyl bis(2-fluoro-2-(4-phenoxyphenyl)acetate) (4.16)

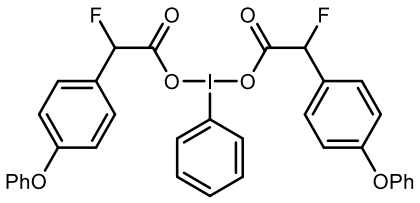

^{1}H NMR (400 MHz, $CDCl_3$) δ 7.96 (d, *J* = 6.7 Hz, 2H), 7.59 (t, *J* = 7.5 Hz, 1H), 7.40 (dt, *J* = 24.6, 8.2 Hz, 8H), 7.29 (s, 2H), 7.16 (t, *J* = 7.4 Hz, 2H), 7.04 (d, *J* = 1.1 Hz, 4H), 6.94 (d, *J* = 8.4 Hz, 4H), 5.70 (d, *J* = 48.0 Hz, 2H); **^{13}C NMR** (101 MHz, $CDCl_3$) δ 172.69 (d, *J* = 27.1 Hz), 158.59, 156.58, 134.80, 132.43, 131.33, 130.02, 129.36 (d, *J* = 20.9 Hz), 128.41, 124.01, 122.96, 119.52, 118.60, 88.33 (d, *J* = 189.0 Hz); **^{19}F NMR** (376 MHz, $CDCl_3$) -173.83 (d, *J* = 48.1 Hz, 1F), -173.85 (d, *J* = 48.1 Hz, 1F); **HRMS** (ESI) *m/z* calculated for $[M + Na]^+$, 717.05561, Found, 717.05588. **IR** (film, cm^{-1}) υ: 3062, 1755, 1677, 1232, 1025.

Phenyl- Λ3-iodanediyl bis(2-([1,1'-biphenyl]-4-yl)-2-fluoroacetate) (4.17)

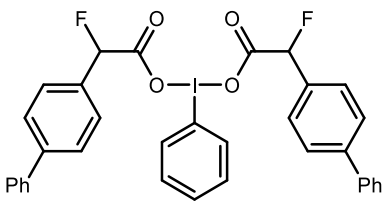

^{1}H NMR (400 MHz, $CDCl_3$) δ 7.97 – 7.89 (m, 2H), 7.56 (dd, *J* = 11.0, 7.9 Hz, 10H), 7.46 (t, *J* = 7.5 Hz, 5H), 7.42 – 7.36 (m, 6H), 5.77 (d, 49.0 Hz, 2H). **^{19}F NMR** (376 MHz, $CDCl_3$) δ -175.90 (d, *J* = 48.7 Hz, 2H).

Phenyl- ʎ3-iodanediyl bis(2-fluoro-2-(4-(trifluoromethyl)phenyl)acetate)

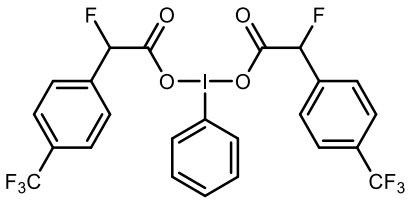

^{1}H NMR (400 MHz, Acetonitrile-d_3) δ 8.06 – 7.86 (m, 2H), 7.73 – 7.55 (m, 5H), 7.56 – 7.33 (m, 6H), 5.92 (d, *J* = 47.9 Hz, 2H). **^{19}F NMR** (376 MHz, Acetonitrile-d_3) δ -178.89 (d, *J* = 48.0 Hz).

Phenyl- ʎ3-iodanediyl bis(2-fluoro-2-(3-methoxyphenyl)acetate)

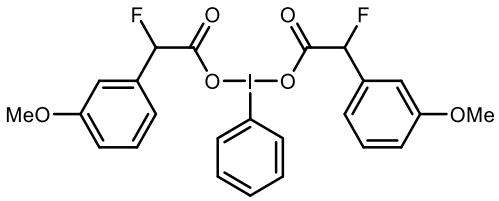

^{1}H NMR (400 MHz, $CDCl_3$) δ 7.84 – 7.73 (m, 2H), 7.51 – 7.38 (m, 1H), 7.37 – 7.27 (m, 2H), 7.23 – 7.12 (m, 2H), 6.93 – 6.65 (m, 6H), 5.61 (d, *J* = 48.4 Hz, 2H), 3.68 (s, 6H). **^{19}F NMR** (376 MHz, $CDCl_3$) δ -176.59 (d, *J* = 48.7 Hz).

Phenyl- ʎ3-iodanediyl bis(2-(3,5-dimethylphenyl)-2-fluoroacetate)

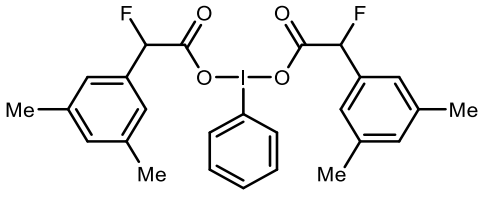

^{1}H NMR (400 MHz, $CDCl_3$) δ 7.83 (d, *J* = 11.2 Hz, 2H), 7.52 – 7.46 (m, 1H), 7.30 (d, *J* = 8.2 Hz, 2H), 6.88 (d, *J* = 20.8 Hz, 6H), 5.56 (d, *J* = 48.7 Hz, 2H), 2.20 (s, 12H). **^{19}F NMR** (376 MHz, $CDCl_3$) δ -174.65 (d, *J* = 48.7 Hz, 1F) , -174.66 (d, *J* = 48.7 Hz, 1F).

Phenyl- ʎ3-iodanediyl bis(2-fluoro-2-(2-methoxyphenyl)acetate)

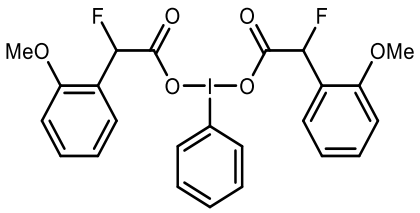

^{1}H NMR (400 MHz, $CDCl_3$) δ 7.96 (s, 2H), 7.56 (t, *J* = 7.4 Hz, 1H), 7.37 (dt, *J* = 21.5, 8.1 Hz, 4H), 7.24 – 7.13 (m, 2H), 7.00 – 6.84 (m, 4H), 6.06 (d, *J* = 48.0 Hz, 2H), 3.77 (s, 6H). **^{19}F NMR** (376 MHz, $CDCl_3$) δ -173.78 (d, *J* = 47.4 Hz).

Phenyl- ʎ3-iodanediyl bis(2-fluoro-2-(6-methoxynaphthalen-2-yl)acetate)

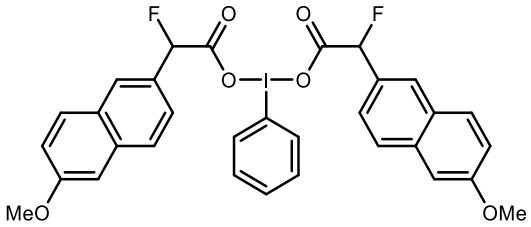

^{1}H NMR (400 MHz, $CDCl_3$) δ 7.70 (dq, *J* = 8.4, 1.9, 1.4 Hz, 2H), 7.60 (ddd, *J* = 16.7, 8.6, 2.3 Hz, 6H), 7.33 – 7.24 (m, 3H), 7.11 – 7.01 (m, 6H), 5.75 (d, *J* = 48.5 Hz, 2H), 3.84 (s, 6H). **^{19}F NMR** (376 MHz, $CDCl_3$) δ -173.76 (d, *J* = 48.7), -173.75 (d, *J* = 48.6 Hz).

Phenyl- ʎ3-iodanediyl bis(2-fluoro-2-(naphthalen-1-yl)acetate)

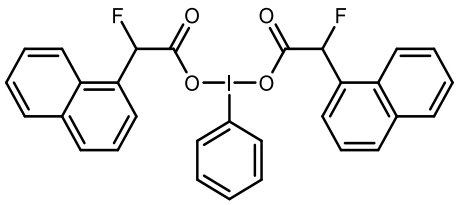

^{1}H NMR (400 MHz, $CDCl_3$) δ 8.03 (d, *J* = 8.4 Hz, 2H), 7.85 (d, *J* = 8.0 Hz, 4H), 7.46 (ddt, *J* = 33.1, 24.3, 9.9 Hz, 11H), 7.15 – 7.05 (m, 2H), 6.27 (d, *J* = 47.6 Hz, 2H). **^{19}F NMR** (376 MHz, $CDCl_3$) δ -174.22 (d, *J* = 47.6 Hz).

Phenyl- ʎ3-iodanediyl bis(2-(2,5-dimethylphenyl)-2-fluoroacetate)

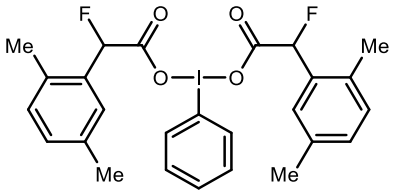

^{1}H NMR (400 MHz, Acetonitrile-d_3) δ 8.03 – 7.96 (m, 1H), 7.72 – 7.60 (m, 1H), 7.56 – 7.42 (m, 2H), 7.38 – 7.19 (m, 1H), 7.22 – 6.97 (m, 6H), 6.07 – 5.82 (d, *J* = 48.2 Hz, 2H), 2.26 (s, 6H), 2.22 (s, 6H), 2.26 (s, 6H). **^{19}F NMR** (376 MHz, Acetonitrile-d_3) δ -174.41 (d, *J* = 48.1 Hz).

Phenyl-ʎ3-iodanediyl bis(2-(4-(2H-1,2,3-triazol-2-yl)phenyl)-2-fluoroacetate)

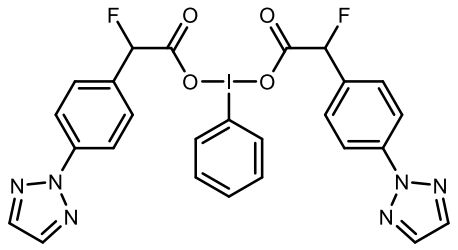

^{1}H NMR (400 MHz, $CDCl_3$) δ 8.03 (d, *J* = 8.7 Hz, 4H), 7.94 – 7.88 (m, 2H), 7.83 (s, 4H), 7.53 (d, *J* = 15.0 Hz, 1H), 7.46 – 7.34 (m, 6H), 5.77 (d, *J* = 48.3 Hz, 2H). **^{19}F NMR** (376 MHz, $CDCl_3$) δ -176.96 (d, *J* = 48.3 Hz, 1F), -176.98 (d, *J* = 48.3 Hz, 1F).

Phenyl-ʎ3-iodanediyl bis(2-fluoro-2-(3-((6-(trifluoromethyl)pyridin-3-yl)oxy)phenyl)acetate)

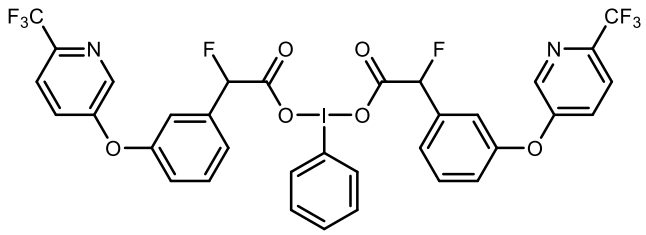

^{1}H NMR (400 MHz, $CDCl_3$) δ 8.34 (s, 2H), 7.91 – 7.65 (m, 4H), 7.65 – 7.22 (m, 6H), 7.17 – 7.05 (m, 5H), 6.94 (d, *J* = 8.6 Hz, 2H), 5.67 (d, *J* = 48.3 Hz, 2H). **^{19}F NMR** (376 MHz, $CDCl_3$) δ -61.64 (s), -178.45 (d, *J* = 48.4 Hz). -178.45 (d, *J* = 48.4 Hz).

Phenyl-ʎ3-iodanediyl bis(2-(dibenzo[b,d]furan-4-yl)-2-fluoroacetate)

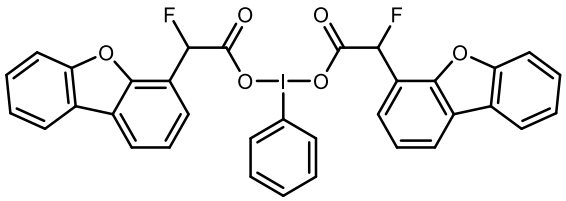

^{1}H NMR (400 MHz, $CDCl_3$) δ 7.84 (d, *J* = 7.6 Hz, 4H), 7.62 – 7.54 (m, 2H), 7.47 – 7.33 (m, 4H), 7.33 – 7.23 (m, 4H), 7.23 – 7.13 (m, 3H), 6.95 – 6.88 (m, 2H), 6.23 (d, *J* = 47.8 Hz, 2H). **^{19}F NMR** (376 MHz, $CDCl_3$) δ -176.02 (d, *J* = 47.8 Hz), -176.04 (d, *J* = 47.8 Hz).

Diisopropyl 2,2'-(((4,4'-(((phenyl-ʎ3-iodanediyl)bis(oxy))bis(1-fluoro-2-oxoethane-2,1-diyl))bis(benzoyl))bis(4,1-phenylene))bis(oxy))bis(2-methylpropanoate)

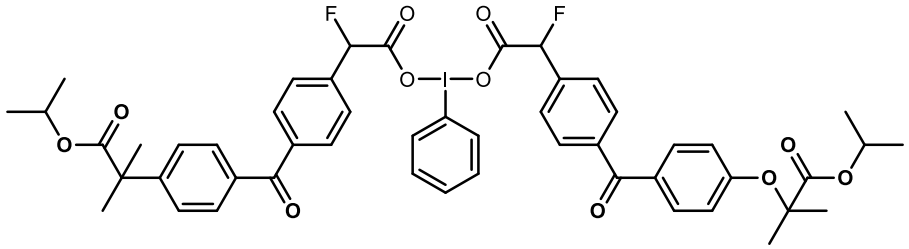

^{1}H NMR (400 MHz, $CDCl_3$) δ 7.84 (d, *J* = 7.9 Hz, 1H), 7.64 (dd, *J* = 23.7, 8.2 Hz, 8H), 7.51 (t, *J* = 7.0 Hz, 1H), 7.35 (d, *J* = 8.4 Hz, 5H), 6.79 (d, *J* = 8.6 Hz, 4H), 5.73 (d, *J* = 48.3 Hz, 2H), 5.02 (p, *J* = 6.4 Hz, 2H), 1.60 (s, 12H), 1.14 (d, *J* = 6.1 Hz, 12H). **^{19}F NMR** (376 MHz, $CDCl_3$) δ -179.56 (d, *J* = 48.3 Hz), -179.58 (d, *J* = 48.3 Hz).

Phenyl-ʎ3-iodanediyl bis(2-fluoro-2-(4-(6-methoxypyridin-3-yl)phenyl)acetate)

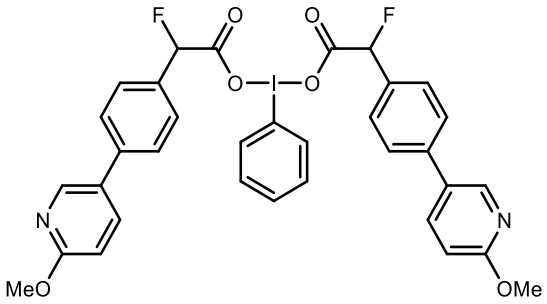

^{1}H NMR (400 MHz, $CDCl_3$) δ 8.39 (d, *J* = 2.3 Hz, 2H), 7.94 (d, *J* = 8.3 Hz, 2H), 7.78 (dd, *J* = 8.6, 2.5 Hz, 2H), 7.61 – 7.52 (m, 2H), 7.48 (d, *J* = 8.1 Hz, 4H), 7.39 (d, *J* = 8.0 Hz, 5H), 6.84 (d, *J* = 8.6 Hz, 2H), 5.76 (d, *J* = 48.4 Hz, 2H), 3.99 (s, 6H). **^{19}F NMR** (376 MHz, $CDCl_3$) δ -176.27 (d, *J* = 48.4 Hz).

Phenyl-ʎ3-iodanediyl bis(2-fluoro-2-(((8R,9S,13S,14S)-13-methyl-17-oxo-7,8,9,11,12,13,14,15,16,17-decahydro-6H-cyclopenta[a]phenanthren-3-yl)oxy)acetate)

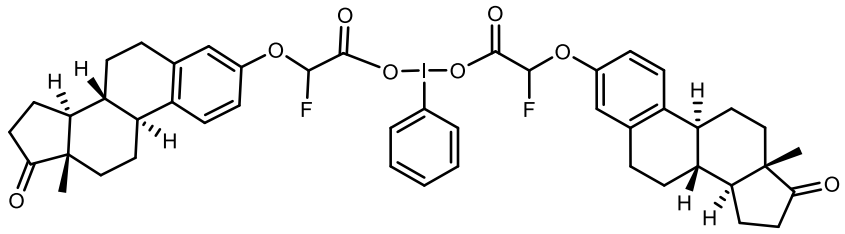

^{1}H NMR (400 MHz, $CDCl_3$) δ 8.13 – 8.03 (m, 2H), 7.63 – 7.54 (m, 1H), 7.47 (dd, *J* = 8.5, 7.2 Hz, 2H), 7.14 (d, *J* = 8.7 Hz, 2H), 6.81 – 6.62 (m, 4H), 5.80 (dd, *J* = 60.3, 1.1 Hz, 2H), 2.81 (dd, *J* = 8.9, 4.2 Hz, 4H), 2.44 (dd, *J* = 18.9, 8.6 Hz, 2H), 2.36 – 2.27 (m, 2H), 2.19 (d, *J* = 11.1 Hz, 2H), 2.13 – 1.84 (m, 8H), 1.63 – 1.29 (m, 12H), 0.84 (s, 6H). **^{19}F NMR** (376 MHz, $CDCl_3$) δ -125.93 (d, *J* = 60.6 Hz), -125.94 (d, *J* = 60.6 Hz)**.**

6.10 Radiochemistry Chapter IV

Procedure for preparation of a solution of [^{18}F]TEAF in MeCN:

A solution of tetraethylammonium bicarbonate (9 mg) in 1 mL of MeCN/H_2O, 4:1 was freshly prepared. [^{18}F]Fluoride (3.0 - 4.0 GBq) was separated from ^{18}O-enriched-water using a Chromafix PSHCO3 ^{18}F separation cartridge (45 mg) and subsequently released with 900 µL (in 6 x 150 µL portions) of the tetraethylammonium bicarbonate solution into a 5 mL V-vial containing a magnetic stir bar in the concentrator. The solution was dried with five cycles of azeotropic drying with MeCN (5 x 200 µL) under a flow of N_2 at 105 °C. The dried [^{18}F]TEAF residue was re-dissolved in anhydrous MeCN (500 - 1000 µL).

Optimisation

Scheme 6.14 Optimisation studies for the [^{18}F]fluorodecarboxylation of **4.31**

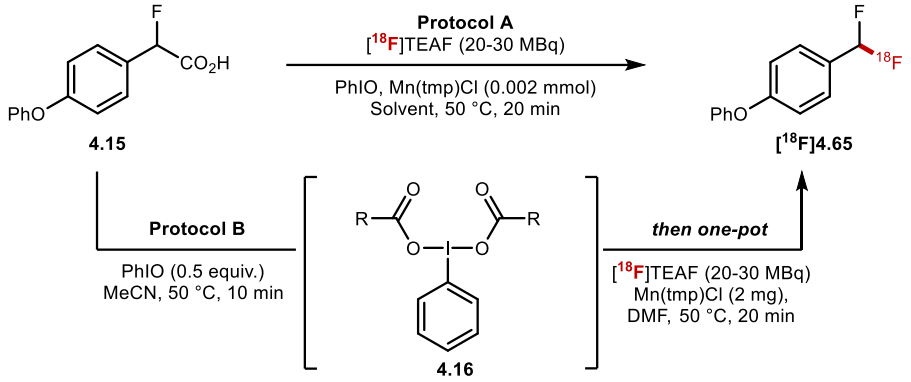

Entry	Starting Material (mmol)	Protocol	Solvent	PhIO (mmol)	RCC[a] (*n* =2)[b]
1	**4.15 (**0.11)	**A**	MeCN[c]	0.33	3% ± 1%
2	**4.15** (0.11)	**A**	MeCN	0.02	6% ± 1%
3	**4.15** (0.11)	**A**	DMF	0.02	7% ± 2%
4	**4.15** (0.055)	**A**	DMF[d]	0.02	22% ± 7%
5	**4.16 (0.014)**	**B**	**DMF[d]**	**-**	**40% ± 10%[e]**
6	**4.16** (0.014)	**B**	DMF[d]	-	0% ± 0%[f]
7	**4.15** (0.014)	**A**	MeCN	0.02	0%± 0%[g]
8	**4.16** (0.014)	**B**	DMF[d]	-	0% ± 0%[h]

[a]Radiochemical conversion. [b]*n* = number of reactions. [c]600 µL of MeCN used. [d]MeCN removed at 100 °C after dispensing [^{18}F]TEAF. [e](*n* = 10). [f]Reaction Temperature = 100 °C. [g]catalyst: Mn(tmp)OTs. [h]No Mn Catalyst.

^{18}F-fluorodecarboxylation competition experiment

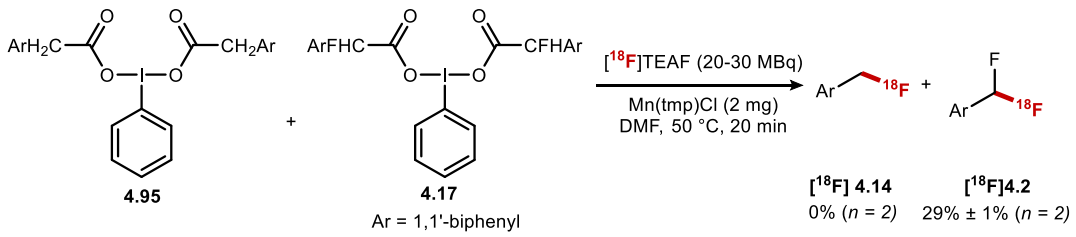

Scheme 6.15 ^{18}F-fluorodecarboxylation competition experiment.

Into a 3 mL vial was weighed phenyl-l3-iodanediyl bis(2-([1,1'-biphenyl]-4-yl)acetate) (0.014 mmol), **4.17** (0.014 mmol) and Mn(tmp)Cl (2 mg). To this vial was dispensed [^{18}F]TEAF (20 – 30 MBq) in a solution of anhydrous MeCN. The MeCN was removed at 100 °C under a flow of nitrogen. Upon cooling, DMF (300 µL) was added to the vial and the reaction was stirred at 50 °C for 20 minutes. The reaction was quenched with water (200 µL) and an aliquot was removed for analysis by radioTLC and radioHPLC for radiochemical conversion and product identity. Analysis was performed using a Waters Nova-Pak C18 column (4 µm, 3.9 x 150 mm) at a flow rate 1 mL/min. Radio-TLC was performed on Merck Kiesegel 60 F254 plates, using DCM/MeOH (9:1) as eluent. Analysis was performed using a plastic scintillator/PMT detector.

General Procedure for the Small Scale ^{18}F-Fluorination towards [^{18}F]4.65 – [^{18}F]4.81

Into a 3 mL vial was weighed substrate (0.014 mmol) and manganese catalyst (2 mgs). To this vial was dispensed [^{18}F]TEAF (20 – 30 MBq) in a solution of anhydrous MeCN. The MeCN was removed at 100 °C under a flow of nitrogen. Upon cooling, DMF (300 µL) was added to the vial and the reaction was stirred at 50 °C for 20 minutes. The reaction was quenched with water (200 µL) and an aliquot was removed for analysis by radioTLC and radioHPLC for radiochemical conversion and product identity. Analysis was performed

using a Waters Nova-Pak C18 column (4 µm, 3.9 x 150 mm) at a flow rate 1 mL/min. Radio-TLC was performed on Merck Kiesegel 60 F254 plates, using DCM/MeOH (9:1) as eluent. Analysis was performed using a plastic scintillator/PMT detector.

HPLC gradient A for small scale ^{18}F-Fluorination towards: [^{18}F]4.65 – [^{18}F]4.81

Water/MeCN, 1 mL/min, Waters Nova-Pak C18 Column, 4 µm, 3.9 x 150 mm 0 - 1 min (5% MeCN) isocratic 1 - 10 min (5% MeCN to 95% MeCN) linear increase 10 - 14 min (95% MeCN) isocratic 14 - 15 min (95% MeCN to 5% MeCN) linear decrease 15 - 17 min (5% MeCN) isocratic.

Radio-HPLC of [^{18}F]4.65 – [^{18}F]4.81

Crude Radio-HPLC traces of the crude mixture following the general procedure, with authentic UV references overlaid are shown below. The solid black line indicates the UV trace for cold reference material and the solid red line is the crude radio-HPLC trace. All samples were run using HPLC gradient A.

[^{18}F]4.2

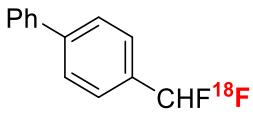

Reaction	Radio-TLC	Radiochemical Conversion
1	13%	10%
2	14%	11%
3	28%	28%
4	30%	30%
Radiochemical Conversion + Standard Deviation		**13% ± 5%**

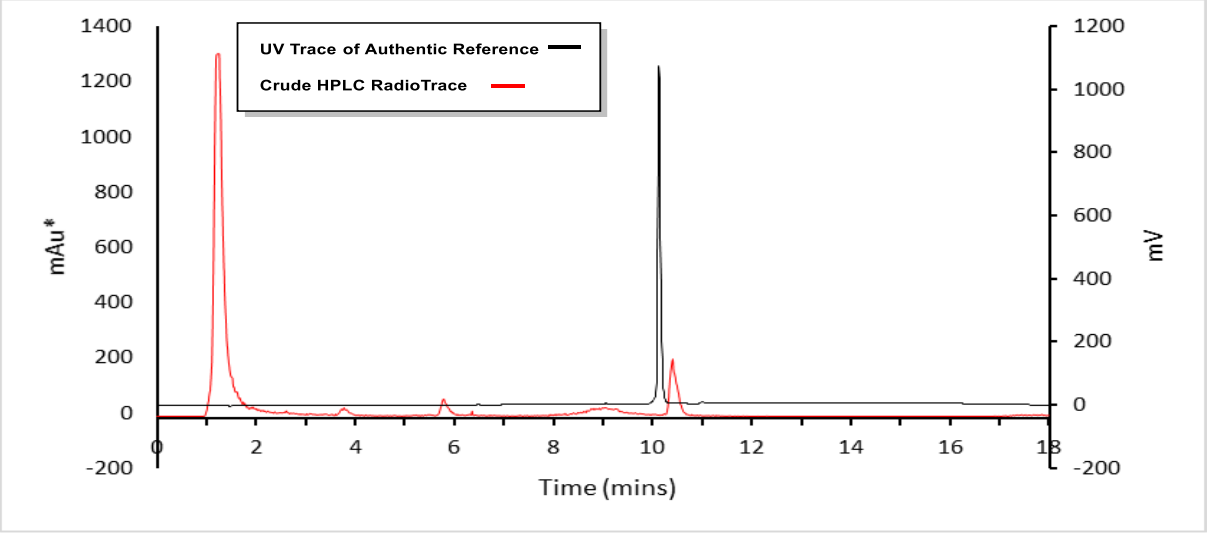

Figure 6.8 HPLC radio-trace of **[^{18}F]4.2** (red) overlaid with HPLC UV-trace (λ = 220 nm) of ^{19}F reference compound (black).

[^{18}F]4.65

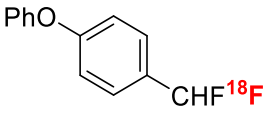

Reaction	Radio-TLC	Radiochemical Conversion
1	50%	50%
2	37%	37%
3	45%	45%
4	37%	37%
5	46%	46%
6	53%	53%
7	34%	34%
8	22%	22%
9	30%	30%
10	43%	43%
Radiochemical Conversion + Standard Deviation		**40% ± 9%**

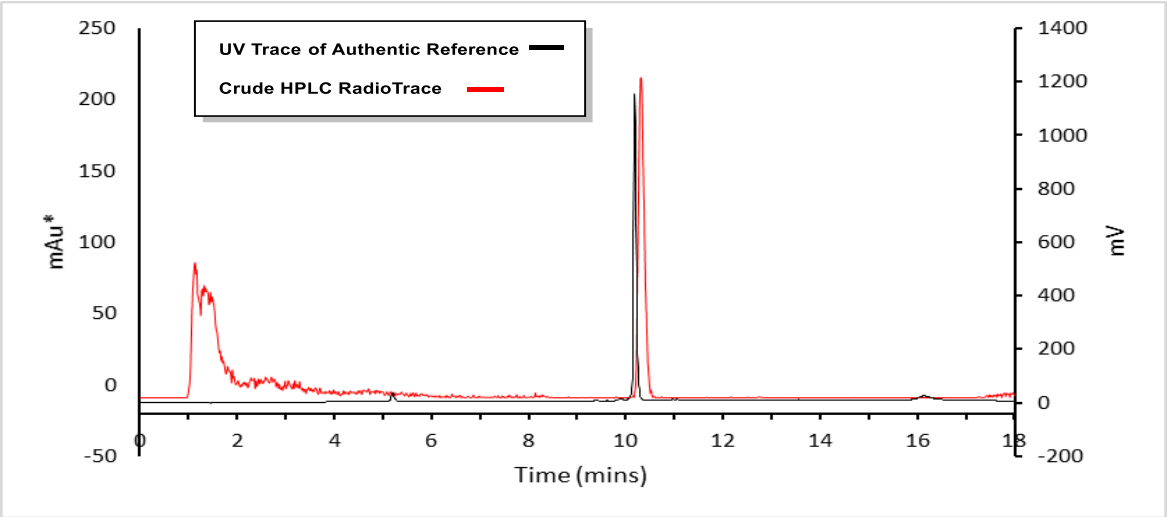

Figure 6.9 HPLC radio-trace of **[^{18}F]4.65** (red) overlaid with HPLC UV-trace (λ = 220 nm) of ^{19}F reference compound (black).

[^{18}F]4.66

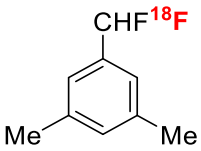

Reaction	Radio-TLC	Radiochemical Conversion
1	20%	20%
2	20%	20%
3	21%	19%
4	27%	26%
Radiochemical Conversion + Standard Deviation		**21% ± 3%**

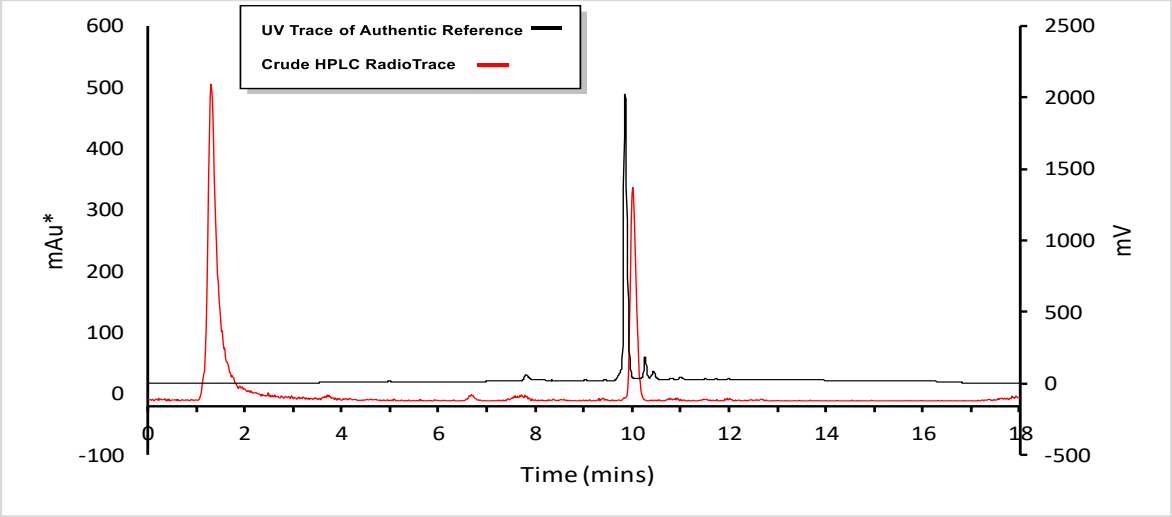

Figure 6.10 HPLC radio-trace of **[^{18}F]4.66** (red) overlaid with HPLC UV-trace (λ = 220 nm) of ^{19}F reference compound (black).

[^{18}F]4.67

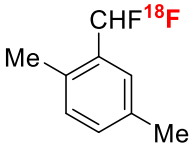

Reaction	Radio-TLC	Radiochemical Conversion
1	36%	34%
2	33%	31%
3	42%	37%
4	36%	32%
Radiochemical Conversion + Standard Deviation		**34% ± 3%**

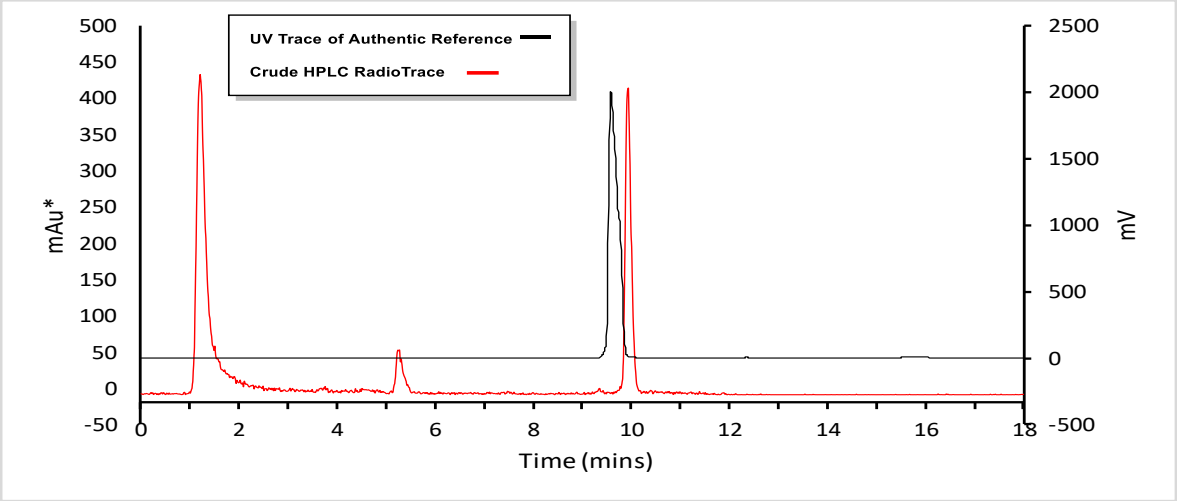

Figure 6.11 HPLC radio-trace of **[^{18}F]4.67** (red) overlaid with HPLC UV-trace (λ = 220 nm) of ^{19}F reference compound (black).

[^{18}F]4.69

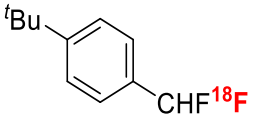

Reaction	Radio-TLC	Radiochemical Conversion
1	33%	33%
2	29%	29%
3	13%	13%
4	36%	36%
Radiochemical Conversion + Standard Deviation		**28% ± 10%**

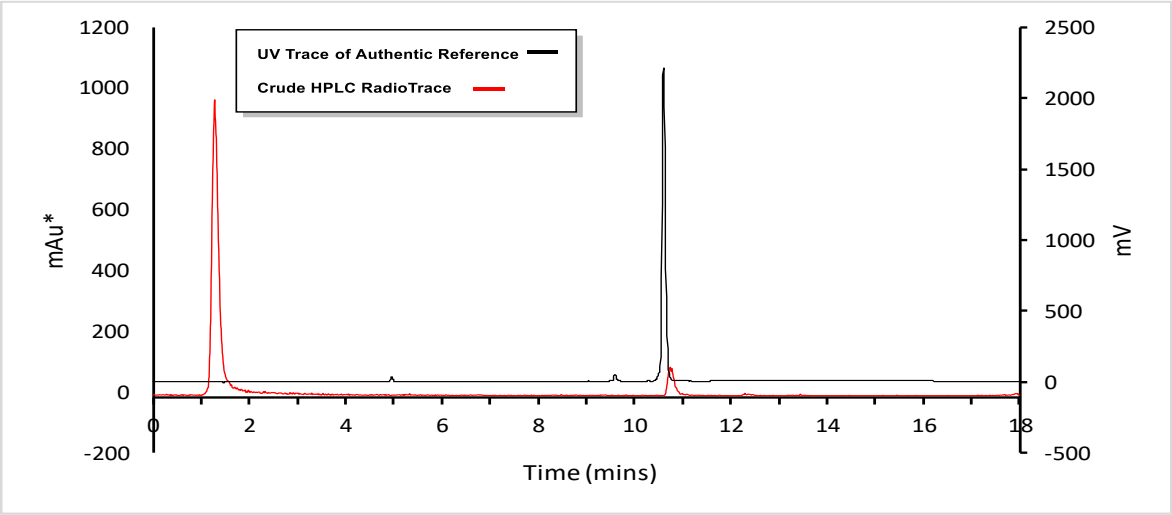

Figure 6.12 HPLC radio-trace of **[^{18}F]4.69** (red) overlaid with HPLC UV-trace (λ = 220 nm) of ^{19}F reference compound (black).

[^{18}F]4.70

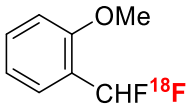

Reaction	Radio-TLC	Radiochemical Conversion
1	27%	23%
2	26%	21%
3	15%	12%
4	8%	7%
Radiochemical Conversion + Standard Deviation		**16% ± 7%**

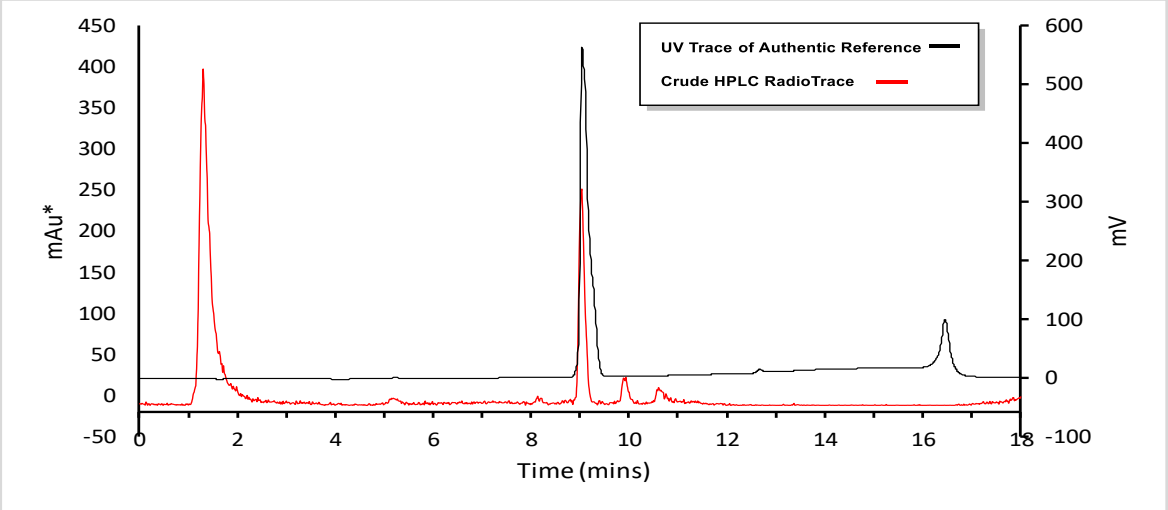

Figure 6.13 HPLC radio-trace of **[^{18}F]4.70** (red) overlaid with HPLC UV-trace (λ = 220 nm) of ^{19}F reference compound (black).

[^{18}F]4.71

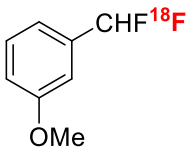

Reaction	Radio-TLC	Radiochemical Conversion
1	23%	21
2	22%	21
3	26%	26%
4	14%	14%
Radiochemical Conversion + Standard Deviation		**21% ± 5%**

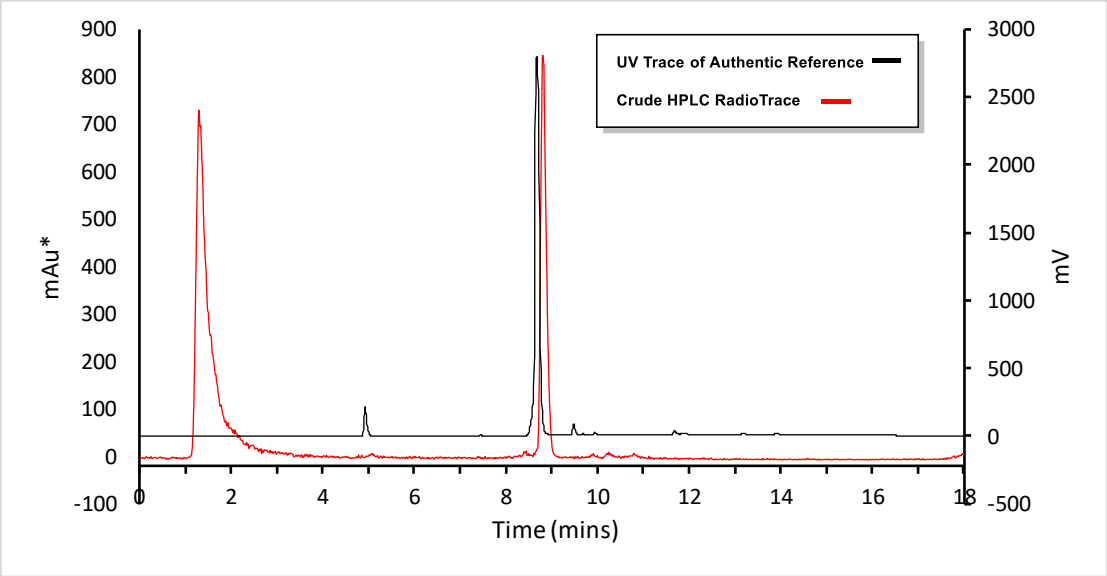

Figure 6.14 HPLC radio-trace of **[^{18}F]4.71** (red) overlaid with HPLC UV-trace (λ = 220 nm) of ^{19}F reference compound (black).

[^{18}F]4.72

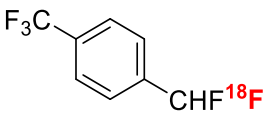

Reaction	Radio-TLC	Radiochemical Conversion
1	16%	5%
2	9%	3%
Radiochemical Conversion + Standard Deviation		**4% ± 1%**

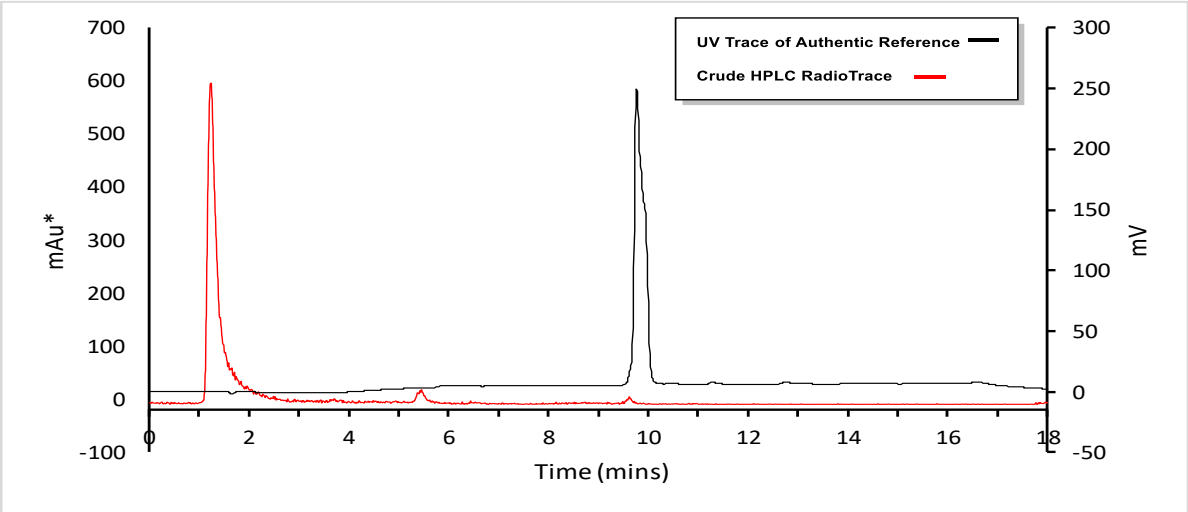

Figure 6.15 HPLC radio-trace of **[^{18}F]4.72** (red) overlaid with HPLC UV-trace (λ = 220 nm) of ^{19}F reference compound (black).

[^{18}F]4.68

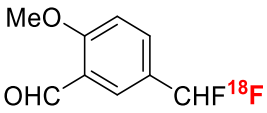

Reaction	Radio-TLC	Radiochemical Conversion
1	10%	10%
2	8%	8%
3	8%	8%
4	10%	10%
Radiochemical Conversion + Standard Deviation		**9% ± 1%**

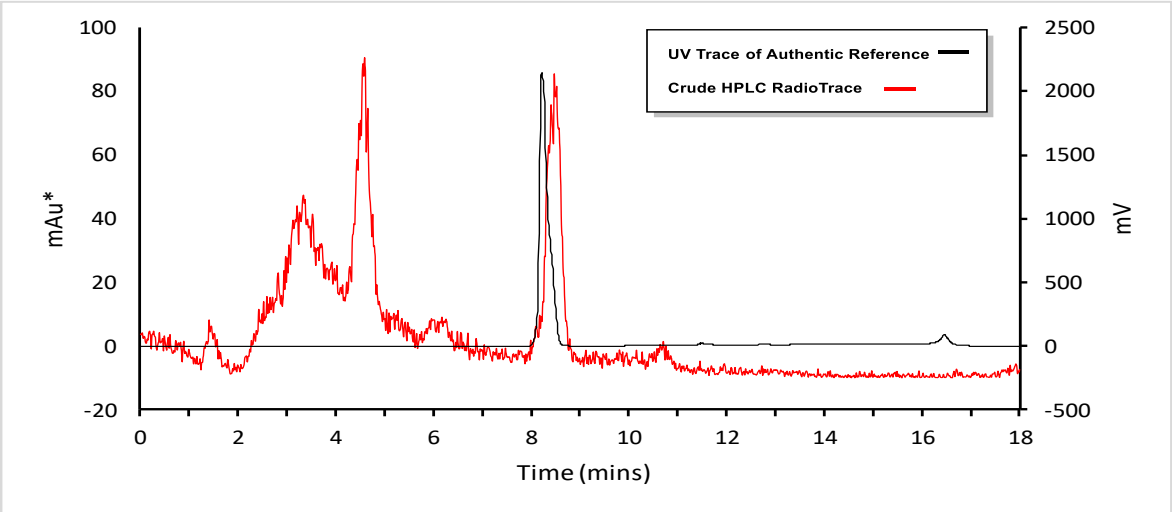

Figure 6.16 HPLC radio-trace of **[^{18}F]4.68** (red) overlaid with HPLC UV-trace (λ = 220 nm) of ^{19}F reference compound (black).

[^{18}F]4.73

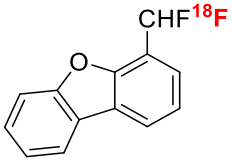

Reaction	Radio-TLC	Radiochemical Conversion
1	27%	27%
2	39%	39%
3	31%	26%
4	43%	35%
Radiochemical Conversion + Standard Deviation		**32% ± 6%**

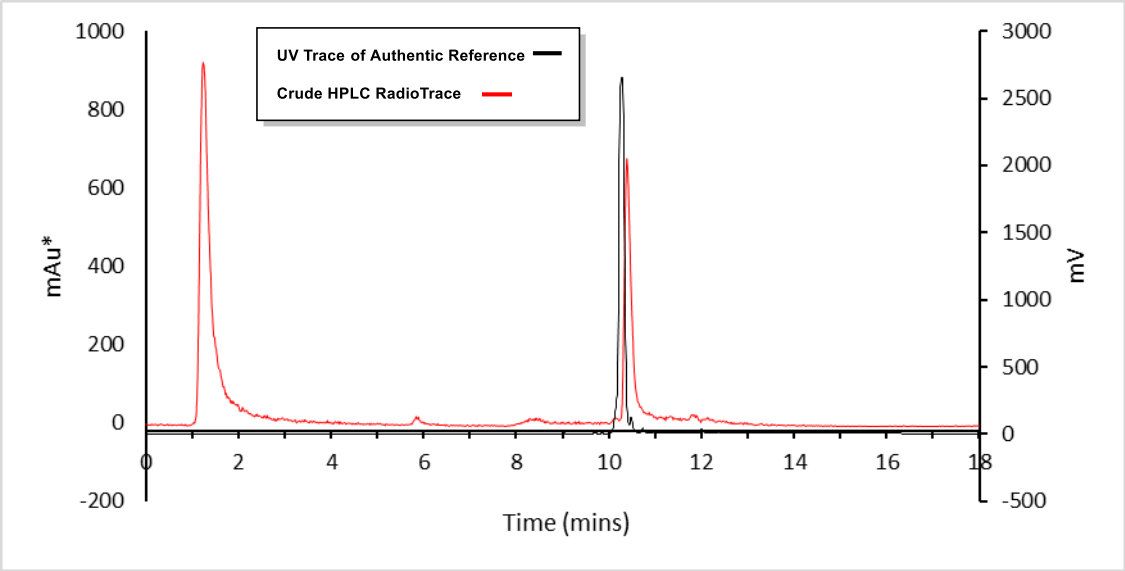

Figure 6.17 HPLC radio-trace of **[^{18}F]4.73** (red) overlaid with HPLC UV-trace (λ = 220 nm) of ^{19}F reference compound (black).

[^{18}F]4.74

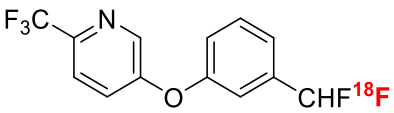

Reaction	Radio-TLC	Radiochemical Conversion
1	23%	21%
2	16%	15%
3	16%	15%
4	14%	13%
Radiochemical Conversion + Standard Deviation		**16% ± 4%**

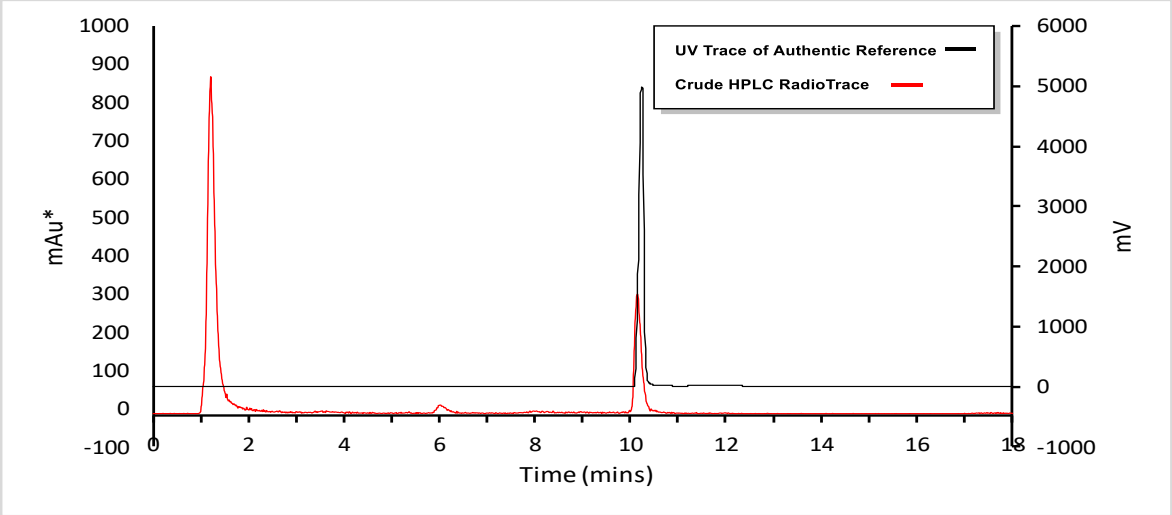

Figure 6.18 HPLC radio-trace of **[^{18}F]4.74** (red) overlaid with HPLC UV-trace (λ = 220 nm) of ^{19}F reference compound (black).

[^{18}F]4.75

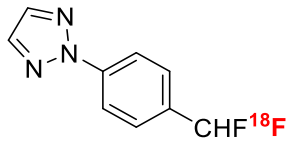

Reaction	Radio-TLC	Radiochemical Conversion
1	18%	11%
2	24%	17%
3	9%	9%
4	8%	8%
Radiochemical Conversion + Standard Deviation		**12% ± 4%**

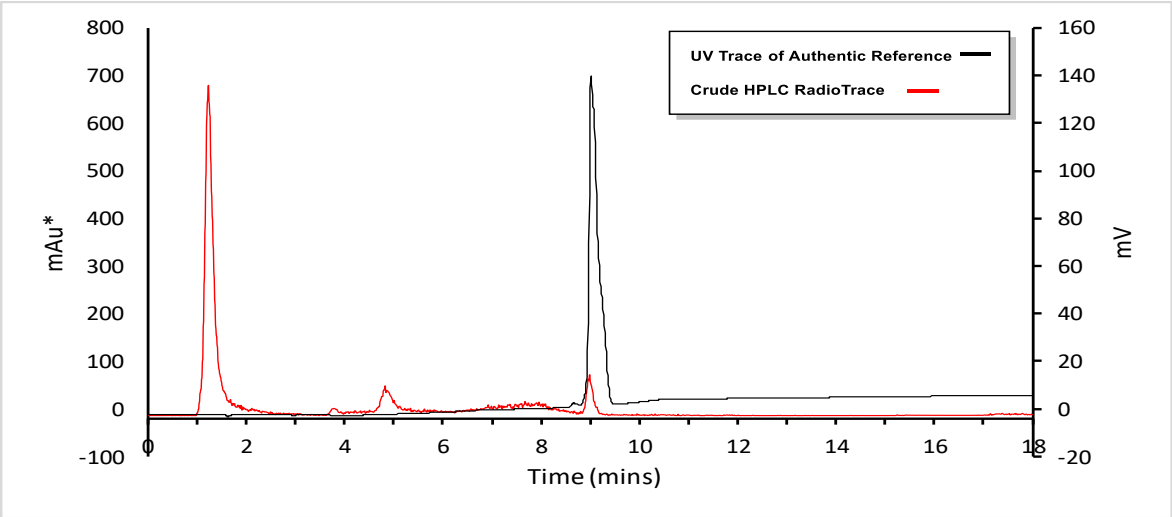

Figure 6.19 HPLC radio-trace of **[^{18}F]4.75** (red) overlaid with HPLC UV-trace (λ = 220 nm) of ^{19}F reference compound (black).

[^{18}F]4.76

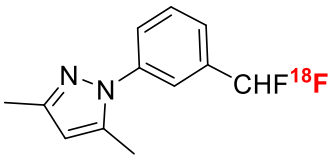

Reaction	Radio-TLC	Radiochemical Conversion
1	20%	16%
2	7%	7%
3	12%	12%
4	19%	19%
Radiochemical Conversion + Standard Deviation		**14% ± 5%**

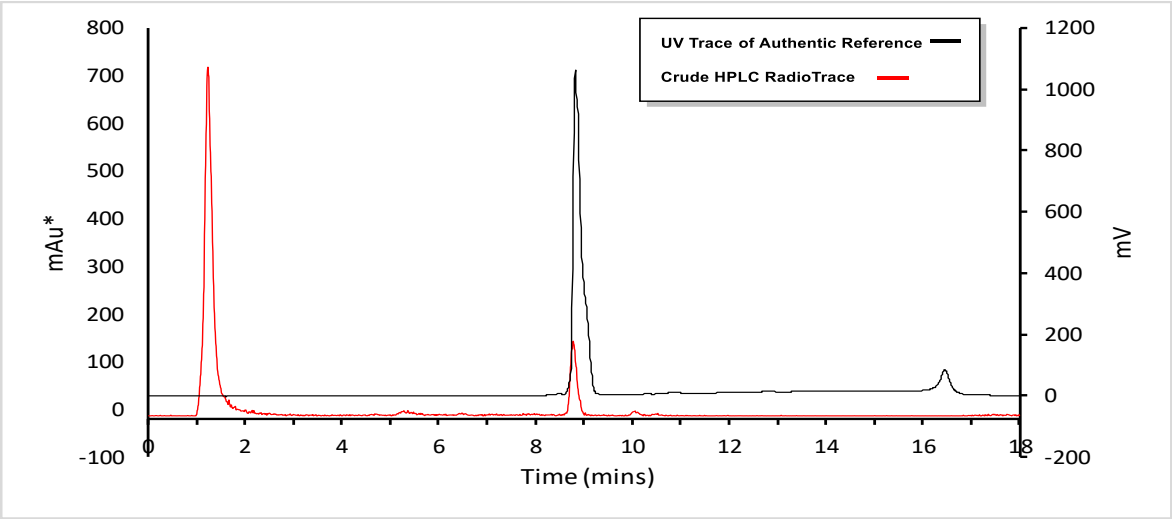

Figure 6.20 HPLC radio-trace of **[^{18}F]4.76** (red) overlaid with HPLC UV-trace (λ = 220 nm) of ^{19}F reference compound (black).

[^{18}F]4.78

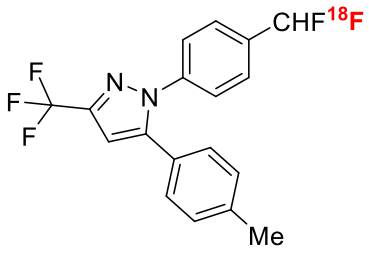

Reaction	Radio-TLC	Radiochemical Conversion
1	30%	30%
2	19%	19%
3	23%	23%
4	12%	12%
Radiochemical Conversion + Standard Deviation		**21% ± 6%**

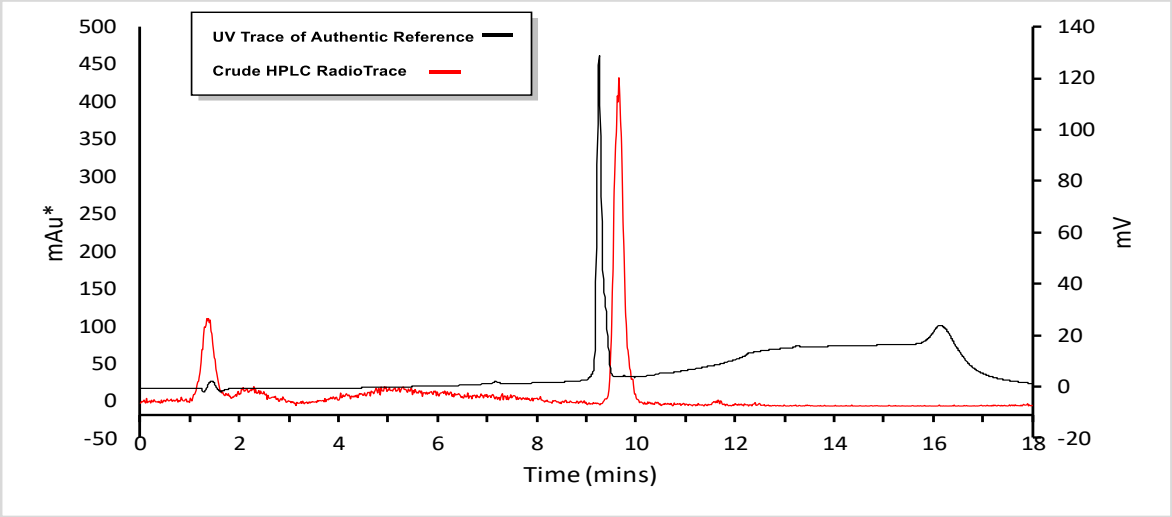

Figure 6.21. HPLC radio-trace of **[^{18}F]4.78** (red) overlaid with HPLC UV-trace (λ = 220 nm) of ^{19}F reference compound (black).

[^{18}F]4.77

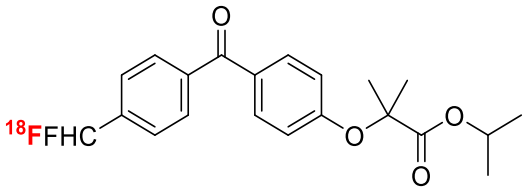

Reaction	Radio-TLC	Radiochemical Conversion
1	23%	21%
2	31%	28%
3	33%	26%
4	26%	20%
Radiochemical Conversion + Standard Deviation		**23% ± 3%**

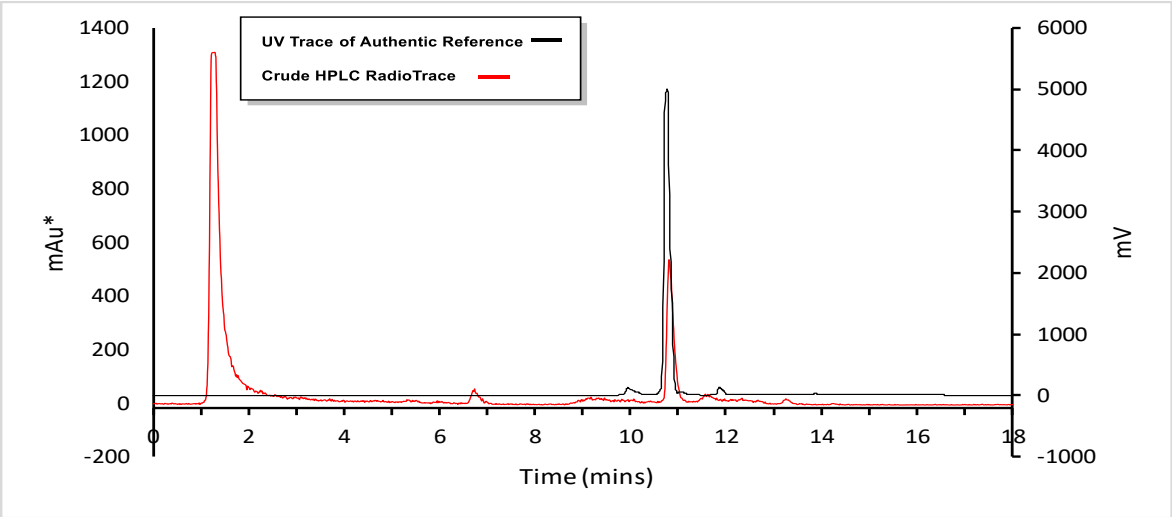

Figure 6.22 HPLC radio-trace of **[^{18}F]4.77** (red) overlaid with HPLC UV-trace (λ = 220 nm) of ^{19}F reference compound (black).

[^{18}F]4.79

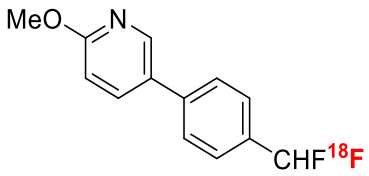

Reaction	Radio-TLC	Radiochemical Conversion
1	30%	30%
2	27%	27%
3	7%	7%
4	31%	31%
Radiochemical Conversion + Standard Deviation		**24% ± 11%**

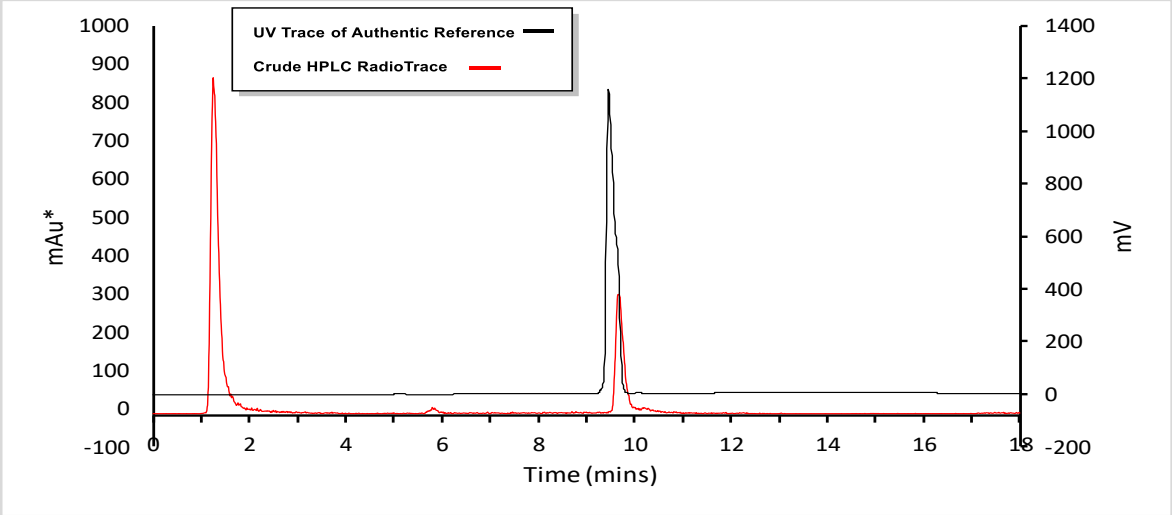

Figure 6.23 HPLC radio-trace of **[^{18}F]4.79** (red) overlaid with HPLC UV-trace (λ = 220 nm) of ^{19}F reference compound (black).

[^{18}F]4.81

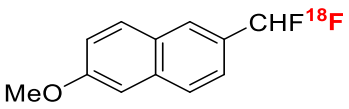

Reaction	Radio-TLC	Radiochemical Conversion
1	40%	40%
2	27%	27%
3	22%	22%
4	34%	34%
Radiochemical Conversion + Standard Deviation		**30% ± 8%**

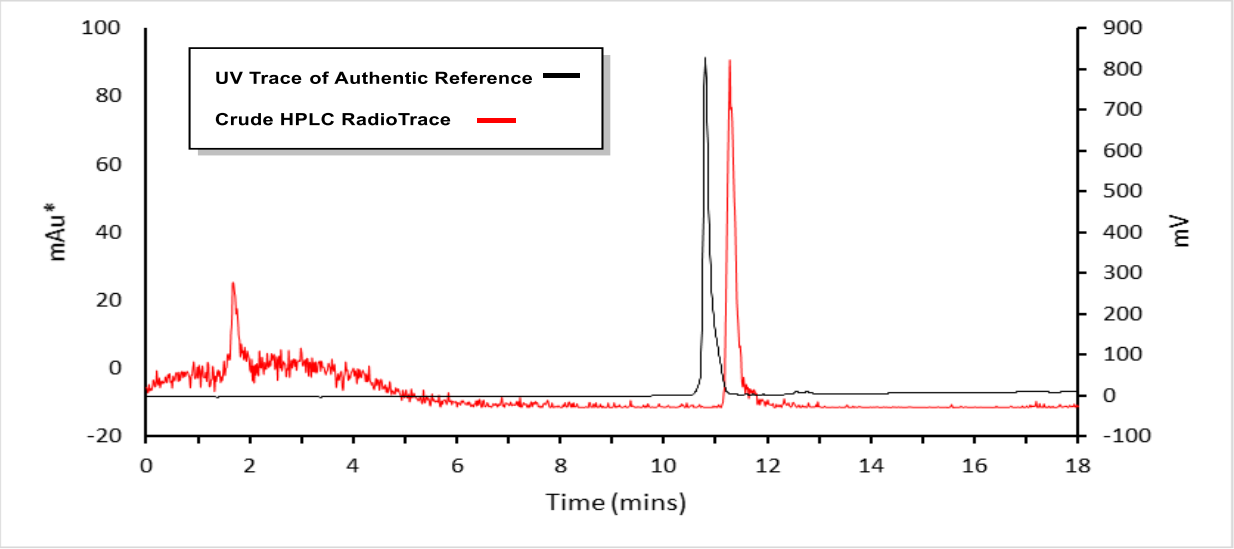

Figure 6.24 HPLC radio-trace of **[^{18}F]4.81** (red) overlaid with HPLC UV-trace (λ = 220 nm) of ^{19}F reference compound (black).

[^{18}F]4.80

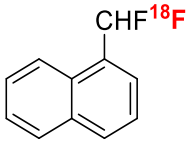

Reaction	Radio-TLC	Radiochemical Conversion
1	49%	47%
2	42%	39%
3	23%	22%
4	36%	34%
Radiochemical Conversion + Standard Deviation		**36% ± 10%**

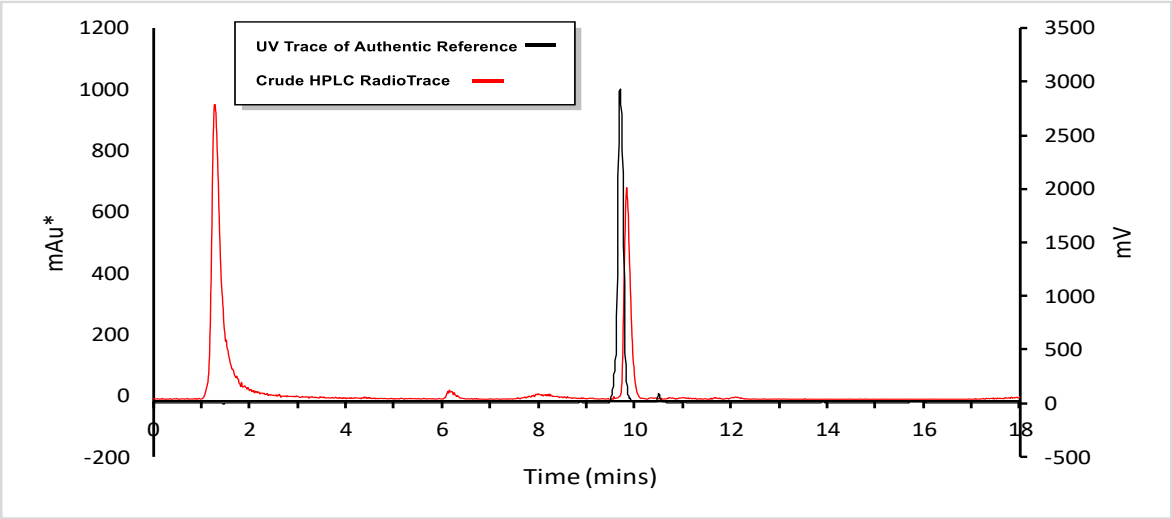

Figure 6.25 HPLC radio-trace of **[^{18}F]4.80** (red) overlaid with HPLC UV-trace (λ = 220 nm) of ^{19}F reference compound (black).

[^{18}F]4.82

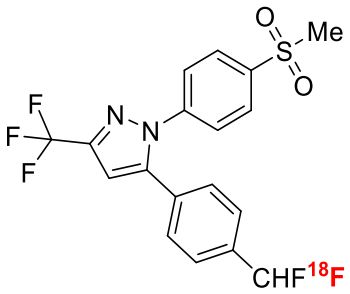

Reaction	Radio-TLC	Radiochemical Conversion
1	18%	17%
2	13%	12%
3	16%	15%
Radiochemical Conversion + Standard Deviation		**15% ± 2%**

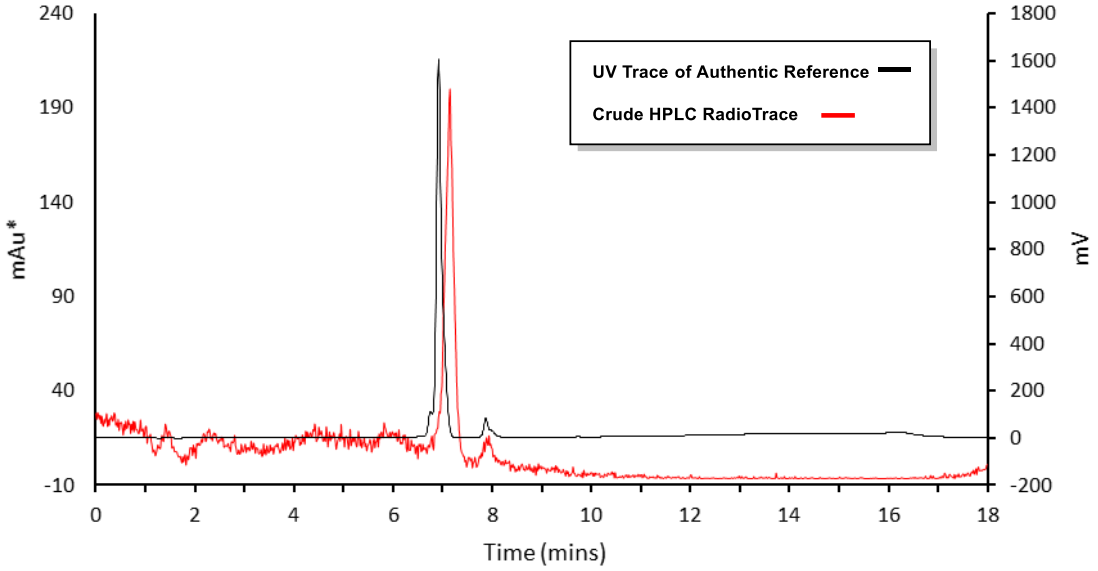

Figure 6.26 HPLC radio-trace of **[^{18}F]4.82** (red) overlaid with HPLC UV-trace (λ = 220 nm) of ^{19}F reference compound (black).

[^{18}F]4.83

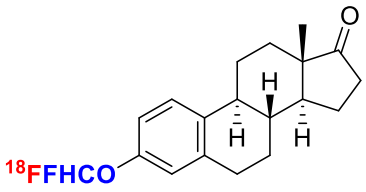

Reaction	Radio-TLC	Radiochemical Conversion
1	18%	18%
2	31%	31%
3	16%	16%
Radiochemical Conversion + Standard Deviation		**21% ± 6%**

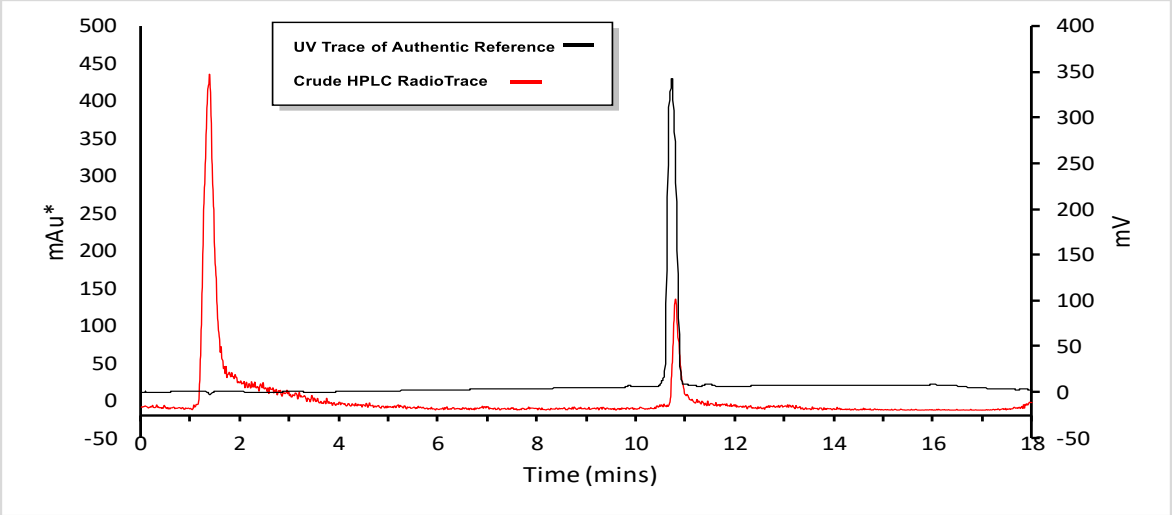

Figure 6.27 HPLC radio-trace of **[^{18}F]4.83** (red) overlaid with HPLC UV-trace (λ = 220 nm) of ^{19}F reference compound (black).

Re-optimisation for Large ^{18}F dose applications:

Elution Procedure:

[^{18}F]Fluoride was separated from ^{18}O-enriched-water using an anion exchange cartridge (Sep-Pak Accell Plus QMA Carbonate Plus Light Cartridge, 46 mg Sorbent per Cartridge, 40 µm particle size, Waters) and released with A solution of Mn(tmp)Cl (8 mg) in 600 µL of anhydrous MeOH into a 5 mL V-vial containing a magnetic stir bar in the concentrator.

Scheme 6.16 Optimisation under Mn(tmp)^{18}F Elution Conditions:

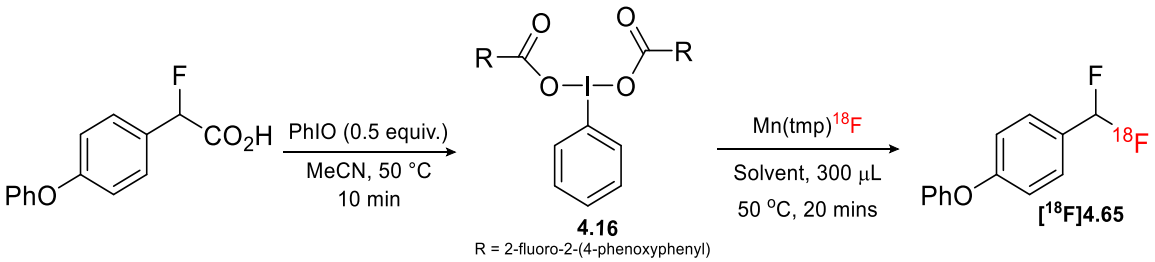

Entry	Substrate (mmol) (5b)	Solvent	RCC (*n* = 2)
1	0.014	DMF	0%
2	0.014	CH_3CN	4% ± 1%
3	0.014	DCM	0%
4	0.014	DCE	25% ± 6%
5	0.056	DCE	3% ± 1%
6[a]	0.056	DCE	10% ± 1%
7	**0.007**	**DCE**	**37% ± 0%**

[a]4 mg of Mn(tmp)Cl spiked into reaction mixture.

Re-optimisation for clinically relevant doses of ^{18}F:

Elution Procedure:

[^{18}F]Fluoride was separated from ^{18}O-enriched-water using an anion exchange cartridge (Sep-Pak Accell Plus QMA Carbonate Plus Light Cartridge, 46 mg Sorbent per Cartridge, 40 µm particle size, Waters) and released with A solution of Mn(tmp)Cl (8 mg) in 600 µL of anhydrous MeOH into a 5 mL V-vial containing a magnetic stir bar in the concentrator.

Procedure for the ^{18}F-fluorination of 4.16 under Batch Scale Isolation:

[^{18}F]Fluoride was separated from ^{18}O-enriched-water using an anion exchange cartridge (Sep-Pak Accell Plus QMA Carbonate Plus Light Cartridge, 46 mg Sorbent per Cartridge, 40 µm particle size, Waters) and released with A solution of Mn(tmp)Cl (8 mg) in 600 µL of anhydrous MeOH into a 5 mL V-vial containing a magnetic stir bar in the concentrator. The methanol was then removed at 80 °C under a flow of N_2. Once dry, the Mn(tmp)^{18}F was dissolved in DCM (1 mL) and transferred to a 5 mL vial. Upon transfer, the DCM was removed at 80 °C under a flow of N_2. Once dry, substrate (0.007 mmol) dissolved in DCE (300 µL) was added and the reaction stirred at 60 °C for 20 minutes. Upon completion, the DCE was removed at 70 °C under a flow of N_2. The crude material was dissolved in DMF (300 µL). Upon cooling, the crude solution was diluted in H_2O (6 mL) and eluted over a C18 SepPak cartridge (preconditioned with 2 mL MeOH followed by 10 mL H_2O). The 5 mL vial was rinsed again with 10% MeCN in H_2O (2 mL) and passed over the C18 SepPak cartridge. The desired product was then eluted of the C18 SepPak cartridge with MeCN (2 mL) upon with RadioHPLC analysis was carried out to confirm the radiochemical purity of the product. Analysis was performed using a Waters Nova-Pak

C18 column (4 µm, 3.9 x 150 mm) at a flow rate 1 mL/min. The overall synthesis time was 60 minutes.

Scheme 6.17 ^{18}F-fluorination of **4.16** under batch scale isolation.

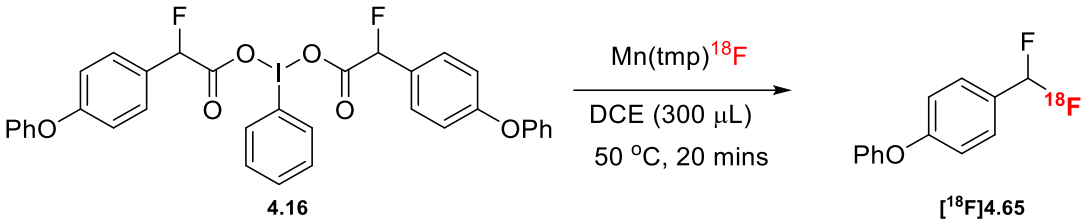

4.16 **[^{18}F]4.65**

Starting Activity (MBq)	Eluted (MBq)	Activity after drying MeOH (MBq)	Activity after transfer and DCM drying (MBq)	Activity after C18 (MBq)	RCY (decay corrected)
841	720	704	594	67	12%

Molar Activity Calculation:

The Molar Activity of [^{18}F]1-(difluoromethyl)-4-phenoxybenzene was assessed by radio-HPLC, using an analytical Analysis was performed using a Waters Nova-Pak C18 column (4 µm, 3.9 x 150 mm) at a flow rate 1 mL/min under HPLC gradient A.

Scheme 6.18 Molar activity measurement.

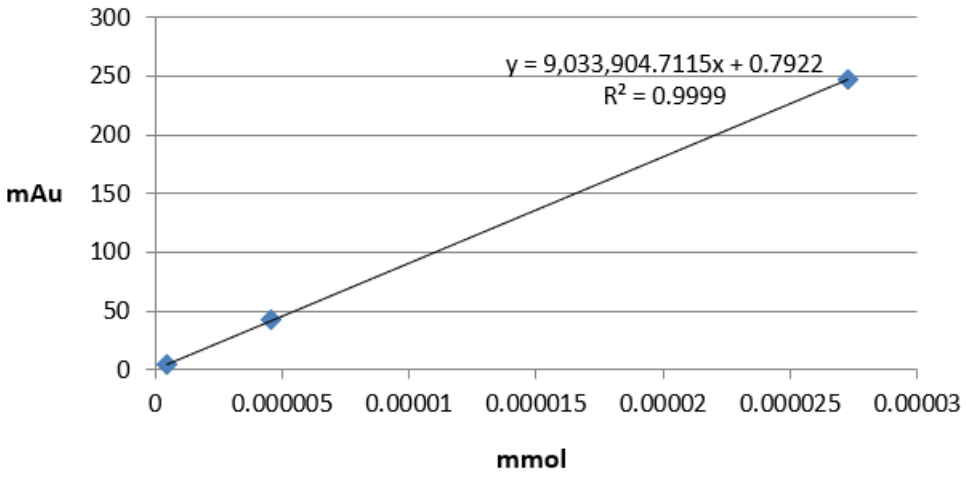

Run	MA (GBq/µmol)	Activity (MBq)	mmol	Area (mAu)
First injection	**3.22**	3.07	9.52412E-07	8.604
Second injection	**2.77**	2.76	9.95915 E-07	8.997

First Injection

y = 9,033,904.7115x + 0.7922 (y = mAu, x = mmol)

Area measured from isolated sample: 8.604 mAu

Activity of isolated sample: 3.07 MBq = 3.07E-03 GBq

mmol of isolated sample = 8.604/9,033,904= 9.52412E-07 mmol

9.52412E-07 mmol = 9.52412E-04 µmol

MA = 0.00307/9.52412E-04= 3.22 GBqµmol^{-1}

Second Injection

y = 9,033,904.7115x + 0.7922 (y = mAu, x = mmol)

Area measured from isolated sample: 8.997 mAu

Activity of isolated sample: 2.76 MBq = 2.76E-03 GBq

mmol of isolated sample = 8.997/9,033,904= 9.95915E-07 mmol

9.95915E-07 mmol = 9.95915E-04 µmol

MA = 0.00276/9.95915E-04= 2.77 GBqµmol^{-1}

Average

MA = 3.0 GBq/µmol

6.11 References Chapter IV

1) W. Liu and J. T. Groves, *Angew. Chem.,* 2013, **125**, 6140.
2) S. Mizuta, I. S. Stenhagen, M. O'Duill, J. Wolstenhulme, A. K. Kirjavainen, S. J. Forsback, M. Tredwell, G. Sandford, P. R. Moore and M. Huiban, *Org. Lett.,* 2013, **15**, 2648.
3) S. Verhoog, L. Pfeifer, T. Khotavivattana, S. Calderwood, T. L. Collier, K. Wheelhouse, M. Tredwell and V. Gouverneur, *Synlett,* 2016, **27**, 25.
4) F. Effenberger, S. Oßwald, *Tetrahedron: Asymmetry.,* 2001, **12**, 279
5) F. Zhang, J. Z. Song, *Tetrahedron Lett.,* 2006, **47**, 7641.
6) Z. Feng, Q. Min, X. Zhang, *Org. Lett.,* 2015, **18**, 44.
7) K. Aikawa, H. Serizawa, K. Ishii, K. Mikami, *Org. Lett.,* 2016, **18**, 3690.
8) H. Shi, A. Braun, L. Wang, S. H. Liang, N. Vasdev and T. Ritter, *Angew. Chem., Int. Ed.,* 2016, **55**, 10786.
9) X. Deng, J. Lin, J. Xiao, *Org. Lett.,* 2016, **18**, 4384.
10) P. S. Fier and J. F. Hartwig, *Angew. Chem. Int. Ed.,* 2013, **52**, 2092
11) Y. Xiao, Q. Min, C. Xu, R. Wang and X. Zhang, *Angew. Chem. Int. Ed.,* 2016, **55**, 5837-5841.
12) Y. Chen, P. R. Murray, A. T. Davies and M. C. Willis, *J. Am. Chem. Soc.,* 2018, **140**, 8781.

6.12 Synthetic Procedures and Characterisation of Compounds Chapter V:

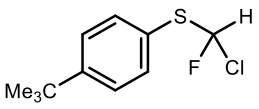

(4-(tert-butyl)phenyl)(chlorofluoromethyl)sulfane (5.65). A solution of (4-(tert-butyl)phenyl) (chloromethyl) sulfane (11.0 g, 90 mmol) in acetonitrile (100 mL) was prepared and cooled down to 0 °C. To this stirring mixture was added Selectfluor™ (1062 mg,3.00mmol) andwas stirred for 30 min at 0 °C under a nitrogen atmosphere.After complete consumption of the starting material, the reaction mixture was evaporated *in vacuo* to remove the MeCN, The resulting suspension was filtered through a glass filter and the filtrate was evaporated in vacuo to provide chlorofluoromethyl phenyl sulfide (25%) as a colourless oil.

^{1}H NMR (400 MHz, $CDCl_3$) δ 7.54 (d, *J* = 8.4 Hz, 2 H), 7.44 (d, *J* = 8.6 Hz, 2 H), 7.04 (d, *J* = 56.3 Hz, 1 H), 1.35 (s, 9 H)

^{19}F NMR (376 MHz, $CDCl_3$) δ -99.13 (d, *J* = 56.2 Hz)

^{13}C NMR (101 MHz, $CDCl_3$) δ 153.58, 134.93, 126.58, 125.72, 104.78 (d, *J* = 282.9 Hz), 34.94, 31.32.

IR (KBr): ν_{max} = 2965, 1490, 1364, 1268, 1194, 1118, 1001, 832, 787 cm^{-1}.

HRMS (EI): Calcd for $C_{11}H_{14}FClS$: 232.0489, Found: 232.0495.

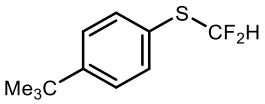

Synthesis of (4-(tert-butyl)phenyl)(difluoromethyl)sulfane (5.68). In an oven-dried round bottom flask with a stirring bar was dissolved 4-(tert-butyl)thiophenol (15 mmol) in MeCN/H_2O (1:1, v/v, 50 mL)). This mixture was cooled down to -78 °C and a solution of KOH (45 mmol, 3 equiv.) was added to the solution. To this mixtusre was added bromodifluoromethyldiethylphosphonate (30 mmol, 2 equiv.) dropwise, and the mixture was stirred at -78 °C for another 15 minutes and then allowed to warm up to room temperature. MeCN was removed under reduced pressure and the resulting mixture was extracted with Et_2O (3 x 50 mL), dried over $MgSO_4$ and concentrated *in vacuo* yielding the title compound as a pale-yellow oil (85%). Spectral data was consistent with literature.[1]

^{1}H NMR (400 MHz, $CDCl_3$) δ 7.43 (m, 2H), 7.28 (m, 2H), 6.90 (t, *J* = 57.0 Hz, 1H), 1.26 (s, 9H).

^{19}F NMR (377 MHz, $CDCl_3$) δ -92.46 (d, *J* = 57.2 Hz).

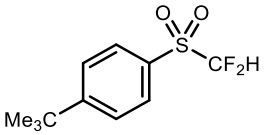

Synthesis of 1-(tert-butyl)-4-((difluoromethyl)sulfonyl)benzene (5.69). To a stirring mixture of (4-(tert-butyl)phenyl)(difluoromethyl)sulfane in DCM at 0 °C was added portion wise *m*-chloroperbenzoic acid (3 equiv.). The mixture was allowed to warm up to room temperature and monitored by TLC until full consumption of the starting material. After this, potential excess *m*-CPBA in the reaction was quenched with aq. 5% Na_2SO_3, diluted with EtOAc and extracted with brine. The combined organic layers were dried over $MgSO_4$ and concentrated *in vacuo*. The crude product was further purified by

column chromatography to yield the title compound as a white solid (74%). Spectral data was consistent with literature.[2]

^{1}H NMR (400 MHz, $CDCl_3$) δ 7.90 (d, *J* = 8.8 Hz, 2H), 7.65 (d, *J* = 8.8 Hz, 2H), 6.18 (t, *J* = 53.5 Hz, 1H), 1.37 (s, 9H).

^{13}C NMR (101 MHz, $CDCl_3$) δ 160.29, 130.62, 128.71, 126.81, 114.77 (t, *J* = 285.3 Hz), 35.64, 31.05.

^{19}F NMR (377 MHz, $CDCl_3$) δ -121.82 (d, *J* = 53.6 Hz).

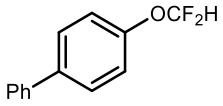

Synthesis of 4-(difluoromethoxy)-1,1'-biphenyl (5.58) To a mixture of [1,1'-biphenyl]-4-ol (0.5 mmol) in DCM (2.0 mL) at 0 °C was added an aqueous KOH solution (20 wt%, 0.7 mL, 3.0 mmol) with vigorous stirring. Then a solution of $TMSCF_2Br$ (203 mg, 1.0 mmol) in DCM (0.5 mL) was added into the mixture at 0 °C. After being stirred at 0 °C for 30 minutes, the reaction mixture was quenched with water (5 mL), followed by extraction with DCM (2 × 15 mL). The organic layers were combined and dried over anhydrous $MgSO_4$. After removal of the solvents *in vacuo*, the residue was subjected to column chromatography (silica gel; petroleum ether/ethyl acetate) to afford the desired title compound as a white solid (74%). Spectral data was consistent with literature.[3]

^{1}H NMR (400 MHz, $CDCl_3$) δ 7.50-7.55 (m, 4H), 7.41 (t, 2H, *J* = 7.6 Hz), 7.33 (t, 1H, *J* = 7.2 Hz), 7.16 (d, 2H, *J* = 8.0 Hz), 6.51 (t, 1H, J = 74.0 Hz).

^{13}C NMR (101 MHz, $CDCl_3$) δ 150.5, 140.0, 138.5, 128.8, 128.4, 127.5, 127.0, 119.7, 116.0 (t, *J* = 258.7 Hz).

^{19}F NMR (377 MHz, $CDCl_3$) δ = -80.7 (d, *J* = 73.1 Hz, 2F).

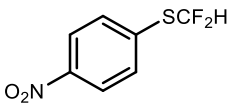

Synthesis of (difluoromethyl)(4-nitrophenyl)sulfane (5.77) To a mixture of 4-nitrobenzenethiol (0.5 mmol) in DCM (2.0 mL) at 0 °C was added an aqueous KOH solution (20 wt%, 0.7 mL, 3.0 mmol) with vigorous stirring. Then a solution of $TMSCF_2Br$ (203 mg, 1.0 mmol) in DCM (0.5 mL) was added into the mixture at 0 °C. After being stirred at 0 °C for 30 minutes, the reaction mixture was quenched with water (5 mL), followed by extraction with DCM (2 × 15 mL). The organic layers were combined and dried over anhydrous $MgSO_4$. After removal of the solvents *in vacuo*, the residue was subjected to column chromatography (silica gel; petroleum ether/ethyl acetate) to afford the desired title compound as a light-yellow oil. Spectral data was consistent with literature.[4]

^{1}H NMR (400 MHz, $CDCl_3$) δ 8.23-8.19 (m, 1 H), 7.72-7.69 (m, 1 H), 6.94 (t, *J* = 55.7 Hz, 1 H)

^{13}C NMR (101 MHz, $CDCl_3$) δ 148.3, 135.1 (t, *J* = 2.8 Hz), 134.3, 124.2, 119.7 (t, *J* = 275.7 Hz).

^{19}F NMR (376 MHz, $CDCl_3$) δ -91.3 (d, *J* = 56.0 Hz, 2 F).

(2,2-difluorocyclopropane-1,1-diyl)dibenzene (5.75)

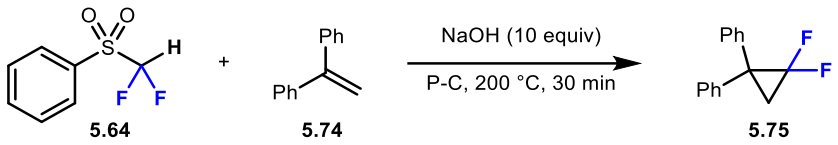

Scheme 6.19 difluorocyclopropanation of ethene-1,1-diyldibenzene.

((difluoromethyl)sulfonyl)benzene (0.1 mmol, 1.0 equiv) and ethene-1,1-diyldibenzene (0.1 mmol, 1.0 equiv) were added to a 4 mL vial containing NaOH (10 mmol, 10 equiv) and propylene carbonate (P-C, 1 mL). The mixture was heated at 200 ˚C for 30 minutes, before cooling. The crude mixture was then subject to HPLC purification to afford the title compound. Compound was obtained as a yellow oil (19%). Spectral data was consistent with literature.[5]

^{1}H NMR (400 MHz, $CDCl_3$) δ 7.40 (d, *J* = 7.3 Hz, 4H), 7.30 (t, *J* = 7.3 Hz, 4H), 7.24 (t, *J* = 7.3 Hz, 2H), 2.10 (t, *J* = 8.6 Hz, 2H).

^{19}F NMR (376 MHz, $CDCl_3$) δ -129.87 (dd, *J* = 11.0, 5.7 Hz, 2F).

^{13}C NMR (101 MHz, $CDCl_3$) δ 138.7, 128.8, 128.6, 127.4, 112.9 (t, J = 287.5 Hz), 40.10 (t, *J* = 10.3 Hz), 23.6 (t, *J* = 9.8 Hz).

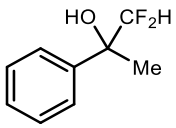

Synthesis of 1,1-difluoro-2-phenylpropan-2-ol (5.89). Under nitrogen, CsF (9 mg, 0.06 mmol, 10 mol%) and 18-crown-6 (16 mg, 0.06 mmol, 10 mol%) were added to a solution of acetophenone (0.60 mmol) in 1,2-dimethoxyethane (DME) (3 mL). Me_3SiCF_2H (149 mg, 160 µL, 1.20 mmol) was added, and the mixture was stirred at room temperature

overnight. TBAF (1.0 mL, 1.0 M in THF) was added, and the whole mixture was stirred for 2 h. HCl (aq. 1.0 M, 1.0 mL) was added and the solution was stirred for another 1 h. The mixture was extracted with ethyl acetate (20 mL × 3). The organic phase was washed with brine and then dried over anhydrous $MgSO_4$. After filtration evaporation of the solvent *in vacuo*, the residue was subjected to silica gel column chromatography using hexane/ethyl acetate as eluent to give the titled product as a transparent oil (63%). Spectral data was consistent with literature.[6]

^{1}H NMR (400 MHz, CDCl3) δ 7.52–7.49 (m, 2H), 7.40–7.28 (m, 3H), 5.70 (t, *J* = 56.3 Hz, 1H), 2.36 (s, 1H), 1.64 (s, 3H).

^{19}F NMR (376 MHz, CDCl3) δ –129.42 (dd, *J* = 275.2, 56.4 Hz, 1F), –130.56 (dd, *J* = 275.2, 56.4 Hz, 1F).

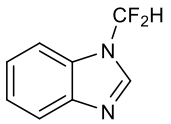

1-(difluoromethyl)-1H-benzo[d]imidazole (5.79). A mixture of 1H-benzo[*d*]imidazole (0.17 mmol, 1 equiv), ethyl bromodifluoroacetate (52 µL, 2 equiv) was dissolved in anhydrous DMF (0.1 M). Lithium hydroxide (19 mg, 4 equiv), was added to the reaction mixture and stirred at room temperature for 18 h. Upon completion, the mixture was diluted with EtOAc (15 mL) and washed with water (50 mL), followed by brine (25 mL). The organic extract was dried over $MgSO_4$, filtered and solvent removed under reduced pressure. The crude mixture was purified by a silica gel column chromatography using (pet ether/EtOAc) to furnish the title compound as a yellow crystal (63%). Spectral data was consistent with literature.

^{1}H NMR (400 MHz, $CDCl_3$): δ 8.15 (s, 1H), 7.84 – 7.82 (m, 1H), 7.61 – 7.59 (m, 1H), 7.43 – 7.40 (m, 2H), 7.36 (t, *J* = 60.0 Hz, 1H).

^{19}F NMR (376 MHz, $CDCl_3$): δ -97.02 (decoupled).[7]

6.13 Radiochemistry Chapter V:

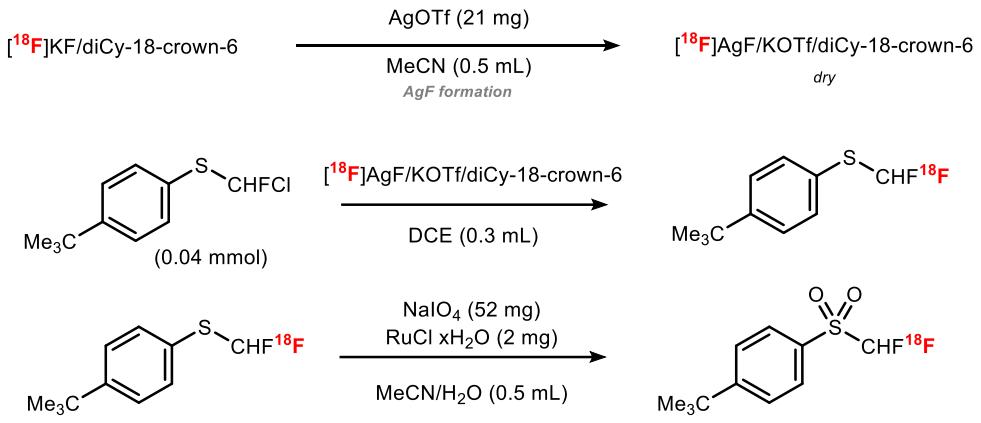

<u>Optimal procedure:</u> [^{18}F]KF/diCy-18-cr-6 capture. ^{18}F-Fluoride was separated from ^{18}O-enriched-water using an anion exchange cartridge (Waters Sep-Pak AccellPlus QMA Carbonate Plus Light Cartridge, activated with H_2O (10.0 mL) prior to use) and released with a solution of diCy-18-cr-6 (14 mg), $K_2C_2O_4$ (4 mg) and K_2CO_3 (0.2 mg) in MeCN/H_2O (1 mL, 4:1, v/v). The solution was dried by azeotropic using dry MeCN (200 µL) under a flow of N_2 at 105 °C (temperature: 105 °C)

[^{18}F]AgF synthesis ([^{18}F]AgF/KOTf/diCy-18-cr-6). To the v-vial containing dried [^{18}F]KF/diCy-18-cr-6 (*vide infra*) was added a solution of *fresh white grains* of AgOTf (21 mg, 80 µmol) in dry MeCN (dry, 0.5 mL) and the solvent was removed by heating at 105 °C (temperature: 105 °C) under a stream of nitrogen (Q = 1.0 L·min^{-1}, *maximum drying time should be 5 minutes*) (*a colour change could be observed to dark red*). After this,

the reaction vial was cooled down prior to the next reaction. A dark red/brown solid was obtained and used for the next step.

Synthesis of **[^{18}F]5.69** step 1: After Cooling 65 ˚C, a solution of (4-(tert-butyl)phenyl)(chlorofluoromethyl)sulfane (11.8 mg, 0.04 mmol) in DCE (300 µL) was added. The resulting brown suspension was allowed to stir at 65 °C for 20 minutes, after which it was allowed to cool to room temperature prior to use in the next step.

Synthesis of **[^{18}F]5.69** step 2: To a v-vial containing the crude reaction mixture in DCE solvent was added $RuCl_3xH_2O$ (20 mol%, 2 mg) and $NaIO_4$ (0.16 mmol, 52 mg) in MeCN/H_2O (1:1, v/v, 0.5 mL). This mixture was stirred at 25 °C (temperature: 36 °C) for 5 minutes, diluted with a solution consisting of water (4.2 mL) and EtOH (0.3 mL) and trapped on a C18 plus cartridge (conditioned 10 mL MeOH, then 10 mL H_2O). **[^{18}F]5.69** was eluted with MeCN (1.0 mL) and loaded onto the HPLC sample-loop for preparative HPLC purification (using isocratic 65% MeCN in 25 mM ammonium formate buffer, Q = 4 mL/min, t_R(**[^{18}F]5.69**) = ~ 8-12 minutes). The ^{18}F-product was collected into H_2O (20 mL), which was then eluted over a C18 Plus cartridge (pre-conditioned with 10 mL MeOH and10 mL of H_2O). HPLC-pure **[^{18}F]5.69** was then released from the C18 Plus cartridge with MeCN (1.0 mL) into a v-vail and used in subsequent ^{18}F-difluoromethylation reactions.

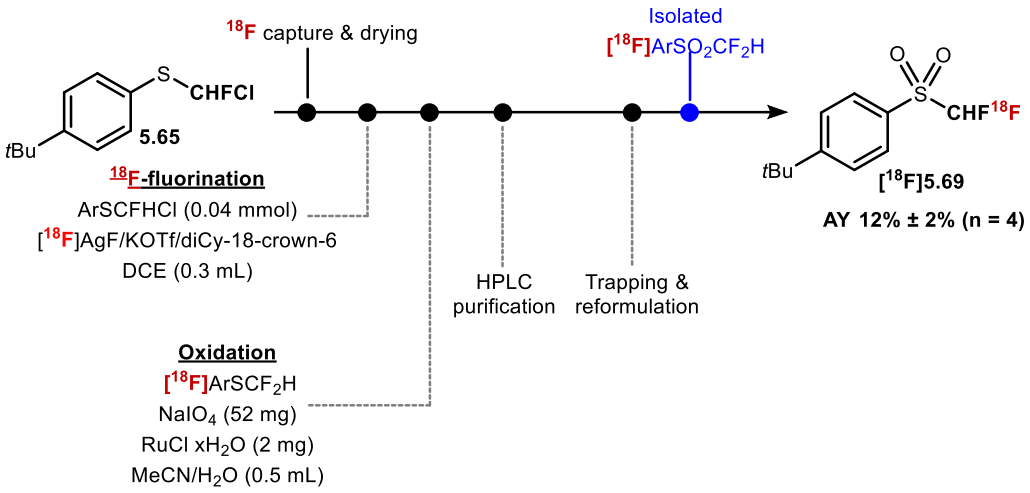

Scheme 6.20 Radiosynthesis for [^{18}F]1-(tert-butyl)-4-((difluoromethyl)sulfonyl)benzene.

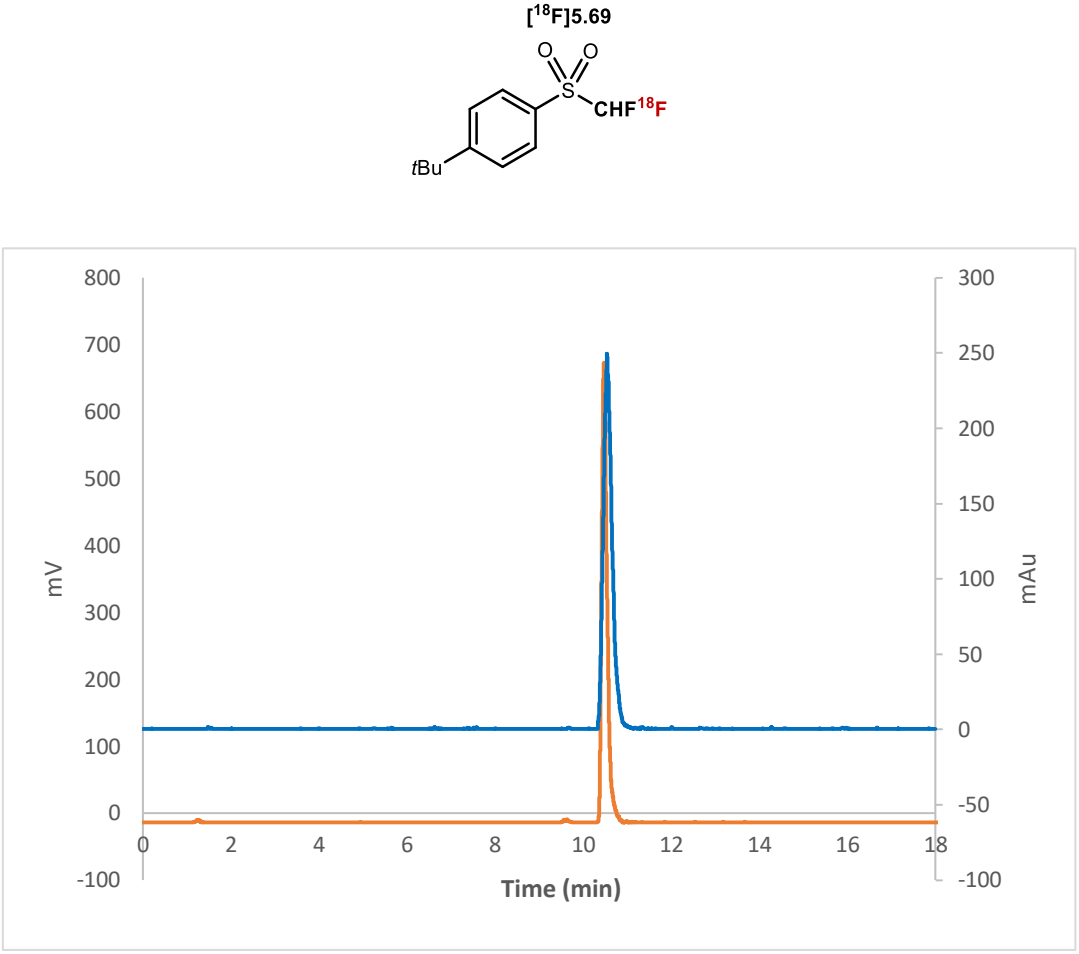

Figure 6.28 HPLC radio-trace of **[^{18}F]5.69** (blue) overlaid with HPLC UV-trace (λ = 220 nm) of ^{19}F reference compound (orange).

[^{18}F]5.75

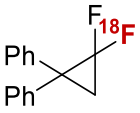

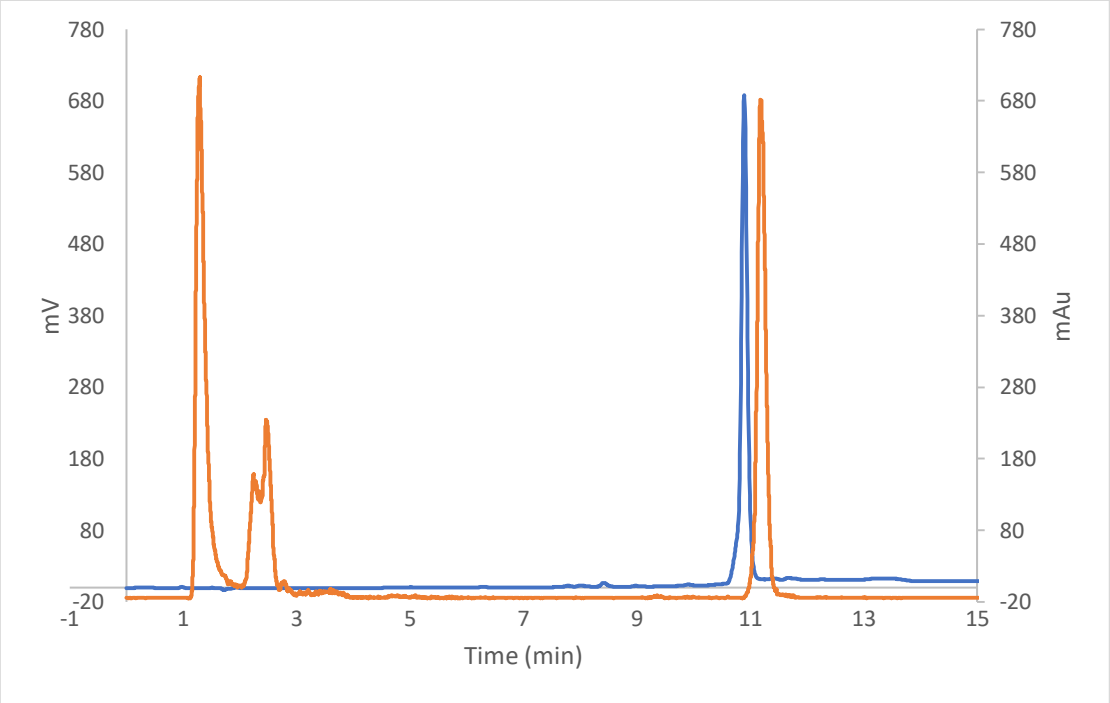

Figure 6.29 HPLC radio-trace of **[^{18}F]5.75** (orange) overlaid with HPLC UV-trace (λ = 220 nm) of ^{19}F reference compound (blue).

[^{18}F]5.58

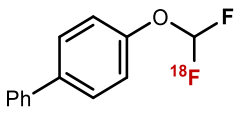

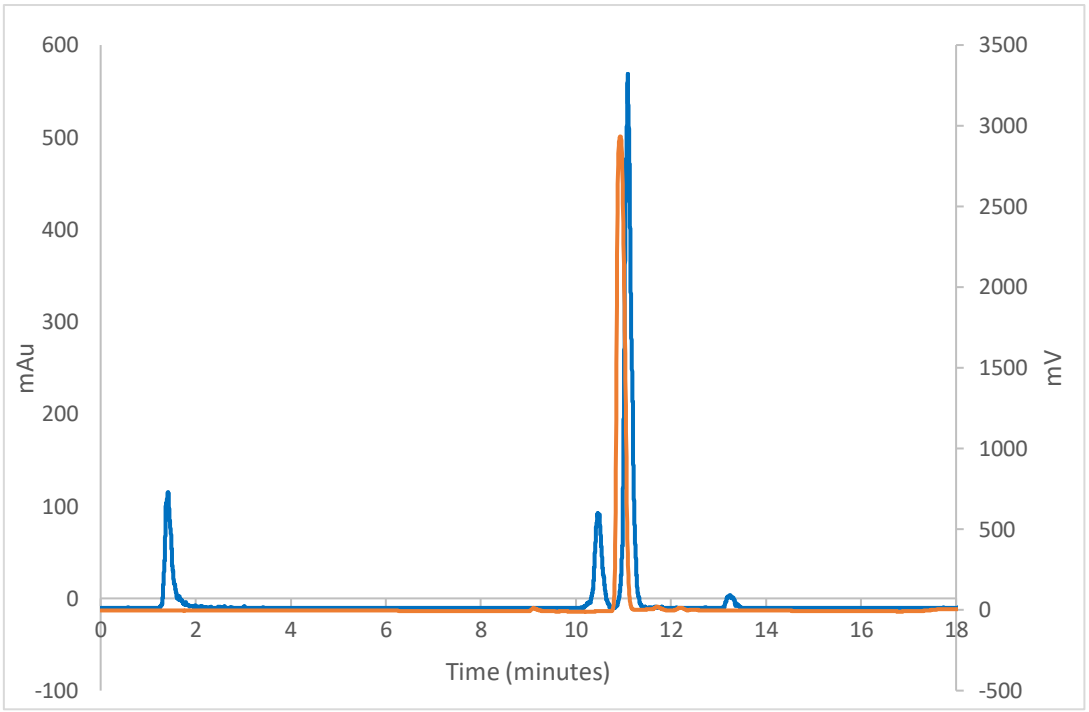

Figure 6.30 HPLC radio-trace of **[^{18}F]5.58** (blue) overlaid with HPLC UV-trace (λ = 220 nm) of ^{19}F reference compound (orange).

[^{18}F]5.77

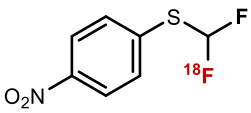

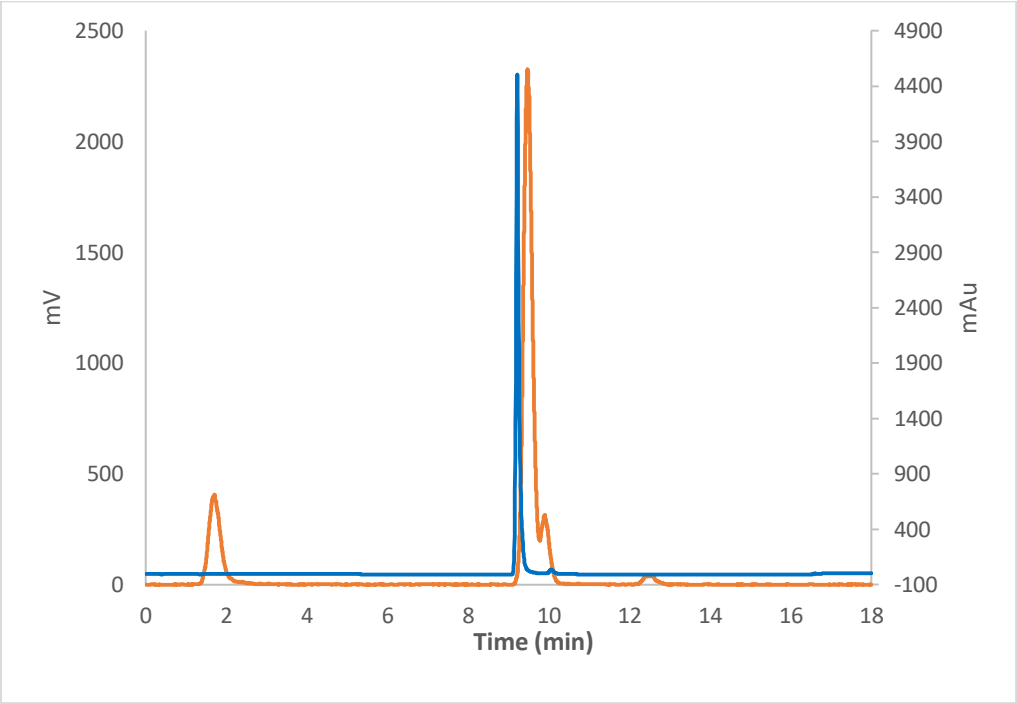

Figure 6.31 HPLC radio-trace of **[^{18}F]5.77** (orange) overlaid with HPLC UV-trace (λ = 220 nm) of ^{19}F reference compound (blue).

[^{18}F]5.79

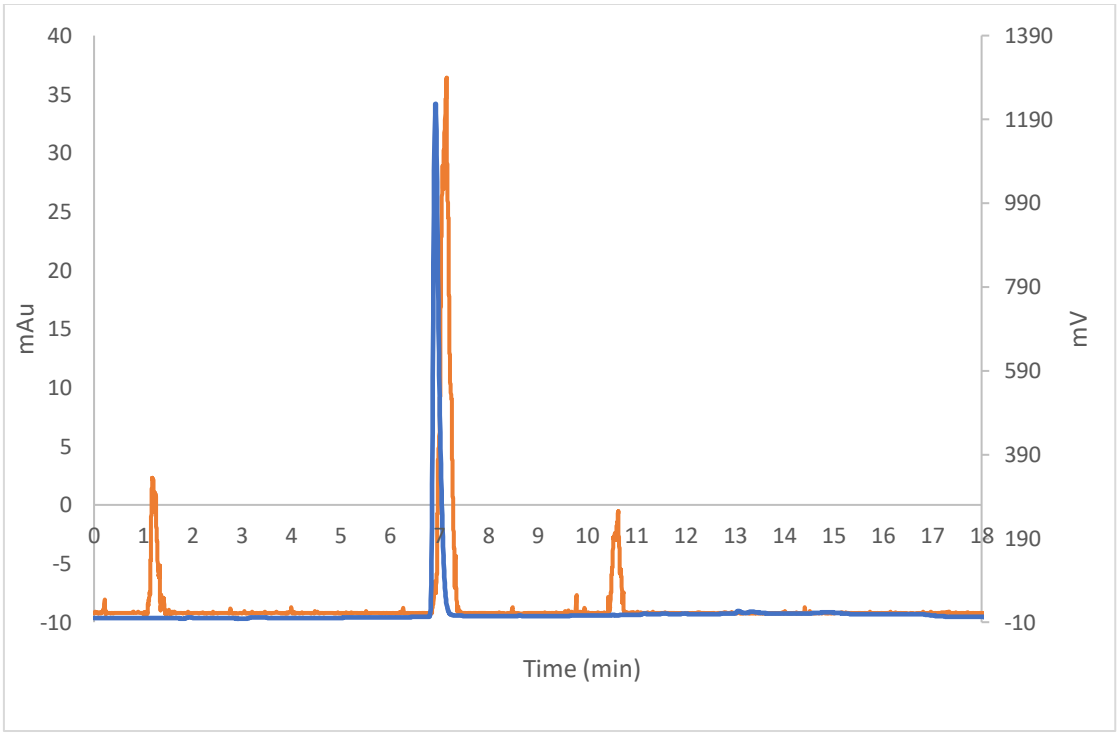

Figure 6.32 HPLC radio-trace of **[^{18}F]5.79** (orange) overlaid with HPLC UV-trace (λ = 220 nm) of ^{19}F reference compound (blue).

[^{18}F]5.81

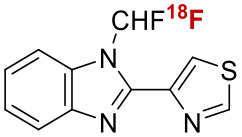

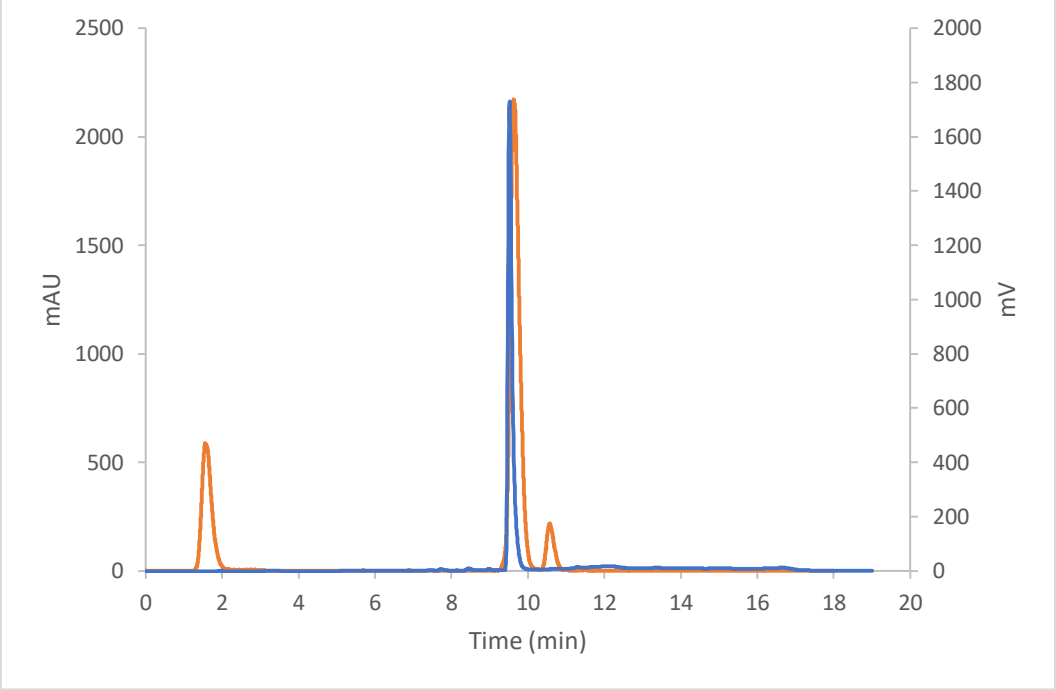

Figure 6.32 HPLC radio-trace of **[^{18}F]5.81** (orange) overlaid with HPLC UV-trace (λ = 220 nm) of ^{19}F reference compound (blue).

[^{18}F]5.89

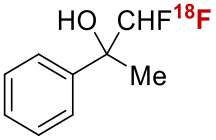

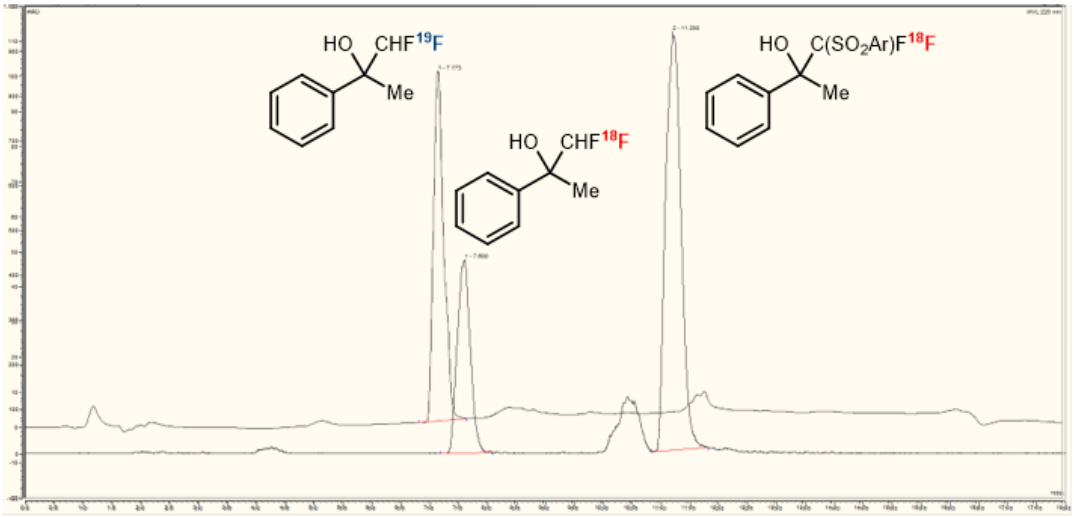

Figure 6.32 Crude reaction mixture of the ^{18}F-difluoromethylation of acetophenone with **[^{18}F]5.69**.

6.14 References Chapter V:

1. W. Wang, S. Zhang, H. Zhao and S. Wang, *Org. Biomol. Chem.,* 2018, **16**, 8565.
2. Q. Zheng, Y. Wei, J. Zheng, Y. Duan, G. Zhao, Z. Wang, J. Lin, X. Zheng and J. Xiao, *RSC Adv.,* 2016, **6**, 82298.
3. L. Li, F. Wang, C. Ni and J. Hu, *Angew. Chem. Int. Ed.* 2013, **52**, 12390.
4. G. Liu, W. Qin, X. Li, L. Lin and H. N. Wong, *J. Org. Chem.,* 2019, **84**, 15948.
5. J. Xu, E. Ahmed, B. Xiao, Q. Lu, Y. Wang, C. Yu and Y. Fu, *Angew. Chem. Int. Ed.,* 2015, **54**, 8231.
6. D. Chen, C. Ni, Y. Zhao, X. Cai, X. Li, P. Xiao and J. Hu, *Angew. Chem. Int. Ed.,* 2016, **55**, 12632.
7. A. Polley, G. Bairy, P. Das and R. Jana, *Adv. Synth. Catal.,* 2018, **360**, 4161.